Integrated Control and Estimation Based on Sliding Mode Control Applied to Electrohydraulic Actuator

A Thesis Submitted to
the College of Graduate Studies and Research
in Partial Fulfillment of the Requirements
for the Degree of Doctor of Philosophy
in the Department of Mechanical Engineering
University of Saskatchewan, Saskatoon
Canada

By
Shu Wang

Permission to Use

In presenting this thesis in partial fulfillment of the requirements for a Postgraduate degree from the University of Saskatchewan, I agree that the Libraries of this University may make it freely available for inspection. I further agree that the permission for copying this thesis in any manner, in whole or in part for scholarly purposes, may be granted by the professors who supervised my thesis work or, in their absence, by the Head of the Department or Dean of the College in which my thesis work was conducted. It is understood that any copying or publication or use of this thesis or parts thereof for financial gain shall not be allowed without my written permission. It is also understood that due recognition shall be given to me and to the University of Saskatchewan in any scholarly use which may be made of any material in my thesis.

Requests for permission to copy or to make other use of material in this thesis, in whole or part, should be addressed to:

Head of the Department Mechanical Engineering
University of Saskatchewan
College of Engineering
57 Campus Drive
Saskatoon, Saskatchewan S7N 5A9
Canada

Abstract

Many problems in tracking control have been identified over the years, such as the availability of systems states, the presence of noise and system uncertainties, and speed of response, just to name a few. This thesis is concerned with developing novel integrated control and estimation algorithms to overcome some of these problems in order to achieve an efficient tracking performance. Since there are some significant advantages associated with Sliding Mode Control (SMC) or Variable Structure Control (VSC), (fast regulation rate and robustness to uncertainties), this research reviews and extends new filtering concepts for state estimation, referred to as the Variable Structure Filter (VSF) and Smooth Variable Structure Filter (SVSF). These are based on the philosophy of Sliding Mode Control.

The VSF filter is designed to estimate some of the states of a plant when noise and uncertainties are presented. This is accomplished by refining an estimate of the states in an iterative fashion using two filter gains, one based on a noiseless system with no uncertainties and the second gain which reflects these uncertainties. The VSF is combined “seamlessly” with the Sliding Mode Controller to produce an integrated controller called a Sliding Mode Controller and Filter (SMCF). This new controller is shown to be a robust and effective integrated control strategy for linear systems. For nonlinear systems, a novel integrated control strategy called the Smooth Sliding Mode Controller and Filter (SSMCF), fuses the SMC and SVSF in a particular form to address nonlinearities. The gain term in the SVSF is redefined to form a new algorithm called the “SVSF with revised gain” in order to obtain a better estimation performance. Its performance is compared to that of the Extended Kalman Filter (EKF) when applied to a particular nonlinear plant.

The SMCF and SSMCF are applied to the experimental prototype of a precision positioning hydraulic system called an ElectroHydraulic Actuator (EHA) system. The EHA system is known to display nonlinear characteristics but can approximate linear behavior under certain operating conditions, making it ideal to test the robustness of the proposed controllers.

The main conclusion drawn in this research was that the SMCF and SSMCF as developed and implemented, do exhibit robust and high performance state estimation and trajectory tracking control given modeling uncertainties and noise. The controllers were applied to a prototype EHA which demonstrated the use of the controllers in a “real world” application. It was also concluded that the application of the concepts of VSC for the controller can alleviate a challenging mechanical problem caused by a slip-stick characteristic in friction. Another conclusion is that the revised form of the SVSF could obtain robust and fast state estimation for nonlinear systems.

The original contributions of the research include: i) proposing the SMCF and SSMCF, ii) applying the Sliding Mode Controller to suppress cross-over oscillations caused by the slip-stick characteristics in friction which often occur in mechanical systems, iii) the first application of the SVSF for state estimation and iv) a comparative study of the SVSF and Extended Kalman Filter (EKF) to the EHA demonstrating the superiority of the SVSF for state estimation performance under both steady-state and transient conditions for the application considered.

The dissertation is written in a paper format unlike the traditional Ph.D thesis manuscript. The content of the thesis discourse is based on five manuscripts which are appended at the end of the thesis. Fundamental principles and concepts associated with SMC, VSF, SVSF and the fused controllers are introduced. For each paper, the objectives, approaches, typical results, conclusions and major contributions are presented. Major conclusions are summarized and original contributions reiterated.

Acknowledgements

The author expresses his gratitude to his supervisors, Dr. S. Habibi and Dr. R.T. Burton for their guidance and advice during the course of this research and the writing of this thesis. The technical assistance of Mr. D.V. Bitner is also gratefully acknowledged. Financial support in the form of graduate student monthly stipend, University of Saskatchewan Graduate Student Scholarship and National Science and Engineering Research Council of Canada is also acknowledged.

Special gratitude must be conveyed to his wife, Lu Gan whose patience and support have been invaluable during my studies. The gratitude is also owned to his son, Clement, for lots of enjoyable and challenge time when his son was born during the author's Ph.D program of study.

He also wishes to express his gratitude to his family, especially to his parents, sisters and brother for their encouragement and support.

Table of Contents

List of Figures

List of Abbreviations

EHA	ElectroHydraulic Actuator system
EKF	Extended Kalman Filter
SMC	Sliding Mode Control
SMCF	Sliding Mode Controller and Filter
SPC	Switched Proportional Controller
SSMCF	Smooth Sliding Mode Controller and Filter
SVSF	Smooth Variable Structure Filter
VSC	Variable Structure Control
VSF	Variable Structure Filter

Chapter 1
Introduction

There exist a wide variety of applications using hydraulic control systems in industrial motion systems, such as robotics, machining plants, mining systems, special purpose machines, and so on [1]. Controlling hydraulic systems is always a challenge due to the presence of nonlinearities which arise from fundamental behavioral properties such as fluid compressibility (due to entrained air, mechanical compliance, dependency on pressure, and temperature), complex flow properties of hydraulic valves (such as pressure losses, transient and turbulent flow conditions), and friction characteristics in hydraulic actuators (due to the combined properties of static, coulomb and viscous friction – slip stick). These challenges are compounded by temporal and operating point parameter variations, and by the presence of measurement and system noise in practical hydraulic applications. Thus, for hydraulic control systems, uncertainties do exist and hence control of these systems over a wide range of operating points and loading conditions is often very difficult to do.

Classical feedback controls (those which are readily tuned manually) are usually applied to deterministic systems (ones without uncertainties). Advanced (model-based) control methods are necessary if high-performance motion control (such as trajectory tracking or model following) is required on stochastic (uncertain or ill defined) systems. Some of these advanced control methods demonstrate robustness in the presence of model and parameter uncertainties and are able to successfully control even when system states and parameters must be estimated.

The objective of this study is to present a novel form of advanced control using concepts based on Sliding Mode Control (SMC) or Variable Structure Control (VSC), which has the capability of controlling a nonlinear plant in the presence of uncertainties associated with parameter estimation and modeling errors. The controller is applied to tracking control of a special hydraulic positioning system which displays many nonlinear characteristics and has shown high positioning accuracy (in the range of 100 nanometers) [2]. The system is called an ElectroHydraulic Actuator (EHA) system. In this system, not all of the actual output trajectories states (or “full states”) can be monitored. Thus, it is

necessary to design an “observer”, or “online filter”, to compute an estimate of the entire state vector when provided with limited measurements of some of the states of the system. The study employs a recently proposed robust state and parameter estimation strategy, referred to as the Variable Structure Filter (VSF) and Smooth Variable Structure Filter (SVSF), in conjunction with SMC, to estimate non-measurable states for the tracking controller, (i.e. full-state feedback), and to control the EHA to follow a set of desired inputs patterns.

The format of this thesis is to first introduce the basic concepts behind the SMC, VSF, SVSF, the Sliding Mode Controller and Filter (SMCF), the Smooth Sliding Mode Controller and Filter (SSMCF) and Extended Kalman Filter (EKF). This introduction contains minimal mathematical derivations. Also, the system of the EHA to which the new controller is applied, is described.

In Chapter 3, a summary of five manuscripts pertinent to the research is presented. This summary contains the manuscripts objectives, approaches, important results, conclusions and significant contributions

Chapter 4 presents overall conclusions and restates the major research contributions of this study.

The Appendices present a compendium of the five manuscripts referred to in the main body.

Chapter 2

Reviews of Basic Concepts

The section will first describe the application of interest, the ElectroHydraulic Actuator (EHA) system, and then introduce the concepts of VSC, VSF and SVSF etc. The mathematics is kept to a minimum with emphasis being placed on the related physical concepts. Details of the equations and their derivations are provided in the appended publications and are referenced accordingly.

2.1 The ElectroHydraulic Actuator (EHA) System

There are two basic types of hydraulic transmission systems used in industry to transfer energy by converting mechanical energy to fluid energy, and then back to mechanical energy: valve controlled and pump controlled hydraulic systems. Valve control is perhaps the most common way to modulate speed of the actuator (load). But this approach has some disadvantages: lower power efficiency (due to pressure drops across the control valve), bulkiness (more components), greater leakage (in the valve itself), and the need to use expensive servo valves. The second approach is to use the pump itself to change the flow rate (and hence the velocity of the load) eliminating pressure drops across a controller orifice (the valve). However, this approach does require additional components for pump control and so trade-offs are often required in assessing the relative benefits of either approach.

The EHA is a typical pump controlled hydraulic system. The EHA system is based on the principle of closed circuit hydraulic transmission and is shown in Figure 2-1 with a schematic representation shown in Figure 2-2. Fluid is delivered by the variable displacement pump directly to the actuator (symmetric and equal piston area in this case) with the exiting fluid being transferred directly back to the pump inlet. The system is thus defined as being “closed” as opposed to an “open” system in which fluid is delivered to a reservoir and then to the pump inlet. An accumulator is located down stream to the actuator motion to ensure that the average return line pressure does not drop resulting in cavitation due to external leakage. The amount of fluid delivered can be varied either by

changing the “displacement” of the pump (via a swash plate) or by varying the “driving” speed of the pump. In this application, a speed controlled pump was used.

A particular EHA system was designed and extensively investigated by Habibi et al [3, 4, 5], in which a symmetric linear actuator (flow in equals flow out) was used. This particular EHA system was capable of moving a load of 20 kg with sub-micron accuracy (100 nanometers) and large stroke (10 cm). As mentioned above, a variable speed pump was used to directly regulate the movement of a hydraulic cylinder (see Figure 2-2). The main constituents of the EHA are: an electrical motor, a bi-directional gear pump, a symmetrical actuator, pressure and position sensors, and an inner accumulator sub-circuit. The electric motor was controlled using an inner loop high gain feedback system to remove dead zone problems [5].

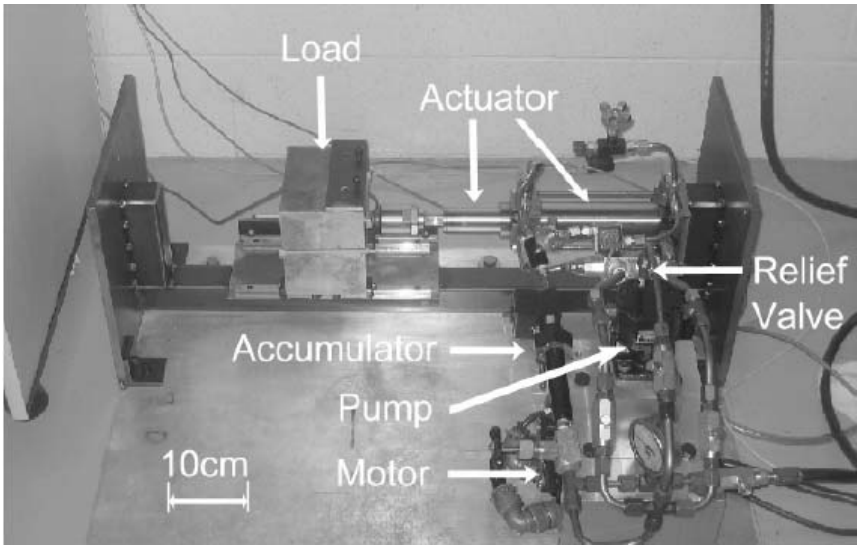

Figure 2-1 The EHA Prototype

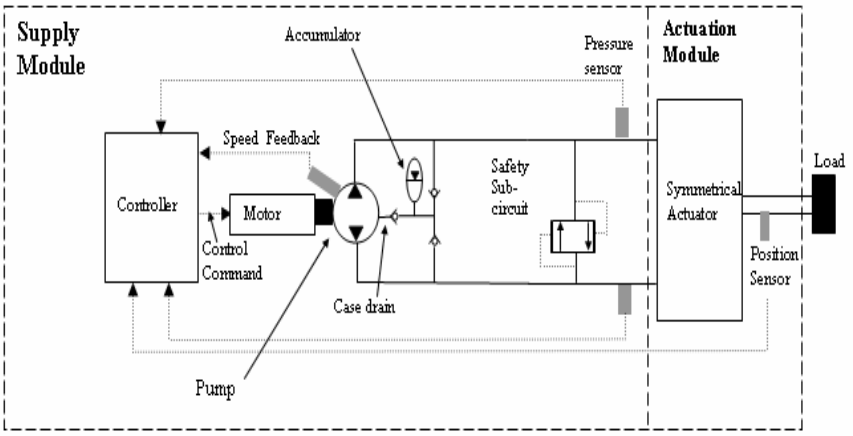

Figure 2-2 Schematic of the Electrohydraulic Actuator (EHA)

Many control studies on the EHA system have been completed. Linear and nonlinear models have been developed and control strategies implemented. A standard proportional controller, a variable gain controller and a fuzzy controller have all been successfully applied to the control of the EHA system [5, 6, 7]. However, the focus of these studies has been on the accurate positioning of the actuator and to a lesser extent on the speed of response of the system. There has been very little research on controlling the tracking capabilities of the EHA system in terms of position, velocity and acceleration and it is with this challenge in mind that this research was initiated.

To facilitate the control of the EHA system, the overall system model can be represented as a simple linearized model [5] at some specified operating condition. The mathematical model of the dominant dynamics of the EHA system can be represented by a third order discrete-time state-space function as [8]:

$$X_{k+1} = \begin{bmatrix} 1 & T_s & 0 \\ 0 & 1 & T_s \\ 0 & -\omega_{nh}^2 T_s & -(2\zeta_h \omega_{nh} T_s - 1) \end{bmatrix} X_k + \begin{bmatrix} 0 \\ 0 \\ \kappa_h \omega_{nh}^2 T_s \end{bmatrix} u_k , \tag{2.1}$$

$$Z_k = \begin{bmatrix} 1 & 0 & 0 \end{bmatrix} X_k , \tag{2.2}$$

where the state vector is $X = [x_1 \quad x_2 \quad x_2]$ and its elements represent the position, velocity, and acceleration of the load in the EHA system, the input u_k is the hydraulic pump speed, and ω_{nh} is the natural frequency of the system ($\omega_{nh} = 198 rad/s$ for this application), ζ_h is the hydraulic damping ratio ($\zeta_h = 0.1$), κ_h is the hydraulic system gain ($\kappa_h = 3.34 \times 10^{-4}$), and T_s is the sampling rate ($T_s = 0.001 s$).

It is worthy to note the output matrix $H = \begin{bmatrix} 1 & 0 & 0 \end{bmatrix}$ signifies that only the position of load may be directly measured by a transducer (in this case an optical encoder in the practical system). It is true that velocity and acceleration, can be calculated through differentiation but the results would be extremely noisy. The use of traditional filters can rectify this situation somewhat but usually at the expense of time delays. Thus, it is very desirable to be able to estimate these states in a more accurate fashion.

As mentioned above, there are many nonlinearities which influence the EHA operation. One very important nonlinearity is associated with the friction characteristics of the actuator. For the EHA prototype fabricated by Habibi et al [3], the friction characteristics were measured and are shown in Figure 2-3. Models for the EHA system described by Eqs. (2.1) and (2.2) assume viscous friction (shown as dot-dash lines in Figure 2-3). The reality is that the friction is dominated by a combination of coulomb, static and viscous friction [9]. Based on the actual friction characteristics, a nonlinear state space model for the EHA system was developed and is given as [10]:

$$\begin{cases} x_{1k+1} = x_{1k} + T_s x_{2k} + T_s w_{1k} \\ x_{2k+1} = x_{2k} + T_s x_{3k} + T_s w_{2k} \\ x_{3k+1} = [1 - T_s a_3] x_{3k} - T_s a_2 x_{2k} - T_s [a_{11} x_{2k} x_{3k} + \\ \qquad a_{12} (x_{2k})^2 + a_{13}] sign(100 x_{2k}) + T_s b u_k + T_s w_{3k} \end{cases}, \tag{2.3}$$

where w_1, w_2, w_3 are system noise. For this system, the coefficients were determined to be:

$a_3 = -71,\ a_2 = 39000,\ a_{11} = 2100,\ a_{12} = 1610,\ a_{13} = 3.5,\ b = 13.1.$

Eqs. (2.1), (2.2) and (2.3) form the model that the new VSF/SVSF and SMC were based. Eq. (2.3) could not be directly applied to the SVSF which required the system model to be continuously differentiable. The mathematical approach which was used to overcome this limitation is the subject of one of the appended manuscript C [11].

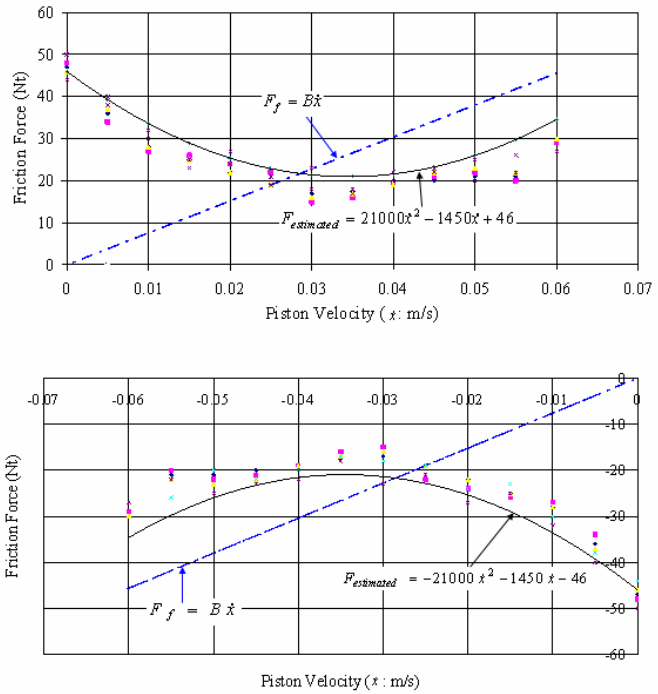

Figure 2-3 Experimental friction in the EHA actuator and showing a linear and quadratic approximation [9]

2.2 The Basic Concepts of SMC

To facilitate the discussion of SMC, the following section will consider the classical control and model based control approaches. This will assist in showing how the SMC, the VSF, and the SVSF operate are developed. The discussion limits the mathematical development of the control and filter strategies and concentrates on "block diagram" representations to illustrate the concepts and ideas. Rigorous mathematical proofs of the developments of filter gains and control stability are referred to the appended papers.

Classical Control:

Depending on the complexity and the linearity of the plant, a first approach to control design is based on "classical control" strategies to control the states of the plant. The purpose of the control law in a closed-loop system is to input appropriate reference signals to the plant in order to force the output states to follow the desired inputs in a stable and accurate fashion, i.e., force the error signals to reach zero. A block diagram of the controller and feedback system is shown in Figure 2-4.

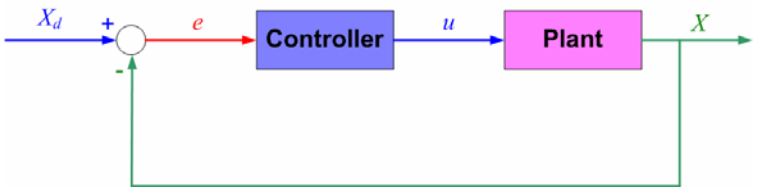

Figure 2-4 A simple "classical" feedback control loop

As stated above, this classical control form is designed to force the system output states to follow the desired inputs based on error signals only. However, this controller does not contain any information about the plant and responds only to the error signal, its derivative and/or its integral; it is called a "non-model-based" controller. Simplistic approaches to tuning of the controller gains would include a trial and error approach and the structured tuning procedures such as the Ziegler-Nichols method [12]. However, the classical controller is not "robust" in terms of performance and stability since its design does not usually directly take into account the existence of external perturbations such as noise.

From Figure 2-4, defining the error signal between the desired input X_d and output X as:

$$e = X_d - X\,, \tag{2.4}$$

a control law can be formulated in the form of a classical PID controller as:

$$u = K_P e + K_I \int e dt + K_D \dot{e}\,, \tag{2.5}$$

where K_P, K_I, K_D are constant gains.

Model-based "Classical" PID Control:

If the dynamics of the plant are known and accurately explained by a model, then the PID control algorithm could be designed to reflect the dynamics of the plant mathematically and to provide a control signal which would force the plant to follow the desired states in a very efficient manner. Classic methods such as root locus and frequency response may be used in the design of the controller. To illustrate this, consider the following. In the state-space form, and in the absence of external disturbances, a typical linear model of a plant may be represented as:

$$\dot{X} = AX + Bu\,, \tag{2.6}$$

where A and B are the system and input matrices which are constant, X is the state vector, and u is the input. Parameters from the dynamic model of Eq. (2.6) are not only used to compute values of controller PID gains (via transfer function and performance constraints), but are also used to provide insight into controller design from parameters such as loop sample time [1].

When a model of a plant is used in conjunction with the classical PID controller to design the performance of the plant analytically, this approach has been defined as a "classical model-based" PID controller [13]. This approach is illustrated in block diagram form in Figure 2-5.

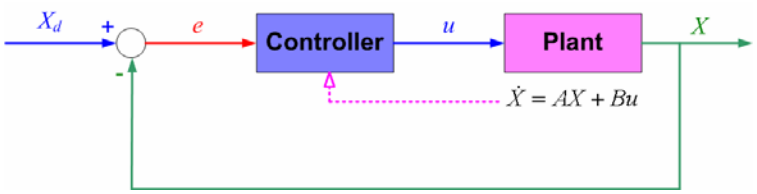

Figure 2-5 Model-based classical PID control

The model defined by Eq. (2.6) is assumed to be a "good" mathematical representation of the dynamics of the plant, and parameters from the plant model are used in the control algorithm directly. But these equations do not provide a comprehensive consideration of uncertainties which exist in a practical plant. Therefore, the "model-based" PID controller does not directly account for uncertainties.

Advanced Control:

When the controller is **not** in the traditional PID format but still requires the use of a plant model defined by Eq. (2.6), then this type of controller has been classified as an "advanced" controller [13]. As in model-based PID controllers, advanced model-based controllers require a model of the plant, obtained either through analytical modeling techniques or through identification techniques. Both the model order and the model coefficients must be "estimated". It becomes a challenge to be able to do so accurately

and online (online because the loading conditions may change during operation, changing the order of the system, for example).

If the system model order is consistent with the plant dynamics, if the parameter values are reasonably defined and if all the states are accurately measured, the outputs of the plant and the model would be very close when subjected to the same inputs. Then an advanced model-based controller can be designed to restrict the plant's dynamical behavior to follow the desired states within the accuracy of the model and within the "saturation" limits of the plant.

To demonstrate this approach, define some error function as:

$$S = Ce, \tag{2.7}$$

where e is the error signal, and , $C \neq 0$, is some constant vector containing the elements which are the coefficients describing the desired dynamics and relationships between the all state errors. It should be noted that choosing the most appropriate C represent a challenge to this type of approach. This is discussed in greater detail in the appended manuscripts A, B, and E [14, 15, 16].

The objective of the control law is to make the actual states or output, X, reach the desired states or input as close as possible. Figure 2-6 shows the "reaching path" of an error signal as it progresses to zero (forced by the feedback control law). With reference to this figure, in the initial time t_0, the error signal $e = X_d - X > 0$, and the error is approaching zero in a downward direction, i.e. the gradient of the reaching path (or the derivative of the error signal) $\dot{e} < 0$. At t_1, $e = 0$, but derivative of the error is still negative. At t_2, the error $e < 0$, but $\dot{e} = 0$. At t_3, the error $e = 0$, but $\dot{e} > 0$. This switching of the sign of $\dot{e}$ occurs until t_n, where the error is equal to zero, $e = 0$, and $\dot{e} = 0$. At this point, the desired output states follows the desired input states. Consequently, two conditions defined as the "reaching conditions" of error signals can be described as [17]:

$$X_d = X \ \text{(because } e = 0\text{)}, \tag{2.8}$$

and

$$\dot{X}_d = \dot{X} \ \text{(because } \dot{e} = 0\text{)}. \tag{2.9}$$

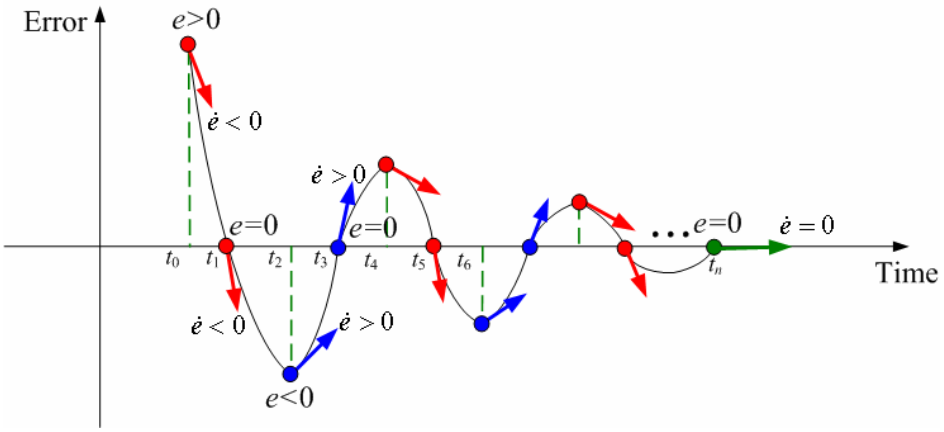

Figure 2-6 Reaching conditions of error signals

S defined as in Eq. (2.7) is essentially a reflection of Eqs (2.8) and (2.9) can thus be written as:

$$S = 0\,, \tag{2.10}$$

and

$$\dot{S} = 0\,. \tag{2.11}$$

From Eqs. (2.4), (2.7), (2.11),

$$C(\dot{X}_d - \dot{X}) = 0\,. \tag{2.12}$$

Substituting Eq. (2.6) into Eq. (2.12) yields:

$$C(\dot{X}_d - AX - Bu) = 0\,. \tag{2.13}$$

Solving for u, the control law may be derived as:

$$u = (CB)^{-1}C(\dot{X}_d - AX)\,. \tag{2.14}$$

For the control of a plant **without** uncertainties, the control law u can be defined as an equivalent control u_{eq}, that is:

$$u_{eq} = (CB)^{-1}C(\dot{X}_d - AX)\,, \tag{2.15}$$

where $C \neq 0$.

The control block diagram is illustrated in Figure 2-7. It is evident that the controller requires information about the plant parameters, the output states, the desired states and the term C.

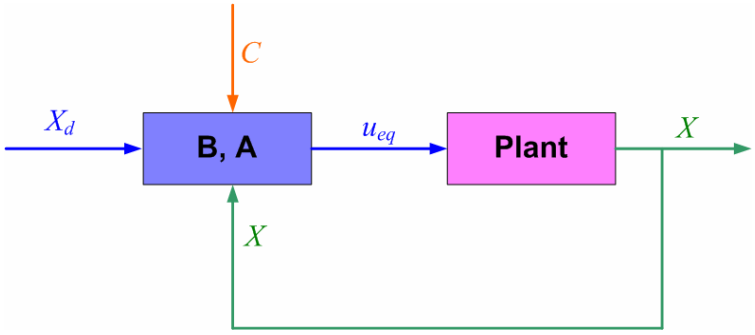

Figure 2-7 Advanced control strategy

Sliding Mode Control:

The equivalent control defined in Eq. (2.15) **does not account** for uncertainties which include such things as errors in model order, parameter errors, non–accounted for nonlinearities and system noise. As a first approximation, all the uncertainties may be lumped together such that the linear model of Eq. (2.6) may be represented as [18]:

$$\dot{X} = AX + Bu + w, \tag{2.16}$$

where w is the lumped system uncertainties. The block diagram of the control strategy can be represented as shown in Figure 2-8 (compared to Figure 2-5):

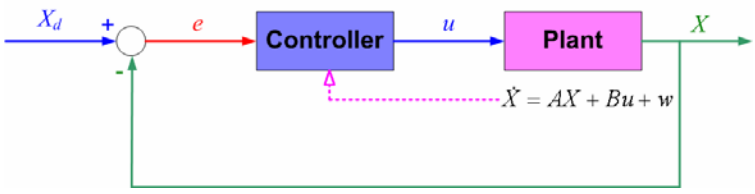

Figure 2-8 Advanced control strategy for systems with uncertainties

Due to the existence of system uncertainties, the system model of Eq. (2.16) is not known exactly because w is random and unknown in the real plant. However, it is reasonable to assume that in practice, the uncertainties w have some maximum limit (an upper bound). If one designs for this upper bound, then the worst case has been

accounted for. Thus the uncertainty is less than this upper bound, the system, may be "over compensated" to some degree.

From Eqs. (2.12) and (2.16):

$$\dot{S} = C(\dot{X}_d - \dot{X}) = C(\dot{X}_d - AX - Bu - w) = 0. \tag{2.17}$$

Thus, the control law may be derived as:

$$u = (CB)^{-1} C(\dot{X}_d - AX - w). \tag{2.18}$$

Using the definition of equivalent control (Eq. (2.15)), Eq. (2.18) can be written as:

$$u = u_{eq} - (CB)^{-1} Cw. \tag{2.19}$$

Thus, the control signal needs something "extra" beside u_{eq} to force $S = 0$ and $\dot{S} = 0$. The control strategy diagram can be represented as shown in Figure 2-9. As will be shown, this diagram forms the basis of a sliding mode controller (SMC).

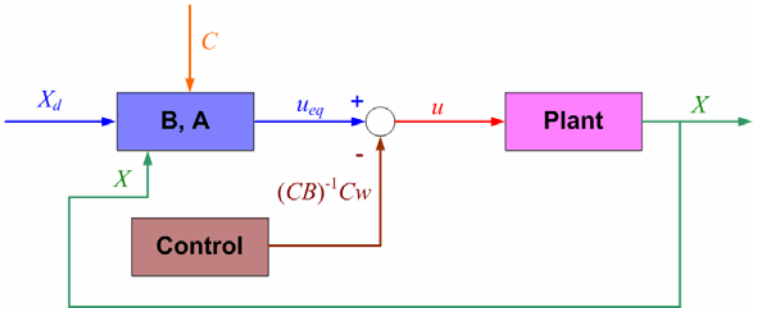

Figure 2-9 Sliding Mode Control Strategy

In Figure 2-9, the challenge is to define a controller which can create a control signal consisting of the uncertain term $CB^{-1}Cw$ and u_{eq}. The problem is that the system uncertainties, w, are not known. It is known that if there are no uncertainties, the equivalent control u_{eq} is able to make the function $S = C(X_d - X) = 0$, i.e. $\dot{X}_d - \dot{X} = 0$ as discussed previously. If matrices A, and B are defined (recognizing that any errors in estimating, measuring or specifying these parameters are included in w), then u_{eq} is known. Thus, $X_d - X$ can be written in terms of w, that is,

$$X_d - X = w. \tag{2.20}$$

Since S is equal to $C(X_d - X)$ for C not equal to zero, then the error function S has the same sign as the uncertainty term w such that:

$$\begin{cases} \text{If } w+, \quad \text{then} \quad S+ \\ \text{If } w-, \quad \text{then} \quad S- \end{cases}, \tag{2.21}$$

where "+" and "-" represent when the values are positive or negative.

Although the uncertainty term w is unknown, it may be assumed the uncertainties are upper bounded by the constant $w_{\max}$. Thus the actual w is always less than this value and hence w can be written as:

$$\left|w\right|_{ABS} \le w_{\max}, \tag{2.22}$$

where $\left|\ \right|_{ABS}$ is the absolute value, and $w_{\max}$ is the absolute maximum value of uncertainties.

Following the form of Eq. (2.19) the controller can be defined as:

$$u = u_{eq} + \Delta u, \tag{2.23}$$

where $u_{eq} = (CB)^{-1}C(\dot{X}_d - AX)$, and

$$\Delta u = K\,\mathrm{sgn}(S), \text{ where } K \ge -(CB)^{-1}Cw_{\max}, \tag{2.24}$$

where sgn( )is the signum function, and K is a constant.

The control law of Eq. (2.23) includes two parts: equivalent control u_{eq} and "switching control" Δu (whose value is dependent on the changing of the sign of the function S). Such a control strategy is commonly referred to as a Sliding Mode Control (SMC). The objective of SMC is the same as for classical controllers, i.e., force the output states to follow the desired input states. However, the SMC is a model-based control strategy in which the controller structure and gains are designed based on the system model. For stochastic systems, uncertainties associated with parameter variations, unknown nonlinear terms, and system and measurement noise exist. Since most of the uncertainties are random in nature, the error signal could be positive or negative. Thus since C, B and $w_{\max}$ are constant parameters, the switching control is essentially of the "bang-bang" type and its sign is dependent on the sign of S (and hence the error

associated with the uncertainties). Because of the bang-bang nature of Δu, the control input can be considered as "discrete" and the set of discrete control inputs is defined as the "switching control", Δu.

When the system errors equal zero, the plant follows the desired trajectory. Under these conditions $S = 0$, and the system state trajectory follows the desired trajectory and is restricted to lie on what is called the "sliding surface" (or "switching surface") $S = 0$. The function S defined in Eq. (2.7) is called the "switching function". It must be emphasized that since $w_{\max}$ is assumed constant and Δu is given by $\Delta u = K\,\mathrm{sgn}(S)$, the switching control will produce a switching signal as the actual states oscillate about the desired values.

The function of the SMC is to produce a discontinuous control signal (due to Δu) which forces the system states to repeatedly cross and then immediately re-cross the sliding surface until it finally slides along the surface $S = 0$. This kind of motion is referred to as "sliding motion".

In sliding mode, due to the discontinuous characteristics of Δu, the states would "switch" about the sliding surface rather than lie directly on it. This switching can occur at a high frequency and is called "chattering". This form of input signal to the plant is highly undesirable, because it can excite un-modeled high-frequency plant dynamics. In the thesis, the term "switching" refers to the oscillatory action that the signal makes about the desired path. The word "chattering" will be also used to describe the high frequency oscillation around the sliding surface. To reduce chattering, the "smoothing boundary layer solution" developed in [19] is applied to the control law of SMC. What this term means is that within the boundary layer, the control action is "smooth" or continuous as opposed to an abrupt bang-bang form outside the boundary, in which a discontinuous control action is applied to achieve the reaching conditions. Thus, the saturation function $sat(S, \Psi)$ is used to replace the sign function $\mathrm{sgn}(S)$ inside of boundary layer, $S \le \Psi$, such that:

$$sat(S, \Psi) = \begin{cases} \mathrm{sgn}(S/\Psi), & \text{for} \mid S/\Psi \mid > 1 \\ S/\Psi, & \text{for} \mid S/\Psi \mid \le 1 \end{cases}. \tag{2.25}$$

To illustrate the sliding motion, consider a simple model of a mass damper (M-D) system with the external disturbance d is described as:

$$M\dot{v} + Bv = u_f + d\,, \tag{2.26}$$

where M is the system mass, B the coefficient of damping, and u_f a control input.

Using the above equations, the SMC control signal for the M-D system can be defined:

$$u_f = u_{f\,eq} - \eta\,\mathrm{sgn}(S) = M\dot{v}_d + Bv - \eta\,\mathrm{sgn}(S)\,, \tag{2.27}$$

where sgn is the signum function, and η is a positive number which is satisfied with $\eta \geq |\,d\,|$, and the external disturbance d is thus assumed to be bounded.

The sliding motion for this example is illustrated in Figure 2-10.

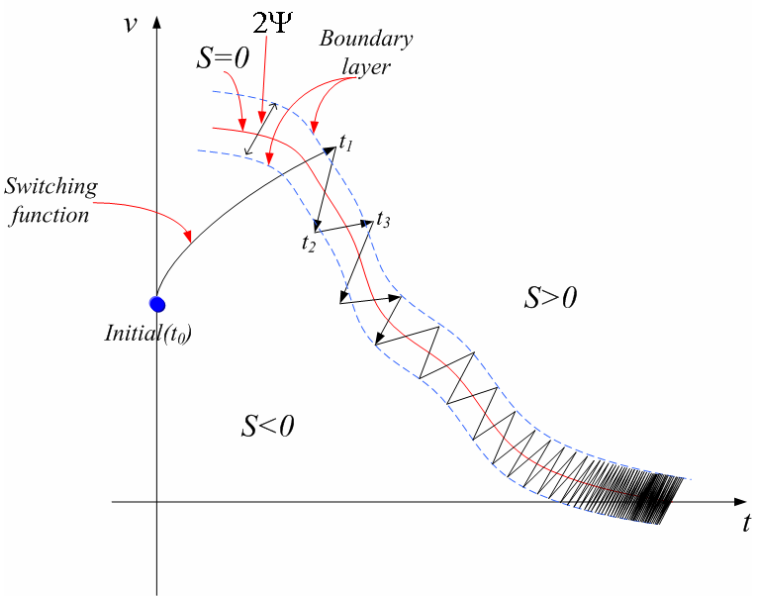

Figure 2-10 Sliding Mode of the M-D system (Note the switching action is of the bang-bang type both outside and inside the boundary layer)

Initially in Figure 2-10, the plant states are at some initial value and hence the error can be large. The SMC does have knowledge of what these states are (either by direct measurement or by some form of estimation scheme). The dynamics defined by the states in the SMC are embedded both in u_{eq} and in the "switching function" S (that is since

$S = C(X_d - X)$, the plant dynamics are defined by the state equations of X). From some initial point on one of the surfaces, (labeled as subspace $S > 0$ or $S < 0$ in Figure 2-10), the sliding surface separates the phase plane into two subspaces i.e. $S > 0$ or $S < 0$. Thus, the control signal will assume different values depending on the two subspaces in the phase plane. The SMC will then try to force the states to follow the desired path by first pushing the states towards the predetermined sliding surface $S = 0$ and then attempting to ensure that the trajectory will oscillate about the sliding surface. Because of uncertainties in the system, the controller can never really achieve the $S = 0$ curve but can oscillate about this condition as the desired input signal follows its desired path.

If in the proceeding example, the saturation function replaces the signum function in the Δu term, then the oscillation will damp out.

It should be noted that the controller based on the SMC can be developed even though the model of the plant is in fact nonlinear. However, the mathematics is very complex and hence its derivation and final form is left to the appended manuscripts A and E [14, 16]. The control signal still consists of two parts: one based on the assumption of no uncertainties, and the second term to compensate for uncertainties. The nonlinearities of the model can be discrete, for instance, Eq. (2.3), in which the coulomb and static friction are considered.

2.3 Introduction to the VSF and SVSF

2.3.1 Variable Structure Filter

Consider a linear plant without uncertainties as shown in Figure 2-5. The dynamic behavior of the plant can be described by n states, i.e. $X_a = \left[x_{a1}, x_{a2}, \cdots, x_{an}\right]$. The model of system is represented by Eq. (2.6). Using the approach of "forward difference" approximation $\dot{x}_i = (x_{ik+1} - x_{ik})/T_s$, where $i = 1,2,\cdots n,$ and T_s is the sampling rate, the discrete model of the plant is:

$$X_{k+1} = \Phi X_k + G u_k, \tag{2.28}$$

where $\Phi = T_s A + 1$, $G = T_s B$, k is the time step, $X = [x_1, x_2, \cdots, x_n]^T$ is the state vector, and $u = [u_1, u_2, \cdots, u_n]^T$ is the input.

In practice, **not all** state variables can be measured due to the cost, accuracy, or availability of appropriate transducers, which means that the number of the measured states is less than the total number of states. This output model can be described by the transducer matrix or output matrix H as:

$$Z_k = HX_k, \tag{2.29}$$

where the output matrix H is $m \times n$ (where $m \le n$), and $Z = [z_1, z_2, \cdots, z_m]^T$ is the output vector. This implies that only m outputs can be measured, which is less than the total number of states, n.

In some of tracking control problems, **all** the states are needed for feedback in order to compare the reference (desired) inputs to those of the output states so that the control signal to the plant can be adjusted in an appropriate fashion. To accommodate this, a state "estimator" or "observer" can be used to predict the plant output states based on a model of the plant. Based on Eq (2.28), a "noiseless estimate model" of the plant is defined and can be written as:

$$\hat{X}_{k+1|k} = \Phi \hat{X}_{k|k} + Gu_k, \tag{2.30}$$

where "^" means estimate states, and "$_{k+1|k}$" means "unrefined" (or priori) states at the $k+1$ time step, and "$_{k|k}$" means "refined" (or posteriori) states at the k th step. Unrefined in this sense means that the estimates of the state have not been adjusted at the beginning of the estimation cycle. Refined means that the states estimates have been adjusted by some form at that point.

The output of the noiseless estimate model is given by:

$$\hat{Z}_{k+1|k} = H\hat{X}_{k+1|k}. \tag{2.31}$$

From Eq. (2.30), the unrefined states of the plant for the beginning of the next cycle are calculated using the refined states of the previous step. The problem is how to obtain the refined states.

Consider Figure 2-11, the plant and the model equations are subjected to the same input. The outputs are the actual states X_a (n elements) and the unrefined states $\hat{X}_{k|k-1}$ (n elements). Since the model of the plant cannot exactly describe the plant, there are some differences between X_a and $\hat{X}_{k|k-1}$ which may be defined as the estimate state error, that is:

$$e_{f\,k|k-1} = X_a - \hat{X}_{k|k-1}, \tag{2.32}$$

where $e_{f\,k|k-1}$ is an $n \times 1$ vector. Note that this is not shown in Figure 2-11.

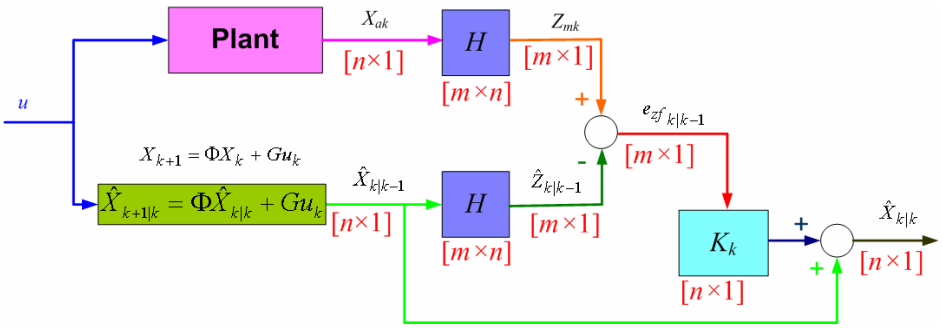

Figure 2-11 Estimation process of a linear plant without uncertainties

Because only m outputs can be measured, outputs $Z_{m\,k}$ (m elements) from the plant and $\hat{Z}_{k|k-1}$ (m elements) calculated from model, are used to obtain the estimated output errors $e_{zf\,k|k-1}$ (shown in Figure 2-11). $e_{zf\,k|k-1}$ is also a vector including m elements, such that:

$$e_{zf\,k|k-1} = Z_{m\,k} - \hat{Z}_{k|k-1}, \tag{2.33}$$

where

$$Z_{m\,k} = HX_{a\,k}, \tag{2.34}$$

$$\hat{Z}_{k|k-1} = H\hat{X}_{k|k-1}. \tag{2.35}$$

Thus,

$$e_{zf\,k|k-1} = H(X_{a\,k} - \hat{X}_{k|k-1}). \tag{2.36}$$

The objective of the estimation process is as follows: using a gain, K_k, compensate the unrefined states $\hat{X}_{k|k-1}$ to obtain the refined states $\hat{X}_{k|k}$ as shown in Figure 2-11, such that,

$$\hat{X}_{k|k} = \hat{X}_{k|k-1} + K_k . \tag{2.37}$$

The gain K_k can be defined in many ways and is usually as a function of the estimate state error $e_{f\,k|k-1}$, that is:

$$K_k = \gamma \cdot e_{f\,k|k-1}, \tag{2.38}$$

where γ is some "tuning" gain, and K_k is a $n \times 1$ vector.

Combining Eqs. (2.32) and (2.36) yields:

$$e_{f\,k|k-1} = X_{a\,k} - \hat{X}_{k|k-1} = H^{+} e_{zf\,k|k-1}, \tag{2.39}$$

where H^{+} is the pseudo inverse matrix of H. A pseudo inverse is required because H may not be a square matrix.

Substituting Eq. (2.39) into Eq. (2.38) yields

$$K_k = \gamma \cdot H^{+} e_{zf\,k|k-1}. \tag{2.40}$$

Following the approach that was used in the introduction to the SMC, a switching function following the form of Eq. (2.7) is defined as:

$$S_f = e_{zf\,k|k-1}. \tag{2.41}$$

Note that in this case, $C = 1$. In the case of the SMC, the $S = 0$ sliding surface was used as a basis for the output states to track the desired states. For estimation, the $S_f = 0$ surface is used as a basis for the estimated states to track the actual states.

The sliding surface of $S_f = 0$ separates the phase plane into two subspaces i.e. $S_f > 0$ or $S_f < 0$ as was the case for SMC. The compensator gain of K_k assumes different values depending on which of the two subspaces in the phase plane the estimated error lies. K_k will then force the estimated states $\hat{X}_{k|k}$ to repeatedly cross and

follow the path of the actual states X_a. For the VSF, the value of K_k is dependent on the sign of estimate output error $e_{zf\ k|k-1}$. Thus, Eq. (2.40) can be written as:

$$K_k = \gamma \cdot H^+ \mid e_{zf\ k|k-1} \mid_{ABS} \operatorname{sgn}(e_{zf\ k|k-1}), \tag{2.42}$$

where $\mid \mid_{ABS}$ is the absolute value, and sgn is the signum function. Details of this derivation are provided in the appended manuscript A [14].

For the estimation of a plant **without** uncertainties, the compensated gain K_k can be defined as an "equivalent" filter gain $K_{eq\,k}$, that is:

$$K_{eq\,k} = \gamma \cdot H^+ \mid e_{zf\ k|k-1} \mid_{ABS} \operatorname{sgn}(e_{zf\ k|k-1}). \tag{2.43}$$

It is useful to note the similarities in the "philosophy" behind the u_{eq} term for the SMC. The derivation of the equivalent filter gain $K_{eq\,k}$ uses only the output estimate model of Eq. (2.31), not the noiseless system estimate model of Eq. (2.30).

The equivalent filter gain defined in Eq. (2.43) does **not** account for system uncertainties w (which were included in Eq. (2.16)). The discrete model of the plant can be derived from Eq. (2.16) using the "forward difference" approximation method as:

$$X_{k+1} = \Phi X_k + G u_k + W_k, \tag{2.44}$$

where $\Phi = T_s A + 1$, $G = T_s B$, $W_k = T_s w$, k is the time step, T_s is the sampling time.

Due to the existence of measured noise caused by the transducer or the feedback loop, the output model of the plant is written as:

$$Z_k = H X_k + V_k, \tag{2.45}$$

where V_k $(m \times 1)$ is the measured noise.

The system uncertainties W_k and measured noises V_k are both unknown random signals. In order to estimate the states, the noiseless estimate model of Eqs. (2.30) and (2.31) is the only available model that can be used. It means that the compensator gain K_k must be redefined somehow to reflect the uncertainties in order to achieve a better "refining performance". As was done in the SMC, it is assumed the system uncertainties W_k and measurement noise V_k are upper limited, such that,

$$\left|W_k\right|_{ABS} \le W_{\max}, \tag{2.46}$$

and

$$\left|V_k\right|_{ABS} \le V_{\max}, \tag{2.47}$$

where $\left|\ \right|_{ABS}$ is the absolute value, and "$_{\max}$" means the maximum value.

The estimation process with uncertainties now included, is shown in Figure 2-12. K_k is now defined as a function of the upper bounds of system uncertainties and measurement noise. Following the same form as was adopted for the SMC, the gain K_k is partitioned into two parts such that:

$$K_k = K_{eq_k} + \Delta K_k, \tag{2.48}$$

where $K_{eq\,k} = \gamma \cdot H^+ \mid e_{zf\ k}\mid_{ABS} \operatorname{sgn}(e_{zf\ k|k-1})$ is the equivalent filter gain, and ΔK_k is the switching filter gain and:

$$\Delta K_k = (F_1 V_{\max} + F_2 W_{\max}) \operatorname{sgn}(e_{zf\ k|k-1}), \tag{2.49}$$

where $F_1 = \Phi^{-1} H^+ \left|H\Phi\right|_{ABS} \cdot [(I + \mid \Phi^{-1}\mid_{ABS}) \cdot \mid H^+\mid_{ABS}$ and $F_2 = \Phi^{-1} H^+ \left|H\Phi\right|_{ABS} \cdot \mid \Phi^{-1}\mid_{ABS}$, (refer to the appended manuscript A [14]).

It should be noted that the switching filter gain ΔK_k is derived from the noiseless system estimate model of Eq. (2.30) and output estimate model Eq. (2.31) as well.

Derivation of these terms are deferred to the appended paper A, but the form is quite similar to the Δu of the SMC. It is should be noted that the switching filter gain ΔK_k is calculated based on the upper bound of uncertainties $W_{\max}$ and $V_{\max}$. These terms will cause the estimated states to always switch around the actual states with the same magnitude even when the estimate errors approach zero. However, the same strategy used in the VSC can be applied to ΔK_k for the filter. The $\operatorname{sgn}(e_{zf\ k|k-1})$ in Eq. (2.49) can be substituted by $sat(e_{zf\ k|k-1})$ to suppress the chattering and force the estimate error to approach zero.

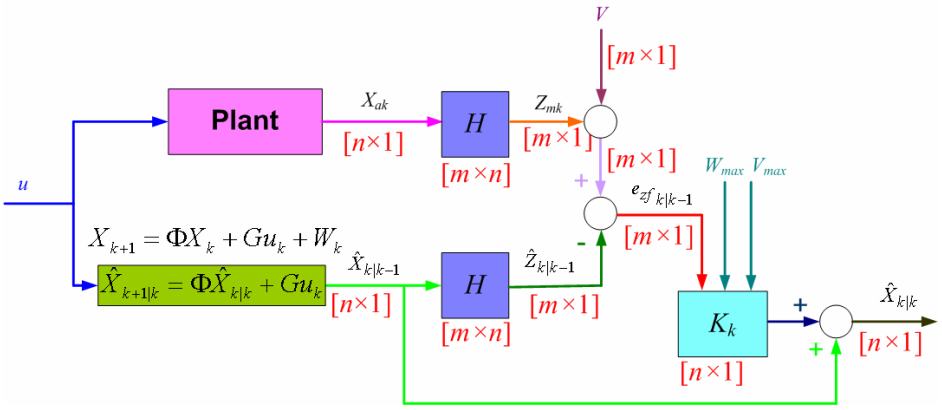

Figure 2-12 Estimation process of an uncertain plant

This kind of estimate strategy has been defined as the Variable Structure Filter (VSF) [20]. As has been illustrated, the VSF is conceptually similar to that of the SMC. The VSF uses a discontinuous gain K_k (defined as the VSF gain) to refine the estimated states $\hat{X}_{k|k}$ to follow the actual states X_{ak} in an oscillatory fashion along the sliding surface $S_f = e_{zf\,k|k-1} = 0$. Since there exist uncertainties in the real plant, the VSF gain is composed of an equivalent filter gain $K_{eq\,k}$ and switching filter gain ΔK_k. The switching gain forces the estimates to oscillate about the sliding surface.

2.3.2 Smooth Variable Structure Filter

The above sections have all assumed a linear plant with and without disturbances. If nonlinearities exist in a plant and cannot be ignored, a nonlinear model should be used to represent the system. This study considers a class of nonlinear systems having a state model nonlinear in the state vector $X(\cdot)$ and linear in the control vector $u(\cdot)$ of the form, such that:

$$\begin{aligned}\dot{X}(t) &= F[X(t), u, w(t)] \\ &= f(X(t)) + b(X(t))u(t) + w(t)\end{aligned}, \tag{2.50}$$

where t is the process time, $X(t) = [x_1(t), x_2(t), \cdots, x_n(t)]^T$ is a $n \times 1$ state vector, $b(X(t)) = [b_1(X(t)), b_2(X(t)), \cdots, b_n(X(t))]^T$ is an $n \times 1$ linear input matrix. $u(t)$ is the input signal and $w(t) = [w_1(t), w_2(t), \cdots, w_n(t)]^T$ is a time-dependent disturbance with a

known upper bound. $F(\cdot)$ is a general form of a nonlinear function, and $f(X(t)) = \left[f_1(X(t)), f_2(X(t)), \cdots, f_n(X(t))\right]^T$ is a **nonlinear** function determining the system characteristics. In this class of nonlinear systems, the control input u is fed into the system through the linear matrix $b(X(t))$ as opposed to being fed through the function $F(\cdot)$ directly. The nonlinear vector is of the form that makes the nonlinear systems controllable [21].

The output of the plant is related to the states by the equation:

$$Z(t) = HX(t) + v(t), \tag{2.51}$$

where $Z(t) = \left[z_1(t), z_2(t), \cdots, z_m(t)\right]^T$ is the $m \times 1$ output vector, H is the $m \times n$ constant output matrix. Because many of the states cannot be measured, $m \le n$.

A discrete model of the plant can be derived by using the "forward difference" approximation and is given by:

$$X_{k+1} = X_k + T_s f(X_k) + T_s b(X_k) u_k + W_k, \tag{2.52}$$

where $W_k = T_s w(t)$ is the system uncertainty, T_s is the sampling time, and k represents the time instant.

The discrete-time form of Eq. (2.51) may be expressed as:

$$Z_k = HX_k + V_k, \tag{2.53}$$

where $V_k = v(t)$.

As mentioned, only m outputs are available in the plant. However, n states have to be known and fed back in order to implement tracking control; thus, an "estimator" or "observer" for a **nonlinear** system is required. The equation for the "noiseless estimate model" which reflects nonlinearities without uncertainties becomes:

$$\hat{X}_{k+1|k} = \hat{X}_{k|k} + T_s f(\hat{X}_{k|k}) + T_s b(\hat{X}_{k|k}) u_k, \tag{2.54}$$

where "^" means estimate states, and "$_{k+1|k}$" means unrefined (or priori) states at the $k+1$ time step, and "$_{k|k}$" means refined states at the k th step. The estimation output model is given by:

$$\hat{Z}_{k+1|k} = H\hat{X}_{k+1|k}. \tag{2.55}$$

The new equations which reflect plant nonlinearities in the model are illustrated in the block diagram of Figure 2-13.

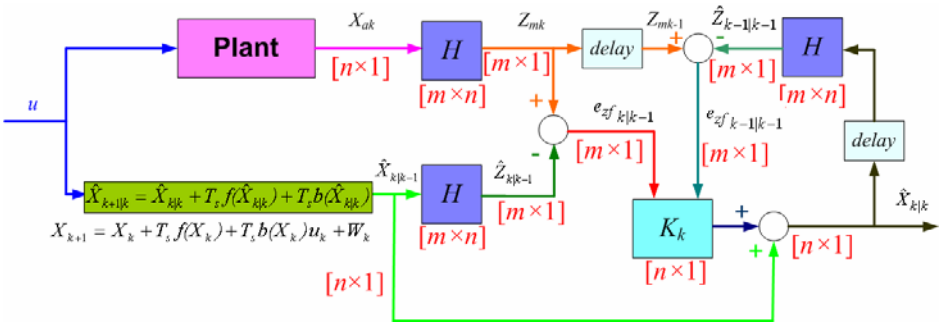

Figure 2-13 Estimation process of a nonlinear plant

As before, the plant contains model and noise uncertainties W_k and V_k. Using the same approach as for the VSF, the refined states $\hat{X}_{k|k}$ is refined by a filter gain, Ks_k based on the unrefined states $\hat{X}_{k|k-1}$, such that,

$$\hat{X}_{k|k} = \hat{X}_{k|k-1} + Ks_k . \tag{2.56}$$

It is useful to compare this form to that of the VSF ($\hat{X}_{k|k} = \hat{X}_{k|k-1} + K_k$). The gain Ks_k is defined as a summation of two parts in the same format as the VSF (see Eq. (2.48)), such that,

$$Ks_k = Ks_{eq_k} + \Delta Ks_k , \tag{2.57}$$

where the equivalent filter gain Ks_{eq_k} is defined in the same form as Eq. (2.43) (because the nonlinear system (Eq. 2.55) has the same noiseless estimate output model as with the linear system (Eq. (2.31)):

$$Ks_{eq_k} = \gamma \cdot H^+ \mid e_{zf_{k|k-1}} \mid_{ABS} \operatorname{sgn}(e_{zf_{k|k-1}}) , \tag{2.58}$$

and $e_{zf_{k|k-1}} = H(X_{a_k} - \hat{X}_{k|k-1})$.

The challenge was to define a new “switching filter” gain ΔKs_k which could reflect the plant nonlinearities and uncertainties. One could certainly use Eq. (2.49) as in the

case of the VSF. However, the use of $F_1 V_{\max} + F_2 W_{\max}$ times the signum function of the error still creates a final solution which oscillates about the sliding path. A different form of ΔKs_k was sought which would not contain constants associated with the upper limits $W_{\max}$ and $V_{\max}$. It was felt that a logical term to incorporate into the ΔKs_k term would be the error itself since as the error approaches zero, so would the magnitude of the switching function (see Eq. 2.60).

The estimation process is a "computing iteration" process. Thus the refined output error for **the last time step** can be calculated and is defined as:

$$e_{zf\,k-1|k-1} = H(X_{a\,k-1} - \hat{X}_{k-1|k-1}). \tag{2.59}$$

Note that the term of $e_{zf\,k-1|k-1}$ is the last time step refined error which reflects the differences between the actual states and estimated states, caused by nonlinearities, system uncertainties and noise. In order to compensate for the uncertainty terms and to facilitate the mathematical calculations, the switching filter gain is now assumed to have a proportional relationship with $e_{zf\,k-1|k-1}$. Using the relationship defined by Eq. (2.39), ΔKs_k was defined as:

$$\Delta Ks_k = \rho \cdot H^+ \mid e_{zf\,k-1|k-1} \mid_{ABS} \operatorname{sgn}(e_{zf\,k|k-1}), \tag{2.60}$$

where ρ is a gain which is to be tuned. Detailed mathematical justification is presented in the appended paper C.

The compensator gain for a plant with modelled nonlinearities becomes:

$$\begin{aligned} Ks_k &= Ks_{eq\,k} + \Delta Ks_k \\ &= H^+(\mid e_{zf\,k|k-1} \mid_{ABS} + \Pi \mid e_{zf\,k-1|k-1} \mid_{ABS}) \operatorname{sgn}(e_{zf\,k|k-1}) \end{aligned}, \tag{2.61}$$

where Π is a "lumped" tuning gain reflecting the gains ρ and γ.

The estimation strategy used in Eqs. (2.56) and (2.61) has been defined as the "Smooth Variable Structure Filter" (SVSF), [22]. The term "Smooth" refers to the fact that the nonlinearity must be smooth (continuous and differentiable). The gain of Ks_k is called the SVSF gain, and uses the estimated output error and the output error value at one step earlier, to refine the states calculated from the nonlinear noiseless estimated

model. Since the switching filter gain ΔKs_k is a function of the refined output errors at the last time step, the magnitude of $|e_{zf_{k-1|k-1}}|_{ABS}$ will decrease and tend to decrease the chattering associated with the SVSF along the sliding surface $S_f = e_{zf_{k|k-1}}$ as the time step is increased. Thus the magnitude of the switching function decreases with error and hence time. Also, the signum function of sgn($e_{zf_{k|k-1}}$) can be substituted by the $sat(e_{zf_{k|k-1}}, \Psi)$, which will force the estimated error to decrease as well. Thus, it can be seen that the SVSF should converge very quickly to the sliding surface (compared to the VSF).

It may be incorrectly concluded that the SVSF can achieve a better estimation performance than the VSF can for all linear and nonlinear plants. The mathematical calculation of $e_{zf_{k|k-1}}$ and $e_{zf_{k-1|k-1}}$ requires that the model of the plant must be continuously differentiable or "smooth" [23]. The SVSF may be applied to a linear plant because it is continuously differentiable but it would take much more "mathematical work" (and hence computational time) than would be the case for the VSF. For some nonlinear cases, such as a mechanical system involving static or coulomb friction, the SVSF cannot be used unlike the SMC which can accommodate discontinuous nonlinearities. (Note: as will be shown, by making such friction characteristics approximately continuous at zero velocity, the SVSF can be applied). To reiterate, the SVSF can only be used on linear or nonlinear systems whose models are composed of infinitely differentiable functions.

2.4 Integration of the SMC with the VSF or SVSF

As stated in Chapter 1, the control problem becomes one of employing an estimation technique to feedback the whole set of states to the control algorithm. This control strategy is called "full-state feedback" control and is illustrated schematically in Figure 2-14. In this figure, the controller requires both the model and all the states ($n \times 1$). However, only m outputs Z_m can be measured. The estimated outputs $\hat{Z}$ ($m \times 1$) of the non-measured states may be calculated from the estimate model of the plant (linear or

nonlinear). The estimate output error e_{zf} $(m\times 1)$ feeds into the estimator for state estimation. The whole set of estimated states $\hat{X}$ $(n\times 1)$ are refined by the estimator and compared with the desired input X_d $(n\times 1)$. The tracking error signal e $(n\times 1)$ between desired input X_d and the estimated states $\hat{X}$, is input into the controller in order to force the output of the plant to follow the desired input.

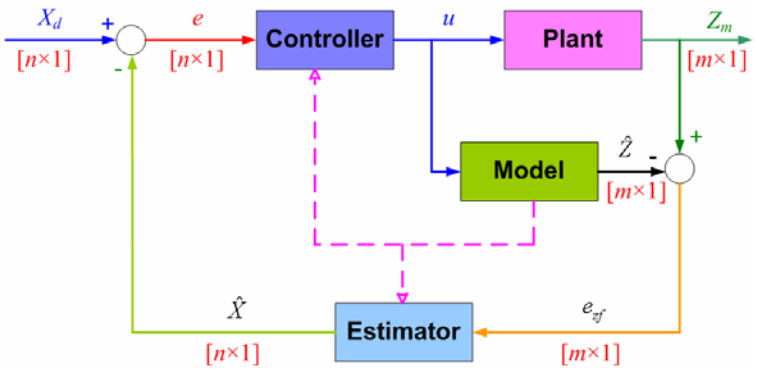

Figure 2-14 Full-state feedback control

In Figure 2-14, the estimate output error e_{zf} and tracking error e are fed into the estimator and controller respectively. The objectives of the controller and estimator are to force the tracking error e and estimation error e_{zf} to be minimum in a very small time frame. It is possible to achieve this objective in an efficient manner if the controller and estimator are "integrated" as an observer-based controller (that is, the estimation and control are done by the same algorithm). Analyzing the properties of this kind of integrated controller based on the basic SMC philosophy has only received limited attention [24]. Some initial work using a sliding mode controller and an asymptotic observer appeared in [25]. In this candidate's research, an objective was therefore to integrate the controller and estimator "seamlessly" into one algorithm since they both originate from the concepts of Variable Structure Systems (VSS).

As defined in the above sections, there exist mathematical relationships between e, e_{zf}, the VSF gain K_k, and the SVSF gain Ks_k, as shown in Eqs. (2.39), (2.43), (2.49) and (2.61). Using these relationships and employing the concepts of SMC, the control

law of the integrated observer-based controller is defined as a function of the VSF/SVSF gain and is composed of two parts, such that:

$$U(Kf_k) = U_{eq}(Kf_k) + \Delta U(Kf_k), \tag{2.62}$$

where U_{eq} is the equivalent control term and ΔU the switching control term of the integrated controller and Kf_k is the VSF or SVSF gain.

For a **linear plant**, the integrated controller embedded with the VSF gain has been defined as the "Sliding Mode Controller and Filter (SMCF)", which combined the SMC and the VSF [8]. The control law of SMCF may be written as [14]:

$$U_k(K_k) = U_{eq_k}(K_k) + \Delta U_k(K_k), \tag{2.63}$$

where the equivalent control is obtained as:

$$u_{eq_k}(K_k) = (C\hat{G})^{-1} C\{X_{d_{k+1}} - \hat{\Phi}[\hat{X}_{k|k-1} - K_k]\}, \tag{2.64}$$

and the switching control $\Delta U_k(K_k)$ is:

$$\Delta U_k(K_k) = -(C\hat{G})^{-1} C[e_{k|k-1} - K_k] + (C\hat{G})^{-1} Kc \cdot sat(C[e_{k|k-1} - K_k]/\psi_c), \tag{2.65}$$

e is the tracking error, K_k is the VSF gain, C is the sliding surface coefficient and $\hat{G}$, $\hat{\Phi}$ are constant matrices of system model, K_c is a constant gain, and ψ_c is the boundary layer width for the controller. Note that the switching control contains the sat term rather than the signum term.

The integrated controller for a **nonlinear system** is defined as the "Smooth Sliding Mode Controller and Filter (SSMCF)", in which the controller contains explicitly the SVSF gain Ks_{k+1}. The control law of the SSMCF may also be divided into two parts: equivalent control and switching control, such that [16]:

$$U_k(Ks_{k+1}) = \frac{\beta^2 + 1}{2\beta}\hat{p}_k + \left[\frac{\beta^2 - 1}{2\beta}|\hat{p}_k| + \frac{\beta K_C}{\hat{b}(\hat{X}_{k|k})\sigma_k}\right] \cdot sign(\hat{S}_k), \tag{2.66}$$

where the equivalent control $U_{eq}(Ks_{k+1}) = \frac{\beta^2 + 1}{2\beta}\hat{p}_k$, and the remaining terms represent the switching control signal [refer to appended paper E]. In addition,

$$\hat{p}_k = \frac{\sigma_k}{T_s \hat{b}(\hat{X}_{k|k})\sigma_k}\left[-T_s \hat{f}(\hat{X}_{k|k}) + \Delta X_{d_k} - Ks_{k+1}\right], \tag{2.67}$$

where Ks_{k+1} is the SVSF gain (Please note that nomenclature for many of the terms are define in the accompanying paper; further details of their derivations are deferred to the appended paper E). The SMCF and SSMCF are original contributions pertaining to this thesis.

2.5 The Kalman Fitler and Extended Kalman Filter (EKF)

In one of the appended papers, the performance of the SVSF is compared to the state estimation characteristics of the EKF. This section will briefly describe how the Kalman filter and its extension to nonlinear systems, i.e. the Extended Kalman Filter, work. A detailed rigorous derivation of the equations is available in the many excellent references on the subject [26].

Consider an uncertain **linear** plant (as shown in Figure 2-12) whose discrete model was described by Eqs. (2.44) and (2.45). Since there exist unknown uncertainties, W_k and V_k, the noiseless estimate model of Eqs. (2.30) and (2.31) is also the only available model that can be used to estimate the states. Define a gain KF_k, (known as the Kalman gain) to estimate and refine the states, such that:

$$\hat{X}_{k|k} = \hat{X}_{k|k-1} + KF_k \cdot e_{zf\,k|k-1}, \tag{2.68}$$

where $e_{zf\,k|k-1} = H(X_{a\,k} - \hat{X}_{k|k-1})$ is the estimate output errors as defined in the Eq. (2.36), $\hat{X}_{k|k-1}$ is the unrefined estimate of the states and $\hat{X}_{k|k}$ the refined estimate. Note the similarity to the form of the VSF in Eq. (2.37).

The objective of the estimation process is to use a gain, KF_k to compensate the unrefined states $\hat{X}_{k|k-1}$ and to obtain the refined states $\hat{X}_{k|k}$ as shown in Eq. (2.68) and illustrated in Figure 2-15. The Kalman gain, KF_k, is derived by first substituting Eq. (2.68) into the state equations, and then determining the mean squared error between the estimated and actual state errors The resulting expression contains covariance matrices of

the error and of the system and the plant noise. This expression contains the Kalman gain and is subsequently differentiated with respect to KF_k to find the particular value of KF_k which minimizes the error. Further to the initial assumptions, initial conditions pertain to the Gaussian distribution of noise and uncertainties. KF_k is an "optimized" expression. Using the above procedure, it can be shown that:

$$KF_k = P_{k|k-1}H[HP_{k|k-1}H + R_{k-1}]^{-1}, \tag{2.69}$$

where H is the output matrix, R_{k-1} is the covariance matrix associated with measured noise V_{k-1}, and $P_{k|k-1}$ is the unrefined (or priori) covariance matrix representing the mean-square error matrix. $P_{k|k-1}$ can be calculated from:

$$P_{k|k-1} = \Phi P_{k-1|k-1}\Phi + Q_{k-1}, \tag{2.70}$$

where Φ_k is the system matrix. Q_{k-1} is the covariance matrix associated with system uncertainties W_{k-1}. $P_{k-1|k-1}$ is the refined covariance matrix associated with the mean-square error and is computed as:

$$P_{k-1|k-1} = [I - KF_{k-1}H]P_{k-1|k-2}, \tag{2.71}$$

In this equation, I is the identity matrix, KF_{k-1} is the Kalman gain at the last time step, and $P_{k-1|k-2}$ is the unrefined covariance matrix associated with mean-square error at the last step.

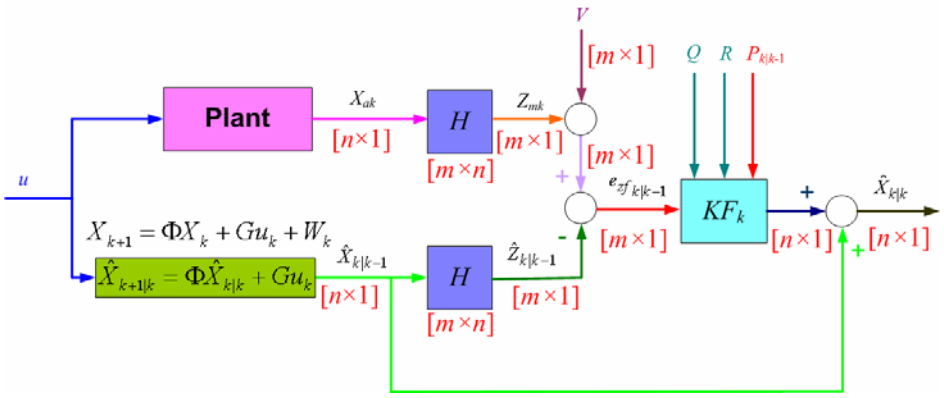

Figure 2-15 Estimation process by Kalman Filter.

(Note that inputs to the filter are the error, and the covariance matrices associated with the mean squared error, the measurement noise and the plant noise.)

From the above equations and Figure 2-15, the Kalman Filter uses the covariance matrices and an predictor-corrector iterative computing method to refine the states in the linear plant which contains system uncertainties and measurement noise. In the Kalman Filter, $P_{k|k-1}$ is used to compensate the estimated output error signal $e_{zf\,k|k-1}$, and Q_{k-1} and R_{k-1} are used to handle the uncertainties and noise. It is noteworthy to see the difference between this approach and the VSF approach which considers the presence of uncertainties as an "add on" to the case with no noise.

For a nonlinear system, such as described by Eqs (2.52) and (2.53), there is a particular challenge in using the Kalman Filter to estimate system states since it was derived assuming a linear system. From Eq. (2.70), in order to calculate the unrefined matrix $P_{k|k-1}$, the system matrix had to be defined as a constant matrix. But for the nonlinear model of Eq. (2.52), the nonlinear function $f(\cdot) = [f_1(\cdot), f_2(\cdot), \cdots, f_n(\cdot)]^T$ precludes defining a constant system matrix. However, if the system is assumed to operate about an operating point, it is a well known approach to approximate the nonlinear function using a Taylor Series approximation, retaining only the first order term. Thus a linear approximation for Eq. (2.52) can be calculated as:

$$\Phi_{k|k} \approx \left. \frac{\partial[\hat{X}_{k|k} + T_s f(\hat{X}_{k|k}) + T_s b(\hat{X}_{k|k}) u_k]}{\partial x} \right|_{x=\hat{x}_{k|k}}, \qquad (2.72))$$

where $\Phi_{k|k}$ is a linearization matrix when $x = \hat{x}_{k|k}$. At the specified operating point, this expression can be assumed constant.

The linear approximation of Eq. (2.72) is substituted into Eq. (2.70) to determine the covariance matrix and to estimate the gain for a nonlinear system. This kind of estimation strategy is called the Extended Kalman Filter (EKF). The EKF uses the same calculation procedure as described by Eqs. (2.68) ~ (2.71) in the Kalman Filter. The only difference is the system matrix in Kalman Filter is replaced by the linear approximation $\Phi_{k|k}$.

Chapter 3

Summary of Manuscripts

In Chapter 2, the basic concepts behind the SMC, VSF, SVSF, SMCF and SSMCF were introduced. This Chapter will consider appropriate papers. In discussing each paper, the same format will be adopted. The objectives of the paper will be defined, the approaches taken to meet the objectives introduced, the results of the studies summarized, the conclusions drawn and finally, the contributions that the paper has made to the area stated. Mathematical details will be included only where necessary. It must be noted that in all cases where states are being estimated, the plant is assumed to be observable, for cases where the plant is to be controlled, the plant is assumed to be observable and controllable. This is a necessary condition.

3.1 "Sliding Mode Controller and Filter applied to an Electrohydraulic Actuator System" (Reference Appendix A)

3.1.1 Objectives

The objective of this paper was to introduce a new integrated control strategy, referred to as a Sliding Mode Controller Filter (SMCF). This controller was applied to a linearized model of a particular hydraulic system, the EHA system (discussed in Chapter 2). It was also an objective to apply the controller to an EHA prototype and to compare the tracking performance of the EHA output states to that of a PID controller.

3.1.2 Approaches

- This paper first proposed combining the Sliding Mode Controller and VSF into one integrated observer-based tracking controller, defined as a Sliding Mode Controller Filter (SMCF). Similar to the operation of a SMC, the SMCF produced two types of control signals, an equivalent signal (based on no noise and no uncertainties) and an error dependent switching signal (inside the boundary layer). An important and original element of this new controller was the fact that the VSF gain was embedded into the controller algorithm.

- A theorem was proposed and verified which established the sufficient conditions for the existence of the discrete sliding mode / filter.
- Since SMC was discontinuous in nature, a “chattering” problem (due to the oscillation of the error signal about the sliding surface) existed in the SMCF. The approach to reduce the chattering caused by the controller and filter was to carefully define realistic boundary layers of the noise and uncertainty for both the SMC and VSF respectively. It was shown that a bypass high frequency loop formed by the SMCF automatically suppressed the chattering of the VSC and VSF individually.
- The stability condition of the SMCF was verified in the Z-domain through a theoretical analysis.
- The SMCF was implemented using only a few simple calculation steps in a predictor-corrector type procedure. The implementation of the SMCF is summarized as six steps.
- To demonstrate the development and use of the SMCF, a linearized model of the EHA was considered and the resulting controller applied to a prototype experimental EHA system. It was known that the EHA system was actually nonlinear. The approach of this paper was to apply the SMCF to this nonlinear system in order to demonstrate its ability to control in a robust sense.
- A PID controller was then applied to the same experimental EHA system and the results were compared to the SMCF.

3.1.3 Results

The VSF was used to estimate system states from only one measured state (position) from the prototype EHA. The controller received the measured and estimated system states from the VSF and subsequently forced the system to follow the desired state trajectories according to the SMCF algorithm. Typical results from applying the SMCF to the control of the prototype EHA are shown in Figure 3-1, Figure 3-2 and Figure 3-3. The estimated states (position, velocity, acceleration) are the dash-dot lines shown in these figures. The measured position resulting from the SMCF is the dashed line shown in Figure 3-1. It is quite evident that the tracking capabilities of the EHA system using the SMCF are excellent for this particular input. In the paper, the first derivative and second derivative of measured position are shown to be very noisy, which demonstrated that the

EHA was a hydraulic plant disturbed by many uncertainties. Thus, these “differentiated” signals could not be fed back to the controller to implement tracking control directly.

The VSF was employed to estimate the velocity and acceleration in the SMCF in Figure 3-1, Figure 3-2 and Figure 3-3, which show the smooth responses of the estimate and actual states, i.e., the SMCF is highly robust for the uncertainty terms in the EHA. In addition, it is noticeable that the high switching action or chattering in the responses are absent in Figure 3-1, Figure 3-2 and Figure 3-3. These results are consistent with other input signal types and frequencies. Although not mentioned in the paper, it should be noted that the tracking error in acceleration tended to grow beyond an input frequency of 10 Hz.

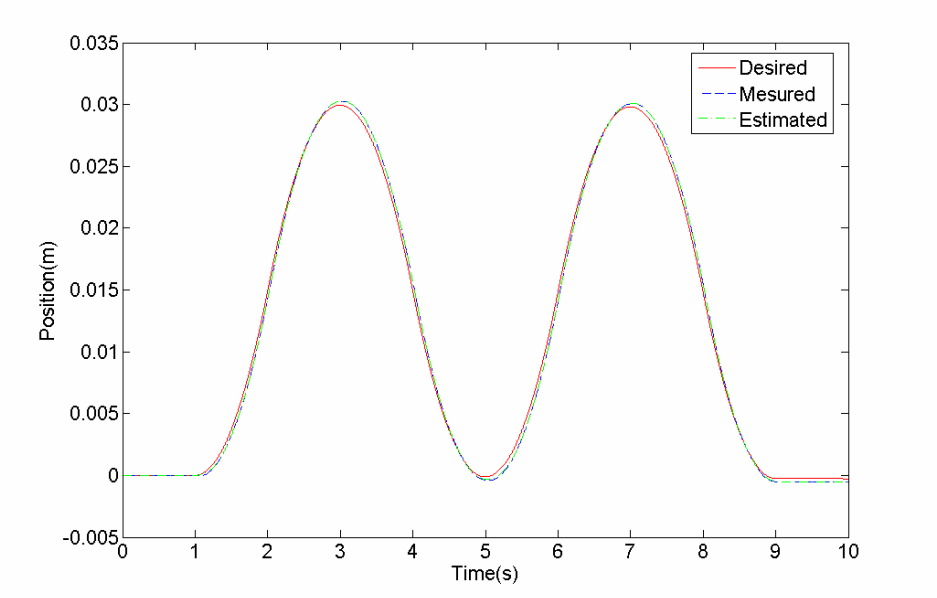

Figure 3-1 The desired, measured and estimated state trajectories associated with position

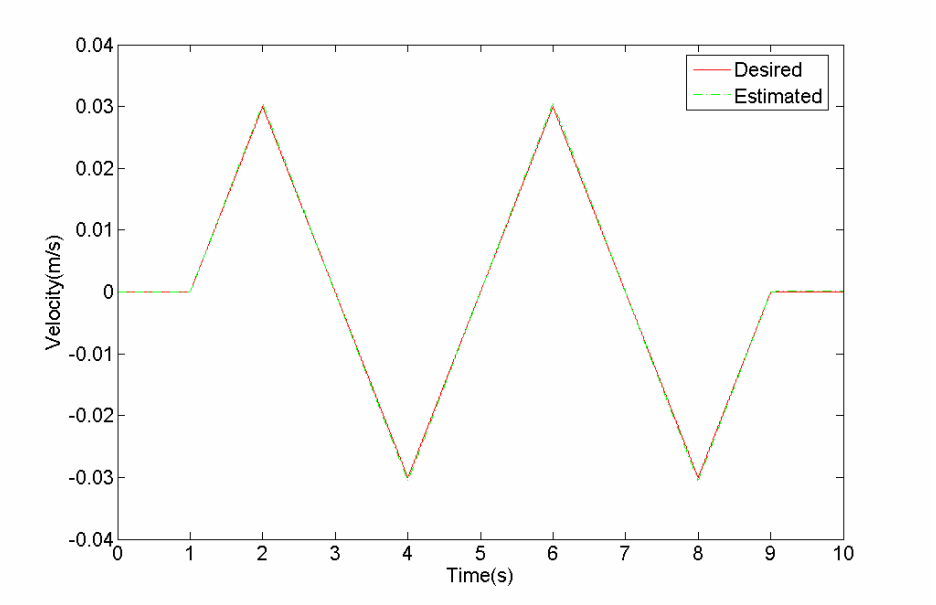

Figure 3-2 The desired and estimated state trajectories associated with velocity

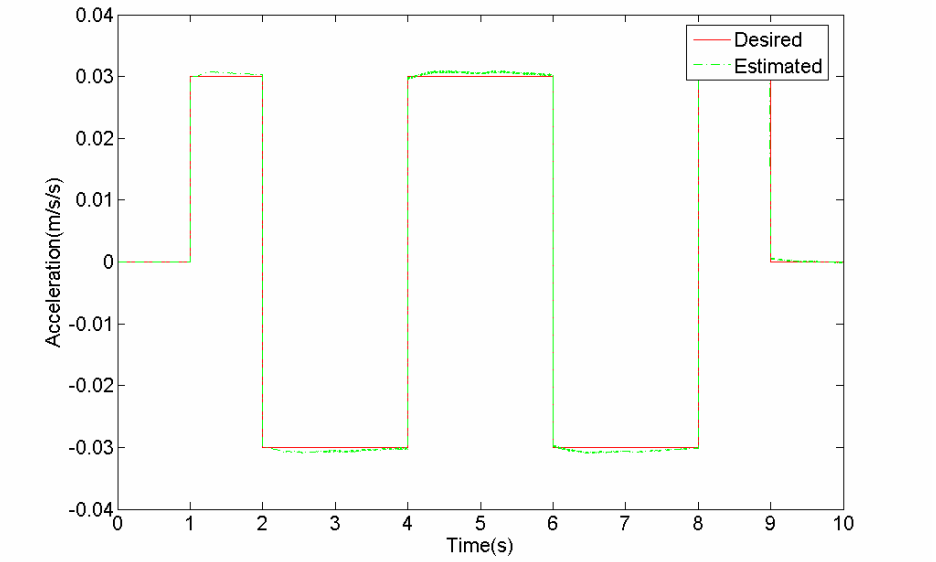

Figure 3-3 The desired and estimated state trajectories associated with acceleration

The EHA system was then controlled using a PID controller. Typical results for the same conditions assumed in Figure 3-1 to Figure 3-3 are shown in Figure 3-4. The velocity and acceleration were obtained using a second order digital filter. It is evident

that the performance is poorer than that of the SMCF. These trends are consistent at other frequencies.

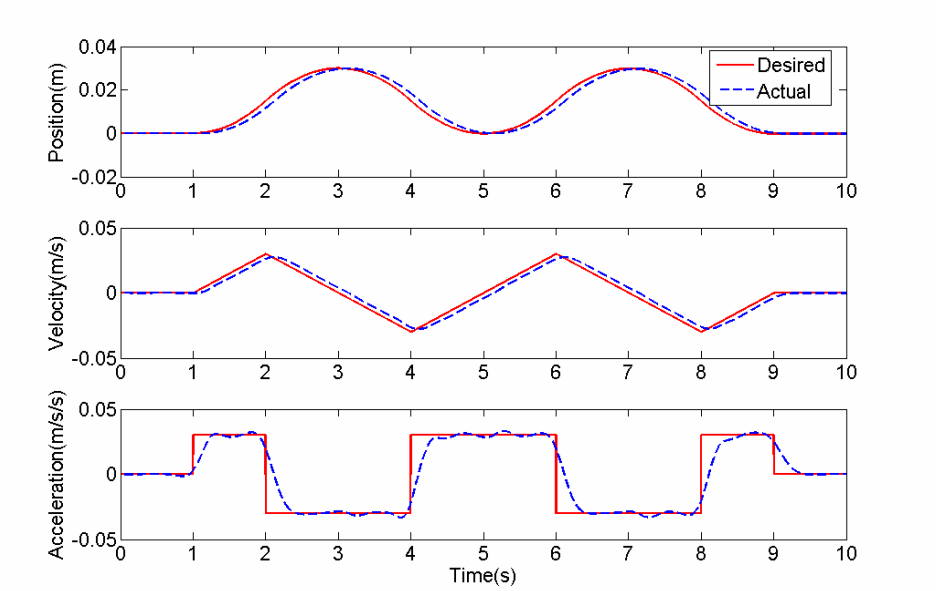

Figure 3-4 Desired and actual states of EHA produced by a PID controller

Other tests which show tacking and estimation errors, Bode plots of the EHA (for PID and SMCF controllers), estimation process of VSF gain, etc., are presented in the paper.

3.1.4 Conclusions and Contributions

It was concluded that, in the presence of bounded parametric uncertainties and noise due to the nonlinearities which exist in the prototype EHA, the SMCF demonstrates a high robustness. The SMCF showed a considerable improvement in performance over a PID type trajectory following controller. In addition, it was concluded that the SMCF effectively suppress the chattering that occurred in both the SMC and VSF.

The unique contribution of this paper is that a novel control strategy, referred to as the SMCF which combines the VSF with the SMC, is proposed. The effectiveness and stability of the SMCF is proven both mathematically and through trial and error tests on the prototype EHA.

3.2 "Sliding Mode Control for an Electrohydraulic Actuator System with Discontinuous Nonlinear Friction" (Reference Appendix B)

3.2.1 Objectives

The objective of this paper was to apply the SMC to both a model of the EHA system and an experimental prototype EHA system which contained uncertainties and showed nonlinear behavioral characteristics, (a consequence of nonlinear friction). It was an objective to use the SMC to overcome the oscillations which occurred as the actuator crossed the zero velocity point. In addition it was an objective to compare the SMC to a controller called a Switched Proportional Controller (SPC) especially developed for the EHA by Sampson et al [6].

3.2.2 Approaches

- It had been established in earlier studies that the friction characteristics of the prototype EHA actuator were very nonlinear displaying slip-stick (static-coulomb) type behavior [9] (see Figure 2-3). A nonlinear model of the EHA system was developed which integrated the nonlinear characteristics in the form of a quadratic function.
- Using this nonlinear model as a basis for the design of the SMC, the SMC was then applied first to a nonlinear model of the EHA. The SMC was then applied to the prototype EHA for comparison purposes. It should be reiterated that the SMC did not require the nonlinearity to be continuous.
- A diffeomorphic transformation matrix T was used to "decompose" the nonlinear model into a linear partition and nonlinear partition. A linear quadratic cost function was defined based on the linear partition. The linear sliding surface coefficients were then determined by solving the discrete Riccati equation (DRE). It was shown that the linear quadratic method could be used to determine the sliding surface for this "discrete" nonlinear problem.
- The boundary layer of the simulated and experimental system was "tuned" manually to better reflect the actual boundary layer conditions.

- A Switched Proportional Controller (SPC), which was developed especially for the EHA by Sampson et al, was then used to control the EHA and the results were compared to the SMC.
- To demonstrate the robustness of the SMC, 20% parametric uncertainty for all coefficients in Eq. (2.3) was injected (by changing the coefficient values 20% in the SMC plant model). The resulting SMC was then applied to the prototype EHA.

3.2.3 Results

The SPC and the SMC were derived and applied to both the simulated and prototype EHA. For the same periodic input signals, the displacement, velocity and acceleration of the simulated EHA for the SPC and SMC are shown in Figure 3-5 and 3-6. It is observed that there are visible transients in the output response of the EHA at the zero velocity cross over points or the maximum position points (such as at time 0, 2, 4, 6 seconds) using the SPC (Figure 3-5). These coincide with regions where the discontinuity in friction occurs. In contrast, observation of Figure 3-6 shows that the oscillations are not present using the SMC.

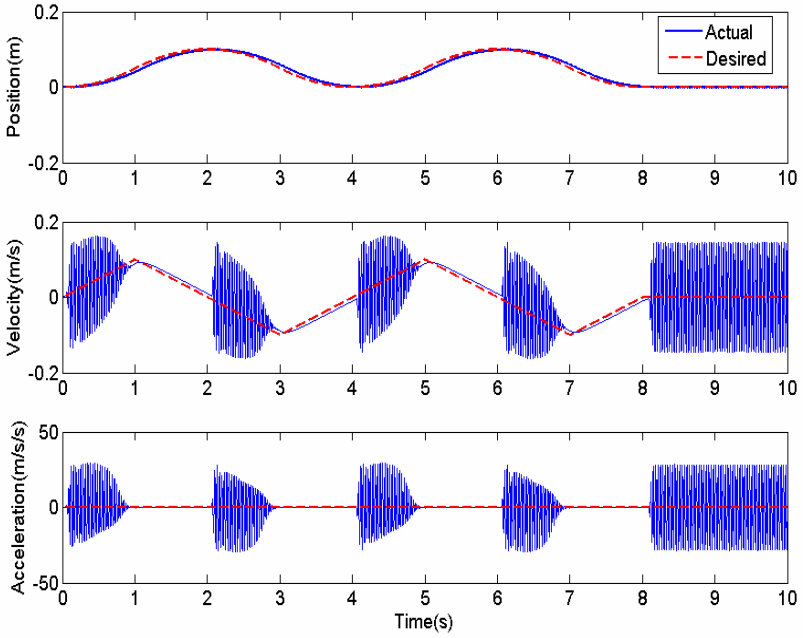

Figure 3-5 Periodic Input Response of SPC (Simulation)

It should be noted that the acceleration plot in Figure 3-5 is in the form of a square wave but the dominance of the oscillations at zero velocity cross-over “dwarf” the results.

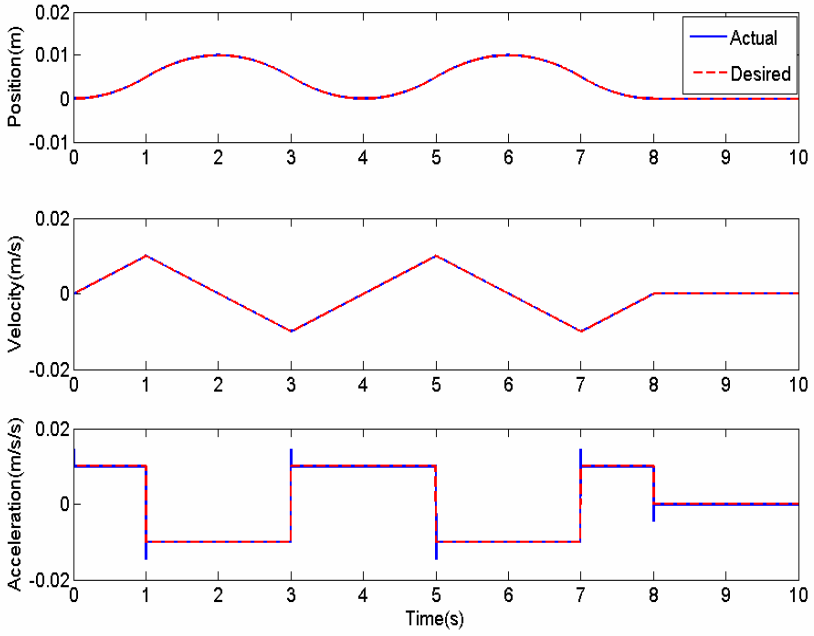

Figure 3-6 Periodic Input Response of SMC (Simulation).

Results for the SPC and SMC when applied to the experimental system show the same trends. These are presented in greater detail in the paper and are not reproduced here because the simulated results demonstrate the cross over problem more clearly. In the paper, the responses for a step input to the system which contained the SMC and SPC are presented and, demonstrate the oscillation problem caused by the nonlinear friction. Other results that are presented include the experimental responses with injected parametric uncertainties showing the robustness of the SMC. These results indicate that the SMC is indeed robust in the presence of parameter uncertainties compared to the

SPC. The maximum errors from the simulation and experiment are also presented to quantify the results.

3.2.4 Conclusions and Contributions

This paper concluded that the Sliding Mode Controller showed little sensitivity to the presence of discontinuous friction and indeed, was instrumental in reducing the oscillations which occurred at the zero velocity crossing points. This was not the case for the SPC. It was also concluded that the VSC demonstrated robustness and performance benefits.

A contribution of this paper is that for the first time, a SMC has been derived and applied to a nonlinear system (simulated and experimental) which displays a slip-stick characteristic in friction. Although not expanded upon in this section, another contribution of the paper is the first application of the "linear quadratic method" to a discrete nonlinear system for the determination of the switching hyperplane.

3.3 "A Smooth Variable Structure Filter for State Estimation" (Reference Appendix C)

3.3.1 Objectives

It was the objective of this paper to review a parameter estimation strategy called a "Smooth Variable Structure Filter (SVSF)", which was based on the SMC. The SVSF was implemented for state estimation of nonlinear systems with uncertainties. To obtain a better estimation performance, it was also an objective to "revise" the estimate gain of the SVSF to decrease the effect of the differential calculation of the noise signal. Another objective was to apply the SVSF to a nonlinear system model displaying discontinuous friction characteristics. The nonlinear model of the EHA system was used as a numerical example. The last objective was to show how the SVSF performed in the presence of large uncertainties in the EHA model.

3.3.2 Approaches

- This paper first introduced type of nonlinearity that has been identified in the application of interest, i.e. the EHA system. For this system the signum function was normally used to describe the discontinuous nonlinear properties. However, this function is not smooth or continuous differentiable and thus the SVSF introduced in other papers, could not be used in the state estimation problem. In order to "smooth" the signum function, the hyperbolic tangent function was chosen to approximate it i.e. $\tanh \lambda x$. The hyperbolic tangent can be differentiated continuously, and is defined as

$$\tanh x = \frac{\sinh x}{\cosh x} = \frac{e^{x} - e^{-x}}{e^{x} + e^{-x}} . \tag{3.1}$$

where sinh and cosh are hyperbolic sine and hyperbolic cosine functions.

- To illustrate the complex mathematics used in the SVSF, the estimation of the SVSF was divided into two processes: the SVSF estimation and the SVSF prediction. Note the "prediction" of the states for the next iteration can be made because a dynamic model of the plant allows a forward projection to be made mathematically.
- In the SVSF estimation, the estimation process is summarized as a 4-steps iteration calculation.
- In the SVSF predication, the transformation matrix $T = [I_n]$ was used to partition the nonlinear model into two parts: measured and unavailable states parts. The inverse function theory was used in different ways to calculate the SVSF gain.
- For the unavailable states parts in the SVSF predication, the calculation of the SVSF gain was derived from the differential of the previous states in the states vector. In order to alleviate the noise magnified by the differential action, an adjusted gain, sampling time T_s , was used to "revise" the SVSF gain and thus the new control algorithm has been renamed "the SVSF with revised gain".
- The stability and reaching conditions of the SVSF with revised gain were proved by a Lyapunov function by using the mathematical identity:

$$\left| e_{zf_{k+1|k+1}} \right|_{ABS} < \left| e_{zf_{k|k}} \right|_{ABS} \tag{3.2}$$

where e_{zf} is estimate output error defined before. This stability condition implied that

the error in state estimation for each step was reduced which meant that the estimated states moved closer to the desired trajectory, i.e., the actual system states.

- The SVSF was used to estimate the states of the EHA with the mathematical approximation of the Signum function. Large parameter uncertainties (20%) were also introduced into the model to illustrate the SVSF robustness (which is similar to the approaches discussed in Section 3.2.2 and paper #2.

3.3.3 Results

The EHA model with the smoothed approximation in the slip stick friction characteristics was applied to the EHA model with the quadratic friction form and was used to illustrate the capability of the SVSF in the presence of uncertainties. In this study, it was assumed that the uncertain parameters were known within 20%. As such, the parameters were changed by 20% in the model and the state estimation capabilities examined. For this case, the three plant and SVSF estimated states (position, velocity and acceleration) are shown in Figure 3-7. The estimated states follow and converge rapidly to the actual states as shown in Figure 3-7. The "filtered error" (the difference between the actual states and estimated states by the SVSF) and the "Non-filtered error" (the difference between actual states and the states directly calculated from the mathematical model without noise and without the SVSF) are shown in Figure 3-8.

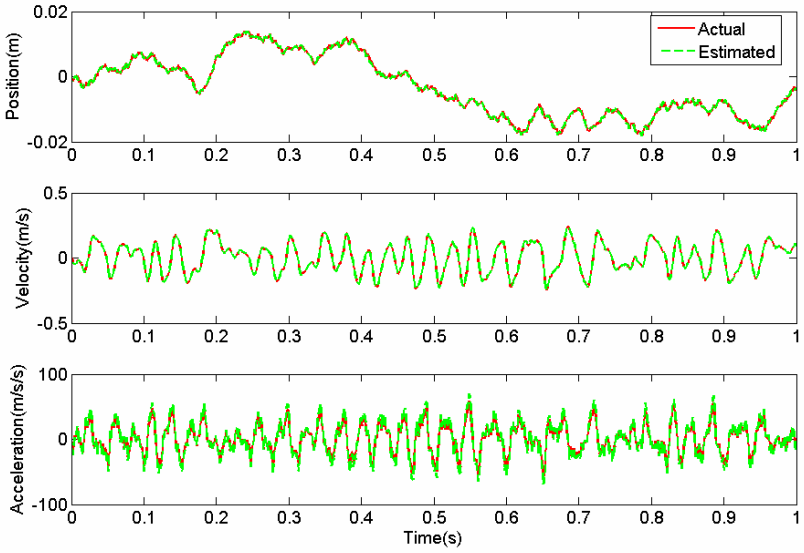

Figure 3-7 Actual and estimated states by SVSF for a model with uncertainties

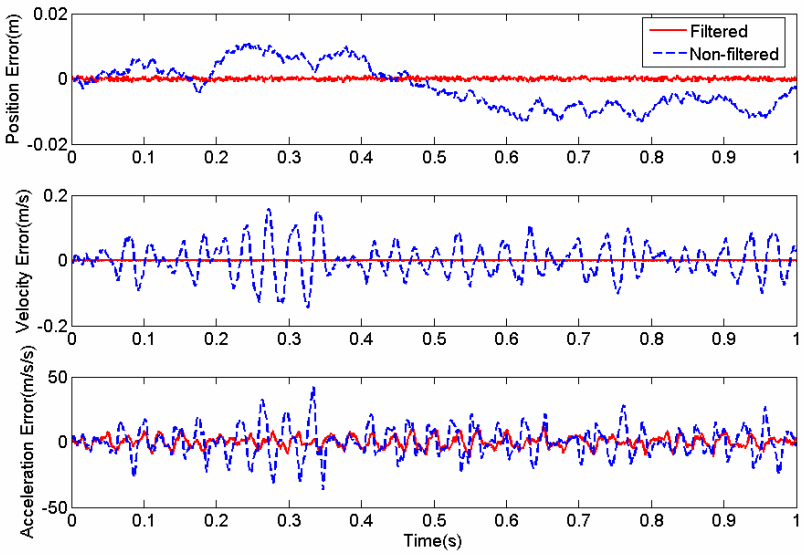

Figure 3-8 State estimation errors by SVSF and Non-filtered errors for a model with uncertainties

The paper presents the estimation states and errors for the EHA model where parametric uncertainties are not present. A very small "filtered error" in these results demonstrates that the SVSF can provide effective and very accurate state estimations.

3.3.4 Conclusions and Contributions

It was concluded that the SVSF with revised gain produces an accurate and effective state estimation. This paper also concludes that the SVSF demonstrates excellent robustness to system noise, measured noise and parameter variations.

The first contribution of this paper was the first application of the SVSF for state estimation. The second contribution was that the paper introduced a revised form of the SVSF gain and presented the stability conditions for it. Another contribution is that a mathematical approximation to models which contain "sign function" type discontinuities can extend the SVSF's application.

3.4 “A Comparative Study of a Smooth Variable Structure Filter and the Extended Kalman Filter” (Reference Appendix D)

3.4.1 Objectives

The objective of this paper was to compare the state estimation performance of the SVSF with the Extended Kalman Filter (EKF) for a nonlinear model of the EHA system which contained uncertainties and noise.

3.4.2 Approaches

- The basic approach of this paper was to use a computer simulation study to illustrate how two filters (the EKF and SVSF) perform when applied to a nonlinear model of the EHA (with nonlinear friction).
- Both the “revised” SVSF (as discussed in Section 3.3.2) and the Extended Kalman Filter (EKF) were introduced and the required equations presented. Both the SVSF and EKF used a predictor-corrector calculation method.
- The SVSF and the EKF were applied to estimate the states of a nonlinear model of the EHA system.
- The EKF used the error covariance matrix (a measure of the estimated accuracy of the state estimates) and a linearized model of the EHA to implement (optimal) estimate of states or parameters.
- The estimation process of the SVSF was based on the nonlinear model of the EHA and a series of transformations were used to calculate the “revised” SVSF gain (see Section 3.3.2).
- As was the case in several of the other papers, large parameter uncertainties (15%) were introduced into the model and used in the estimation process of both the EKF and SVSF in order to compare the robustness of these two methods.

3.4.3 Results

Figure 3-9 and 3-10 show the EKF and SVSF estimate errors for acceleration during the transient conditions (0-0.02s) and steady-state (0.3-0.7s) when the nonlinear model of the EHA was used. The SVSF showed a much faster estimation in the transient state than

the EKF does. Under steady state conditions the SVSF estimation error is significantly smaller than the EKF estimation error.

In this paper, the actual (output from the plant with uncertainties), and “Non-filtered” (output from the model without noise and without the SVSF) states are also illustrated. The estimated states from both the EKF and SVSF were compared with the “Non-filtered” ones in the paper, which showed that both the EKF and SVSF can achieve good performance in state estimation. This can be observed from Figure 3-9 and 3.10, in which the SVSF demonstrates better estimations compared to the EKF for both the transient and steady-state conditions for the EHA system examined. When the nonlinear model was injected with 15% parameter variations, the results using the SVSF also demonstrated a better estimation performance than the EKF did.

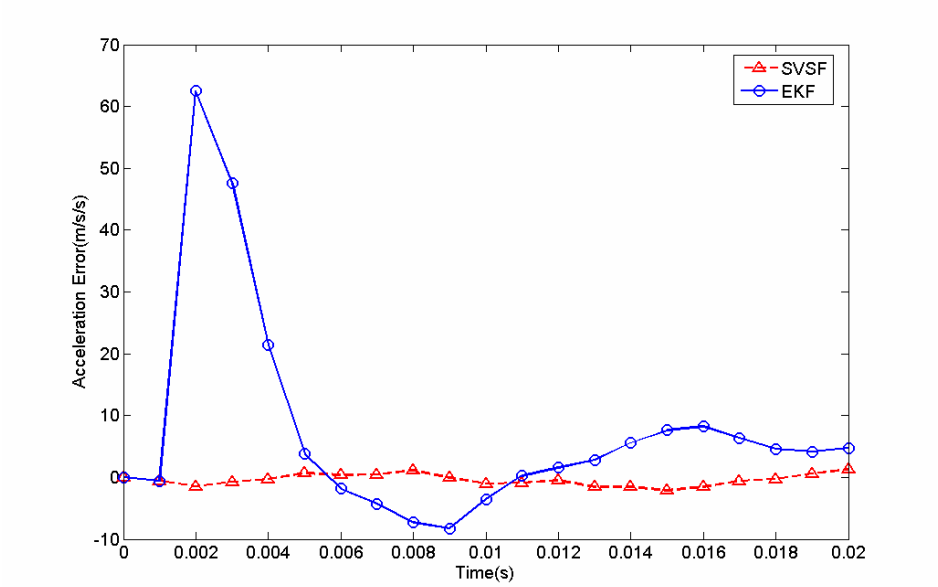

Figure 3-9 Transient state estimation acceleration errors by the SVSF and the EKF (from 0.00s~0.02s)

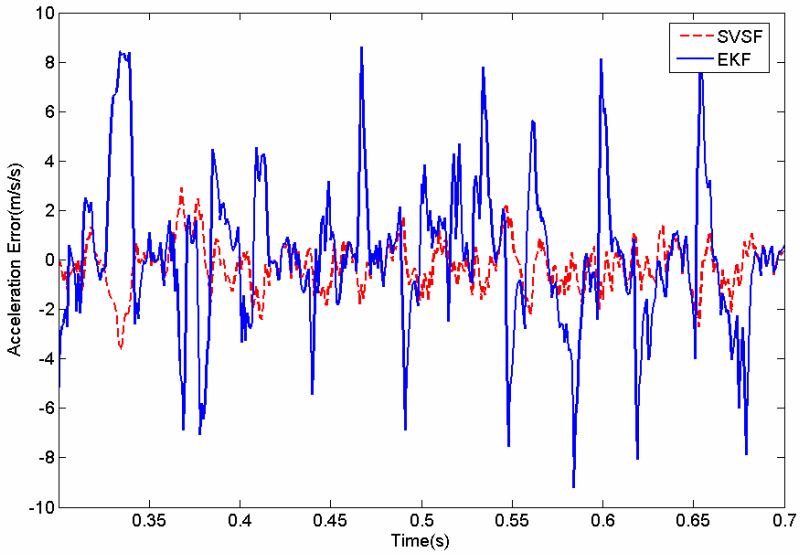

Figure 3-10 Steady state estimation acceleration errors by SVSF and the EKF (from 0.3s~0.7s)

3.4.4 Conclusions and Contributions

It was concluded in this paper that the SVSF can demonstrate a higher convergent estimation rate than the EKF for this particular example because of the Variable Structure Control (VSC) nature of the SVSF. It was also concluded the SVSF can improve the estimation accuracy significantly under steady state considerations compared to the EKF (again, for the system considered in the paper). A third conclusion was that the SVSF can demonstrate a higher robust property than the EKF when uncertainties were included into the EHA nonlinear model. However, it must be emphasized that these results could not be generalized to a broader range of applications at this point.

The contribution of the paper was that the study demonstrated the potential of the SVSF to obtain a higher accurate state estimation for full-feedback control for a particular system, the EHA, than could be accomplished using the EKF.

3.5 "Smooth Sliding Mode Controller and Filter (SSMCF)" (Reference Appendix E)

3.5.1 Objectives

It was the objective of the paper to present the SMC and SVSF as an "integrated" tracking controller for a class of nonlinear systems (as defined by Eq. (2.50)). This integrated control strategy was defined as the Smooth Sliding Mode Controller and Filter (SSMCF). Another objective was to experimentally and mathematically verify the effectiveness, stability and robustness of SSMCF on the EHA system.

3.5.2 Approaches

- The control law of the SSMCF was derived using discrete-time Lyapunov stability theory to make the tracking errors or switching function approach the reaching conditions. The following steps were followed in developing the equations for the controller.
- A sliding surface was defined:

$$\hat{S}_k = \hat{S}(e_{c\,k}) = 0\,, \tag{3.3}$$

where $e_{c_k} = X_{d_k} - \hat{X}_{k|k}$, X_{d_k} is the desired trajectory, and $\hat{X}_{k|k}$ is the estimated states.

- A Lyapunov function was chosen to be:

$$V_k = \hat{S}_k^2\,, \tag{3.4}$$

where the sliding surface $\hat{S} = 0$ was attractive (achieved the reaching conditions) if

$$V_{k+1} < V_k \Rightarrow \hat{S}_{k+1}^2 < \hat{S}_k^2 \quad \forall k \geq 0\,, \tag{3.5}$$

where k is the time step, and V is the Lyapunov function, and $\hat{S}$ is the switching function. This condition means that for time steps $k \geq 0$, if the values of the Lyapunov function (i.e. square of the switching function) decrease for every step, the tracking error will also decrease and hence satisfy the reaching condition as defined in Eqs. (2.8) and (2.9).

- An integrated control law was divided into two parts: equivalent control and switching control. The derivation of the SSMCF was implemented by substituting the

definition of the sliding surface (Eq. (3.3)), the nonlinear model equations (in the paper), and upper limits of uncertainties, into the condition of Eq. (3.5). The SVSF gain term is embedded in the control law (a discontinuous control signal), but can be smoothed by the boundary layers for the SMC and SVSF individually.

- The stability of the SSMCF was established using an "integration" of three processes: the Estimation Process (EP), the Control Process (CP), and the Integrated Process (IP). In the development of these three processes, three different types of errors were introduced: the EP error ($e_{f\,k|k} = X_k - \hat{X}_{k|k}$), the CP error ($e_{c\,k} = X_{d\,k} - \hat{X}_{k|k}$), and the IP error ($e_{w\,k} = X_{d\,k} - X_k$) where X_k, $\hat{X}_{k|k}$, $X_{d\,k}$ are actual, estimated and desired states respectively. The stability for each of these three processes were considered individually and it was shown that all satisfied the required stability condition such that:

$$\left|e_k\right|_{ABS} < \left|e_{k+1}\right|_{ABS} \tag{3.6}$$

where *e* represents these three errors. This condition meant that the error in every process was reduced as the time step increased and the actual states were forced to approach the desired states.

- The SSMCF was applied to a prototype EHA in which zero and 20% parameter uncertainties were injected into the nonlinear model (used by the controller). All these tests were oriented towards verifying the robustness and stability of the SSMCF.

3.5.3 Results

In the experimental tests, the desired trajectories of position, velocity and acceleration were in a periodic form, as shown in Figure 3-11. For the position plot, the actual, the measured and the estimated EHA positions are shown in Figure 3-11. It is observed that the output states of the plant follow the desired trajectory effectively. The estimated states shown as dash-dot lines in Figure 3-11 also track the desired states very well which imply that the estimation is very accurate and stable. Figure 3-12 show the error signals, e_c (for the Control Process (CP)) and e_f (for the Integrated Process (IP)) separately. The results show that the SSMCF provided a effective tracking control and stability. The paper also showed the experimental responses which result when 20% parameter uncertainties were

introduced. These results indicate that the SSMCF can force the actual states to track the desired trajectories very well. The only difference is that the CP and IP errors increased compared to the errors which occurred under conditions without parameter uncertainties (see Figure 3-12).

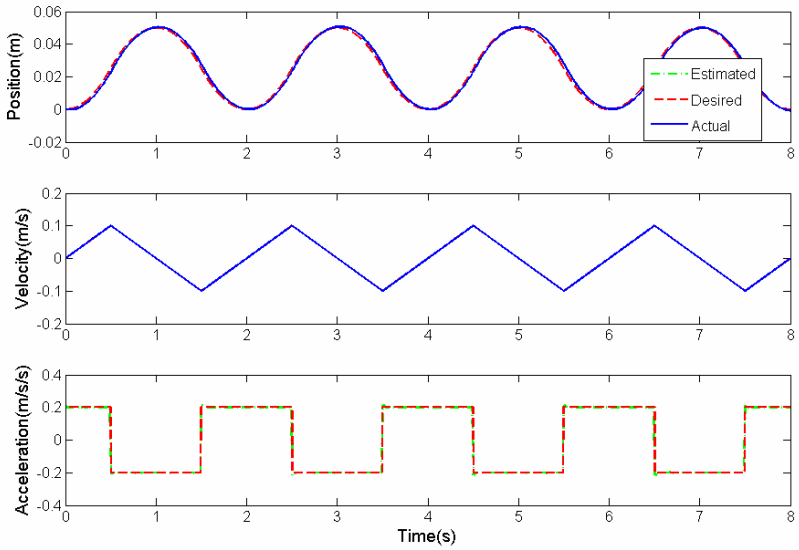

Figure 3-11 The estimated, actual and desired states of the EHA with the SSMCF

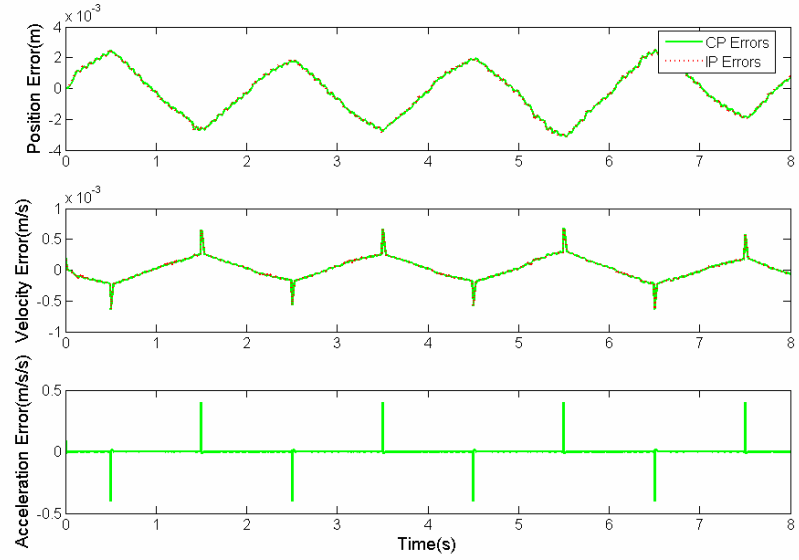

Figure 3-12 The CP and IP Errors of the EHA with the SSMCF

3.5.4 Conclusions and Contributions

It was concluded that the SSMCF can be used on a class of nonlinear systems defined by Eq. (2.50) to provide a robust and high performance state estimation and trajectory tracking control given modeling uncertainties. The paper also concludes that the stability of the SSMCF is guaranteed given bounded uncertainties.

The significant contribution of this paper is the introduction of a novel combined control and estimation strategy (SSMCF) for a special class of nonlinear systems.

Chapter 4

Conclusions, Key Results and Contributions

In this dissertation, the basic principles and concepts associated with the VSC, the VSF, the SVSF, the SMCF and the SSMCF used in the research work were introduced using a number of block diagrams and basic equations. Five Journal papers that have been submitted for review were summarized with respect to the objectives, approaches, results, conclusions and research contributions. The overall objective of the research work was to introduce novel integrated full feed-back control strategies, which included tracking control and state estimation, for a stochastic system. A particular hydraulic positioning system defined as the EHA was used in all papers as the "Plant to be controlled". This research considered a form of discontinuous control (called SMC or VSC), and reviewed, analyzed and augmented a new form of online estimation (VSF, SVSF), Nonlinearities (nonlinear friction in the EHA), and uncertainties (parameter variations, unknown nonlinear terms, and system and measurement noise) were key to the study. The VSF and SVSF were integrated with the VSC to form new controllers called SMCF and SSMCF.

The key conclusions and results of this research are summarized as following.

1. It is concluded that a novel control strategy, referred to as the SMCF can be obtained by the combination of the VSF and the SMC in a "seamless" fashion in order to control a linear or piece-wise linear plant. It was also concluded that in the presence of bounded parametric uncertainties and noise (such as that experienced in the prototype EHA), the SMCF demonstrates a high robustness and efficiency in tracking performance. The stability and alleviation of chattering were proven both mathematically and through experimental tests on the prototype EHA.
2. It is concluded that a "linear quadratic method" can be applied to a discrete nonlinear system for the determination of the switching hyperplane for a SMC controller. A discontinuous controller based on the concepts of SMC and which uses this linear quadratic method was applied to a specific nonlinear system (simulated and experimental) called the EHA and demonstrated little sensitivity to the "slip-stick" characteristics associated with friction in the actuator.

3. It is concluded that the “SVSF with revised gain” could obtain robust and fast state estimations of nonlinear systems. The study revealed that the revised SVSF showed faster estimation rates, higher accuracy and superior robustness than the EKF for the particular system that was considered, namely the EHA system. This conclusion could not be generalized to all systems.
4. Finally, with regards to a nonlinear model of the EHA system, it is concluded that the novel SSMCF can display a robust and high performance state estimation and trajectory tracking control given modeling uncertainties and noise.

The major contributions of the research can summarized as follows:
1) This research has introduced a novel controller/filter called a SMCF, which combines the VSF with the SMC. The SMCF has been applied to a prototype EHA demonstrating the effectiveness and stability of the SMCF.
2) This research has, for the first time, derived a SMC which can be applied to a particular type of nonlinear system to alleviate cross-over oscillations caused by the slip-stick characteristic often associated with friction.
3) This research has applied the SVSF and its “revised” form, for state estimation to a specific application, the EHA.
4) The research has demonstrated that for a particular application, the SVSF can obtain a more accurate and faster convergence rate state estimation for full-feedback control for a particular system than could be obtained using the EKF.
5) This research has introduced a novel combined control and estimation strategy called the SSMCF for a special class of nonlinear systems.

References

[1] Jelali, M., and Kroll, A., 2003, “Hydraulic Servo-systems: Modelling, Identification and Control”, Springer-Verlag London Limited.
[2] Habibi, S. R., Burton, R., and Sampson, E., “High Precision Hydrostatic Actuation Systems for Micro-and-Nano Manipulation of Heavy Loads”, ASME Journal of Dynamic Systems, Measurement and Control, 128(4), pp. 778-787.
[3] Habibi, S., and Goldenberg, A., 1999, Design and analysis of a symmetrical linear actuator for hydraulic systems, Transactions of the CSME, vol. 23, pp. 377–397
[4] Habibi, S. R., and Goldenberg, A., 2000, “Design of A New High-Performance ElectroHydraulic Actuator”, IEEE/ASME Transactions on Mechatronics, 5(2), pp. 158-164.
[5] Habibi, S. R. and Singh, G., 2000, “Derivation of Design Requirements for Optimization of A High Performance Hydrostatic Actuation System”, International Journal of Fluid Power, 2, pp. 11-27.
[6] Sampson, E., Habibi, S., Burton, R., and Chinniah, Y., 2004, “Effect of controller in reducing steady-state error due to flow and force disturbances in the electrohydraulic actuator system”, International Journal of Fluid Power, 5(2), pp. 57-66.
[7] Sampson, E., 2005, “Fuzzy Control of the ElectroHydraulic Actuator”, The M. of S. Thesis, University of Saskatchewan.
[8] Wang, S. Burton, R., and Habibi, S., 2005, “Sliding Mode Controller and Filter applied to A Model of An Electrohydraulic Actuator System”, in ASME Fluid Power Systems and Technology Division Publication – 2005 International Mechanical Engineering Congress and Exposition, Orlando, U.S., no. IMECE2005-80305.
[9] Chinniah, Y. A., 2004, “Fault Detection in the Electrohydraulic Actuator Using Extended Kalman Filter”, Ph.D Dissertation, Dept. of Mechanical Engineering, University of Saskatchewan.
[10] Wang, S., and Habibi, S., and Burton, R., 2006, “Sliding Mode Control for A Model of An Electrohydraulic Actuator System with Discontinuous Nonlinear Friction”, The Proceedings of 2006 American Control Conference, Minneapolis, Minnesota USA, 2006, pp. 5898-5904.
[11] Wang, S., Habibi, S., and Burton R., 2006, “A Smooth Variable Structure Filter for State Estimation”, Journal of Control and Intelligent Systems (Accepted).
[12] Franklin, G. F., Powell, J. D., and Emami-Naeini A., 2002, “Feedback Control of Dynamic Systems”, Prentice Hall, Inc., Upper Saddle River, New Jersy.
[13] Murray-Smith, R., and Johansen, T. A., 1997, “Multiple Model Approaches to Modelling and Control”, Taylor & Francis Ltd.
[14] Wang, S., Burton, R., and Habibi, S., 2006, “Sliding Mode Controller and Filter applied to An Electrohydraulic Actuator System”, ASME Journal of Dynamic Systems, Measurement and Control (under review).
[15] Wang, S., Habibi, S., and Burton, R., 2006, “Sliding Mode Control for an Electrohydraulic Actuator System with Discontinuous Nonlinear Friction”, ASME Journal of Dynamic Systems, Measurement and Control (under review).

[16] Wang, S., Habibi, S., and Burton, R., 2006, “Smooth Sliding Mode Controller and Filter (SSMCF)”, IEEE Transactions on Automatic Control (under review)
[17] Utkin, V. I, 1977, “Variable structure system with sliding modes.” IEEE Transactions on Automatic Control, AC-22, pp. 212-222.
[18] Misawa, E. A., 1997, “Discrete-Time Sliding Mode Control: The Linear Case”, ASME Journal of Dynamic Systems, Measurement, and Control, 119, pp. 819-821.
[19] Slotine, J. –J. E., 1984, “Sliding Controller design for nonlinear Systems”, International Journal of Control, 40, pp. 421-434.
[20] Habibi, S. R. and Burton, R., 2003, “The Variable Structure Filter” ASME Journal of Dynamic Systems, Measurement and Control, 125, pp. 287-293.
[21] Choi, H. and Lim, J. 2005, “Stabilizing a Class of Nonlinear Systems Based on Approximate Feedback Linearization”, IEICE Transactions on Fundamentals of Electronics, Communications and Computer Sciences, E88-A(6), pp. 1626-1630.
[22] Habibi, S. R and Burton, R., 2004, “Parameter identification for a high performance hydrostatic actuation system using the variable structure filter concept”, American Society of Mechanical Engineers, The Fluid Power and Systems Technology Division (Publication) FPST, 11, pp. 93-101.
[23] Wang, S., Habibi, S., and Burton, R., 2006, “A Smooth Variable Structure Filter For State Estimation”, In The 25th IASTED International Conference on Modelling, Identification, and Control, MIC 2006, Lanzarote, Spain, no. 500-172.
[24] Christopher Edwards & Sarah K. Spurgeon, 1998, “Sliding Mode Control: Theory and Applications”, Taylor & Francis Ltd.
[25] Utkin, V. I., 1992, “Sliding Modes in Control Optimization”, Berlin: Springer-Verlag.
[26] Grewal, M. S. and Andrews, A. P., 2001, “Kalman Filtering: Theory and Practice Using MATLAB”, New York: John Wiley.

Copyright Permission

The following papers have been submitted for review. At the time of the publication of this thesis, only the paper "A Smooth Variable Structure Filter for State Estimation" has been accepted for final publication, but contents of the remaining manuscripts will change in accordance to the reviewers' comments and hence will not necessarily be in the same form as appears here. Regardless, permission to include these submitted manuscripts has been sought and responses from the publishers are appended. Where copyright issues have been raised, permission to include in the thesis, the paper has been given.

The permissions by E-mail responses from each publisher are included as follows:

1. The permission for the Appendix A

Date: Thu, 03 Aug 2006 22:07:46 -0500
From: Suhada Jayasuriya <sjayasuriya@tamu.edu>
Reply-To: Suhada Jayasuriya <sjayasuriya@tamu.edu>
Subject: RE: Permission to use the ASME journal paper
To: Shu Wang <shw750@mail.usask.ca>, pli@me.umn.edu

Yes, you may do that as long as you say that the paper is under review or submitted for review. Thanks.

Suhada Jayasuriya
Kotzebue Endowed Professor
Department of Mechanical Engineering
Texas A&M University
College Station, TX 77843-3123
Phone: (979) 845-0271
Fax: (979) 845-3081
Email: sjayasuriya@tamu.edu

-----Original Message-----
From: Shu Wang [mailto:shw750@mail.usask.ca]
Sent: Wednesday, August 02, 2006 12:57 PM
To: pli@me.umn.edu
Cc: Suhada Jayasuriya; Shu Wang
Subject: Permission to use the ASME journal paper

Dear Dr. Li
*I am Shu Wang, the author of paper of "Sliding Mode Controller and Filter Applied to an Electrohydraulic Actuator System" (paper No.: DS-06-1035) in Journal of Dynamic Systems, Measurement and Control.***

I am writing my Ph.D dissertation. Could you give me the permission to add this paper as one of the appendix in the thesis? I will appreciate it very much.
Thanks.

Best regarding,
Shu Wang

2. The permission for the Appendix B

Yes, you may do that as long as you say that the paper is under review for JDSMC or is submitted for review. You may also want to check with your graduate school about the internal requirements. Thanks.

Suhada Jayasuriya
Kotzebue Endowed Professor
Department of Mechanical Engineering
Texas A&M University
College Station, TX 77843-3123
Phone: (979) 845-0271
Fax: (979) 845-3081
Email: sjayasuriya@tamu.edu

-----Original Message-----
From: Shu Wang [mailto:shw750@mail.usask.ca]
Sent: Wednesday, August 02, 2006 2:06 PM
To: gchiu@purdue.edu
Cc: Suhada Jayasuriya; Shu Wang
Subject: Permission to use the ASME journal paper

Dear Dr. Chiu
I am Shu Wang, the author of paper of "Sliding Mode Control for an Electrohydraulic Actuator System (EHA) with Discontinuous Nonlinear Friction" (paper No.: DS-06-1130) in Journal of Dynamic Systems, Measurement and Control.

I am writing my Ph.D dissertation. Could you give me the permission to add this paper as one of the appendices in the thesis? I will appreciate

it very much.
Thanks.

Best regards,
Shu Wang

3. The permission for the Appendix C

Date: Tue, 08 Aug 2006 09:04:24 -0600
From: journals <journals@actapress.com>
Reply-To: journals <journals@actapress.com>
Subject: Paper 201-1831
To: shw750@mail.usask.ca

Dear Shu Wang,

Yes, you can use this paper in your thesis, however, we ask that you refer to it as a submitted paper or as a paper under review, as it has not yet been accepted for publication. If you have any questions, please do not hesitate to contact me. Thanks!

Best Wishes!

Sincerely,

Erin Green
Publisher
ACTA Press/IASTED

4. The permission for the Appendix D

Date: Thu, 03 Aug 2006 09:18:44 -0400
From: Mmm Mecheng <mmm.mecheng@mcgill.ca>
Reply-To: Mmm Mecheng <mmm.mecheng@mcgill.ca>
Subject: RE: Permission to use the CSME Transactions paper
To: Shu Wang <shw750@mail.usask.ca>

Dear Shu Wang,

You have the permission of CSME Transactions. Please specify that the paper is currently under review.

Good luck with your dissertation,
Myrosia

Myrosia Cap
Tel: (514) 398-7201
Fax: (514) 398-7365
-----Original Message-----
From: Shu Wang [mailto:shw750@mail.usask.ca]
Sent: Wednesday, August 02, 2006 5:35 PM
To: Mmm Mecheng
Cc: sassani@mech.ubc.ca; Shu Wang
Subject: Permission to use the CSME Transactions paper

Dear Dr. Cap,
*I am Shu Wang, the author of paper of "A Comparative Study of A Smooth Variable Structure Filter and The Extended Kalman Filter** " (paper No.:*

06-CSME-06) in CSME Transactions. I am writing my Ph.D dissertation. Could you give me the permission to add this paper as one of the appendices in the thesis? I will appreciate it very much.
Thanks.

Best regards,
Shu Wang

5. The permission for the Appendix E

Date: Mon, 20 Nov 2006 11:38:23 -0500
From: "Christos G. Cassandras" <cgc@bu.edu>
Reply-To: "Christos G. Cassandras" <cgc@bu.edu>
Subject: Fwd: Re: 06-334
To: shw750@mail.usask.ca

>>From: shw750@mail.usask.ca
>>Date: Mon, 20 Nov 2006 10:15:53 -0600
>>To: IEEE Transactions on Automatic Control <trac@bu.edu>
>>Cc: habibi@univmail.cis.mcmaster.ca, richard.burton@usak.ca
>>Subject: Re: 06-334
>>X-Originating-IP: 207.16.136.21
*>>X-Score-Level: ** 2.438*
>>Status:
>>Thank you very much. This is the first time I get this letter,
>>probably I there
>>are some problems for my email address.
>>In addition, I still need your permission to append this paper in the my Ph.D
>>thesis. Thanks.

**** Dear Mr. Wang:*
If I understand your question correctly, you wish to include the
manuscript that you submitted to the TAC as part of your PhD thesis.
Since there is no publication decision made as yet, you can of course
use your manuscript as you wish.

Sincerely,

C.G. Cassandras
Editor-in-Chief
****
* *Christos G. Cassandras*
* *Editor-in-Chief,*
* *IEEE Transactions on Automatic Control*
*
****** *Dept. of Manufacturing Engineering*
****** *15 St. Mary's St.*
****** *Boston University*
****** *Brookline, MA 02446*
* ----------
****** *PHONE: (617) 353-7154*
****** *FAX: (617) 353-4830*
* ----------
****** *E-MAIL: cgc@bu.edu*
****** *WWW: http://vita.bu.edu/cgc*
****

Appendix A: Sliding Mode Controller and Filter applied to an Electrohydraulic Actuator (Wang, et al [2006]) *

* This paper is under review by the ASME Journal of Dynamic Systems, Measurement and Control. This paper is included with the express permission of the journal's publishers.

Sliding Mode Controller and Filter Applied to an Electrohydraulic Actuator System

Shu Wang **Richard Burton** **Saeid Habibi**

Department of Mechanical Engineering, University of Saskatchewan
57 Campus Drive, Saskatoon, SK, S7N 5A9 Canada
Phone: 1-306-966-5463 Fax: 1-306-966-5427
shw750@mail.usask.ca

ABSTRACT

A common problem pertaining to linear stochastic systems is the design of a combined robust control and estimation strategy that can effectively deal with noise and uncertainties. The Variable Structure Control (VSC) and its special form of Sliding Mode Control (SMC) show superb robustness with regards to uncertainties, though their performance can be severely degraded by noise. As such they can benefit from using state estimates obtained from filters. In this regard, this paper considers the use of a recently proposed robust state and parameter estimation strategy referred to as the Variable Structure Filter (VSF) in conjunction with SMC. The contribution of this paper is a new strategy that combines Sliding Mode Control with the Variable Structure Filter. In the presence of bounded parametric uncertainties and noise, this combined method guarantees robust stability both in terms of control and state estimation. Furthermore, the combined strategy can be used to achieve high regulation rates or short settling time. The combined VSF and SMC strategy is demonstrated by its application to a high precision hydrostatic system, referred to as the Electrohydraulic Actuator System (EHA).

Keywords: SMCF, Sliding mode control, Variable Structure Filter, Hydraulic

1 INTRODUCTION

It is often an objective to force a plant to follow a prescribe path or state trajectory (referred to as trajectory tracking control). The presence of noise and nonlinearities in the actual plant makes this task very difficult to realize precisely. Trajectory tracking controllers have to estimate the system states and modulate the inputs such that the error between the desired and actual paths is minimized. Trajectory tracking controllers are commonly model-based. They project an estimate of the state by using their internal model and correct this estimate through measurements. Their performance is thus severely affected by the presence of measurement and plant noise, as well as uncertainties in their plant model. The main problem then becomes one of developing an appropriate control strategy which can accommodate noise and uncertainties. In this paper, the Variable Structure System concept that has been proven to be very effective with respect to uncertainties, in its special form of sliding mode control (SMC) is considered. A combined

method consisting of a SMC and a newly proposed filtering concept referred to as the Variable Structure Filter (VSF) is proposed. This combined method is referred to as the Sliding Mode Controller and Filter (SMCF).

The Sliding Mode control (SMC) component of this new strategy requires the specification of several "operational modes". The term operational mode refers to a state of operation with an associated sliding hyperplane (or mode) "*S*". The most common operational modes of SMC are regulation (usually for regulator systems) [1], trajectory following (usually mechanical motion, such as robot manipulator trajectory) [2], model following (usually encountered in the application of optimal control system), [3], and observation (for systems requiring state estimation) [4]. Each mode entails a specific method for the definition of its associated hyperplane, *S*.

The techniques considered in this paper are model based, requiring a plant model. In this case, the plant is represented as a linear stochastic system. Sensor noise is common in stochastic systems and is often attributed to Electromagnetic interference. A second category of noise referred to as system noise is mainly a consequence of the fact that the plant model is not exactly known, or that only an approximation of it is available.

Many studies on modeling plant uncertainties have focused on establishing the "matching conditions" where the uncertainties lie in the "image" of the input matrix [5, 6]. What this really means is that the uncertainties can only affect the plant dynamics through the same channels as the plant's input. To illustrate this, the following definition of a nonlinear model with uncertainties can be used:

$$\dot{X}(t) = [f(x,t) + \Delta f(x,t)] + [B(x,t) + \Delta B(x,t)]u(x,t) + d(t) \quad (1)$$

where Δf and ΔB are system uncertainties, and *d(t)* is an external disturbance. If Δf, ΔB and $d(t)$ lie in the image of *B(x, t)* for all *x* and *t*, they can all be lumped into a single vector function $\Delta D(x,t,d,u)$, such that:

$$\dot{X}(t) = f(x,t) + B(x,t)u(x,t) + B(x,t)\cdot\Delta D(x,t,d,u) \quad (2)$$

Thus, uncertainties in this system will be considered to satisfy the matching condition if the model can be expressed in the form of Eq. (2). Many system uncertainties, however, cannot satisfy this requirement and pose a challenge for control.

Misawa proposed a robust sliding mode controller with uncertainties which did not satisfy the matching conditions [7]. His approach allowed the SMC design for the more general problem of uncertain systems in the stochastic environment.

Central to trajectory tracking control is the requirement for state estimation. An estimator that is commonly used is the Kalman filter, and has been the subject of much research in the past. There are, however, other strategies which have been applied for state and parameter estimation and are called "sliding mode" observers such as proposed in [4, 8, 9]. A new strategy referred to as Variable Structure Filter (VSF) has recently been proposed [10]. The VSF is model-based and can be used for estimating the states of an observable system. The VSF uses concepts closely related to the Variable Structure Control. However similarly to the Kalman Filter, it has a predictor-corrector structure.

In this paper, a new combined sliding mode control and filtering strategy is proposed and is referred to as the Sliding Mode Controller and Filter (SMCF) and represents the original contribution of this research. The SMCF is conceptually robust to noise and system uncertainties. The SMCF approaches the estimation and control problem by separating the filtering and control law into different function blocks, but then can be implemented by several simple iteration calculation steps. This separation facilitates understanding the attributes associated with the system's performance. In addition, the SMCF can handle general uncertainties, i.e. unmatched uncertainties.

The paper is organized as follows. The nomenclature used in this paper is listed in Section 2. The system definition and problem statement is presented in Section 3. Section 4 proposes the Sliding Mode Controller and Filter. Its application to a Hydrostatic system referred to as the Electrohydraulic Actuator (EHA) is provided in Section 5. Comparative analysis and some are given in Section 6 and Section 7. The conclusions are provided in Section 8.

2 NOMENCLATURE

Table 1 provides a listing of all parameters and coefficients.

Table 1 Nomenclature

Symbol	Comments	Dimensions
$\hat{\cdot}$	Denotes uncertain values	
$\lvert\ \rvert_{ABS}$	Absolute value	
$(\cdot)_{\max}$	Subscripts 'max' means upper bound of the variables	

$A,\ B,\ \Delta A\ ,\ \Delta B$	Matrix	
C	Sliding coefficient	1×n
$d, \Delta D$	External disturbance and lumped uncertainties.	
e_c	Control state error	n×1
e_f	State estimation error	n×1
$e_{fz_{k\|k}}, e_{fz_{k\|k-1}}$	Output estimation error calculated by using the a posteriori and a priori output estimates	m×1
f_k, F_k	Vector and its upper bound	n×1
$f, \Delta f$	Nonlinear system function and uncertainties	n×1
$G, \hat{G}$	Input matrix	n×p
G_h	Transfer function	
$H,\ \hat{H}$	Output matrix	m×n
i, j	Subscripts used to identify elements of matrices and vectors	1×1
k	Calculation step index	1×1
Kc	Sliding gain	1×1
K_k	VSF gain	n×1
k_P, k_I, k_D	PID controller gain	1×1
m	Number of measurements	1×1
n	Number of states	1×1
p	Number of inputs	1×1
$S,\ \hat{S}, \hat{S}_f$	Switching function	m×1
sat	Saturation function	
sgn	Sign function	
T_s	Sampling period	
u, u_{eq}	Control input and equivalent	1×1
$v, V_{\max}$	Measurement noise and its upper bound	m×1
$w, W_{\max}$	System noise and its upper bound	n×1
x, x_o	System states and their initial condition	n×1
X, X_d, e_c	States vector and desired state vector and their error vector	n×1
$\hat{X}_{k\|k}, \hat{X}_{k\|k-1}$	A posteriori and a priori state estimates	n×1
Z	Measured output	m×1
$\hat{Z}_{k\|k}, \hat{Z}_{k\|k-1}$	A posteriori and a priori output estimates	m×1
$\delta\ ,\ \hat{\delta}\ ,\ \widetilde{\delta}\ ,\ \xi\ ,\ \hat{\xi}\ ,\ \widetilde{\xi}\ ,\ \widetilde{H}$	Modeling uncertainties	
δ, σ	Arbitrary positive number	1×1
$\Phi, \hat{\Phi}$	System matrix	n×n
γ	Constant diagonal gain matrix with elements $\gamma_{ij} \geq 1$	n×n
ψ, ψ_c, ψ_f	Boundary layer	n×1

3 SYSTEM DEFINITION AND PROBLEM STATEMENT

Consider a discrete-time mathematical model of the plant given as,

$$X_{k+1} = \Phi X_k + G u_k + w_k .$$

$$Z_k = H X_k + v_k , \tag{3}$$

where the matrix pair (Φ, G) is controllable.

In trajectory following problems, the sliding surface is defined in terms of the error rather than the state as is the case in regulation control. Assume that the control problem is for the state vector X to follow a prescribed trajectory X_d. Let:

$$X_{d_k}(k) = [x_{d_k}, \dot{x}_{d_k}, \cdots, x_{d_k}^{(n-1)}] . \tag{4}$$

The sliding hyperplane is defined by using the desired and actual state trajectories as follows.

Definition 3.1: Defining the sliding hyperplane to be:

$$S_k = C e_{c_k} = 0 , \tag{5}$$

where $e_{c_k} = X_{d_k} - X_k$, $S(k) = C e_c(k)$ is referred to as the switching function, and C is a real-valued constant vector such that the product $CG \neq 0$, where G is the input matrix as defined in Eq. (3).

The objective of the controller is to force the states onto the sliding hyperplane as shown in Fig. 1 for the case of a second order sliding surface. If $S(k) = 0$, then all states are on the surface and follow exactly the desired path.

A "reaching condition" (a condition which guarantees that the states will reach $S = 0$) can be stated as [11], [12]:

$$S_i \dot{S}_i < 0 \quad \mathrm{i} = 1, \cdots, \mathrm{m} . \tag{6}$$

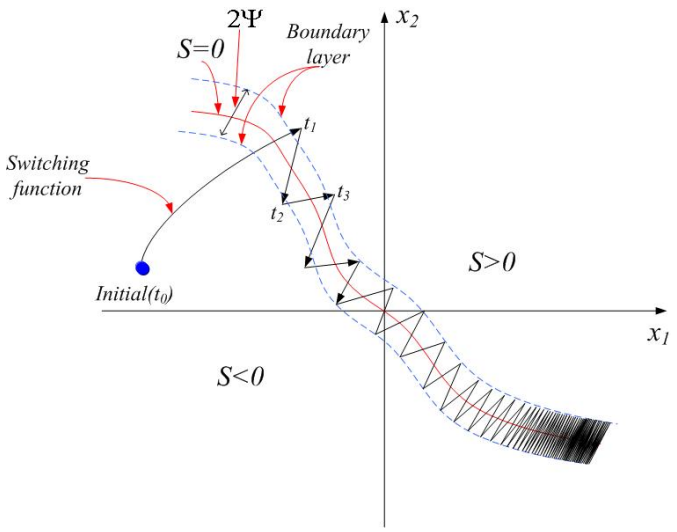

Fig. 1 Sliding mode of discrete-time second order systems

Corollary 3.1: For the discrete-time system, the pseudo-sliding mode (the discrete version of the continuous sliding surface) is said to exist if the following condition is satisfied:

$$\nabla S_k S_k < 0 \ , \tag{7}$$

where $\nabla S_k = S_{k+1} - S_k$.

Another sufficient but not necessary condition can also be defined as [13]:

$$|S_{k+1}| < |S_k| \ . \tag{8}$$

In real sliding mode [5], the states chatter and remain within a neighborhood of the sliding hyperplane. This chattering can be removed by using smoothing boundary layers as follows.

Definition 3.2: Let a boundary layer be specified in terms of the distance of the states from the switching hyperplane as:

$$S_{\Psi_k} = \{e_{c_k} \mid\mid S(e_{c_k}) | \leq \Psi, \ \Psi > 0\} \ . \tag{9}$$

Boundary layers are essential for implementation of sliding mode strategies in real applications as described in the following section.

4 SLIDING MODE CONTROLLER AND FILTER (SMCF)

Using the concepts and the definitions presented in Section 3, it is now possible to introduce the SMCF structure. Consider Fig. 2. From the actual plant, only some of the outputs may be physically measured, and those that can, may contain measurement uncertainties. These outputs are fed into the Variable Structure Filter to extract and estimate the full set of internal states of the system. If the estimated states follow the

actual plant states to within acceptable boundaries, then these states may be integrated into a trajectory following Sliding Mode Controller. The Sliding mode controller uses the estimated states and the reference input *r* to produce a discontinuous control signal to attain trajectory following.

Sliding mode control has an inherent switching action as shown in Fig. 1. This switching and discontinuous control action can lead to a phenomenon known as chattering. This problem is addressed in the SMCF through the introduction of a boundary layer [14]. Inside the boundary layer, the control input is interpolated into a continuous approximated form. In addition, since the VSF is a special form of Observer chattering can be further alleviated by a bypass high frequency loop, which is formed by SMC and VSF shown in Fig. 2 [15].

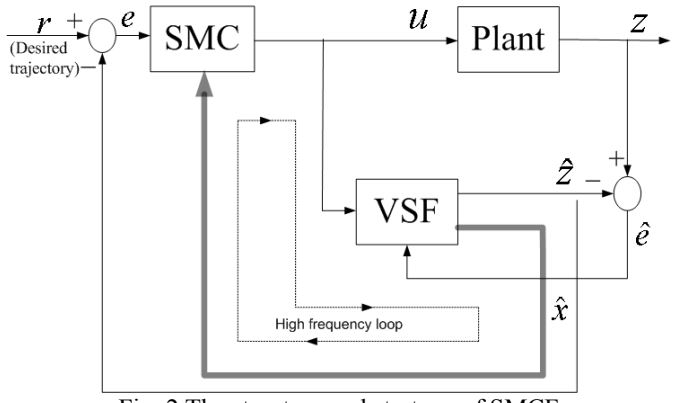

Fig. 2 The structure and strategy of SMCF

Consider a system which is described by a discrete-time linear time-invariant model as specified in Eq. (3). In practice, the matrices Φ, *G*, *H* are not exactly known, and the system may be written assuming unmatched modeling uncertainties as:

$$X_{k+1} = \hat{\Phi} X_k + \hat{G} u_k + w_k \tag{10}$$

$$Z_k = \hat{H} X_k + v_k , \tag{11}$$

where $X = [x_1, x_2, \cdots, x_n]^T$ is the state vector, $Z = [z_1, z_2, \cdots, z_m]^T$ is the measurement vector, ($m \le n$), $u_k \in \Re^{p\times 1}$ is the control input. $w_k \in \Re^{n\times 1}$ and $v_k \in \Re^{m\times 1}$ are random variables representing the system and measurement noise respectively and are both upper bounded. $\hat{\Phi}, \hat{G}$ and $\hat{H}$ are the system, input and output matrices in the known model, respectively. The pair of $(\hat{\Phi}, \hat{G})$ is assumed to be completely

controllable, and the pair of $(\hat{\Phi}, \hat{H})$ is assumed be completely observable. The index k indicates the *k-th* sampling step and sampling period is indicated as T_s. It is for this general system that a controller and an observer are to be designed as follows.

4.1 Sliding Mode Controller

To facilitate the introduction of the definitions for sliding mode control, consider a simple case which is a second order system and where only one control input is involved. The sliding surface $S = 0$ about which the control signal changes, is illustrated graphically in Fig. 1. "Sliding motion" will occur when the system state repeatedly crosses and immediately re-crosses the sliding or switching surface $S = 0$, because all motions in the neighborhood of the surface are directed towards it. For a stable controller, once the states reach the surface, they remain on the surface and are said to be in the "sliding mode".

Based on the uncertain model with unmatched modeling uncertainties as specified in Eqs. (10) and (11), the sliding hyperplane can be defined in the form of (5) as:

$$\hat{S}_k = Ce_{c_k} = 0\,, \tag{12}$$

where $\hat{S}_k$ is a switching function for the uncertain model.

Because of imperfections in controllers such as delays in the switching action, real sliding mode may occur. In real sliding mode, the states would chatter about the switching hyperplane rather than strictly remain on it. This high-frequency chattering effect is synonymous to artificial noise, is highly undesirable, and can excite unmodeled high-frequency plant dynamics. To reduce chattering, the smoothing boundary layer solution [16] is applied to the control law such that: (i) outside the smoothing boundary layer, a discontinuous control action is applied for stability, but (ii) within the layer, the continuous control action is used as a function of the distance of the states from the hyperplane. This means that within the boundary layer, the control action is smooth as opposed to an abrupt bang-bang input. In implementing a boundary layer, the saturation function $sat(\hat{S}, \Psi)$ is used to replace the sign function $\mathrm{sgn}(\hat{S})$ inside of boundary layer, $\hat{S}_k \le \Psi$, such that:

$$sat(\hat{S}, \Psi) = \begin{cases} \mathrm{sgn}(\hat{S}/\Psi), & \text{for } |\hat{S}/\Psi| > 1 \\ \hat{S}/\Psi, & \text{for } |\hat{S}/\Psi| \le 1 \end{cases}. \tag{13}$$

The discrete-time system in the sliding mode involves two control subsystems which is the same as its continuous counterpart: a slow and fast subsystem. The slow subsystem is the system when it is in the sliding mode (i.e. on the *S*=0 surface) yielding "equivalent" control. The equivalent control is the continuous input that results in the ideal condition of sliding mode, i.e.

$$\hat{S}_{k+1} = \hat{S}_k = 0 . \tag{14}$$

The fast subsystem is the high switching control input that prevents the system from leaving the surface.

Consider the ideal system model without uncertainties and system noise:

$$X_{k+1} = \hat{\Phi} X_k + \hat{G} u_k . \tag{15}$$

Substituting (5), (15) into (14), the equivalent control can be determined as:

$$u_{eq_k} = (C\hat{G})^{-1} C(X_{d_{k+1}} - \hat{\Phi} X_k) . \tag{16}$$

Thus, equivalent control can be considered as the perfect control signal that in the absence of noise and uncertainties, would force the error between all the actual and the desired states to zero. However, in the presence of uncertainties, the actual states will oscillate or switch about this ideal condition and hence the equivalent control signal will be augmented by a fast acting switching control signal and as discussed previously, give rise to "chattering". Instead of residing on the surface, the states would remain in a boundary layer neighboring the sliding surface $\hat{S} = 0$, defined as

$$\{e_{c_k} \,||\, \hat{S}_k \,|=| Ce_{c_k} \,| \le \psi_c, \psi_c > 0\} , \tag{17}$$

whose thickness is $2\,\Psi_c$.

Theorem 4.1. For a system with bounded uncertainties, a sufficient condition for the existence of the discrete sliding mode is that there exists a k_0 such that

$$(a). \quad |\hat{S}_{k+1}| < |\hat{S}_k|, \; k \ge k_0 ; \tag{18}$$

$$(b). \quad \hat{S}_k \Delta \hat{S}_k < -\frac{1}{2} \Delta \hat{S}_k^2, \; k \ge k_0 . \tag{19}$$

The above two conditions are equivalent.

Proof: The Lyapunov function is chosen as

$$V_k = \hat{S}_k^2 = (\hat{S}(e_{c_k}))^2 . \tag{20}$$

It has been shown in [17] that the condition $V_{k+1} - V_k < 0$ guarantees the existence of sliding motion, that is:

$$\hat{S}^2{}_{k+1} < \hat{S}_k^2 . \tag{21}$$

Thus, if condition (a) is satisfied, the existence of a sliding mode is guaranteed.

Let $\Delta\hat{S}_k = \hat{S}_{k+1} - \hat{S}_k$, then Eq. (21) may be rewritten as

$$\begin{aligned} &[\hat{S}_{k+1} + \hat{S}_k][\hat{S}_{k+1} - \hat{S}_k] \\ &= \Delta\hat{S}_k[\Delta\hat{S}_k + 2\hat{S}_k] < 0 \end{aligned}, \tag{22}$$

which is equivalent to Eq. (19). Thus, condition (b) is also a sufficient condition for the existence of a sliding mode. Conditions (a) and (b) are equivalent.

Using the existence of Theorem 4.1, the control law is given as [18]:

$$u_k = u_{eq_k} - (C\hat{G})^{-1}\hat{S}_k + (C\hat{G})^{-1}Kc \cdot sat(\hat{S}_k / \psi_c) , \tag{23}$$

where the sliding mode control gain $Kc = (Cw)_{\max} + \Delta$, $\psi_c > (Cw)_{\max} + \sigma$,

$$sat(S_k / \psi_c) = \begin{cases} \hat{S}_k / \psi_c & |\hat{S}_k| \le \psi_c \\ sign(\hat{S}_k / \psi_c) & \text{otherwise} \end{cases},$$

in which $(Cw)_{\max}$ is the upper bound of Cw_k, Δ and σ are arbitrary positive number. It should be noted that *Kc* is chosen as a constant value. The derivation of control law (23) is summarized in APPENDIX A.

4.2 Variable Structure Filter

The function of the variable structure filter is to estimate the states of a system. The VSF uses concepts closely related to VSC. As discussed in reference [15], sliding observers use a constant feedback gain and a discontinuous vector to correct the predicted estimates of the system dynamics. The VSF uses a discontinuous component called a VSF gain, to correct state estimates. The VSF is a predictor-corrector method and its gain formulation K_k is different from other sliding observers as follows.

Consider a linear system with unmatched uncertainties as described in Eqs. (10) and (11). Define an observer switching function of the system

$$\hat{S}_f = e_{fz} = Z_d - \hat{Z} , \tag{24}$$

where $e_{fz} = Z_d - \hat{Z}$ is the estimation error for the output and $e_f = X_d - \hat{X}$ is the estimation error for the states, and $\hat{X}$ and $\hat{Z}$ are estimates of the state and output vectors from the filter. Thus for the output estimation error to be zero, the switching hyperplane equation associated with the filter should be

$$\hat{S}_f = e_{fz} = 0 . \tag{25}$$

This switching hyperplane is identical in concept to that in the VSC. VSF however is a predictor-corrector method and follows a similar calculation process for state estimation as the Kalman filter. Here, the a priori state estimate ($\hat{X}_{k|k-1}$) is obtained from the plant model (albeit uncertain) and is then refined into an a posteriori state estimate ($\hat{X}_{k|k}$) by using a switching function of the output estimation error e_{fz}. Note, a priori estimate can be interpreted as an "unrefined" estimate, and a posteriori as a "refined" estimate. Thus $\hat{X}_{k|k}$ is a combination of $\hat{X}_{k|k-1}$ and a prediction error function defined as the VSF gain. In the VSF, the structure of the gain changes with the error such that:

$$\begin{aligned} K_k &= f(e_{fz}, \mathrm{sgn}(e_{fz}), \widetilde{\Xi}_{\max}, V_{\max}, W_{\max}) \\ &= \begin{cases} K_k^+ = f(e_{fz}, +|\mathrm{sgn}(e_{fz})|, \widetilde{\Xi}_{\max}, V_{\max}, W_{\max}) & e_{fz} > 0 \\ K_k^- = f(e_{fz}, -|\mathrm{sgn}(e_{fz})|, \widetilde{\Xi}_{\max}, V_{\max}, W_{\max}) & e_{fz} < 0 \end{cases} \end{aligned} , \tag{26}$$

where **sgn** is the sign function of e_{fz}, V_{max} and W_{max} are the upper bounds of system noise and measurement noise respectively, and the subscripts max also signifies the upper bound on uncertain dynamics attributed to uncertainties in Φ, G and H , which is $\widetilde{\Xi}_{\max}$.

A block diagram of the model for the VSF estimation process is shown in Fig. 3, where K_k is the VSF gain and is applied to obtain the a posteriori state estimate such that:

$$\hat{X}_{k|k} = \hat{X}_{k|k-1} + K_k , \tag{27}$$

The a priori (or unrefined) output estimate for the next step is predicted by using a model of the plant as:

$$\hat{Z}_{k+1|k} = \hat{H}(\hat{\Phi}\hat{X}_{k|k} + \hat{G}u_k) , \tag{28}$$

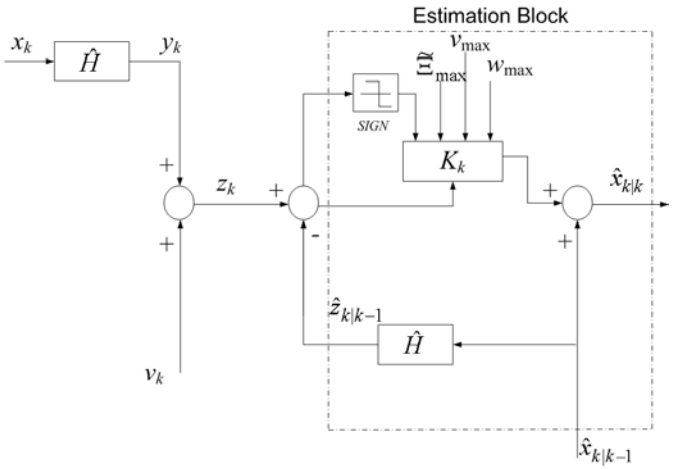

Fig. 3 The model for the estimation phase in VSF

The essential feature of the variable structure filter is the use of the VSF gain K_k. In deriving K_k., a switching hyperplane is used to restrict the estimated states to within a subspace of the actual system states. The VSF gain K_k. can be derived by the asymptotic stability condition, which is based on the existence condition described by Corollary 3.1 for what is termed as the reachability phase when estimated states are forced towards a neighborhood of the actual system states:

$$| e_{fz_{i_{k|k}}} | < | e_{fz_{i_{k|k-1}}} | , \tag{29}$$

where i is the element number of states vector, k and k-1 are the calculation step index.

Condition (29) is sufficient for stability. A further condition that is NOT sufficient for stability, but is instrumental to the derivation of the VSF gain is:

$$e_{fz_{i_{k+1|k}}} \operatorname{sgn}(e_{fz_{i_{k|k-1}}}) < 0 . \tag{30}$$

Making the system noise w_k and measurement noise v_k bounded by V_{max} and W_{max} respectively, then the VSF gain can be obtained as (detailed in APPENDIX B):

$$\begin{aligned} K_k = & \\ & \hat{\Phi}^{-1}\hat{H}^{+}\cdot\{|\hat{H}\hat{\Phi}|_{ABS}\cdot[\mathrm{Y}\cdot|\hat{H}^{+}|_{ABS}\cdot|e_{z_{k|k-1}}|_{ABS}+|\hat{\Phi}^{-1}\hat{H}^{+}\tilde{\xi}_{\max}z_k|_{ABS} \\ & +|\hat{\Phi}^{-1}\hat{H}^{+}|_{ABS}\cdot(|\hat{\xi}+\tilde{\xi}_{\max}|_{ABS}+I)V_{\max}+|\hat{\Phi}^{-1}\hat{H}^{+}\tilde{\delta}_{\max}u_k|_{ABS} \\ & +(|\hat{\Phi}^{-1}|_{ABS}+|\hat{\Phi}^{-1}\hat{H}^{+}\tilde{H}_{\max}|_{ABS})\cdot W_{\max}]\}\cdot\operatorname{sgn}(e_{z_{k|k-1}}) \end{aligned} , \tag{31}$$

where γ is a diagonal matrix with elements $\gamma_{ii} \geq 1$, and the superscript "+" on $\hat{H}$ denotes the pseudo-inverse, $\tilde{\xi}_{\max}, \tilde{\delta}_{\max}$ and $\tilde{H}_{\max}$ are upper bounds on modeling uncertainties of ξ, δ and H, and $\delta = HG,\ \hat{\delta} = \hat{H}\hat{G},\ \tilde{\delta} = \delta - \hat{\delta},\ \xi = H\Phi H^{+},\ \hat{\xi} = \hat{H}\hat{\Phi}\hat{H}^{+},\ \tilde{\xi} = \xi - \hat{\xi},\ \tilde{H} = H - \hat{H}$ [19].

To avoid chattering, from Definition 3.2, a smoothing boundary layer is also used for the VSF as:

$$\begin{aligned} &\{e_{z_{ik}} \ \| \hat{S}_f(k) | = | e_{fz_k} | \leq \psi_{fi}, \\ &where\ \ \psi_f = | \hat{H}\hat{\Phi} |_{ABS} \cdot \{ | \hat{\Phi}^{-1}\hat{H}^{+}\tilde{\xi}_{\max} z_{f\max} |_{ABS} \\ &+ | \hat{\Phi}^{-1}\hat{H}^{+} |_{ABS} \cdot (| \hat{\xi} + \tilde{\xi}_{\max} |_{ABS} + I)V_{\max} + | \hat{\Phi}^{-1}\hat{H}^{+}\tilde{\delta}_{\max} u_{\max} |_{ABS} \\ &+ (| \hat{\Phi}^{-1} |_{ABS} + | \hat{\Phi}^{-1}\hat{H}^{+}\tilde{H}_{\max} |_{ABS}) \cdot W_{\max} \} \end{aligned}, \tag{32}$$

and where $e_{fz_{ik}}$ are the elements of outputs, the elements of ψ_f is $\psi_{fi}(i = 1, \cdots m)$, and $z_{f\max}$ and $u_{\max}$ are the saturation level of the measured signal and the maximum magnitude of the input respectively.

The term of $\mathrm{sgn}(e_{z_{k|k-1}})$ in (31) may be replaced by saturation function as follows:

$$sat(e_{fz_{k|k-1}} / \psi_f) = \begin{cases} e_{fz_{k|k-1}} / \psi_f & | e_{fz_{k|k-1}} | \leq \psi_f \\ sign(e_{fz_{k|k-1}} / \psi_f) & \text{otherwise} \end{cases}. \tag{33}$$

A small boundary layer width in (23) and (33) improves the control and estimation accuracy of the filter.

4.3 Sliding Mode Controller and Filter

Both the SMC and VSF are based on the same basic concept of discontinuous control theory. The Sliding Mode Controller and the Variable Structure Filter are described in earlier Sections and are both derived by using the same definitions and existence conditions, (i.e. Definition 3.1, Definition 3.2 and Corollary 3.1). These allow the SMC and the VSF to be smoothly "fused" together in order to achieve a satisfactory control objective.

The objective is trajectory following control for the uncertain system of Eqs. (10) and (11); this requires full-state feedback. However, in practice not all state variables are measured due to the cost of instrumentation, accuracy, or availability of appropriate transducers. The Variable Structure Filter can be formulated as a full-state observer as presented in Section 4.2. The estimated states by the VSF may be fed back to the sliding mode controller to obtain a discontinuous control signal to drive the plant to follow the

desired state trajectory. Using the a posteriori estimated states to replace the actual states in Eq. (12), the sliding hyperplance of the controller is obtained as:

$$\hat{S}(k) = C[X_{d_k} - \hat{X}_{k|k}] = C[X_{d_k} - \hat{X}_{k|k-1} - K_k] = C(e_{c_{k|k-1}} - K_k) \\ = 0 \quad (34)$$

where K_k is the state estimator (or the VSF) gain and the control error $e_{c_{k/k-1}} = X_{d_{k-1}} - \hat{X}_{k|k-1}$.

Optimal control deals with the problem of finding a control law for a given system such that a certain optimality criterion is achieved. The design criteria for the combined Sliding Mode Controller and Filter (SMCF) are i) driving the systems states to follow the desired states; ii) and considering the size of control "effort". The sliding surface design in SMCF is chosen by using the Linear Quadratic approach that is commonly used in optimal control [20]. In this method, the cost function penalizes the control energy (measured in a quadratic form) and the time it takes the system to reach the desired trajectory. In addition, not all the states X_k for the system are known, but they can be estimated by the VSF, which means that the X_k can be substituted by the a posteriori estimate $\hat{X}_{k|k}$. As such, the cost function is defined as following:

$$J = \sum_{k_{sm}}^{\infty} [e_{c1_{k|k}}^T Q e_{c1_{k|k}} + u_{o_k}^T R u_{o_k}], \quad (35)$$

where u_o is the optimal control signal, Q is the state weighting matrix, and R is the control weighting matrix, such that the states response time and control energy will be kept small by adjusting the Q and R.

Thus the sliding surface definition becomes the design of optimal controller as previously stated in Eq. (35) such that:

$$u_o = F e_{c1_{k|k}} = C_2^{-1} C_1 e_{c1_{k|k}}, \quad (36)$$

where F is the optimal feedback gain derived from the switching function coefficients C_1 and C_2. These coefficients in turn define the sliding surface and are determined by solving a standard Linear Quadratic Regulator (LQR) problem solution to the discrete Algebraic Riccati Equation (ARE). The sliding surface design will inherit the important property of LQR, i.e. guaranteed robustness [21].

Replacing the X_k by $\hat{X}_{k|k}$ in Eq. (23) and substituting Eq. (27) into it, the control law may be obtained as:

$$\begin{aligned} u_k &= u_{eq_k} - (C\hat{G})^{-1} C[X_{d_k} - \hat{X}_{k|k-1} - K_k] \\ &\quad + (C\hat{G})^{-1} Kc \cdot sat(C[X_{d_k} - \hat{X}_{k|k-1} - K_k]/\psi_c) \\ &= u_{eq_k} - (C\hat{G})^{-1} C[e_{c_{k|k-1}} - K_k] + (C\hat{G})^{-1} Kc \cdot sat(C[e_{c_{k|k-1}} - K_k]/\psi_c) \end{aligned}, \quad (37)$$

where the equivalent control is obtained as:

$$u_{eq_k} = (C\hat{G})^{-1} C\{X_{d_{k+1}} - \hat{\Phi}[\hat{X}_{k|k-1} - K_k]\}, \quad (38)$$

and K_k is the VSF gain defined by Eq. (31). The sign and magnitude of K_k is dependent on the estimation error which will affect the system stability as discussed later. Furthermore, The controller's sliding gain *Kc* is chosen as a constant which is a upper bound of the term of (Cw), i.e.

$$Kc = (Cw)_{\max} + \Delta, \quad (39)$$

where Δ is any positive number that affects the controller performance in terms of stability and speed of response as indicated in Appendix A and as follows. The sliding constant *Kc* will make sure the sliding motion is maintained despite system uncertainties. The choice of a bigger value of *Kc* (and thus Δ) will lead to a faster system response faster; however, in the case of real sliding mode that occurs in systems with switching delay, a larger *K*c or Δ leads to excessive control action and chattering. The boundary layer of the controller is chosen as: $\psi_c > (Cw)_{\max} + \sigma$.

where σ is a positive number that relates to the upper bound of system uncertainties.

The design of combined Sliding Mode Controller and Filter (SMCF) can be regarded as a predictor-corrector control strategy, the implementation process of SMCF may be summarized as the following steps:

1. The a priori state estimate $\hat{X}_{k|k-1}$ and the a priori estimates of measurements, $\hat{Z}_{k|k-1}$ may be predicted by using the estimated model as following:

$$\hat{X}_{k|k-1} = \hat{\Phi}\hat{X}_{k-1|k-1} + \hat{G}u_{k-1}, \quad (40)$$

$$\hat{Z}_{k|k-1} = \hat{H}\hat{X}_{k|k-1}. \quad (41)$$

2. A corrective VSF gain $K_k \in \Re^n$ is calculated as a function of the estimate error $e_{fz_{k|k-1}}$ by Eq. (31).

3. The sliding hyperplane and sliding mode control gain *Kc* is calculated and determined based on the VSF gain K_k by Eqs. (34) and (39) respectively.

4. The control input application to the system is obtained as a function of control error signal and VSF gain as indicated in Eqs. (37) and (38).

5. The a priori state estimate is refined into an a posteriori state estimate such that:

$$\hat{X}_{k|k} = \hat{X}_{k|k-1} + K_k \,. \tag{42}$$

6. Steps 1 to 5 are iteratively repeated.

The VSF can be formulated to provide convergence for the estimated the states to the existence boundary subspace in only one sampling interval. This leads to only one time step lag in the estimation errors as shown in Eq. (31). This high convergent rate is independent of the convergence of the controller or the closed-loop system.

Consider a desired trajectory following control system problem in which the system states would track the desired states X_d such that:

$$X_{d_k} = \hat{\Phi} X_{d_{k-1}} + \hat{G} u_{d_{k-1}} \,, \tag{43}$$

where the desired control signal can be chosen as the ideal control, i.e. equivalent control in Sliding Mode Control.

Subtract both sides of Eq. (43) by Eq. (40), yields:

$$e_{c_{k|k}} = \hat{\Phi} e_{c_{k|k-1}} + \hat{G}[u_{eq_{k-1}} - u_{k-1}] \,. \tag{44}$$

Substitute the lag step of Eqs. (31) and (37) into Eq. (44), given as:

$$\begin{aligned} e_{c_{k|k}} &= \hat{\Phi} e_{c_{k|k-1}} + \hat{G}\{u_{eq_{k-1}} - u_{eq_{k-1}} + (C\hat{G})^{-1} C[e_{c_{k-1|k-2}} - K_{k-1}] \\ &\quad - (C\hat{G})^{-1} Kc \cdot sat(C[e_{c_{k-1|k-2}} - K_{k-1}]/\psi_c)\} \\ &= \hat{\Phi} e_{c_{k|k-1}} + \aleph e_{c_{k-1|k-2}} + \Im \end{aligned} \,, \tag{45}$$

where $\aleph = \hat{G}(C\hat{G})^{-1} C$, and

$$\begin{aligned} \Im = \hat{G}(C\hat{G})^{-1} C[&\hat{\Phi}^{-1}\hat{H}^{+} \cdot |\hat{H}\hat{\Phi}|_{ABS} \cdot \{\Upsilon \cdot |\hat{H}^{+}|_{ABS} |e_{fz_{k|k-1}}|_{ABS} \\ &+ |\hat{\Phi}^{-1}\hat{H}^{+}\tilde{\xi}_{\max} z_{k-1}|_{ABS} + |\hat{\Phi}^{-1}\hat{H}^{+}|_{ABS} \cdot (|\hat{\xi} + \tilde{\xi}_{\max}|_{ABS} + I) V_{\max} \\ &+ |\hat{\Phi}^{-1}\hat{H}^{+}\tilde{\delta}_{\max} u_{k-1}|_{ABS} + (|\hat{\Phi}^{-1}|_{ABS} + |\hat{\Phi}^{-1}\hat{H}^{+}\tilde{H}_{\max}|_{ABS}) \cdot W_{\max}\} \\ &\cdot \mathrm{sgn}(e_{fz_{k-1|k-2}})] - \hat{G}(C\hat{G})^{-1} Kc \cdot sat(C[e_{c_{k-1|k-2}} - K_{k-1}]/\psi_c) \end{aligned} \,.$$

The choice of the coefficients of the SMC's switching function, *C*, and gain *Kc* together with the VSF's gain matrix *Y* determines the stability, speed, and manner of convergence for the controller. This may be verified by taking the Z transform of (45), such that:

$$e_{c_{k|k}} = \frac{\Im}{\mathbf{I} - z^{-1}\hat{\Phi} - z^{-2}\aleph}, \qquad (46)$$

where **I** is the identity matrix and *z* is the Z transform factor.

Thus, the poles of discrete transfer function of (46) can be placed within the unit circle by design, leading to a stable SMCF process.

5 APPLICATION TO AN EHA SYSTEM

The ElectroHydraulic Actuator (EHA) is a high performance actuation system based on the principle of closed circuit hydrostatic transmission as shown in Fig. 4. In this system, a variable speed pump is used to directly regulate the movement of a hydraulic cylinder as shown in Fig. 5. The main constituents of EHA are: an electrical motor, a bi-directional gear pump, a symmetrical actuator, pressure and position sensors, and an inner accumulator sub-circuit. Details of its operation can be found in the references cited.

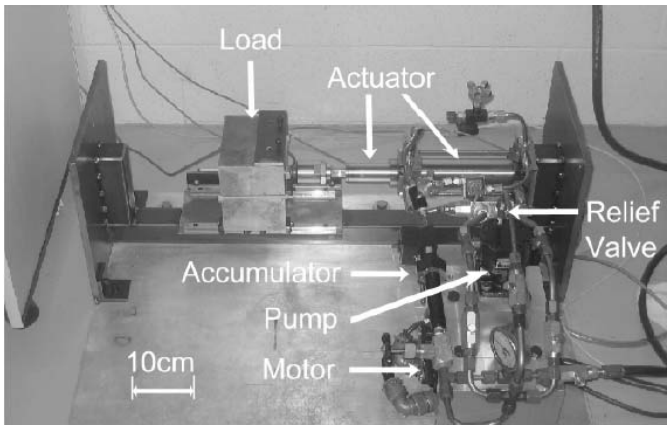

Fig. 4 The EHA Prototype

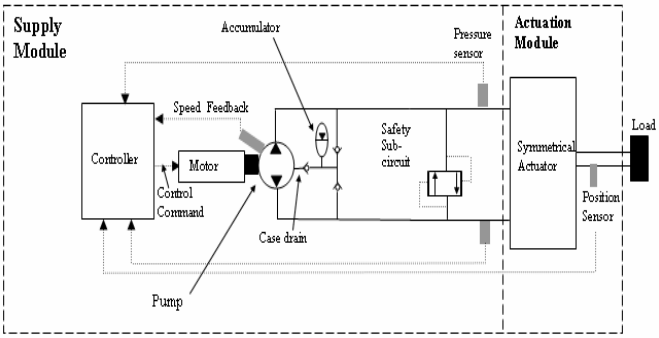

Fig. 5 Schematic of the Electrohydraulic Actuator (EHA) [22]

The EHA is capable of moving large loads with sub-micron precision. All of the results reported in this section are unique to this work and have been experimentally generated by using a prototype of the EHA system as shown in Fig. 4.

A mathematical model of the dominant dynamics of the EHA system can be represented by a third order transfer function as follows [22]:

$$G_h(s) = \frac{13.1}{s(s^2 + 39.53s + 39165)}. \tag{47}$$

The discrete state-space equation of the EHA may be approximated with a sampling period $T_s = 0.001s$ to:

$$X(k+1) = \begin{bmatrix} 1 & 0.001 & 0 \\ 0 & 1 & 0.001 \\ 0 & -39.165 & 0.9605 \end{bmatrix} X(k) + \begin{bmatrix} 0 \\ 0 \\ 0.0131 \end{bmatrix} u(k), \tag{48}$$

$$Z(k) = \begin{bmatrix} 1 & 0 & 0 \end{bmatrix} X(k). \tag{49}$$

Based on the EHA system, some coefficients, such as sliding gain, sliding surface coefficients, boundary layer and so on, are consistent with and estimated from experimental tests. Considering the stability of the system and the optimal system performance, the sliding surface can be determined by solving the unique solution of the ARE of Eq. (35) given as:

$$S(k) = CX_e(k) = \begin{bmatrix} 358.0318 & 196.2450 & 35.8423 \end{bmatrix} X_e(k). \tag{50}$$

The gain Kc is chosen as 10, which satisfies the condition of $Kc > (Cw)_{\max} + \Delta$. It is assumed the maximum of system noise is given as:

$w_{\max} = [0.001 \quad 0.001 \quad 0.001]^T$ and the upper bound of measurement noise is $v_{\max} = 0.001$. The choice of *K*c will affect the system response such that the bigger gain will obtain a high regulation rate, but could conceivably cause system instability. The boundary layer of Sliding Mode Controller if chosen to be $\psi_c = 5$ which makes $\psi_c > (Cw)_{\max} + \sigma$.

For the filter, the boundary layer width is evaluated as the VSF gain reaches the maximum value such that all states can be contained within the boundary,

$$\begin{aligned}\psi_f &= |\Phi^{-1}H^+|_{ABS}\{|[|H\Phi|_{ABS}((\mathrm{I}+|\Phi^{-1}|_{ABS})|H^+|_{ABS}v_{\max} \\ &\quad +|\Phi^{-1}|_{ABS}|w_{\max})]|_{ABS}\} \\ &= [3\times10^{-2} \quad 3\times10^{-5} \quad 3\times10^{-5}]^{\mathrm{T}}\end{aligned}, \tag{51}$$

and the diagonal matrix Y is chosen as

$$Y = \begin{bmatrix} 1.9 & 0 & 0 \\ 0 & 1.9 & 0 \\ 0 & 0 & 1.9 \end{bmatrix}. \tag{52}$$

The choice of Y is initially somewhat arbitrary and is based on the stability of the system (see Eq. (46)).

The EHA system is third order and has three states associated with position, velocity and acceleration. The only measured signal available from the EHA system is from a position encoder with a resolution of 50nm. For the experimental system tested, the EHA system was at rest and therefore its initial states were known and set at $X_0 = [0 \quad 0 \quad 0]$.

The reference input (i.e. the desired trajectory of all states) was chosen to be as illustrated by the solid lines in Fig. 6, Fig. 7 and Fig. 8.

The VSF is used to estimate the system states from the only measurement (position) from the EHA. The controller receives the measured and estimated system states from the VSF and subsequently forces the system to follow the desired state trajectories. The estimated states (position, velocity, acceleration) are the dash-dot lines shown in Fig. 6, Fig. 7 and Fig. 8. The measured position resulting from the SMCF is the dashed line shown in Fig. 6. The errors between the desired and actual system position and the estimation errors, i.e. the difference between the desired and estimated states, are shown in Fig. 9, Fig. 10 and Fig. 11. It is evident that the magnitude of the transient errors between the desired and the actual states are very

small and thus it can be concluded that in the presence of uncertainties, the SMCF can obtain a high degree of robustness and accurate control without an actual measurement of the velocity and the acceleration. The chattering that is evident in the error plots can be further suppressed by adjusting the boundary layer designed for the SMCF.

It is recognized that an alternative to using the VSF to estimate the velocity and acceleration states is to estimate them directly through direct differentiation. Since the position of load can be measured directly, its first derivative and second derivative can be directly obtained as shown in Fig. 12. The presence of noise is very evident in this plot. The measured position is differentiated and then filtered to provide a derived filtered velocity. The same procedure is applied to the filtered velocity to obtain the smooth filtered acceleration. This procedure is referred to as Derivative-filtered approach. The measured position and filtered velocity and acceleration are shown in Fig. 13. The maximum cut-off frequency of the second order digital filter was set to 2.25Hz. It is evident that the cut-off frequency is very low which will limit the system in response to a rapidly changing input signal. The results in Fig. 13 show that the digital filter strategy discussed above cannot follow the desired states very effectively when compared to the VSF shown in Fig. 6, Fig. 7, and Fig. 8. It is evident that the magnitude of the errors as shown in Fig. 14 between the derivative-filtered approach and desired states is substantively larger than for the VSF approach for velocity and acceleration.

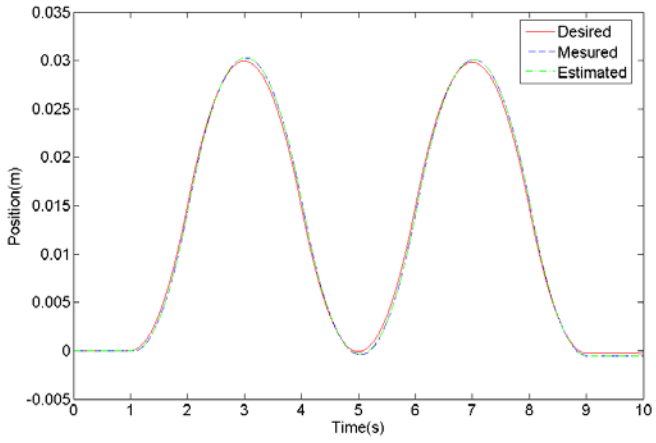

Fig. 6 The desired, measured and estimated state trajectories associated with position

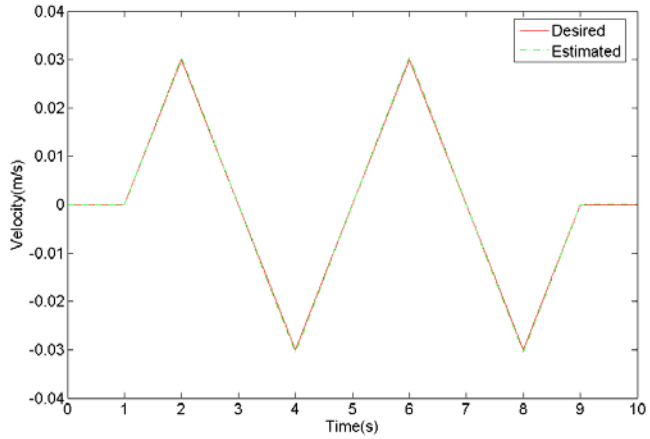

Fig. 7 The desired and estimated state trajectories associated with velocity

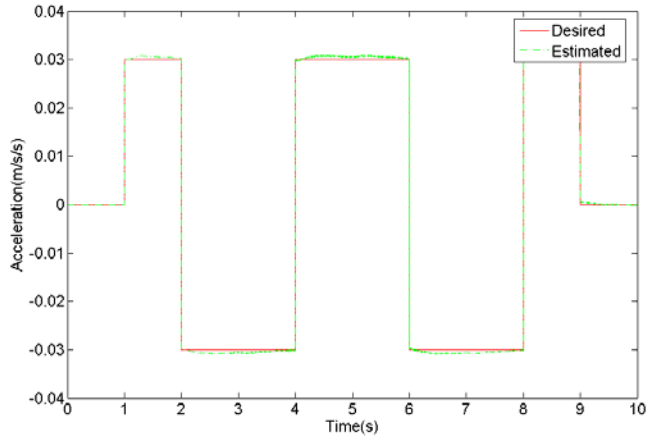

Fig. 8 The desired and estimated state trajectories associated with acceleration

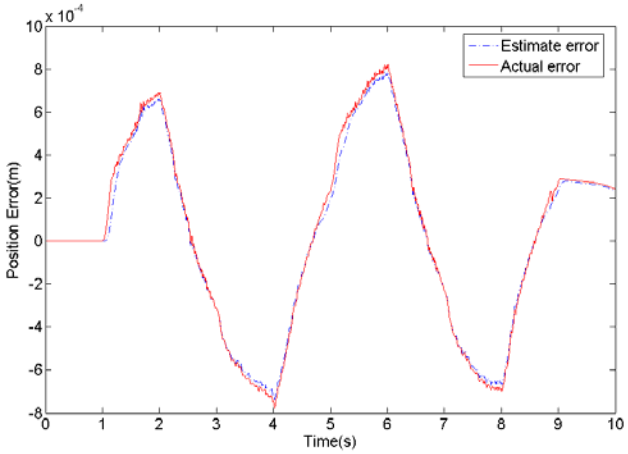

Fig. 9 The trajectory following error associated with position using the measured signal compared to that of the VSF state estimate.

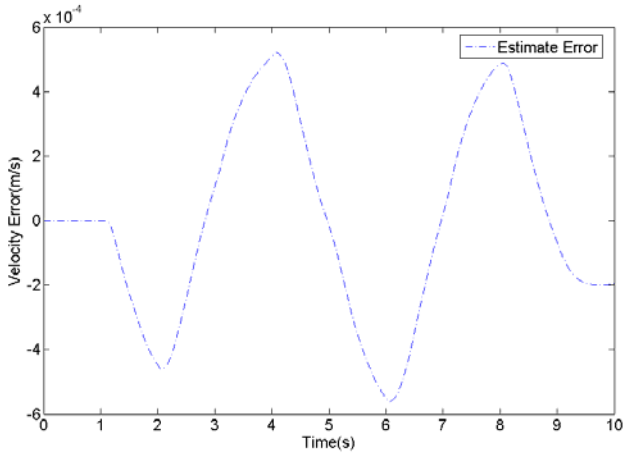

Fig. 10 The trajectory following error associated with velocity obtained by using the associated VSF state estimate (note only the estimate error is shown since the actual velocity is not known).

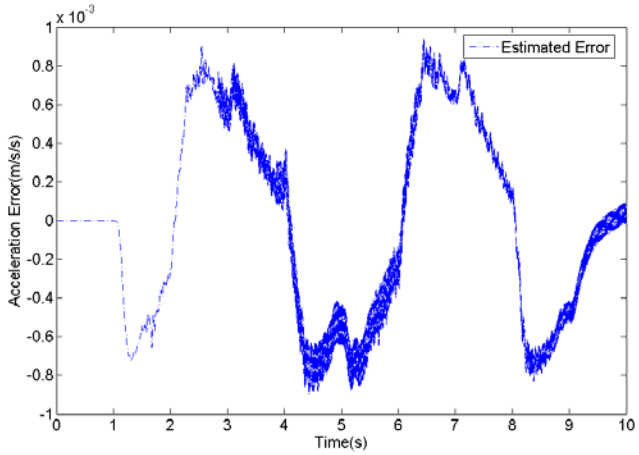

Fig. 11 The trajectory following error associated with acceleration obtained by using the associated VSF state estimate.

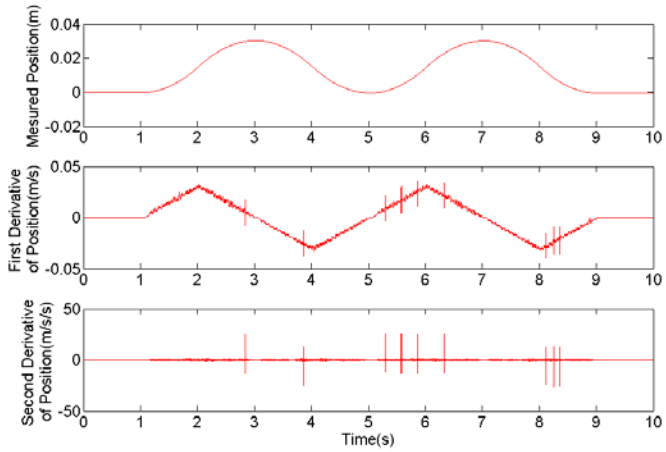

Fig. 12 The measured position and its first derivative and second derivative

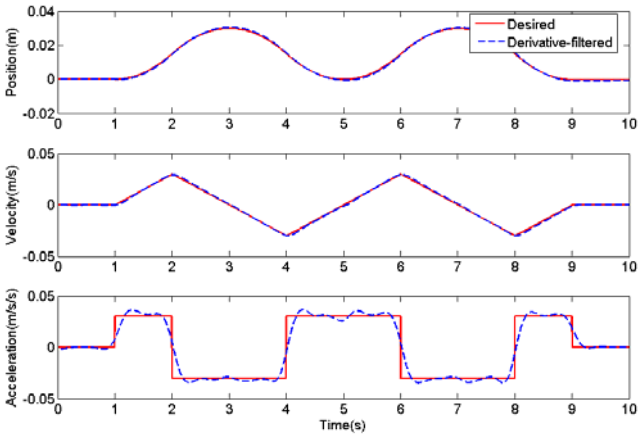

Fig. 13 The measured position and its first filtered derivative and filtered second derivative and desired states.

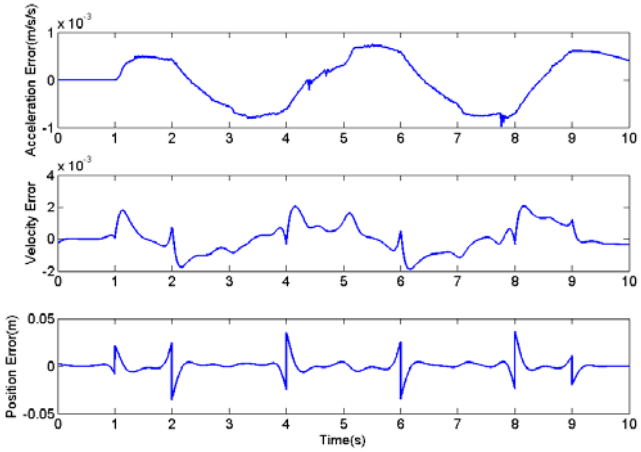

Fig. 14 The errors between Derivative-filtered and desired states

6 COMPARITIVE ANALYSIS

In the previous sections, the concepts of the SMCF and its application to the EHA system have been presented. In this section to facilitate comparison to a classical controller, a form of a PID controller was introduced and tuned using standard practices [22]. This controller is shown in Figure 14.

It was of interest to apply this well known controller to the EHA model subject to follow the desired state trajectories of Fig. 6 to Fig. 8.

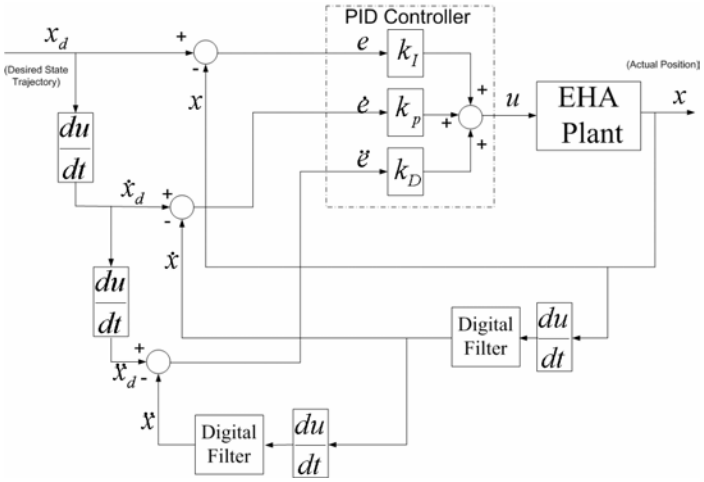

Fig. 15 PID form controller designed for an EHA

With this PID controller, the actual output position of EHA system, its first and second filtered derivative (using second order digital filtering as described in Section 5) are shown in Fig. 16. From this experimental result, it is obvious that there is a significant trajectory following error with the PID controller. Comparing these results with those of the SMCF (Fig. 6, Fig. 7, Fig. 8), the SMCF achieves much better performance in terms of tracking accuracy and settling times.

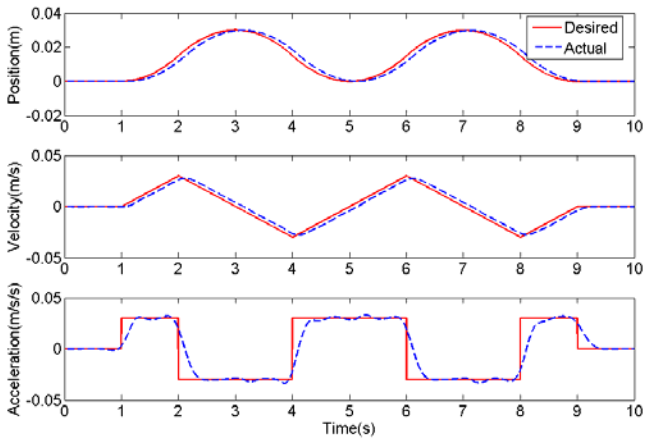

Fig. 16 Desired and actual position of EHA produced by a PID controller

7 OBSERVATIONS

An examination of the system bandwidth resulting from the implementation of the SMCF is necessary to confirm the ability of the controller to regulate the system in tracking the input trajectories. A large bandwidth corresponds to a small rise time, or fast response. For the EHA system, one design objective for the SMCF was to maximize the bandwidth of the EHA. In this case, a swept sinusoid signals with

magnitude of 1 volt and frequency range from 0.1Hz to 200Hz, was input into the EHA plant directly without any controller. The open loop bandwidth of the EHA was determined to be approximately 6Hz shown in Fig. 17. The Bode diagram of the EHA with the SMCF implemented is illustrated in Fig. 18. The bandwidth of the closed-loop system with SMCF was approximately 40Hz. As such, the SMCF improves the bandwidth of EHA system by more than 6 times than the system in the open loop. The closed loop bandwidth with the PID trajectory following controller is shown in Fig. 19. It is apparent that the SMCF's performance is better by a factor of two. It must be stated that the poorer performance was in part due to the low cut-off frequency of digital filter used in PID controller as explained Section 6. If however, the filter cutoff frequency was increased, the performance of the PID controller rapidly deteriorated.

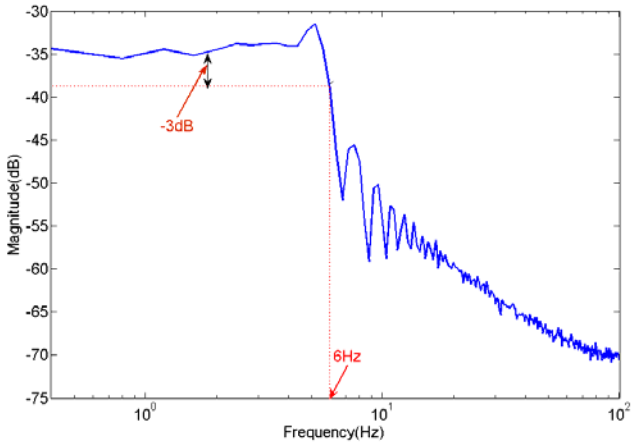

Fig. 17 Bode plot of EHA plant

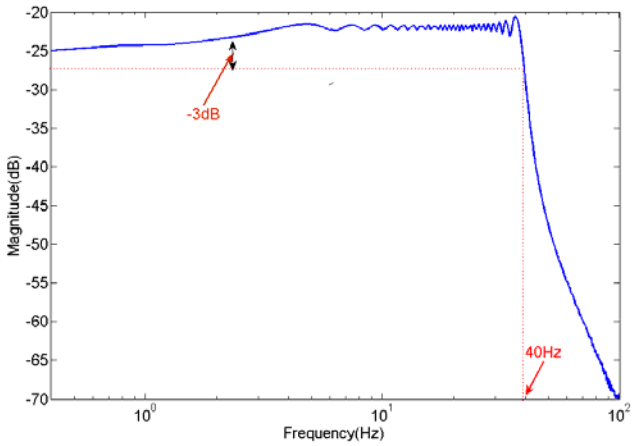

Fig. 18 Bode plot of EHA plant with SMCF

In the SMCF system, the VSF was used for state estimation. The response of the filter should be faster than the convergence rate of the controller such that the dynamics of the VSF is insignificant as seen by the

SMC. The VSF gain K_k that is used to refine the estimated position is shown in Fig. 20. The corresponding a priori and a posteriori states are shown in Fig. 21. It is clear from this figure that the estimated state lags the actual state by only one sampling interval, which is 0.001s. It may be said that the convergence speed of the VSF is experimentally 1000Hz, which is 25 times faster than that of the of the combined closed loop system (given that the bandwidth of the system with SMC is 40Hz).

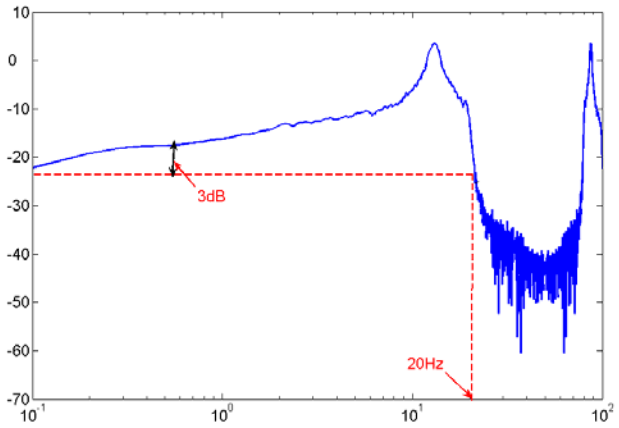

Fig. 19 Bode plot of EHA plant with PID

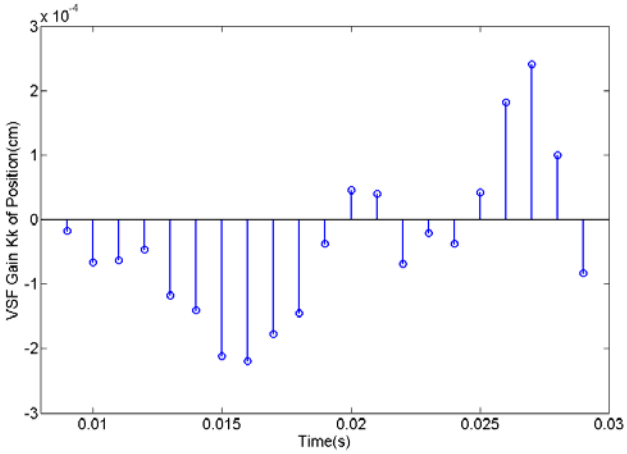

Fig. 20 VSF gain compensating the position

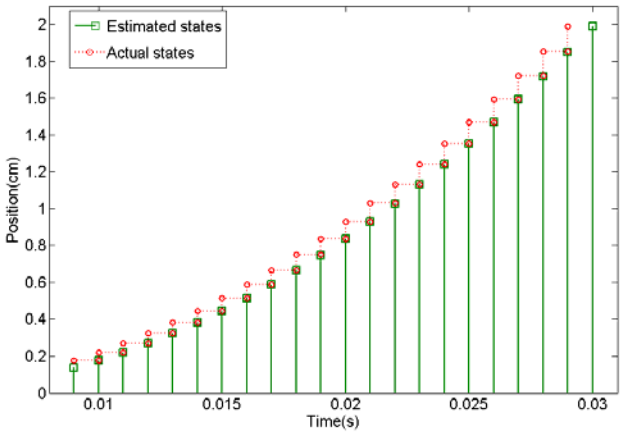

Fig. 21 The actual and estimated position (the estimated states lag the actual states by one time step)

8 CONCLUSIONS

A new control strategy, referred to as the SMCF is proposed based on the concepts of Variable Structure Control and Filter and represents the unique contribution of this paper. Meanwhile, the SMCF can easily be implemented by several iteration calculation steps in the same form as a predictor-corrector method, although it is composed of different function blocks, i.e., Controller and Filter. Also, the advantages of the proposed controller include robustness and faster system response. The SMCF was applied to an experimental high performance hydrostatic actuation system referred to as the EHA. Experimental results indicate that SMCF can deal with a stochastic system with unmatched modeling uncertainties.

In the paper, the stability of SMCF is proven by the mathematical derivation. The chattering problem can be alleviated by introducing a boundary layer and internal high frequency loop in the SMCF. The comparison between SMCF with a form of the classical PID controller with digital filters is provided. The SMCF provides a very considerable improvement in performance over a PID type trajectory following controller.

ACKNOWLEDGEMENTS

The author would like to acknowledge the financial support of the University of Saskatchewan and National Science and Engineering Research Council of Canada.

APPENDIX A: DERIVATION OF SMC

For the case of $\hat{S}_k > 0$, from Eq. (18)

$$\hat{S}_{k+1} < \hat{S}_k \,, \tag{53}$$

where

$$\hat{S}_{k+1} = Ce_{c_{k+1}} = C(X_{d_{k+1}} - \hat{\Phi} X_k - \hat{G}u_k - w_k) \,. \tag{54}$$

Substituting (16) into (54)

$$\hat{S}_{k+1} = C\hat{G}u_{eq_k} - C\hat{G}u_k - Cw_k \,. \tag{55}$$

Thus Eq. (53) may be rewritten as:

$$C\hat{G}u_{eq_k} - C\hat{G}u_k - Cw_k < \hat{S}_k \,, \tag{56}$$

For the case of $\hat{S}_k < 0$, the existence condition (18) may be written as:

$$\hat{S}_{k+1} > \hat{S}_k \,. \tag{57}$$

The existence condition of (18) is satisfied if:

$$C\hat{G}u_{eq_k} - C\hat{G}u_k - Cw_k > \hat{S}_k \,. \tag{58}$$

Thus the control law may choose the maximum or minimum value of the last term on the left hand side of inequality of (56) and (58) which depends on the sign of switching function, such that:

$$u_k = u_{eq_k} - (C\hat{G})^{-1}\hat{S}_k + (C\hat{G})^{-1} Kc \cdot \mathrm{sgn}(\hat{S}_k) \,, \tag{59}$$

where the gain $Kc = (Cw)_{\max} + \Delta$, in which Δ and σ are arbitrary positive number.

To handle the chattering, the sign function of $\mathrm{sgn}(\hat{S}_k)$ in (59) may be replaced by saturation function as follows:

$$sat(\hat{S}_k)/\psi_c) = \begin{cases} \hat{S}_k / \psi_c & |\hat{S}_k| \le \psi_c \\ sign(\hat{S}_k / \psi_c) & \text{otherwise} \end{cases},$$

where $\psi_c > (Cw)_{\max} + \sigma$, in which $(Cw)_{\max}$ is the upper bound of Cw_k.

APPENDIX B: DERIVATION OF VSF GAIN

In the discrete form, define the a priori and a posteriori estimated errors in terms of measured output signals as in a vector form:

$$e_{z_{k|k}} = Z_k - \hat{Z}_{k|k} \,, \tag{60}$$

$$e_{z_{k|k-1}} = Z_k - \hat{Z}_{k|k-1} . \tag{61}$$

Similarly

$$e_{z_{k+1|k}} = Z_{k+1} - \hat{Z}_{k+1|k} . \tag{62}$$

Substitute the system model as defined by Eq. (3) and the next a priori state estimate Eq. (28) into Eq. (62) to yield:

$$\begin{aligned} e_{z_{k+1|k}} &= Z_{k+1} - \hat{Z}_{k+1|k} \\ &= HX_{k+1} + v_{k+1} - \hat{H}(\hat{\Phi}\hat{X}_{k|k} + \hat{G}u_k) \\ &= H(\Phi X_k + Gu_k + w_k) + v_{k+1} - \hat{H}(\hat{\Phi}\hat{X}_{k|k} + \hat{G}u_k) \end{aligned} . \tag{63}$$

Rearranging Eq. (63) and substituting Eqs. (27) and (3) into Eq. (63) yields:

$$\begin{aligned} e_{z_{k+1|k}} &= H(\Phi X_k + w_k) - \hat{H}\hat{\Phi}\hat{X}_{k|k} + (HG - \hat{H}\hat{G})u_k + v_{k+1} \\ &= \hat{\xi} e_{z_{k|k-1}} + \tilde{\xi} Z_k - (\hat{\xi} + \tilde{\xi})v_k + \tilde{\delta}u_k + (\hat{H} + \tilde{H})w_k \\ &\quad + v_{k+1} - \hat{H}\hat{\Phi}K_k \end{aligned} , \tag{64}$$

where $\delta = HG,\ \hat{\delta} = \hat{H}\hat{G},\ \tilde{\delta} = \delta - \hat{\delta}$, $\xi = H\Phi H^+$, $\hat{\xi} = \hat{H}\hat{\Phi}\hat{H}^+$, $\tilde{\xi} = \xi - \hat{\xi}$, $\tilde{H} = H - \hat{H}$.

Substituting $e_{z_{k+1|k}}$ from Eq. (64) into $e_{z_{i_{k+1|k}}} \operatorname{sgn}(e_{z_{i_{k|k-1}}})$ of Eq. (30):

$$\begin{aligned} & e_{z_{k+1|k}} \operatorname{sgn}(e_{z_{k|k-1}}) \\ &= \hat{H}\hat{\Phi} \cdot [\hat{H}^+ e_{k|k-1} + \hat{\Phi}^{-1}\hat{H}^+\tilde{\xi}Z_k - \hat{\Phi}^{-1}\hat{H}^+(\hat{\xi} + \tilde{\xi})v_k + \hat{\Phi}^{-1}\hat{H}^+ v_{k+1} \\ &\quad + \hat{\Phi}^{-1}\hat{H}^+\tilde{\delta}u_k + \hat{\Phi}^{-1}\hat{H}^+(\hat{H} + \tilde{H})w_k - K_k] \cdot \operatorname{sgn}(e_{z_{k|k-1}}) \end{aligned} . \tag{65}$$

Let

$$\begin{aligned} f_k &= \hat{H}^+ e_{k|k-1} + \hat{\Phi}^{-1}\hat{H}^+\tilde{\xi}Z_k - \hat{\Phi}^{-1}\hat{H}^+(\hat{\xi} + \tilde{\xi})v_k + \hat{\Phi}^{-1}\hat{H}^+ v_{k+1} \\ &\quad + \hat{\Phi}^{-1}\hat{H}^+\tilde{\delta}u_k + \hat{\Phi}^{-1}\hat{H}^+(\hat{H} + \tilde{H})w_k \end{aligned} \tag{66}$$

Eq. (65) becomes,

$$e_{z_{k+1|k}} \operatorname{sgn}(e_{z_{k|k-1}}) = \hat{H}\hat{\Phi} \cdot [f_k - K_k] \cdot \operatorname{sgn}(e_{z_{k|k-1}}) . \tag{67}$$

From Eq. (30), the $e_{z_{k+1|k}} \operatorname{sgn}(e_{z_{k|k-1}})$ is negative definite. The VSF gain K_k may be defined as the following so that it can satisfy the condition of Eq. (30). Thus K_k may be derived from Eq. (67) as:

$$K_k \cdot = \hat{\Phi}^{-1}\hat{H}^+[|\hat{H}\hat{\Phi}|_{ABS} \cdot |F_k|_{ABS} \cdot \operatorname{sgn}(e_{z_{k|k-1}})] , \tag{68}$$

where F_k is the upper bound of f_k,

$$
\begin{aligned}
F_k = & [\mathrm{Y}\cdot|H^+|_{ABS}\cdot|e_{z_{k|k-1}}|_{ABS}+|\hat{\Phi}^{-1}\hat{H}^+\tilde{\xi}_{\max}Z_k|_{ABS} \\
& +|\hat{\Phi}^{-1}\hat{H}^+|_{ABS}\cdot(|\hat{\xi}+\tilde{\xi}_{\max}|_{ABS}+I)V_{\max}+|\hat{\Phi}^{-1}\hat{H}^+\tilde{\delta}_{\max}u_k|_{ABS}, \\
& +(|\hat{\Phi}^{-1}|_{ABS}+|\hat{\Phi}^{-1}\hat{H}^+\tilde{H}_{\max}|_{ABS})\cdot W_{\max}]
\end{aligned}
\tag{69}
$$

and the modeling uncertainties of $\tilde{\xi}$, $\tilde{\delta}$, $\tilde{H}$, and also system noise and measured noise w_k and v_k are respectively upper bounded by $\tilde{\xi}_{\max}$, $\tilde{\delta}_{\max}$, $\tilde{H}_{\max}$, $W_{\max}$ and $V_{\max}$, where Y is a diagonal matrix with elements $\gamma_{ij}\geq 1$.

The VSF gain of a model with an explicit consideration of modeling uncertainties can be written as:

$$
\begin{aligned}
K_k = & \\
& \hat{\Phi}^{-1}\hat{H}^+\cdot\{|\hat{H}\hat{\Phi}|_{ABS}\cdot[\mathrm{Y}\cdot|H^+|_{ABS}\cdot|e_{z_{k|k-1}}|_{ABS} \\
& +|\hat{\Phi}^{-1}\hat{H}^+\tilde{\xi}_{\max}Z_k|_{ABS}+|\hat{\Phi}^{-1}\hat{H}^+|_{ABS}\cdot(|\hat{\xi}+\tilde{\xi}_{\max}|_{ABS}+I)V_{\max}\cdot \\
& +|\hat{\Phi}^{-1}\hat{H}^+\tilde{\delta}_{\max}u_k|_{ABS}+(|\hat{\Phi}^{-1}|_{ABS}+|\hat{\Phi}^{-1}\hat{H}^+\tilde{H}_{\max}|_{ABS}) \\
& \cdot W_{\max}]\}\cdot\mathrm{sgn}(e_{z_{k|k-1}})
\end{aligned}
\tag{70}
$$

REFERENCES

[1] Utkin, V. I, 1977, "Variable structure system with sliding modes." IEEE Transactions on Automatic Control, AC-22, pp. 212-222.

[2] Corradini, M., and Letizia, and Leo, T., and Orlando, G., 2002, "Experimental Testing of a Discrete-time Sliding Mode Controller for Trajectory Tracking of A Wheeled Mobile Robot in the Presence of Skidding Effects", J. of Robotic systems 19(4), pp. 177-188.

[3] Zinober, A.S.I, El-Ghezawi, O.M.E. and Billings, S.A., 1982, "Multivariable-Structure Adaptative Model-following Control Systems", Proceedings of IEEE, 129, pp. 6-12.

[4] Slotine, J. –J. E., Hedrick, J.K. and Misawa, E. A., 1987, "On Sliding Observers for Nonlinear Systems", J. of Dynamic Systems, Measurement and Control, 109, pp. 245-252

[5] Decarlo, R. A., and Zak, S. H. and Matthews G. P., 1988, "Variable Structure Control of Nonlinear Multivariable Systems: A Tutorial", Proceedings of the IEEE, 76, No. 3, 212-232.

[6] Furuta, K., 1990, "Sliding Mode Control of A Discrete System," System & Control Letters, 14, pp. 145-152.

[7] Misawa, E. A., 1997, "Discrete-Time Sliding Mode Control for Nonlinear Systems with Unmatched Uncertainties and Uncertain Control Vector", ASME Journal of Dynamic Systems, Measurement, and Control, 119, pp. 503-512.

[8] Utkin, V. I., 1992, "Sliding Modes in Control Optimization,", Springer-Verlag Berlin.

[9] Walcott, B. L. and Zak, S. H., 1987, " State Observation of Nonlinear Uncertain Dynamical Systems," IEEE Transaction on Automatic Control, 32, pp. 166-170.

[10] Habibi, S. R. and Burton, R., 2003, "The Variable Structure Filter" ASME Journal of Dynamic Systems, Measurement and Control, 125, pp. 287-293.

[11] Emelyanov, S.V., 1967, "Variable Structure Control Systems", Moscow: Nauka (in Russian).

[12] Utkin, V. I., 1978, "Sliding Mode and Their Application in Variable Structure Systems", English translation, Mir Publication, Moscow.

[13] Sarpturk, S. Z., Istefanopulos Y., and Kaynak, O., 1987, "The Stability of Discrete-time Sliding Mode Control Systems IEEE Transactions on Automatic Control, Vol. 32, pp.930-932.

[14] Slotine, J. –J. E and Sastry, S. S, 1983, "Tracking Control of Nonlinear Systems Using Sliding Surfaces, with Application to Robot Manipulators", International Journal of Control, 38, pp. 465-492.

[15] Utkin, V. I., and Guldner, J., and Shi, J., 1999, "Sliding Mode Control in Electromechanical Systems", Taylor & Francis London.
[16] Slotine, J. –J. E., 1984, "Sliding Controller design for nonlinear Systems", International Journal of Control, 40, pp. 421-434.
[17] Itkis, Y., 1976, "Control Systems of Variable Structure", New York: Wiley.
[18] Misawa, E. A., 1997, "Discrete-Time Sliding Mode Control: The Linear Case", ASME Journal of Dynamic Systems, Measurement, and Control, 119, pp. 819-821
[19] Campbell, S.L. and Meyer, C.D. Jr, 1991, "Generalized Inverses of Linear Transformations", New York: Dover.
[20] Zinober, A. S. I. (Ed.), 1994, "Variable Structure and Lyapunov Control", Springer-Verlag London Limited.
[21] Lewis, F. L., 1996, "Optimal Control", in W. S. Levine, editor, The Control Handbook, CRC Press, Boca Raton, FL, pp. 759-778.
[22] Habibi, S. R. and Singh, G., 2000, "Derivation of Design Requirements for Optimization of A High Performance Hydrostatic Actuation System", International Journal of Fluid Power, 2, pp. 11-27.

Appendix B: Sliding Mode Control for an Electrohydraulic Actuator System with Discontinuous Nonlinear Friction (Wang, et al [2006])*

* This paper is under review by the ASME Journal of Dynamic Systems, Measurement and Control. This paper is included with the express permission of the journal's publishers.

Sliding Mode Control for an Electrohydraulic Actuator System (EHA) with Discontinuous Nonlinear Friction

Shu Wang **Saeid Habibi** **Richard Burton**

Department of Mechanical Engineering, University of Saskatchewan
57 Campus Drive, Saskatoon, SK, S7N 5A9 Canada
Phone: 1-306-966-5463 Fax: 1-306-966-5427
shw750@mail.usask.ca

ABSTRACT

This paper considers the application of Sliding Mode Control (SMC) to a high precision Electrohydraulic Actuator (EHA) system with nonlinear discontinuous friction effect. An important consideration in such systems is the oscillations that occur in the system response due to friction for small input signals at cross-over regions where the velocity changes sign. A new model for a high precision hydrostatic actuation system is developed for investigating the effects of discontinuous and nonlinear friction. This model is used in the development of a sliding mode control strategy. A significant result from this study is that the SMC can suppress such oscillations. In addition, the paper introduces for the first time, a linear quadratic approach for defining a discrete-time sliding surface for nonlinear systems.

A comparative study involving the application of the proposed SMC versus a gain-scheduled proportional controller is presented. This comparison demonstrates the performance improvements resulting from the SMC and the added robustness of this strategy given large modeling uncertainties.

Keywords: Sliding mode control, Discontinuous nonlinear friction, Transient oscillations, Electrohydraulic Actuator

1 INTRODUCTION

Nonlinear friction exists in all hydraulic systems which have sliding surfaces aided by lubricating oil. It is very difficult to model friction characteristics in most simulation studies and hence often the approach is to approximate the friction characteristic by an “equivalent” linear viscous friction term. Friction can lead to tracking errors, undesirable “stick-slip” motion and even limit cycle oscillations. [1]. A general survey of friction and control was done by Armstrong-Helouvry et al in 1994, [2]. Seven representations of friction were considered including Viscous, Coulomb, Static+Coulomb+Viscous, Stribech, Rising Static Friction, Frictional Memory, and Presliding Displacement. For these cases, black box and model-based control strategies have been investigated extensively by many researchers. Black box compensation for friction have included stiff PD control [3], adaptive pulse-width control (PWC) [4], and neural network

control [5] amongst others. Model-based-control approaches have included compensation [6] and adaptive control [7]. A unique two-relay system configuration method was proposed in [8] to identify and control a system with a dominant Coulomb friction effect.

In this manuscript, friction compensation in a novel hydrostatic actuation system referred to as the Electrohydraulic Actuator (EHA) is considered. This actuation system is the first reported hydrostatic system that has achieved an experimental sub-micron resolution of 50nm and is hence used as the subject of this paper. In [9], a linearized mathematical model of the EHA was derived and used as a basis for model identification. A prototype model of the EHA system was fabricated and extensively tested. Experimental studies indicated that coulomb, static and viscous friction exist in the linear actuator [10]. Further to experimental results of [10], a typical friction characteristic from a prototype of the EHA is shown in Fig. 1. This friction characterization is adopted in the simulation and experimental study of this actuator in order to faithfully reproduce the associated physical effects of friction. Ability to compensate for friction is particularly important for achieving a higher level of precision and resolution with the EHA system. The control strategy presented in this paper includes friction compensation and is particularly relevant to precision trajectory tracking.

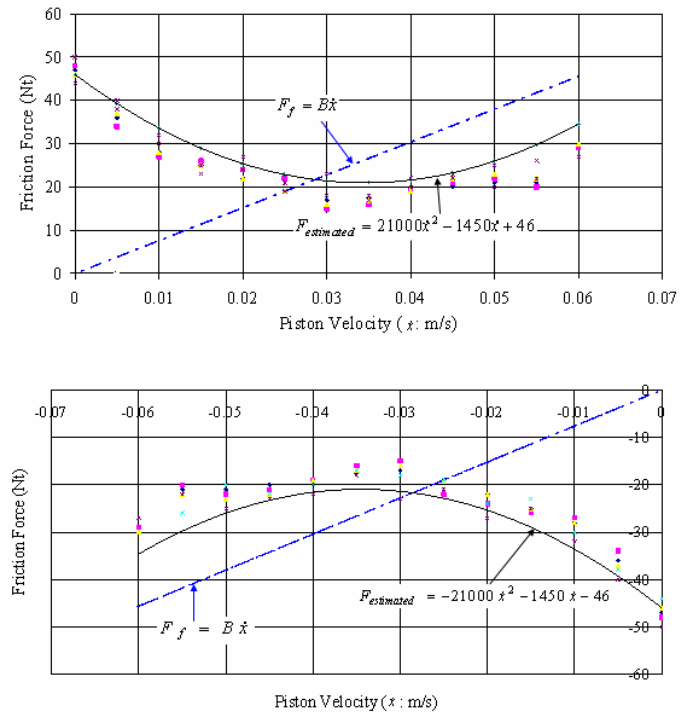

Fig. 1. Experimental friction in the EHA and the linear and quadratic approximation

In [11], a linearized model of the EHA was presented that assumed a linear characteristic for the load friction (as illustrated in Fig. 1). Based on this model, proportional control and nonlinear proportional control were applied to the EHA in [12] and [13] respectively. The challenge was to be able to achieve a high trajectory tracking performance in the presence of severe nonlinear friction but with a higher dynamic performance. Thus the objective of this study was to investigate nonlinear type controllers to achieve this goal. This paper will first present a revised nonlinear model of the EHA which includes static, coulomb and viscous friction in the actuator. A controller is then presented that is based on the concept of sliding mode control (SMC).

Sliding Mode Control (SMC), a subclass of variable structure systems (VSSs) theory, is a popular nonlinear control method that forces a prescribed structural response from a system. SMC achieves this effect by using a switching nonlinear input that drives the state trajectory to a predetermined sliding surface and then retains them on that surface. The dynamic response of the system is then determined by the choice of the switching surface. Although the derivation of a suitable control signal (u) is relatively simple and straightforward, the analysis and choice of the switching surface can be challenging, [14]. Utkin and Young have proposed three methods for designing the sliding surface in SMC systems: desirable placement of eigenvalues of the plant's system matrix, optimal quadratic performance, and optimal quadratic performance with equivalent control defined in the cost function, [15]. All of these methods apply to both continuous and discrete linear systems. The sliding surface for the discrete linear system using a Lyapunov function was proposed by Spurgeon in 1992 [16]. DeCarlo, et al in 1996 proposed a sliding surface design approach using a "regular" form (the form of the plant equations after a diffeomorphic transformation) of the plant dynamics for one class of continuous nonlinear systems [17]. In 1984, Slotine presented a sliding mode controller for tracking a class of continuous nonlinear time-varying multivariable systems in the presence of disturbances and parameter variations, [18]. In 1988, Decarlo et al published a tutorial paper about variable structure control (VSC) of nonlinear systems in which VSC design developments were described and several approaches were summarized, [19]. In 1997, Misawa proposed a discrete-time sliding mode controller with uncertainties which did not require the controller to satisfy the "matching conditions" for nonlinear systems, [20].

In a study on friction compensation, it has been reported that as the velocity of an actuator changes direction (or sign), small oscillatory transients are observed at the crossover point when using a classical PID controller, [21]. This effect can be attributed to nonlinear friction and to alleviate it, Qian et al [1] proposed a combined PID/Neural Network controller that suppressed these crossover transients. Their control strategy did reduce the magnitude of the transient at the crossover points, but could not completely remove them.

The objective of this paper is to apply a nonlinear controller to the EHA system to compensate in part its nonlinear friction characteristics to implement trajectory tracking. The proposed method will use some of the concepts introduced in [15] and [16]; in particular, the diffeomorphic transformation is used and the linear optimal quadratic method (similar in concept to the optimal quadratic performance) is applied to a discrete nonlinear system to determine the sliding surface. In this paper, the nomenclature is provided in Section 2. In Section 3, the EHA system and its nonlinear model are described. In Section 4, the design of a sliding mode controller and its application to the EHA system are presented. The implementation results in a simulated and experimental study are considered in Section 5. Section 6 contains the concluding remarks.

2 NOMENCLATURE

Before the theoretical and experimental study, it should be clarified several terminologies used in this paper. In the paper, the term "plant" will refer to either the physical system or a set of nonlinear equations and measured parameters that best represent the physical plant. The term "nonlinear model" will refer to the equations that are used to formulate the Sliding Mode Controller.

Table 1 gives all parameters and coefficients and their values. Matrices and vectors are denoted by using bold letters.

Table 1: Nomenclature (Experimental values for the prototype EHA were obtained from [10]).

Symbol	Comments	Values and Units
$\hat{\cdot}$	Denotes uncertain values	
A	Pressure area in symmetrical actuators	$5.051\times10^{-4}\,m^2$
a_1, a_2, a_3	Coefficients of the quadratic function of nonlinear function	2.1×10^{4}, -1450, 46
B	Viscous friction coefficient	$760\,Ns/m$
b , $\Delta b(\cdot)$	Input vector and its scalar uncertainty factor	
$C(k)$	Real-valued constant vector	
$\frac{L}{2}+\xi$	Lumped pump and actuator leakage coefficient	$5\times10^{-13}\,m^3/sPa$
D_p	Pump volumetric displacement	$1.6925\times10^{-7}\,m^3/rad$
$f, \hat{f}, \Delta f$	Nonlinear function, uncertain nonlinear function and its uncertainties	
i, j	Subscripts used to identify elements of matrices and vectors	
J	linear quadratic cost function	

K	Calculation step index	
K	Sliding gain	
K_{pipe}	Pipe coefficient relating pressure drop to flow	$2.5\times10^{12}\ Pas^2/m^6$
L	Leakage coefficient	m^3/sPa
P_1, P_2	Actuator chamber pressures	Pa
P_a, P_b	Pump port pressures	Pa
P_{pipe}	The modeled pressure drop for the pump/actuator pipe connection	Pa
P_r	The accumulator pressure	Pa
P_gain	Scheduled proportional gain	
Q_a, Q_b	Pump flow	m^3/s
Q_L	Load flow	m^3/s
S	Switching function	
T	Diffeomorphic transformation matrix	
T_s	Sampling period	
u, u_{eq}, u_c	Control input, equivalent control and correct term of control	
$\mathbf{V}$	Optimal control	
V_a, V_b	Pump section volumes associated with its two ports	m^3
V_0	Total mean volume	$6.85\times10^{-5}m^3$
$V_{0_{ac}}$	Pipe plus mean actuator chamber volume	m^3
$w_i, W_{\max}$	Lumped disturbance and its upper bound	
x_0, x	Pump section volumes associated with its two ports	m^3
$\mathbf{x}, \mathbf{x}_d, \mathbf{x}_e$	System states and their desired value and desired/actual error	
$\mathbf{z}, \mathbf{z_d}, \mathbf{z_e}$	Transformed states and their desired value and desired/actual error	
β, γ	Adjustment gain	
β_e	Effective bulk modulus of hydraulic oil	$2.1\times10^8\ Pa$
ε	Arbitrary positive constant	
$\delta_i(k), \sigma$	Numerical approximation errors	
$\Delta_i(k), \Sigma$	Lumped uncertainty term	
ξ	Pump cross-port leakage coefficient	m^3/sPa
Φ, Q, Γ	Matrix	
Ψ, ϕ	Boundary layer and its element	
ω_p	Pump angular velocity	rad/s

3 EHA NONLINEAR MODEL

A schematic of the EHA system is shown in Fig. 2. The EHA uses a bi-directional, fixed displacement gear pump to supply oil to the actuator and symmetrical actuator to provide high accurate motion by simply varying the speed of the electric motor. A simplified pump/actuator model was developed in [12] and is given as:

$$D_p\omega_p = A\dot{x} + \frac{V_o}{\beta_e}\left(\frac{dP_1}{dt} - \frac{dP_2}{dt}\right) + \xi\left(P_1 - P_2\right) + 2\xi P_{pipe} + \frac{L}{2}\left(P_1 - P_2\right) \tag{1}$$

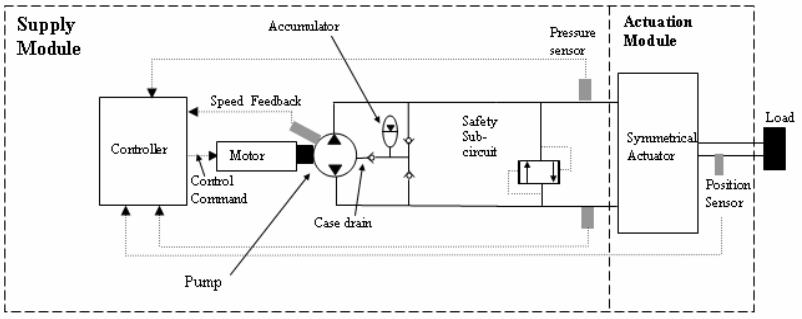

Fig. 2. Schematic of the Electrohydraulic Actuator (EHA)

The EHA system is connected to a horizontal sliding mass and the equation of motion for the actuator is obtained as follows:

$$(P_1 - P_2)A = M\ddot{x} + F_f \tag{2}$$

where friction F_f is written as a summation of three terms including Static (F_{static}), Coulomb ($F_{coulomb}$)and Viscous friction ($F_{viscous}$) such that

$$F_f = F_{static} + F_{coulomb} + F_{viscous} . \tag{3}$$

In [11, 12], coulomb and static friction were neglected for the derivation of a linear model for EHA. Chinniah in 2004 [10] used the Extended Kalman Filter to estimate the nonlinear friction. A quadratic form of the friction, which combined static, coulomb and viscous friction characteristic, was considered as follows:

$$F_f = a_1\dot{x}^2 + a_2\dot{x} + a_3 \qquad \dot{x} > 0$$

$$F_f = -a_1\dot{x}^2 + a_2\dot{x} - a_3 \qquad \dot{x} < 0 \tag{4}$$

where a_1, a_2, a_3 are the experimental coefficients whose values are given in Table 1 for the prototype of the EHA, and $\dot{x}$ is the load velocity. The nonlinear friction based on Eq. (4) and the actual EHA experimental friction coefficients are shown in Fig. 1.

Substituting (4) into (2) yields,

$$(P_1 - P_2)A = M\ddot{x} + a_1\dot{x}^2 + a_2\dot{x} + a_3 \qquad \dot{x} > 0$$

$$(P_1 - P_2)A = M\ddot{x} - a_1\dot{x}^2 + a_2\dot{x} - a_3 \qquad \dot{x} < 0 \tag{5}$$

This can be written as

$$(P_1 - P_2)A = M\ddot{x} + a_2\dot{x} + (a_1\dot{x}^2 + a_3)sign(\dot{x}) \tag{6}$$

Taking the derivative of both sides of Eq. (5) yields:

$$\frac{dP_1}{dt} - \frac{dP_2}{dt} = \frac{M}{A}\dddot{x} + \frac{2a_1\dot{x}\ddot{x}}{A} + \frac{a_2}{A}\ddot{x} \qquad \dot{x} > 0$$

$$\frac{dP_1}{dt} - \frac{dP_2}{dt} = \frac{M}{A}\dddot{x} - \frac{2a_1\dot{x}\ddot{x}}{A} + \frac{a_2}{A}\ddot{x} \qquad \dot{x} < 0\,, \tag{7}$$

which can be written as:

$$\frac{dP_1}{dt} - \frac{dP_2}{dt} = \frac{M}{A}\dddot{x} + \frac{a_2}{A}\ddot{x} + \frac{2a_1\dot{x}\ddot{x}}{A}sign(\dot{x})\,. \tag{8}$$

Note: the transient impulse due to the derivative of sign ($\dot{x}$) at 0 is neglected in this model.

A second nonlinearity which arises in the EHA system is due to pipe/entrance losses. Due to the symmetry of the EHA, the pump/actuator pipe connection is modeled as a pressure drop, P_{pipe}, which is a function of flow. In the EHA system, P_{pipe} is approximately modeled by using Darcy's pipe flow equation as:

$$P_{pipe} \approx K_{pipe}Q_L^2 \approx K_{pipe}D_p^2\omega_p^2 \tag{9}$$

Although it is most desirable to include all identifiable nonlinearities in the model, it is recognized that the resulting complexity would interfere with the proposed controller in the first instance. Preliminary studies showed that this nonlinearity was known to be small compared to the actuator friction effects and hence it was decided to linearize pipe flow. Thus in a linearized form:

$$\Delta P_{pipe} \approx 2K_{pipe}D_p^2\omega_{p0}\Delta\omega_p \tag{10}$$

Substituting Eqs (6), (8) and (10) into Eq. (1) yields,

$$\begin{aligned} &D_p\left(1 - 4K_{pipe}\xi D_p\omega_{p0}\right)\omega_p = \frac{MV_0}{A\beta_e}\dddot{x} \\ &+ \left(\frac{a_2V_0 + M\beta_e(\xi + L/2)}{2A\beta_e}\right)\ddot{x} + \frac{A^2 + a_2(\xi + L/2)}{A}\dot{x} \\ &+ \frac{2a_1V_0\dot{x}\ddot{x} + \beta_e(\xi + L/2)(a_1\dot{x}^2 + a_3)}{A\beta_e}sign(\dot{x}) \end{aligned} \tag{11}$$

In practice, $4K_{pipe}D_p\xi\omega_{p0} << 1$. Choosing the state variables, x_i, as shown in Eq (12) it is more convenient to convert these state equations into a discrete form. Assuming the presence of system noise, and using the sampling period, T_s, replacing the input term ω_p as u (a more general form of the input), the state-space discrete equations may be approximated (using the "forward difference" approach to discretization) as:

$$\begin{cases} x_1(k+1) = x_1(k) + T_s x_2(k) + T_s w_1(k) \\ x_2(k+1) = x_2(k) + T_s x_3(k) + T_s w_2(k) \\ x_3(k+1) = \left[1 - T_s \left(\dfrac{a_2 V_0 + M\beta_e(\xi + \frac{L}{2})}{MV_0} \right) \right] x_3(k) \\ \quad - T_s \dfrac{(A^2 + a_2(\xi + \frac{L}{2}))\beta_e}{MV_0} x_2(k) \\ \quad - T_s \dfrac{2a_1 V_0 x_2(k) x_3(k) + \beta_e(\xi + \frac{L}{2})[a_1 (x_2(k))^2 + a_3]}{MV_0} sign(x_2(k)) \\ \quad + T_s \dfrac{AD_p\beta_e}{MV_0} u(k) + T_s w_3(k) \end{cases} \tag{12}$$

The discrete equation can be now represented by the more generic form:

$$\mathbf{x}(k+1) = \mathbf{x}(k) + T_s \hat{f}(\mathbf{x}(k)) + T_s b(\mathbf{x}(k))u(k) + T_s \Delta(k) \tag{13}$$

4 SLIDING MODE CONTROL

SMC is fairly simple to implement and has been effective in controlling against external disturbances and parameter variations [22]. The theory and application of SMC design can be broken down into two steps:

1. design of a sliding surface that represents the desired system dynamics, and,
2. development of a control law that makes the sliding surface "attractive" (which means that there exists a part of surface in the neighborhood of which all the state trajectories are directed towards.).

Before designing the controller, it is necessary to represent mathematically a generic discrete model which includes uncertainties. Consider the following class of uncertain systems:

$$\dot{\mathbf{x}}(\mathbf{t}) = \hat{F}(\mathbf{x}, t, u) = \hat{f}(\mathbf{x}, t) + \hat{b}(\mathbf{x}, t)u(\mathbf{x}, t) + \Delta f(\mathbf{x}, t) \tag{14}$$

where $x(t) \in R^n$ is the state vector , $u(t)$ is the input signal and $\Delta f(x,t)$ is the time-dependent parameter uncertainties with known upper bound. $\hat{f}(x,t)$ and $\hat{b}(x,t)$ are known functions determining the system characteristics, where

$$\hat{f}(\mathbf{x},t) = \left[\hat{f}_1(\mathbf{x},t) \quad \hat{f}_2(\mathbf{x},t) \quad \cdots \quad \hat{f}_n(\mathbf{x},t)\right]^T ,$$

$$\hat{b}(\mathbf{x},t) = \left[\hat{b}_1(\mathbf{x},t) \quad \hat{b}_2(\mathbf{x},t) \quad \cdots \quad \hat{b}_n(\mathbf{x},t)\right]^T$$

$$\begin{aligned} \Delta f(\mathbf{x},t) &= \left[\Delta f_1(\mathbf{x},t) \quad \Delta f_2(\mathbf{x},t) \quad \cdots \quad \Delta f_n(\mathbf{x},t)\right]^T \\ &= \left[\hat{f}_1(\mathbf{x},t) - f_1(\mathbf{x},t) \quad \hat{f}_2(\mathbf{x},t) - f_2(\mathbf{x},t) \quad \cdots \quad \hat{f}_n(\mathbf{x},t) - f_n(\mathbf{x},t)\right]^T \end{aligned} \tag{15}$$

where $f(.) = \left[f_1(.) \quad f_2(.) \quad \cdots \quad f_n(.)\right]$ is the function describing the plant, which is unknown in practice due to system uncertainties. The unknown exact input matrix *b* can be written as the product of the uncertain input matrix $\hat{b}$ and a scalar uncertainty factor $\Delta b(\cdot)$, which is bounded such that $1/\beta \le \Delta b \le \beta$ for $\beta > 1$, and

$$b(x(k)) = \hat{b}(\mathbf{x}(k))\Delta b(\cdot) \tag{16}$$

The approach of "forward difference" approximation is used in the discretization of the state space model at any time T_s and given by:

$$\begin{aligned} &\dot{x}_i = \frac{x_i(k+1) - x_i(k)}{T_s} + \delta_i(k) \\ &i = 1,2,\cdots n \end{aligned} \tag{17}$$

where T_s is the sampling time and the term $\delta_i(k)$ denotes the numerical approximation error. The discrete form of Eq. (14) can be written in the form of Eq (13). The general form of Eq (13) will now be used to design the sliding surface and the controller.

4.1 Sliding Surface Design

In sliding mode control, the full-order discrete-time system given in Eq. (13) is transformed into the cascade of two reduced-order subsystems, referred to as the "regular" form,

$$\mathbf{z}_1(k+1) = \mathbf{z}_1(k) + T_s \hat{f}_1(\mathbf{z}(k)) + T_s \Delta_1(k) \tag{18}$$

$$\mathbf{z}_2(k+1) = \mathbf{z}_2(k) + T_s \hat{f}_2(\mathbf{z}(k)) + \hat{b}_2 u(k) + T_s \Delta_2(k) \tag{19}$$

where $\mathbf{z}_1(k) \in R^{n-m}$, $\mathbf{z}_2(k) \in R^m$. This decomposition is done by applying a linear transformation, $\mathbf{z}(k) = T\mathbf{x}(k)$, where T is a diffeomorphic transformation. In order to design a linear sliding surface, only Eq. (18) is required. However, in this form, only z_2 contains the input variable. Thus it is necessary to choose a different form of T to define a new equation that does contain the input but is still linear. One such transformation is given by: $T\hat{b} = [0 \quad \hat{b}_2]^T$, [23]. It is assumed without loss of generality that Eq. (18) is linear such that it can be written in the form:

$$\mathbf{z}_1(k+1) = [\hat{\Phi}_{11} \quad \hat{\Phi}_{12}] \begin{bmatrix} \mathbf{z}_1(k) \\ \mathbf{z}_2(k) \end{bmatrix} + T_s \Delta_1(k) \tag{20}$$

where $\hat{\Phi}_{11}, \hat{\Phi}_{12}$ are constants. As an example and referring to the EHA model of equations of (12) and (13), $\hat{\Phi}_{11}, \hat{\Phi}_{12}$ can be obtained using diffeomorphic transformation matrix T=[$\boldsymbol{I}_3$] such that $\hat{\Phi}_{11} = \begin{bmatrix} 1 & T_s \\ 0 & 1 \end{bmatrix}, \hat{\Phi}_{12} = \begin{bmatrix} 0 \\ T_s \end{bmatrix}$.

In the derivation of the sliding surface, the known part of the dynamic model will be used and the uncertainties such as the term $T_s \Delta_1(k)$ are assumed small and negligible.

In state tracking or trajectory following problems, the sliding surface is defined in terms of the error. The control problem becomes one of constraining the states $\boldsymbol{x}$ to follow a prescribed trajectory $\boldsymbol{x}_d$. Let

$$\mathbf{x_d}(k) = [x_d(k), \dot{x}_d(k), \cdots, x_d^{(n-1)}(k)] \tag{21}$$

Defining the sliding surface is very problem dependent. For tracking control, it is not unusual to assume:

$$S(k) = \frac{\partial S(k)}{\partial \mathbf{x}_e} \mathbf{x}_e(k) = C(k)\, \mathbf{x}_e(k) = 0 \tag{22}$$

where. $\mathbf{x}_e(k) = \mathbf{x}_d(k) - \mathbf{x}(k)$. $C(k) = \dfrac{\partial S(k)}{\partial \mathbf{x}_e}$ is a real-valued vector.

In discrete form, $S(k+1) - S(k) = C(k)[\mathbf{x}_e(k+1) - \mathbf{x}_e(k)] + \sigma(k)$, where $\sigma(k)$ is the numerical approximation error for the sliding surface.

Using the transformation T, the parameter matrix of the switching function can be partitioned as:

$$S(k) = CT^T T\mathbf{x}_e(k) = [C_1 \quad C_2]\begin{bmatrix}\mathbf{z}_{1e}(k)\\ \mathbf{z}_{2e}(k)\end{bmatrix} \tag{23}$$

During an ideal sliding motion, the $\mathbf{z}_{2e(k)}$ can be expressed in terms of $\mathbf{z}_{1e(k)}$:

$$\mathbf{z}_{2e}(k) = -F\mathbf{z}_{1e}(k) \tag{24}$$

where $F = C_2^{-1}C_1$.

Assuming that the desired states satisfy the nonlinear model for a "hypothetical" control input [24], such that:

$$\mathbf{z}_{1d}(k+1) = [\hat{\Phi}_{11} \quad \hat{\Phi}_{12}]\begin{bmatrix}\mathbf{z}_{1d}(k)\\ \mathbf{z}_{2d}(k)\end{bmatrix}, \tag{25}$$

then,

$$\mathbf{z}_{1e}(k+1) = [\hat{\Phi}_{11} \quad \hat{\Phi}_{12}]\begin{bmatrix}\mathbf{z}_{1e}(k)\\ \mathbf{z}_{2e}(k)\end{bmatrix}, \tag{26}$$

where $\mathbf{z}_{1e}(k)$=$\mathbf{z}_{1d}(k)$-$z_1(k)$, $\mathbf{z}_{2e}(k)$=$\mathbf{z}_{2d}(k)$-$\mathbf{z}_2(k)$.

Consider the linear quadratic cost function:

$$J = \sum_{ksm}^{\infty} \mathbf{x}_e^T(k) Q \mathbf{x}_e(k), \tag{27}$$

where $Q > 0$ are symmetric matrices, and k is the step in which the sliding motion is starting. The objective is to choose the coefficients of the linear sliding surface such as to minimize this cost function. By using the same transformation T as for the states, and by partitioning the matrix Q, then

$$TQT^T = \begin{bmatrix}Q_{11} & Q_{12}\\ Q_{21} & Q_{22}\end{bmatrix}, \tag{28}$$

Defining, [22]:

$$\Gamma = Q_{11} - Q_{12}Q_{22}^{-1}Q_{21}, \tag{29}$$

and for:

$$\mathbf{v}(k) = \mathbf{z}_{2e}(k) + Q_{22}^{-1}Q_{21}\mathbf{z}_{1e}(k), \tag{30}$$

the quadratic cost function given in Eq. (27) can be written as:

$$J = \sum_{ksm}^{\infty} [\mathbf{z}_1^T(k)\Gamma\mathbf{z}_1(k) + \mathbf{v}^T(k)Q_{22}\mathbf{v}(k)] \tag{31}$$

where $Q_{22} > 0$ ensured by $Q > 0$ so that Q_{22} is nonsingular, and $\Gamma > 0$.

Combining Eqs. (26) and (30) to eliminate the $\mathbf{z}_{2e}$, the constraint equation may be written as:

$$\mathbf{z}_{1e}(k+1) = \hat{\Phi}\mathbf{z}_{1e}(k) + \Phi_{12}\mathbf{v}(k) \tag{32}$$

where $\hat{\Phi} = \Phi_{11} - \Phi_{12}Q_{22}^{-1}Q_{21}$.

A positive-definite unique solution *P* is guaranteed by the discrete algebraic Riccati equation defined as:

$$P\hat{\Phi} + \hat{\Phi}^T P - P\Phi_{12}Q_{22}^{-1}\Phi_{12}^T P + \Gamma = 0. \tag{33}$$

Thus the problem becomes one of minimizing the function of Eq (31) constrained by Eq (32), which can be restated as a standard optimal control law $\mathbf{v}(k)$ given as:

$$\mathbf{v}(k) = -Q_{22}^{-1}\Phi_{12}^T P\mathbf{z}_{1e}(k). \tag{34}$$

Substituting (34) into (30) yields:

$$\mathbf{z}_{2e}(k) = -Q_{22}^{-1}(Q_{21} + \Phi_{12}^T P)\mathbf{z}_{1e}(k) = -F\mathbf{z}_{1e}(k) \tag{35}$$

From this equation, $F = Q_{22}^{-1}(Q_{21} + \Phi_{12}^T P)$ and by hence $C_2 = Q_{22}$ and $C_1 = (Q_{21} + \Phi_{12}^T P)$.

Thus the sliding surface coefficients (embedded in F) can be determined by solving the discrete Riccati Eq. (33). This, then, is the first application of the linear quadratic method to a discrete nonlinear problem for sliding surface determination and is considered to be a very important contribution to this area. This optimally defined sliding surface is used in the following section in the derivation of the control law.

4.2 Controller

Sliding mode control (SMC) is a powerful control methodology for both linear and nonlinear systems because of its robustness to parameter changes, external disturbances and unmodelled dynamics. The equivalent control method for nonlinear systems was proposed by Utkin in 1977 [25]. The control law may be selected such that a "candidate" Lyapunov function satisfies Lyapunov stability criteria. The control signal will then ensure existence of a sliding mode on the surface *S*=0, which is determined as:

$$u(t) = \hat{u}_{eq}(t) + u_c(t) \tag{36}$$

where $\hat{u}_{eq}(t)$ is the estimated equivalent control and $u_c(t)$ is the corrective control or discontinuous term.

u_{eq} is the continuous input that would maintain the system on the sliding hyperplane in the absence of a corrective term. In practice, the presence of uncertainties makes an exact calculation of the equivalent control input impossible. Slotine in 1984 proposed a sliding mode controller for continuous nonlinear systems in the presence of parametric variations and uncertainties, [18]. A discrete but similar approach is considered in this paper. For discrete-time nonlinear systems with large uncertainties, the discrete controller proposed by Misawa [20] is adopted here. This controller is expressed as

$$u(k) = \frac{\beta^2 + 1}{2\beta}\hat{p}(k) + \left[\frac{\beta^2 - 1}{2\beta}\,|\,\hat{p}(k)\,| + \frac{\beta K}{\hat{b}(\mathbf{x}(k))C(k)}\right]\cdot sat\left(\frac{S(k)}{\phi(k)}\right) \tag{37}$$

where

$$\hat{p}(k) = \frac{C(k)}{\hat{b}(x(k))C(k)}\left[-\hat{f}(\mathbf{x}(k)) + \frac{\Delta\mathbf{x}_d(k)}{T_s}\right] \tag{38}$$

and $\Delta\mathbf{x}_d = \mathbf{x}_d(k+1) - \mathbf{x}_d(k)$. K is the sliding mode gain which is specified as $K = \sigma(k) - T_s C(k)\Delta(k) + 2\varepsilon$, where ε is an arbitrary positive constant and β is an adjustment coefficient. In the general case of nonlinear systems, the sliding surface can be chosen as a nonlinear function with an associated time index as shown in Eqs. (37) and (38). But for the controller implemented in this paper, the sliding surface is taken as linear and $C(k)$ is a constant vector determined by solving Eq. (33) as indicated in the previous section.

To remove the chattering caused by the discontinuous control signal, a smoothing boundary layer is defined as:

$$\Psi = \{\mathbf{x}_e(k)\,||\,S(\mathbf{x}_e(k)) \le \phi(k)\} \tag{39}$$

In this result, Misawa [20] has defined the value of $\phi(k)$ (evaluated to be a maximum value which depends on $\Delta b(\cdot)$) is selected as β or $1/\beta$ based on the sign of S and $\hat{p}(k)$. But, the width of the boundary layer is a conservatively large number as first proposed in [20]. To obtain a more accurate trajectory following, the boundary layer can be adjusted by some gain γ to make the boundary layer width smaller, such that,

$$\phi(k) \geq \frac{T_s}{2}\{\hat{b}(\mathbf{x}(k))C(k)\frac{(\beta^2-1)}{2\beta^2}\cdot\gamma\cdot[(3\beta^2+1)\mid \hat{p}(k)\mid + (\beta^2-1)\hat{p}(k)sat\left(\frac{S(k)}{\phi(k-1)}\right)] + (1+\beta^2)\Sigma(k) + 2\beta^2\varepsilon\} \quad (40)$$

where $0<\gamma<1$, $\Sigma(k)=\sigma(k)-T_s C(k)\Delta(k)$ [20].

Further to above, the control law is defined by Eqs. (37), (38) and (40)) and by solving the Riccati Eq. (33) for the definition of the sliding surface. The numerical values for the control law as they pertain to the EHA system are provided in the following Section 5.

5 SIMULATION AND EXPERIMENTAL RESULTS

The model of the EHA can be expressed in the form of Eq. (12). This model contains uncertainties where the parameters such as $\hat{a}_1, \hat{a}_2, \hat{a}_3, \hat{A}, \hat{M}, \hat{C}_T, \hat{D}_p, \hat{\beta}_e, \hat{V}_0$ are not exactly known and may be subject to perturbations. As such, w_i's are used to denote lumped disturbances and uncertainties. Consider the following cases that assume different levels of uncertainty. These cases are presented by using computer simulation and are complemented by experimental tests on the EHA plant.

Case I

In this simulation, the variations in the parameters are assumed to be zero (therefore the model is assumed to be known). A gain scheduled proportional controller, proposed by Sampson et al [13] was used on the nonlinear EHA plant in order to provide a comparison with the performance of the Sliding Mode Controller. The nonlinear gain scheduled proportional controller (SPC) is illustrated in Fig. 3. The proportional gain is switched from 6980 to 42800 depending on whether the error signal was greater or less than $5\times10^{-4}\,m$. In this simulation study, the acceleration waveform was chosen such the position signal waveform resembled a step input for the period under consideration. Thus in all appropriate figures (Fig. 4, for example), the desired position input is not a "perfect" step waveform and is defined as a "quasi-step". The simulated EHA output position tracking and its desired trajectory are shown in Fig. 4. For final position control, the steady-state error is shown in Fig. 5. The oscillation effects caused by discontinuous friction are evident in these results.

In applying the SMC to the same plant, the sliding surface coefficients are chosen as $C(k)=[30.5 \quad 33.1 \quad 1]$ and the gains set to $\beta=1$ (assumed there are no uncertainties in model), and

$\gamma = 0.5$ (which is dependent on a best accuracy obtained in simulation results). The output displacement and positional error for these conditions are shown in Fig. 6 and Fig. 7. These results show the sliding mode controller can demonstrate a very fast response with a "more accurate motion" (compared to the SPC) given the nonlinear EHA plant. The maximum error (Fig. 6) is less than $4\times10^{-5}\,m$ in simulation. From these results, it is observed that the SMC produces a much shorter rise or settling time than the SPC and no oscillation in steady-state.

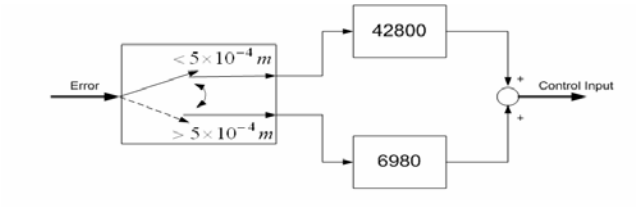

Fig. 3. Scheduled Proportional Controller for the EHA (after Sampson et al [13])

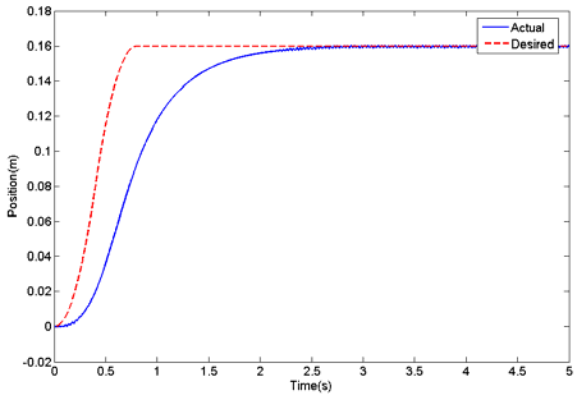

Fig. 4. Quasi-step Response of the SPC (Simulation)

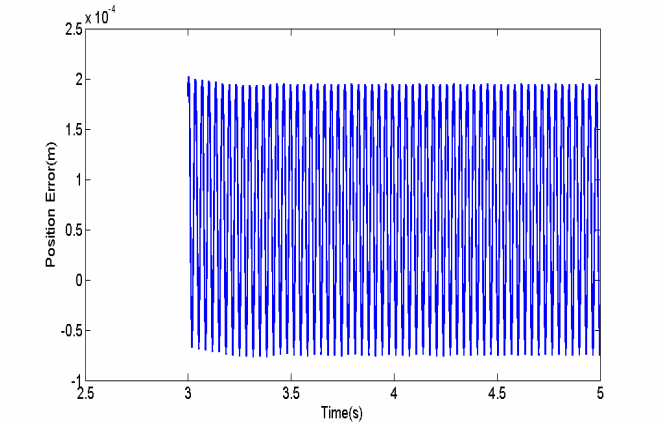

Fig. 5. Quasi-step Response Error of the SPC (Simulation)

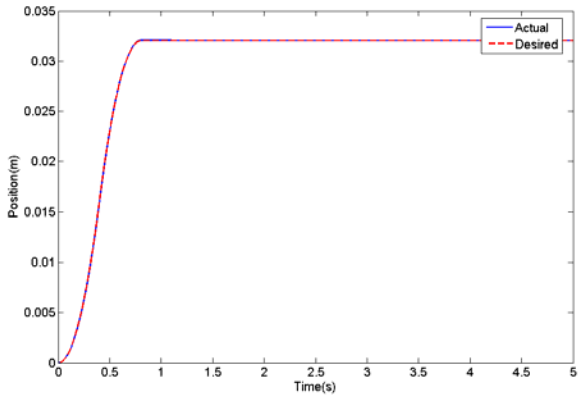

Fig. 6. Quasi-step Response of SMC (Simulation)

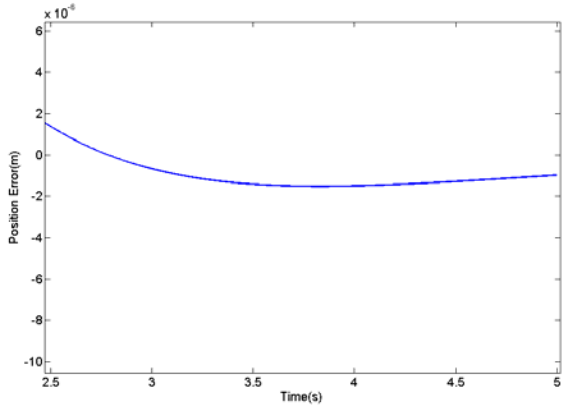

Fig. 7. Step Response Steady state Error of SMC (Simulation).

(Note that the error is "smooth" as compared to the oscillations observed SPC in Figure 5)

Case II

In order to improve the settling time of the SPC on the nonlinear EHA plant, the switched gain was increased by a factor of 4 such that:

$$\begin{cases} P\_gain = 27920 & \text{error} > 5\times10^{-4}\,m \\ P\_gain = 171200 & \text{error} \le 5\times10^{-4}\,m \end{cases}.$$

where *P_gain* is the scheduled proportional gain.

The step response with the new switched gain is shown in Fig. 8. The results show that the SPC also can obtain a very fast response with higher switched gains. However, because of discontinuous friction, oscillatory effects can also be observed in the system response as shown in Fig. 8 (just visible at steady

state) and Fig. 9 (quite dominant).

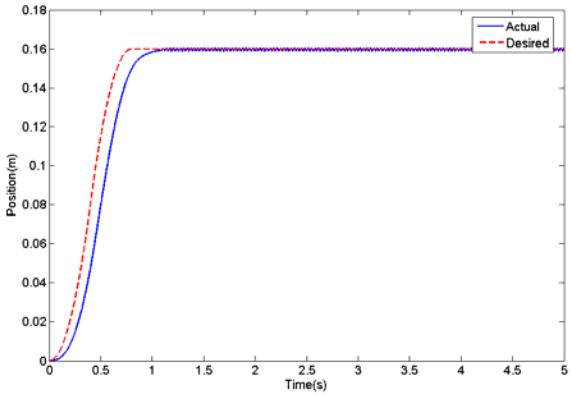

Fig. 8. Step Input Response of SPC (Simulation)

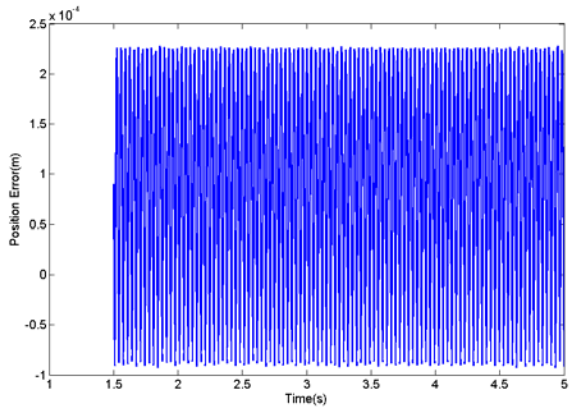

Fig. 9. Step Input Response Error of SPC (Simulation)

For the computer simulation study, it is should be noted that all the states (Position, Velocity, and Acceleration) of the system are available and can be used to verify the effectiveness of control performance. Given periodic input signals, the displacement, velocity and acceleration of the actuator for the SPC controller are shown in Fig. 10. The maximum errors between desired and actual states are summarized in Table 1 (presented after Case III).

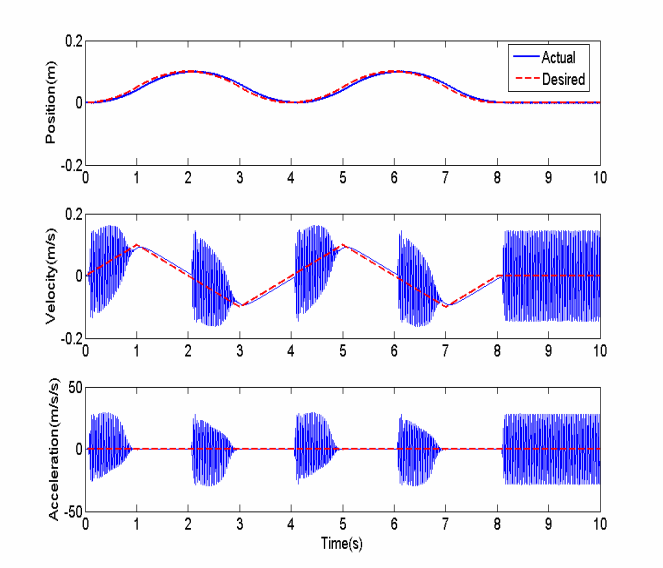

Fig. 10. Periodic Input Response of SPC (Simulation)

(Note that the desired acceleration is periodic square wave, but in this figure it does not appear as such due to the magnitude of the transient oscillation in acceleration)

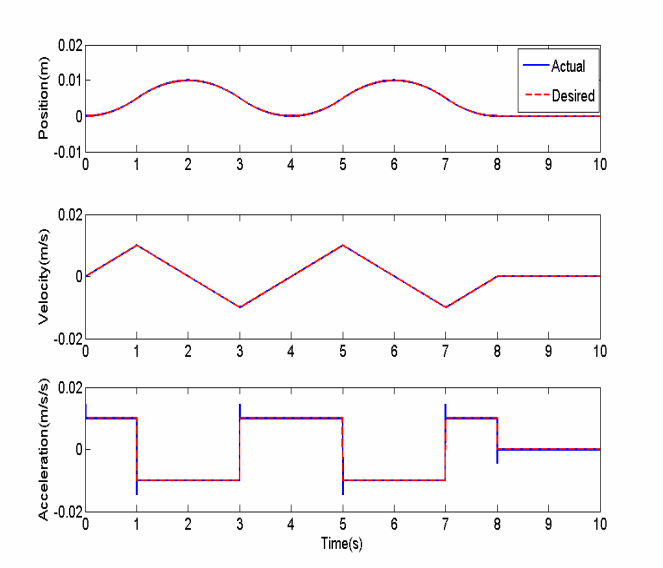

Fig. 11. Periodic Input Response of SMC (Simulation).

(This result can be compared to Figure 10 which demonstrates that the severe oscillations of the SPC are not evident here)

The EHA has been prototyped as shown in Fig. 12. Experimental studies from this prototype are used here to confirm the observations made by simulation. In practical experimental tests, only the position can be measured in the EHA system. But in this work, SMC is a full-feedback controller, which means all the states are needed for feedback. As a first step, the Extended Kalman Filter is used to provide an on-line

estimate of the states in the experimental tests and then these estimated states are fed back to the controller.

The SPC control law was applied to the EHA prototype as shown in Fig. 13. The same desired reference input as for the simulation case as shown in Fig. 10 is used to implement the experiment tests. The experimental results from this application of the SPC are shown in Fig. 14 to 15.

From the above simulation and experimental results, it is observed that there are visible transients in the output response of the EHA at the zero velocity cross over points or the maximum position points (such as at time 0, 2, 4, 6 seconds) using the SPC (Fig. 14). The SPC provides significant "kicks" at these time points. These coincide with regions where the discontinuity in friction occurs and support the hypothesis stipulated in [1].

For the sliding mode controller, the same periodic input signals are used as inputs to the experimental EHA prototype The same sliding surface and adjustment gains β , γ as in Case I, were chosen. The control law and its transient responses from experiments are shown in Fig. 16 and Fig. 17. The simulation results (as shown in Fig.11) and experimental results demonstrate that the oscillations in the output that are attributed to nonlinear friction have been removed by the application of the SMC without compromising the speed of system response (the maximum states errors are indicated in Table 1). There are no obvious "kicks" occurred in SMC control signal than in SPC.

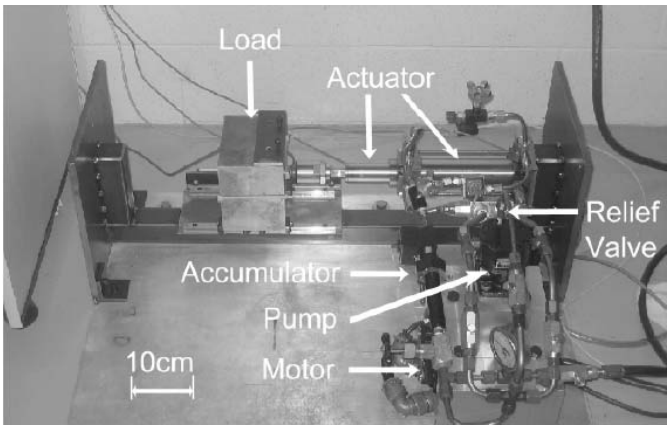

Fig. 12. The EHA Prototype

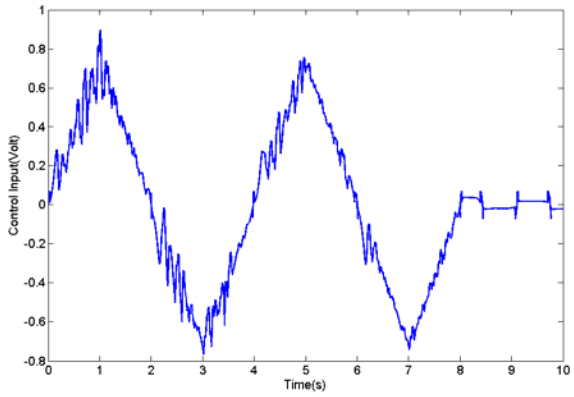

Fig. 13. The Control Law of Periodic Input of SPC (Experiment)

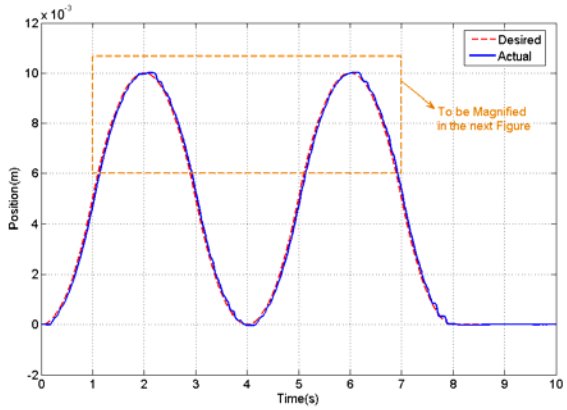

Fig. 14. The Position Response of Periodic Input of SPC (Experiment)

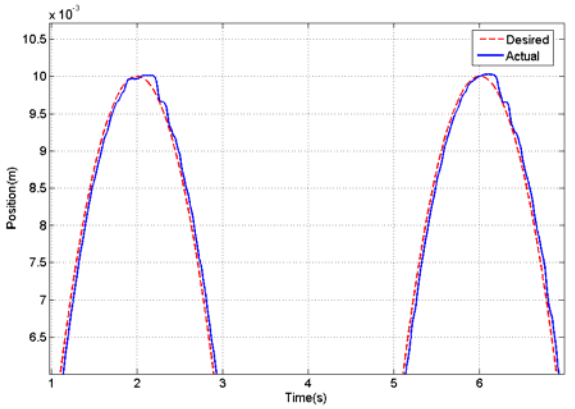

Fig. 15. The Magnified Position Response of Periodic Input of SPC (Experiment)

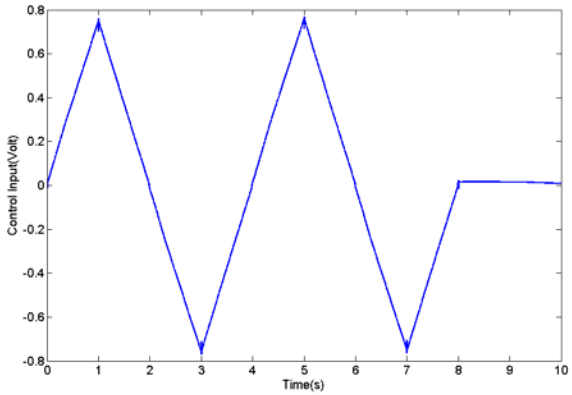

Fig. 16. The Control Law of Periodic Input of SMC (Experiment) (Note that this result is compared to Fig 13 which demonstrates that the "kicks" which are observed at the transient points of the SPC does not occur here)

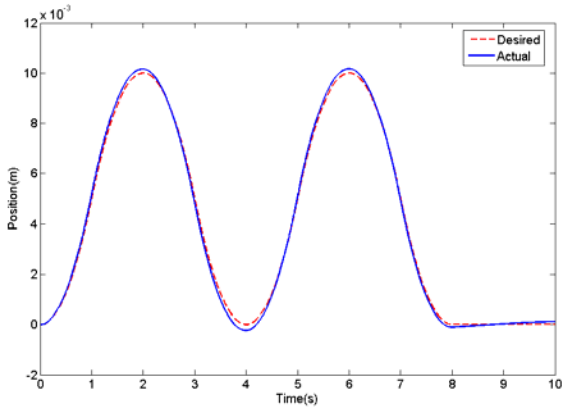

Fig. 17. The Position Response of Periodic Input of SMC (Experiment)

Case III.

The most important characteristic of SMC is its insensitivity to parametric variations, uncertainties, and rejection of external disturbances, i.e. robustness. In this case a 20% of parametric error (uncertainty) for all coefficients is injected into the nonlinear model of EHA at the same time such that:

$$[\hat{a}_1, \hat{a}_2, \hat{a}_3, \hat{A}, \hat{M}, \hat{C}_T, \hat{D}_p, \hat{\beta}_e]^T$$
$$= (1+0.2)*[a_1, a_2, a_3, A, M, C_T, D_p, \beta_e]^T .$$

The same periodic reference input was used as in case II. The sliding surface was defined by the discrete linear quadratic approach as $C(k) = [100 \quad 106 \quad 1]$ and adjustment gains $\beta = 1.1$ (considering the 20% uncertainties) and $\gamma = 0.5$ (which is dependent on the best performance obtained in practical tests). The simulated transient response of the states with respect to the desired input is shown in Fig. 18. The

position of load in the experimental tests is demonstrated in Fig. 19.

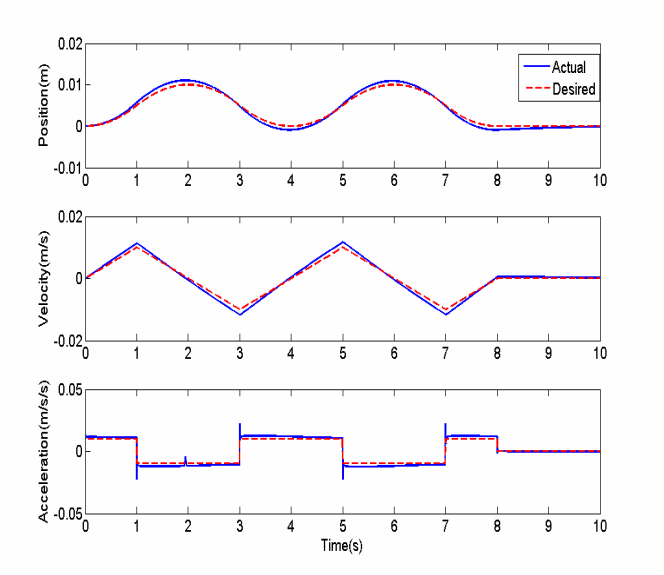

Fig. 18. Periodic Input Response of SMC for Nonlinear Model with 20% Uncertainties (Simulation)

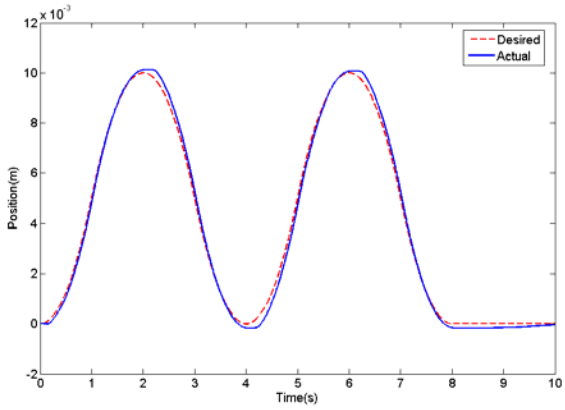

Fig. 19. The Position Response of Periodic Input of SMC with Nonlinear Model with 20% Uncertainties (Experiment)

		Maximum Errors from Simulation			Maximum Errors from Experiment
		Position (m)	**Velocity(m/s)**	**Acceleration(m/s^2)**	**Position(m/s)**
Case I	**SPC**	2×10^{-4}			
	SMC	3.5×10^{-5}			
Case II	**SPC**	0.01	0.15	20	3.5×10^{-4}
	SMC	5×10^{-6}	2×10^{-5}	0.02	3×10^{-4}
Case III	**SMC**	1×10^{-3}	2×10^{-3}	0.03	4×10^{-4}

Table 1 Maximum Errors of simulation and experiment study

The results show that even with 20% variation in the parameters, the proposed SMC shows an excellent trajectory following capability with minimal transient effects at the cross over points (maximum error of $4\times10^{-4}\,m$). But the steady state error of states is increased compared to Case II due to the large level of uncertainties.

The controller is successful in both cases (involving a known model and the nonlinear model allowing for uncertainties) in compensating the oscillations due to static friction (observed in Fig. 10 and Fig. 14). The effect of the controller can be explained by considering the elements that make up the control signal. In essence, the control signal (input to the plant) consists of two elements that are its continuous and its discontinuous (switching) elements. There is a limit in the size of the gains associated with the continuous element of the controller that is determined by the stability of the closed loop system. To alleviate the effect of static friction this gain would need to increase at the expense of stability. In the controller presented in this paper, the gain of the continuous element of the control signal is indeed set to a conservative level that satisfies the stability considerations. The added control action needed for compensating for static friction is provided by the discontinuous element of the control signal. The discontinuous terms comes into effect only when the error is greater than the width of the smoothing boundary layer. In this case, it compensates the uncertainty due to friction in the small error margins that the static friction is significant and thus alleviates its effects without causing instability or oscillations.

The importance of the presented controller becomes evident when considering the application that is considered in this paper. The EHA actuator is capable of moving large loads with extreme precision. Static friction is an important limiting factor for this level of precision. The SMC controller compensates static friction here without the necessity of implementing high gains that could result in instability.

6 CONCLUSIONS

The paper considers the application of sliding mode control to a hydrostatic actuation system with discontinuous and nonlinear friction effects. The associated sliding surface design is defined by using a linear quadratic cost function. This is the first application of the linear quadratic method to a discrete nonlinear problem for the determination of the switching hyperplane.

An important controller design consideration for systems with discontinuous friction is the oscillations that can occur given small input signals at crossover regions where the sign of the velocity changes. The Sliding Mode Controller proposed in this paper shows little sensitivity to discontinuous friction and

alleviates the above mentioned oscillations. A comparative study with a gain-scheduled proportional controller demonstrates the robustness and performance benefits of the SMC.

ACKNOWLEDGEMENTS

The authors would like to acknowledge the financial support of the University of Saskatchewan and National Science and Engineering Research Council of Canada (NSERC).

REFERENCES

[1] Qian, W., Burton, R., Schoenau, G., and Ukrainetz, P., 1998, "Comparison of a PID controller to a neural net controller in a hydraulic system with nonlinear friction", in Proceedings of the 1998 ASME International Mechanical Engineering Congress and Exposition, 5, pp. 91-98.
[2] Armstrong-Helouvry, B., Dupont, P., and Canudas de Wit, C., 1994, "Asurvey of models, analysis tools and compensation methods for the control of machines with friction", Automatica, 30(7), pp. 1083–1138..
[3] Dupont, P. E., "Avoiding stick-slip through PD control", IEEE Transactions on Automatic Control, 39(5), pp. 1059-1097.
[4] Yang, S., and Tomizuka, M., 1988, "Adaptive pulse width control for precise positioning under the influence of stiction and Coulomb friction", Journal of Dynamic Systems, Measurement and Control, 110(3) pp. 221-227.
[5] Qian, W., 1999, "Neural Network Control of Nonlinear Hydraulic System", Master Thesis, Dept. of Mechanical Engineering, University of Saskatchewan.
[6] Dupont P. E., 1993, "The effect of friction on the forward dynamics problem", International Journal of Robotics Research, 12(2), pp. 164-179.
[7] Friedland , B., and Park, Y., 1992, "On adaptive friction compensation", IEEE Transactions on Automatic Control, 37(10), pp. 1609-1612.
[8] Besan-con-Voda, A., and Blaha, P., 2002, "Describing function approximation of a two-relay system configuration with application to Coulomb friction identification", Control Engineering Practice, 10, pp.655–668.
[9] Habibi, S. R., Pastrakujic, V., and Goldenberg, A. A., 2000, "Model identification of a high performance hydrostatic actuation system", American Society of Mechanical Engineers, The Fluid Power and Systems Technology Division (Publication) FPST, 7, pp. 113-119.
[10] Chinniah, Y. A., 2004, "Fault Detection In the Electrohydraulic Actuator Using Extended Kalman Filter", Ph.D Dissertation, Dept. of Mechanical Engineering, University of Saskatchewan.
[11] Habibi, S. R., and Goldenberg, A., 2000, "Design of A New High-Performance ElectroHydraulic Actuator", IEEE/ASME Transactions on Mechatronics, 5(2), pp. 158-164.
[12] Habibi, S. R., and Singh, G., 2000, "Derivation of Design Requirements for Optimization of A High Performance Hydrostatic Actuation System", International Journal of Fluid Power, 2, pp. 11-27.
[13] Sampson, E., Habibi, S., Burton, R., and Chinniah, Y., 2004, "Effect of controller in reducing steady-state error due to flow and force disturbances in the electrohydraulic actuator system", International Journal of Fluid Power, 5(2), pp. 57-66.
[14] Utkin, V., 1978, "Sliding Mode and Their Application in Variable Structure Systems", English translation, Mir Publication, Moscow.
[15] Utkin, V. I, and Yang, K. D., 1978, "Methods for constructing discontinuity planes in multidimensional variable structure systems", Automation and Remote Control, 39, pp. 1466-1470.
[16] Spurgeon, S. K., 1992, "Hyperplane Design Techniques for Discrete-Time Variable Structure Control Systems", International Journal of Control, 55(2), pp.445-456.
[17] DeCarlo, R. A., Zak, S. H., and Drakunov, S. V., 1996, "Variable structure, sliding-mode controller design", in W. S. Levine, editor, The Control Handbook, CRC Press, Boca Raton, FL, pp. 941-951.
[18] Slotine, J.-J. E., 1984, "Sliding Controller Design for Non-linear Systems", International Journal of Control, 40(2), pp.421-434.
[19] Decarlo, R. A., Zak, S. H., and Matthews, G. P., 1988, "Variable Structure Control of Nonlinear Multivariable Systems: A Tutorial", in Proceedings of the IEEE, 76(3), pp. 212-232.
[20] Misawa, E. A., 1997, "Discrete-Time Sliding Mode Control for Nonlinear Systems with Unmatched Uncertainties and Uncertain Control Vector", ASME Journal of Dynamic Systems, Measurement, and Control, 119, pp. 503-512.
[21] Yasuda, Y., Mano, S. , Mori, N. , Azegami, T. , and Crotty, S., 1990, "PID controller with overshoot suppression algorithm", Proceedings of the ISA '90 International Conference and Exhibition Part 4 (of 4), 45(pt4), pp. 1849-1857.
[22] Edwards, C., and Spurgeon, S. K., 1998, "Sliding Mode Control: Theory and Applications", Taylor & Francis Ltd.
[23] Hunt L. R., Su, R., and Meyer, G., 1983, "Global Transformations of Nonlinear Systems", IEEE Transactions on Automatic Control, 28(1), pp. 24-31.
[24] Misawa, E. A., 1997 "Discrete-Time Sliding Mode Control: The Linear Case", ASME Journal of Dynamic Systems, Measurement, and Control, 119, pp. 819-821.
[25] Utkin, V. I., 1977, "Variable structure system with sliding modes", IEEE Transactions on Automatic Control, AC-22, pp. 212-222.

Appendix C: A Smooth Variable Structure Filter for State Estimation (Wang, et al [2006])[*]

[*] This paper is under reviewed by the Journal of Control and Intelligent Systems. This paper is included with the express permission of the journal's publishers.

[1]A SMOOTH VARIABLE STRUCTURE FILTER FOR STATE ESTIMATION

Shu Wang* Saeid Habibi** Richard Burton***

Abstract

A new method of filtering strategy, referred to as the Smooth Variable Structure Filter (SVSF) is reviewed and applied to the problem of state estimation. The reaching stability of the SVSF (closely related to that of Variable Structure Control (VSC)), is verified by a mathematical proof. The mathematical foundation behind, and the methodology of SVSF are presented. The robustness of SVSF to system noise, measured noise and parameter variations is verified by a numerical example.

Key Words

Smooth Variable Structure Filter, State Estimation, Inverse Function

1. Introduction

A "full-state feedback" control system is based on the assumption that all the state variables can be measured. However, in practice not all state variables are available due to the cost, accuracy, or availability of appropriate transducers [1]. Under some circumstances, it is possible to estimate the states which are then fed to the controller rather than actual states.

One of the earliest approaches to state estimation (also referred to as filtering) was forwarded by Kalman who defined a systematic approach to linear filtering based on the method of least-squares [2] and [3]. An introduction to stochastic/random processes and

*College of Engineering, University of Saskatchewan, 57 Campus Drive, Saskatoon, SK, S7N 5A9, Canada, shw750@mail.usask.ca,
**Department of Mechanical Engineering, McMaster University, 1280 Main Street West, Hamilton, Ontario, L8S 4L7, Canada, habibi@univmail.cis.mcmaster.ca
***College of Engineering, University of Saskatchewan, 57 Campus Drive, Saskatoon, SK, S7N 5A9, Canada, richard.burton@usask.ca

both the theoretical and practical aspects of Kalman filtering are provided in [4]. The concept of an "observer" for a dynamic system was introduced in 1966 by Luenberger which was used to estimate unavailable state variables [5]. An adaptive filter was used to perform satisfactorily in an environment where knowledge of relevant statistics is not available [6]. The unscented filter was introduced for nonlinear systems indicating more accurate than the Extended Kalman Filter (EKF) [7]. The Particle filters, known as Sequential Monte Carlo Methods, are introduced as a sophisticated model estimation techniques based on simulation [8, 9, 10].

A filtering strategy defined as a Variable Structure Filter (VSF) [11] for state estimation was proposed by Habibi and Burton to be used for estimating the states of an observable Linear Time Invariant (LTI) systems. This filter was designed to estimate the states of systems with uncertainties and was found to be very robust in the presence of noise. As an extension of this work, a Smooth Variable Structure Filter (SVSF) was first presented in 2004 [12]. The SVSF is reviewed in this paper and modified to accommodate a limited class of discontinuities. The SVSF uses concepts closely related to Variable Structure Control. However, its implementation procedure is similar to the Kalman Filter [13]. Usually sliding observers use a constant feedback gain and a discontinuous vector to correct the predicted estimates of the system dynamics [14]. Although SVSF can be regarded as a special form of sliding observer, the function of the SVSF is to directly estimate the states of a system by a discontinuous component. This discontinuous component called a "SVSF gain", (which is calculated by transformation), is used to correct state estimates. The form of the SVSF gain, however, is different from the sliding observer gain and this will be expanded upon.

The SVSF is a novel state estimation strategy which is stable and has a simple formulation. An estimate of the state trajectory is generated by using an uncertain model of the system. The SVSF forces the estimated state trajectory towards the true state trajectory until it reaches a subspace referred to as the "existence subspace". The SVSF is a predictor corrector method and involves two stages. In the first stage of prediction, a model of the system under consideration is used to predict the state trajectories. In the second stage of correction, an SVSF gain is calculated and used to refine the estimated state variables.

2. Mathematical Background

In SVSF theory, it is required that an inverse function can be calculated from the system dynamical model. A "smooth function" is defined as one that is infinitely differentiable, i.e., has derivatives of all finite orders [15]. Thus, a necessary condition to obtain its inverse function is possessed by a smooth function. Given a smooth function $f:\Re^n \to \Re^n$, if the Jacobian is invertible at 0, then there is a neighbourhood U containing 0 such that $f:U \to f(U)$ is a diffeomorphism. That is, there is a smooth inverse $f^{-1}: f(U) \to U$, [16].. For a function f to have a valid inverse, it must be a bijection, which means the system is completely observable and completely controllable

In many systems, discontinuous behaviour appears in the operation of the plant or in the case of a VSC, the controller. To make the nonlinear terms compatible to the SVSF, several requirements associated with inverse functions must be satisfied. In the presence of discontinuous nonlinear terms (for example, caused by coulomb friction) in some control problems, it is impossible to obtain the inverse function. Here, an approximation may be used for smoothing out the discontinuity from the function, e.g. a sign function

being replaced by the hyperbolic tangent function as an example. For the function tanh(Cx), as C increases, then the tanh function approaches the sign function in the limit. The inverse of the hyperbolic tangent is often called the arc hyperbolic tangent function: $\operatorname{arctanh}(x) = \ln\left(\frac{\sqrt{1-x^2}}{1-x}\right)$. As such, this approximation is used for calculate the inverse function for the Smooth Variable Structure Filter.

3. SVSF Estimation

Control system models with no stochastic elements are called deterministic. Among the models with stochastic elements, the least complex are those with a single uncertain vector, containing additive noise terms while more complicated models have uncertain parameters, measurement errors, uncertain initial state vectors and time-varying parameters. For the SVSF, an estimate of the state trajectory is generated using a deterministic albeit uncertain model. The estimated trajectory is forced towards the true state trajectory by the use of a discontinuous gain until it reaches a neighbourhood of actual state trajectory; the size of this neighbourhood determines the accuracy of SVSF. This neighbourhood is referred to here as the "existence subspace". The existence subspace will enclose the actual state trajectory [12]. The SVSF is formulated such that once the estimated trajectory reaches the existence subspace; it remains confined within this neighbourhood without leaving, switching back and forth along the actual state trajectory.

Consider a nonlinear system which may be expressed by a smooth function, i.e. which can be infinitely differentiable, such that:

$$\dot{\mathbf{x}}(\mathbf{t}) = F(\mathbf{x}, t, u, w) = f(\mathbf{x}(t)) + b(\mathbf{x}(t))u(t) + d(\mathbf{x}, t) \quad (1)$$

where $f(\mathbf{x}(t))$ and $b(\mathbf{x}(t))$ are differentiable functions determining the system characteristics.

It is assumed that the relationship between the measurement signals and the states is linear, or at least piece-wise linear, such that:

$$\mathbf{z}(t) = H\mathbf{x}(t) + v(t) \tag{2}$$

where H is a constant matrix, and $v(t)$ is the measurement noise.

The approach of "forward difference" approximation is used in the discretization of the state space model at any time $T_s(k)$ and is given by:

$$\dot{x}_i = \frac{x_i(k+1) - x_i(k)}{T_s} + \delta_i(k) \;\; i = 1,2,\cdots n \tag{3}$$

where T_s is the sampling time and the terms of $\delta_i(k)$ are the numerical approximation errors. The discrete model of (1) can be written as:

$$\mathbf{x}_{k+1} = \mathbf{x}_k + T_s f(\mathbf{x}_k) + T_s b(\mathbf{x}_k) u_k + w_k \tag{4}$$

where $w_k = T_s[d_k - \delta_k]$ is the lumped uncertainty term.

The discrete-time form of (2) may be expressed as:

$$\mathbf{z}_k = H\mathbf{x}_k + v_k \tag{5}$$

The system w_k and measured v_k noise are assumed to have Gaussian distributions. To a high level probability, they are assumed to be amplitude bounded. Furthermore, the systems and measurement noise are assumed to be uncorrelated and upper bounded.

The SVSF is a predictor-corrector method that uses an internal model to predict an a priori estimate of states. The a priori estimate is corrected into an a posteriori state estimate through a corrective term K_{k+1}.

The SVSF estimation process is summarized as follows, [12]:

1. The a priori state estimate is predicted by using the estimated model of the system such that:

$$\hat{\mathbf{x}}_{k+1|k} = \hat{\mathbf{x}}_{k|k} + T_s \hat{f}(\hat{\mathbf{x}}_{k|k}) + T_s \hat{b}(\hat{\mathbf{x}}_{k|k}) u_k \quad (6)$$

The state estimate in (6) is obtained by using the previous a posteriori state estimate $\hat{\mathbf{x}}_{k|k}$ or at the inception of the process, by using the initial conditions, $\hat{\mathbf{x}}_0$. The estimated states are then used for predicting the a priori estimates of measurements such that:

$$\hat{\mathbf{z}}_{k+1|k} = \hat{H}\hat{\mathbf{x}}_{k+1|k} \quad (7)$$

2. A corrective gain $K_{k+1} \in \Re^n$ is calculated as a function of the error in the predicted output.

3. The a priori state estimate is refined into an a posteriori state estimate such that:

$$\hat{\mathbf{x}}_{k+1|k+1} = \hat{\mathbf{x}}_{k+1|k} + K_{k+1} \quad (8)$$

4. Steps 1 to 3 are iteratively repeated.

In the following section, a derivation for the corrective gain of stage 2 is provided.

4. SVSF Prediction

Let a surface be defined in the continuous time as:

$$S = \Lambda e \quad (9)$$

where the estimation error is $e = \mathbf{x} - \hat{\mathbf{x}}$, $\lambda_{ij} > 0$ are the components of vector of Λ. Thus the stability condition for the sliding mode may be stated as:

$$s_i \frac{d(s_i)}{dt} < 0 \quad (10)$$

where s_i are elements of S in (9).

Since constant $\lambda_{ij} > 0$, from (9) and (10), the stability condition may be written as:

$$e_i \frac{d(e_i)}{dt} < 0 \tag{11}$$

In practice, the states are not available for the calculation of the estimated error; hence, the measured output, $\mathbf{z}_k$, must be used in state estimation. In the discrete form, the a priori and a posteriori estimated errors in terms of measured output signals are defined as:

$$e_{z_{i_{k+1|k+1}}} = z_{i_{k+1}} - \hat{z}_{i_{k+1|k+1}} \tag{12}$$

$$e_{z_{i_{k+1|k}}} = z_{i_{k+1}} - \hat{z}_{i_{k+1|k}} \tag{13}$$

where $\hat{z}_{i_{k+1|k+1}}$ and $\hat{z}_{i_{k+1|k}}$ are elements of the following estimated output vectors:

$$\hat{\mathbf{z}}_{k+1|k+1} = \hat{H}\hat{\mathbf{x}}_{k+1|k+1} \tag{14}$$

$$\hat{\mathbf{z}}_{k+1|k} = \hat{H}\hat{\mathbf{x}}_{k+1|k} \tag{15}$$

The corrective term K_{k+1} is a discontinuous term that is designed to guarantee the stability of the estimation process. The SVSF gain K_{k+1} is used to force the estimated states to approach the desired trajectory. In order to derive the SVSF gain, a stability Lemma has to be considered.

Lemma 1: the stability condition of (11) is satisfied if:

$$\left| e_{z_{i_{k+1|k+1}}} \right|_{ABS} < \left| e_{z_{i_{k|k}}} \right|_{ABS} \tag{16}$$

It is should be noted that the physical meaning of the *Lemma 1* is that the error in state estimation for each step is reduced which means that the estimated states move closer to the desired trajectory, i.e., the actual system states.

Proof: Let a Lyapunov function be defined such that $\nu_k = e^2_{z_{k|k}}$. The estimation process is stable if $\left(\Delta\nu_{k+1} = e^2_{z_{k+1|k+1}} - e^2_{z_{k|k}}\right) < 0$. This stability condition is satisfied by equation (16).

For a completely controllable and a completely observable system model, the stability of the output estimate implies the stability of the state estimate.

The SVSF gain that would satisfy *Lemma 1* can be found from theorem 1 which states:

Theorem 1: Based on the stability condition, the SVSF gain may be chosen in the form of:

$$K_{k+1} = \hat{H}^{+}(\left|e_{z_{k+1|k}}\right|_{ABS} + \gamma\left|e_{z_{k|k}}\right|_{ABS})\,\mathrm{sgn}(e_{z_{i_{k+1|k}}}) \tag{17}$$

where $\gamma \in \Re^{m\times m}$ diagonal matrix, and its elements $0 \le \gamma_{ii} < 1$.

Proof: See Appendix A.

If the system is completely observable and completely controllable or bijective in the case of nonlinear systems, it is possible to construct a full state observer, i.e. SVSF. In the prediction stage of SVSF, the state vector may be divided into two parts: the state estimates with explicit measurements associated with them denoted as $y_k^{(m)}$ and the remaining state estimation $y_k^{(u)}$. To facilitate the development of the SVSF, a new form of output vector is defined that would correspond to the above mentioned state vector partition as follows:

$$\mathbf{y}_{k+1} = T\mathbf{x}_{k+1} = \begin{bmatrix} \mathbf{y}_{k+1}^{(m)} \\ \mathbf{y}_{k+1}^{(u)} \end{bmatrix} \tag{18}$$

where T is a transformation matrix, the superscripts of $^{(m)}$ and $^{(u)}$ means measured and unavailable state variables.

Thus, the upper partition of (18) can be replaced by the actual measured output described by (5). Now the output can be written as a summation of measured output vector (with a noise term) and estimated output vector as:

$$\mathbf{y}_{k+1} = \begin{bmatrix} \mathbf{z}_{k+1} \\ \mathbf{y}_{k+1}^{(u)} \end{bmatrix} \tag{19}$$

The problem now is to estimate $\mathbf{y}_k^{(u)}$ associated with the unavailable state partition of (19). For the discrete system model (4), rewriting the equation using the transformation T yields:

$$\Theta(\mathbf{y}_k, u_k, w_k, v_k) = T\mathbf{x}_{k+1} = T\{\mathbf{x}_k + T_s f(\mathbf{x}_k) + T_s b(\mathbf{x}_k)u_k + w_k\} \tag{20}$$

where T=[I_n], and I_n is a identity matrix with the dimension of $n \times n$.

The transformation model may be written as:

$$\mathbf{y}_{k+1} = \begin{bmatrix} \mathbf{z}_{k+1} \\ \mathbf{y}_{k+1}^{(u)} \end{bmatrix} = \Theta(\mathbf{y}_k, u_k, w_k, v_k) \tag{21}$$

For a reduced order form of the system, the transformed model (20) can be partitioned as two parts as:

$$\mathbf{y}_{k+1} = \begin{bmatrix} \mathbf{z}_{k+1} \\ \mathbf{y}_{k+1}^{(u)} \end{bmatrix} = \begin{bmatrix} \Theta_1(\mathbf{z}_k, \mathbf{y}_k^{(u)}, u_k, w_k, v_k) \\ \Theta_2(\mathbf{z}_k, \mathbf{y}_k^{(u)}, u_k, w_k, v_k) \end{bmatrix} \tag{22}$$

Since the model of (1) assumes all smooth functions, and assumes Θ_1 *and*, Θ_2 are both smooth functions inherently (because the transformation T=[I_n]), the estimated output $\mathbf{y}_k^{(u)}$ can be calculated by the unique inverse functions from (22) as:

$$\begin{bmatrix} \mathbf{y}_k^{(u)} \\ \mathbf{y}_k^{(u)} \end{bmatrix} = \begin{bmatrix} \Theta_1^{-1}(\mathbf{z}_k, \mathbf{z}_{k+1}, u_k, w_k, v_k) \\ \Theta_2^{-1}(\mathbf{z}_k, \mathbf{y}_{k+1}^{(u)}, u_k, w_k, v_k) \end{bmatrix} \tag{23}$$

Similarly, as in the estimated model of (6) and (7), the a posteriori and priori estimation can be expressed as estimated functions following the form of (23). Define an estimated term for the upper partition of (23) without noise term as:

$$\hat{\sigma}_{k+1} = \hat{\Theta}_1^{-1}(\mathbf{z}_k, \mathbf{z}_{k+1}, u_k) \tag{24}$$

The priori estimated states can be derived from the lower partition of (23) as:

$$\hat{\mathbf{y}}_{k+1|k}^{(u)} = \hat{\Theta}_2(\mathbf{z}_k, \hat{\sigma}_k, u_k) \tag{25}$$

Thus, unavailable state estimate are refined by the SVSF gain K_{k+1} as:

$$\hat{\mathbf{y}}_{k|k}^{(u)} = \hat{\mathbf{y}}_{k|k-1}^{(u)} + K_{k+1}^{(u)} \tag{26}$$

where the $K_{k+1}^{(u)}$ are the elements for unavailable states in the SVSF gain vector.

The a priori error between the estimations from the measured state partition and unavailable state partition of the output matrix may be defined as:

$$e_{y_{k+1|k}}^{(u)} = \hat{\sigma}_{k+1} - \hat{\mathbf{y}}_{k+1|k}^{(u)} = \hat{\Theta}_1^{-1}(z_k, z_{k+1}, u_k) - \hat{\Theta}_2(z_k, \hat{\sigma}_k, u_k) \tag{27}$$

The a posteriori error can therefore be defined as:

$$e_{y_{k|k}}^{(u)} = \hat{\sigma}_k - \hat{\mathbf{y}}_{k|k}^{(u)} \tag{28}$$

Since the estimated term $\hat{\sigma}_{k+1}$ is derived from the canonical form of the discrete nonlinear model, the calculation process resembles the differential of the previous states in the states vector. The system noise may also be magnified by this calculation process

which is dependent on the sampling time. The SVSF corrective gain of the unavailable states may be adjusted by a gain which is sampling time T_s, and can be defined in the same form of (17) as:

$$K_{k+1}^{(u)} = T_s(\left|e_{y_{k+1|k}}^{(u)}\right|_{ABS} + \gamma^{(u)}\left|e_{y_{k|k}}^{(u)}\right|_{ABS})\,\mathrm{sgn}(e_{y_{k+1|k}}^{(u)}) \tag{29}$$

Note that as an example, the output matrix $\hat{H}$ is of the commonly used form in engineering systems which is a pseudo-diagonal matrix with elements equal to 1 such that $\hat{H} = [I_{m\times n}]$.

For the measured state partition, since all the elements of this partition can be measured, the SVSF gain can be written as:

$$K_{k+1}^{(m)} = (\left|e_{z_{k+1|k}}\right|_{ABS} + \gamma^{(m)}\left|e_{z_{k|k}}\right|_{ABS})\,\mathrm{sgn}(e_{z_{i_{k+1|k}}}) \tag{30}$$

Thus, the corrective SVSF gain can be expressed as a combination of (29) and (30):

$$K_{k+1} = \begin{bmatrix} K_{k+1}^{(m)} \\ K_{k+1}^{(u)} \end{bmatrix} = \begin{bmatrix} (\left|e_{z_{k|k-1}}\right|_{ABS} + \gamma^{(m)}\left|e_{z_{k|k}}\right|_{ABS}) \\ T_s(\left|e_{y_{k|k-1}}^{(u)}\right|_{ABS} + \gamma^{(u)}\left|e_{y_{k|k}}^{(u)}\right|_{ABS}) \end{bmatrix} \circ \begin{bmatrix} \mathrm{sgn}(e_{z_{i_{k|k-1}}}) \\ \mathrm{sgn}(e_{y_{k|k-1}}^{(u)}) \end{bmatrix} \tag{31}$$

The sign function in equation (31) leads to a high frequency switching effect that is referred to as chattering. To remove the chattering, the sgn(*vec*) in (31) may be replaced by the saturation function $sat(vec, \Psi)$ with elements defined as follows [17]:

$$sat(vec, \Psi) = \begin{cases} (vec_i / \Psi_i) \Leftrightarrow |\, vec_i / \Psi_i \,| \le 1 \\ sign(vec_i / \Psi_i) \Leftrightarrow |\, vec_i / \Psi_i \,| > 1 \end{cases} \tag{32}$$

$$K_{k+1} = \begin{bmatrix} K_{k+1}^{(m)} \\ K_{k+1}^{(u)} \end{bmatrix} = \begin{bmatrix} (\left|e_{z_{k+1|k}}\right|_{ABS} + \gamma^{(m)}\left|e_{z_{k|k}}\right|_{ABS}) \\ T_s(\left|e_{y_{k+1|k}}^{(u)}\right|_{ABS} + \gamma^{(u)}\left|e_{y_{k|k}}^{(u)}\right|_{ABS}) \end{bmatrix} \circ \begin{bmatrix} sat(e_{z_{k+1|k}}, \Psi_z) \\ sat(e_{y_{k+1|k}}^{(u)}, \Psi_y^{(u)}) \end{bmatrix} \tag{33}$$

The gain K_k obtained by (33) is used in the SVSF process to refine the a priori state estimates as indicated by (8).

5. Numerical Example

A nonlinear hydraulic system, referred to as ElectroHydraulic Actuator (EHA) system, is used in this section to illustrate the application of the SVSF method for state estimation. The EHA system was developed as a typical pump control hydrostatic system and based on the principle of closed circuit hydrostatic transmission as shown in Fig. 1. The particular EHA system was capable of moving large loads with sub-micron precision and large stroke. A nonlinear model with considering discontinuous and nonlinear friction effects in the EHA, is considered for the SVSF application. . A third order system which in its state space form is given by [18, 19].

$$\begin{cases} \dot{x}_1 = x_2 \\ \dot{x}_2 = x_3 \\ \dot{x}_3 = -a_3 x_3 - a_2 x_2 - [a_{11} x_2 x_3 + a_{12} x_2^{\,2} + a_{13}]\,\mathrm{sgn}(x_2) + bu \end{cases} \tag{34}$$

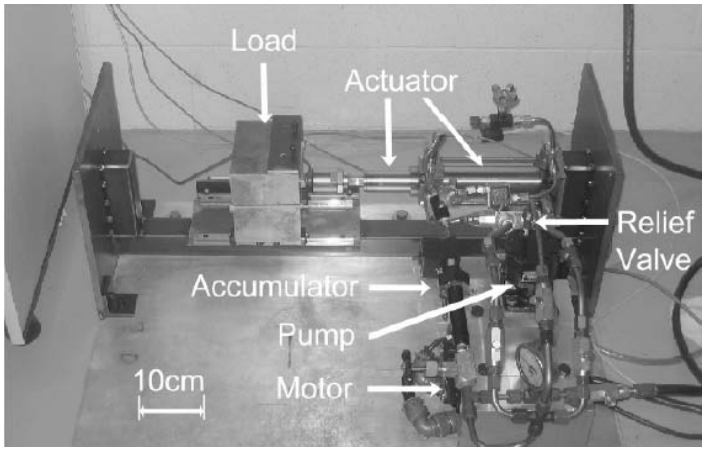

Figure 1. The EHA system

The model of this system is nonlinear and contains a discontinuous term involving a sign function $\mathrm{sgn}(x_2)$ of the second state x_2. In order to satisfy the smoothness requirement, the hyperbolic tangent with a high gain of 100, i.e. $\tanh 100x_2$, was used to

approximate to the term $\text{sgn}(x_2)$ based on the discussion in Section 2. A discrete system model is obtained as [20, 21]:

$$\begin{cases} x_1(k+1) = x_1(k) + T_s x_2(k) + T_s w_1(k) \\ x_2(k+1) = x_2(k) + T_s x_3(k) + T_s w_2(k) \\ x_3(k+1) = \left[1 - T_s a_3\right] x_3(k) - T_s a_2 x_2(k) - T_s [a_{11} x_2(k) x_3(k) + \\ \qquad a_{12}(x_2(k))^2 + a_{13}] \tanh(100 x_2(k)) + T_s b u(k) + T_s w_3(k) \end{cases} \tag{35}$$

In this system model, it is assumed that displacement and velocity can be measured only and acceleration is not available. In (35), the sampling time is T_s =0.001*s*. The maximum amplitude of system noise is set as: $W_{\max} = \begin{bmatrix} \max(T_s w_1(k)) \\ \max(T_s w_2(k)) \\ \max(T_s w_3(k)) \end{bmatrix} = \begin{bmatrix} 0.001 \\ 0.01 \\ 0.1 \end{bmatrix}$. The measurement from the system pertains to position and velocity and all the measurements are subjected to white noise of maximum amplitude of: $V_{\max} = \begin{bmatrix} \max(v_1) \\ \max(v_2) \end{bmatrix} = \begin{bmatrix} 0.001 \\ 0.001 \end{bmatrix}$. The initial condition of states is $\mathbf{x}_0 = [0 \quad 0 \quad 0]^T$. The input to the system is a random signal with amplitude in the range of -1000 to 1000 that correspond to the demanded pump speed in revolutions per minute in the hydrostatic system example. The coefficients of (35) are set as: $a_3 = -71$, $a_2 = 78100$, $a_{11} = 2100$, $a_{12} = 1610$, $a_{12} = 3.5$. The diagonal matrix γ is chosen as $\begin{bmatrix} 0.1 & 0 & 0 \\ 0 & 0.1 & 0 \\ 0 & 0 & 0.1 \end{bmatrix}$.

In a real application, the state variables are not available and therefore the exact value of the estimation error is unknown. However, in this study, the states and the estimation error are available and can be used to evaluate the effectiveness of the SVSF since the

study is based on computer simulation. The three actual (plant) and estimated states that represent position, velocity and acceleration are shown in Figure 2. The estimated states follow and converge rapidly to the actual states as shown in Figure 2. The estimation error and the error between actual states and unrefined states from estimated model of (6) and (7), referred to as "Non-filtered error", are shown in Figure 3. Fig. 3 shows that the use of the SVSF provides an improved performance for state estimation.

In practice, there exist uncertain parameter variations since the exact model is unknown, which means the coefficients in (35), such as $a_{11}, a_{12}, a_{13}, a_3, a_2$ are not exactly known. In the second simulation study, it was assumed that the uncertain parameters were known within 20%, i.e. as such an error is deliberately injected in the estimated filter model such that $[\hat{a}_{11}, \hat{a}_{12}, \hat{a}_{13}, \hat{a}_3, \hat{a}_2] = 120\% \times [a_{11}, a_{12}, a_{13}, a_3, a_2]$. The simulation results of estimated states and estimation errors are illustrated in Figure 4 and Figure 5, respectively. These results show that SVSF is robust against uncertainties as predicted by *Lemma 1*.

6. Conclusions

The paper reviews and applies a recently proposed state estimation strategy, referred to as Smooth Variable Structure Filter (SVSF). The derivation of SVSF gain and the stability of the SVSF process are provided. The SVSF estimation process in its original form only applies to smooth differentiable functions. In paper a mathematical approximation is used in order to allow the SVSF's application to models that contain sign function discontinuities. Simulation results pertaining to the application of the SVSF to a hydraulic system described by a nonlinear discontinuous model are presented.

Acknowledgements

The authors would like to acknowledge the financial support of the University of Saskatchewan and National Science and Engineering Research Council of Canada.

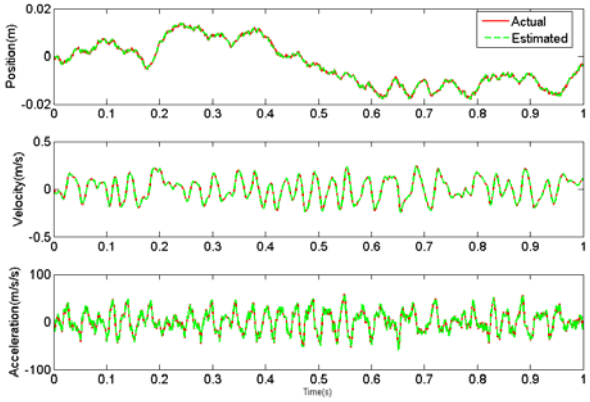

Figure 2. Actual and estimated states by SVSF

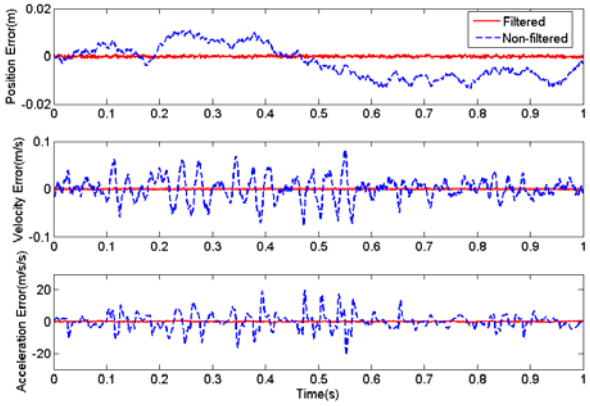

Figure 3. State estimation errors by SVSF and Non-filtered errors

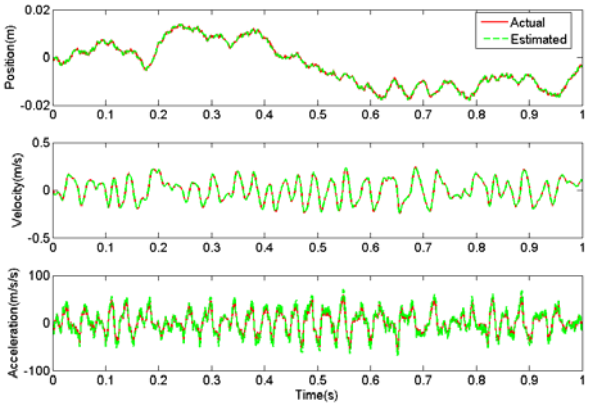

Figure 4. Actual and estimated states by SVSF for a model with uncertainties

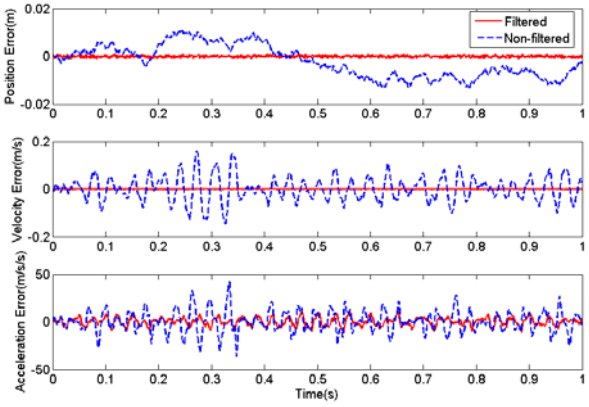

Figure 5. State estimation errors by SVSF and Non-filtered errors for a model with uncertainties

Appendix A: Proof of Theorem 1

It is necessary to prove *Theorem 1* which established that the SVSF is stable according to *Lemma 1*. The states must first be "refined" using the SVSF with (8) written as:

$$\hat{x}_{k+1|k+1} = \hat{x}_{k+1|k} + K_{k+1} \tag{36}$$

Pre-multiply both sides of (36) by output matrix of $\hat{H}$ such that:

$$\hat{H}\hat{x}_{k+1|k+1} = \hat{H}\hat{x}_{k+1|k} + \hat{H}K_{k+1} \tag{37}$$

Substitute (12), (13), (14) and (15) into (37) yields:

$$e_{z_{k+1|k+1}} = e_{z_{k+1|k}} - \hat{H}K_{k+1} \tag{38}$$

Thus:

$$\left|\hat{H}K_{k+1}\right|_{ABS} = \left|e_{z_{k+1|k}} - e_{z_{k+1|k+1}}\right|_{ABS} \tag{39}$$

From (16) and (39), it can be derived as:

$$\left|\hat{H}K_{k+1}\right|_{ABS} < \left|e_{z_{k+1|k}}\right|_{ABS} + \left|e_{z_{k|k}}\right|_{ABS} \tag{40}$$

And then:

$$\hat{H}K_{k+1}\,\mathrm{sgn}(\hat{H}K_{k}) < \left|e_{z_{k+1|k}}\right|_{ABS} + \left|e_{z_{k|k}}\right|_{ABS} \tag{41}$$

Rewriting (41) yields:

$$K_{k+1}\,\mathrm{sgn}(\hat{H}K_{k+1}) < \hat{H}^{+}(\left|e_{z_{k+1|k}}\right|_{ABS} + \left|e_{z_{k|k}}\right|_{ABS}) \tag{42}$$

Hence, from (42) and (50), the SVSF gain can be chosen as a moderate gain with a bound which is the right side of inequality of (42) such that:

$$K_{k+1} = \hat{H}^{+}(\left|e_{z_{k+1|k}}\right|_{ABS} + \gamma\left|e_{z_{k|k}}\right|_{ABS})\,\mathrm{sgn}(e_{z_{k+1|k}}) \tag{43}$$

where $\gamma \in \Re^{m\times m}$, and its elements $0 \le \gamma_{ii} < 1$.

To verify the stability condition, assume on the $k+1^{th}$ step there exists:

$$|\, e_{z_{k+1|k}}\,|_{ABS} < |\, \hat{H}K_{k+1}\,|_{ABS} \tag{44}$$

Thus, from (38) and the assumption of (44), the sign of $e_{z_{k+1|k+1}}$ depends on value of $\hat{H}K_{k+1}$, namely

$$\mathrm{sgn}(e_{z_{k+1|k+1}}) = -\mathrm{sgn}(\hat{H}K_{k+1}) \tag{45}$$

Then from (38):

$$e_{z_{k+1|k}} = | e_{z_{k+1|k+1}} |_{ABS} \ \mathrm{sgn}(e_{z_{k+1|k+1}}) + | \hat{HK}_{k+1} |_{ABS} \ \mathrm{sgn}(\hat{HK}_{k+1}) \quad (46)$$

Substituting (45) into (46) yields:

$$e_{z_{k+1|k}} = (| \hat{HK}_{k+1} |_{ABS} - | e_{z_{k+1|k+1}} |_{ABS}) \cdot \mathrm{sgn}(\hat{HK}_{k+1}) \quad (47)$$

Substituting (38) into (47) gives:

$$e_{z_{k+1|k}} = (| \hat{HK}_{k+1} |_{ABS} - | \hat{HK}_{k+1} - e_{z_{k+1|k}} |_{ABS}) \cdot \mathrm{sgn}(\hat{HK}_{k+1}) \quad (48)$$

From (44) and (48):

$$e_{z_{k+1|k}} = | e_{z_{k+1|k}} |_{ABS} \cdot \mathrm{sgn}(\hat{HK}_{k+1}) \quad (49)$$

which results in :

$$\mathrm{sgn}(e_{z_{k+1|k}}) = \mathrm{sgn}(\hat{HK}_{k+1}) \quad (50)$$

From (44) and (50), (40) may be written as:

$$\left| e_{z_{k+1|k}} - \hat{HK}_{k+1} \right|_{ABS} < \left| e_{z_{k|k}} \right|_{ABS} \quad (51)$$

Substituting (38) into (51), the stability condition of ***Lemma 1*** is satisfied for the state estimate, i.e.:

$$\left| e_{z_{k+1|k+1}} \right|_{ABS} < \left| e_{z_{k|k}} \right|_{ABS} \quad (52)$$

Appendix B: Nomenclature

lists all the constants and variable used in this paper. Vectors of state and output are denoted by using bold letters. Their elements are denoted by italic lower case letters with *i* and or *j*. *k* denotes calculation step. Subscripts *k*|*k* and *k*|*k*-1 are used to identify a posterori and a priori estimates. The symbol "^" is used to identify uncertain parameters and to denote estimated value for state variables.

Symbol	Comments	Dimension
^	Estimated variable and uncertain parameter	

(m), (u)	Superscripts for measured and unavailable states	
$\left\| \right\|_{ABS}$	Absolutely value	
$a_{11}, a_{12}, a_{13}, a_3, a_2$	Coefficients of system model.	1×1
b	Input matrix	$m\times1$
e	State estimation error	$n\times1$
$e_{z_{k\|k}}, e_{z_{k\|k-1}}$	Output estimation error calculated by using the a posteriori and a priori output estimates	$m\times1$
f, F	Nonlinear function	
H	Output matrix	$m\times n$
I_m	Identity matrix	$m\times m$
i, j	Subscripts used to identify elements of matrices and vectors	1×1
k	Calculation step index	1×1
K_k	SVSF gain	$n\times1$
m	Number of measurements	1×1
n	Number of states	1×1
S	Switching function	
sat	Saturation function	
sgn	Signum function	
tanh, sinh, cosh	Hyperbolic tangent, sine and cosine function	
T	Transformation matrix	$n\times n$
T_s	Sampling time	1×1
u	Input	1×1
vec	Any vector	
v, $V_{\max}$	Measurement noise and its upper bound	$m\times1$
w, $W_{\max}$	System noise and its upper bound	$n\times1$
$\mathbf{x}, \mathbf{x}_0$	System states and their initial condition	$n\times1$
$\hat{\mathbf{x}}_{k\|k}, \hat{\mathbf{x}}_{k\|k-1}$	A posteriori and a priori state estimates	$n\times1$
$\mathbf{y}$	Transformed system state	$n\times1$
$\mathbf{z}$	Measured output	$m\times1$
$\hat{\mathbf{z}}_{k\|k}, \hat{\mathbf{z}}_{k\|k-1}$	A posteriori and a priori output estimates	$m\times1$
Λ	Constant diagonal matrix with elements $\lambda_{ij} > 0$	$n\times n$
Θ	Differentiable function	
γ	Constant diagonal gain matrix with elements $\gamma_{ij} \geq 1$	$n\times n$
Ψ	Boundary layer	$n\times1$

Table 1 Nomenclature

References

[1] N. S. Nise, *Control systems engineering*, (Hoboken, NJ, John Wiley, 2004).

[2] R. E. Kalman, A new approach to linear filtering and prediction problems, *Journal of Basic Engineering, 82*(1), 1960, 35-46.
[3] R.E. Kalman, & R.S. Bucy, New results in linear filtering and prediction theory, *ASME Journal of Basic Engineering, 83* (Series D), 95-108, 1961.
[4] M.S. Grewal, & A.P. *Andews, Kalman filtering: theory and practice, 2nd edition*, (New York, N.Y.: John Wiley & Sons inc., 2001).
[5] D Luenberger, Observers for multivariable systems, *IEEE Transaction on Automatic Control, 11*, 1966, 190-197.
[6] S. Haykin., *Adaptive filter theory, third edition* (Englewood Cliffs, NJ: Prentice-Hall, 1996).
[7] S. Julier, J. Uhlmann, & H.F. Durrant-White, A new method for nonlinear transformation of means and covariances in filters and estimators, *IEEE Transactions on Automatic Control, 45*(3), 2000, 477-482.
[8]N.J. Gordon, D.J. Salmond, & A.F.M. Smith, Novel approach to nonlinear/non-Guassian Bayseian state estimation, *IEE Proc.-F, 140*, 1993, 107-113.
[9] A. Doucet, N. de Freitas, & N.J. Gordon, *Sequential monte carlo methods in Practice*, (Springer Verlag, 2001).
[10] B. Ristic, S. Arulampalam, & N. Gordon, *Beyond Kalman Filter: Particle Filters for Tracking Applications*, (Artech House Publishers, 2004)
[11] S. R. Habibi, & R. Burton, The variable structure filter, *ASME Journal of Dynamic Systems, Measurement and Control, 125*, 2003, 287-293.
[12] S. R Habibi, & R. Burton, Parameter identification for a high performance hydrostatic actuation system using the variable structure filter concept, *American Society of Mechanical Engineers, The Fluid Power and Systems Technology Division (Publication) FPST, 11*, 2004, 93-101.
[13] M. S. Grewal, & A. P. Andrews, *Kalman Filtering: theory and practice using MATLAB, 2nd Edition*, (Englewood Cliffs, N.J.: Prentice-Hall. 2001).
[14] B. L. Walcott, & S. H. Zak, State observation of nonlinear uncertain dynamical systems, *IEEE Transaction on Automatic Control, 32*, 1987, 166-170.
[15] R. A. Adams, *Calculus: a complete course*, (Don Mills, Ontario, Addison-Wesley Longman, 1999).
[16] *http://mathworld.wolfram.com/*
[17] J. –J. E. Slotine, Sliding controller design for nonlinear systems, *International Journal of Control, 40*, 1984, 421-434.
[18] S. R. Habibi, & G. Singh, Derivation of design requirements for optimization of a high performance hydrostatic actuation system, *International Journal of Fluid Power, 2*, 2000, 11-27.
[19] S. Wang, S. Habibi, & R. Burton, Sliding mode control for a model of an electrohydraulic actuator system with discontinuous nonlinear friction, *The Proc. of 2006 American Control Conference*, Minneapolis, MN, 2006, 5898-5904.
[20] S. R. Habibi, & G. Singh, Derivation of design requirements for optimization of a high performance hydrostatic actuation system, *International Journal of Fluid Power, 2*, 2000, 11-27.
[21] S. Wang, S. Habibi, & R. Burton, Sliding mode control for a model of an electrohydraulic actuator system with discontinuous nonlinear friction, *The Proc. of 2006 American Control Conference*, Minneapolis, MN, 2006, 5898-5904.

Appendix D: A Comparative Study of a Smooth Variable Structure Filter and the Extended Kalman Filter (Wang, et al [2006])*

* This paper is under reviewed by the Transactions of the CSME. This paper is included with the express permission of the journal's publishers.

A COMPARATIVE STUDY OF A SMOOTH VARIABLE STRUCTURE FILTER AND THE EXTENDED KALMAN FILTER

Shu Wang Saeid Habibi Richard Burton
College of Engineering, University of Saskatchewan
57 Campus Drive, Saskatoon, SK, S7N 5A9
Canada
Shw750@mail.usask.ca

ABSTRACT
A new method of filtering strategy, referred to as the Smooth Variable Structure Filter (SVSF) is applied to the problem of state estimation on a class of nonlinear system. A comparative study is presented in which the Extended Kalman Filter (EKF) is applied to the same nonlinear system model. The estimation convergence and accuracy of the SVSF and EKF are comparable. The robustness of the SVSF to parameter variations is established though simulation results. This study is important because it allows the new SVSF to be critically compared to a standard technique such as the EKF.

KEY WORDS
Smooth Variable Structure Filter, Extended Kalman Filter, State Estimation, Inverse Function

1 Introduction

The extended Kalman filter (EKF) has been extensively studied and applied to state estimation and tracking in the control engineering area because of its simplicity and robustness. The EKF can be applied to some nonlinear systems by linearizing the model about an operating point so that the traditional linear Kalman filter can be applied [1]. However, this linearization at each time step can introduce large errors and in some instances, can result in divergence of the filter [2]. When the EKF is applied to a complex system a problem which sometimes arises is the computation of the state transition matrix which requires calculation of the Jacobian matrix and its matrix exponential. Often, the Jacobian may be difficult to evaluate, and time consuming to carry out (especially for a complex and higher order system). Furthermore, The Jacobian must be re-evaluated at every prediction step of the filter [1, 3]. Higher order Kalman filters have been developed to minimize the linearization errors, but they are more difficult to implement and prone to instability [4].

The Smooth Variable Structure Filter (SVSF) as applied to parameter estimation was first proposed by Habibi and Burton in 2004 [5]. This filtering strategy can also be used to estimate system states for Linear Time Invariant (LTI) and nonlinear systems with system and measured uncertainties [6]. In this paper, the Smooth Variable Structure Filter (SVSF) structure introduced in [5] and [6] is reviewed and subsequently revised using a canonical control system form of an "adjusting" gain. The SVSF uses concepts closely related to Variable Structure Control. However, its implementation procedure is similar to the Kalman Filter [4]. The SVSF can be regarded as a special form of a sliding observer. The function of the SVSF is to directly estimate the states of a system by a discontinuous component. This discontinuous component called a "SVSF gain", (calculated by a series transformation) is used to correct state estimates.

In this paper, both the "revised" SVSF gain and EKF are used to predict the states of a nonlinear hydraulic model. The transient dynamics and steady-state conditions of both filters are compared. An advantage of using this form of the SVSF is that it inherently contains the robust properties for uncertainties (which, in fact stem from the basic properties of Variable Structure Control). Thus the robustness of the SVSF and EKF are compared in this paper. The original contributions of this paper lie in the presentation of the revised form of the SVSF and in the crucial comparison to a standard estimation technique, the EKF.

This paper is organized as follows: Section 2 describes the filtering strategy of the SVSF. Section 3 reviews the implementation procedure of the EKF. Simulation results and comparison analysis of a numerical example applied using the SVSF and EKF are illustrated in Section 4. Section 5 concludes the paper and the Appendix provides the transformation process of SVSF and the nomenclature.

2 Smooth Variable Structure Filter

Much of the following description has appeared in [5, 6], but for continuity and clarity, it is repeated in this section. The description of the "transformation process" appears in this section and Appendix A. For the SVSF, an estimate of the state trajectory is generated using a stochastic model. It is the objective of any observer to estimate specified (unknown) states of the system as the states change over time (state trajectory) As shown in Fig.

1, the estimated trajectory is forced towards the true state trajectory by the use of a discontinuous gain, referred to as SVSF gain, until it reaches a neighborhood of the actual state trajectory. This neighborhood is referred to here as the "existence subspace". The size of existence subspace determines the accuracy of the SVSF. The SVSF is formulated such that once the estimated trajectory reaches the existence subspace; it remains confined within this neighborhood without leaving, switching back and forth along the actual state trajectory. Thus the existence subspace always encloses the actual state trajectory [5].

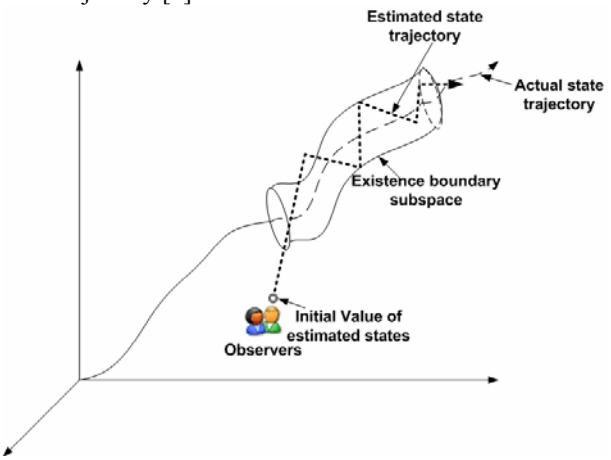

Fig. 1 SVSF State Estimation

Consider a nonlinear system which may be expressed by a smooth function, (infinitely differentiable), such that,

$$\dot{\mathbf{x}}(\mathbf{t}) = F(\mathbf{x},t,u,w) = f(\mathbf{x}(t)) + b(\mathbf{x}(t))u(t) + d(\mathbf{x},t) \qquad (1)$$

where $\mathbf{x}(t) \in R^n$ is the state vector , b is the input matrix. $u(t)$ is the input signal and $d(\mathbf{x},t)$ is a time-dependent disturbance with known upper bound. $f(\mathbf{x}(t))$ and $b(\mathbf{x}(t))$ are differentiable functions determining the system characteristics, where

$$f(\mathbf{x}(t)) = \begin{bmatrix} f_1(\mathbf{x}(t)) & f_2(\mathbf{x}(t)) & \cdots & f_n(\mathbf{x}(t)) \end{bmatrix}^T ,$$

$$b(\mathbf{x}(t)) = \begin{bmatrix} b_1(\mathbf{x}(t)) & b_2(\mathbf{x}(t)) & \cdots & b_n(\mathbf{x}(t)) \end{bmatrix}^T$$

It is assumed that the relationship between the measurement signals and the states is linear, or at least piece-wise linear, such that

$$\mathbf{z}(t) = H\mathbf{x}(t) + v(t) . \qquad (2)$$

where H is a constant matrix, and $v(t)$ is the measurement noise.

The approach of "forward difference" approximation is used in the discretization of the state space model at any time $T_s(k)$ and is given by:

$$\dot{x}_i = \frac{x_i(k+1) - x_i(k)}{T_s} + \delta_i(k) \qquad (3)$$

$$i = 1,2,\cdots n$$

where T_s is the sampling time and the terms of $\delta_i(k)$ are the numerical approximation errors.

The discrete model of (1) can be written as:

$$\mathbf{x}_{k+1} = \mathbf{x}_k + T_s f(\mathbf{x}_k) + T_s b(\mathbf{x}_k)u_k + w_k \qquad (4)$$

where $w_k = T_s[d_k - \delta_k]$ is the lumped uncertainty term.

The discrete-time form of (2) may be expressed as:

$$\mathbf{z}_k = H\mathbf{x}_k + v_k . \qquad (5)$$

The system w_k and measured v_k noise are assumed to have Gaussian distributions. To a high level of probability, the system measured and system noise are assumed to be amplitude bounded. Furthermore, they are assumed to be uncorrelated and upper bounded.

The SVSF is a predictor-corrector method that uses an internal model to predict an a priori (unrefined) estimate of states. The a priori estimate is corrected into an a posteriori (refined) state estimate through a corrective term K_k.

The SVSF estimation process detailed in [5] is summarized as follows:

1. The a priori state estimate is predicted by using the estimated model of the system such that:

$$\hat{\mathbf{x}}_{k+1|k} = \hat{\mathbf{x}}_{k|k} + T_s \hat{f}(\hat{\mathbf{x}}_{k|k}) + T_s \hat{b}(\hat{\mathbf{x}}_{k|k})u_k \qquad (6)$$

where the hat symbol "^" denotes an estimated state, function, or parameter, (it should be noted that as such, a "^" on the f and b means an uncertain function or parameter). The state estimate in (6) is obtained by using the previous a posteriori state estimate $\hat{\mathbf{x}}_{k|k}$ or at the inception of the process, by using the initial conditions, $\hat{\mathbf{x}}_0$. These estimated states are then used for predicting the a priori estimates of measurements such that:

$$\hat{\mathbf{z}}_{k+1|k} = \hat{H}\hat{\mathbf{x}}_{k+1|k} \qquad (7)$$

2. A corrective gain $K_{k+1} \in \Re^n$ is calculated as a function of the error in the predicted output.

3. The a priori state estimate is refined into an a posteriori state estimate such that:

$$\hat{\mathbf{x}}_{k+1|k+1} = \hat{\mathbf{x}}_{k+1|k} + K_{k+1} . \qquad (8)$$

4. Steps 1 to 3 are iteratively repeated.

It should be noted that the order of the steps can be changed, that is, the unrefined state estimate is adjusted with the corrective gain first to give the refined states, and then projected forward to the next time step using Eq. (6) which in turn becomes the unrefined estimate for the next cycle.

In practice, the states are not available for the calculation of the estimated error; hence, the measured output, $\mathbf{z}_k$, must be used in state estimation. In the discrete form, the a priori and a posteriori estimated errors of the k+1 step in terms of measured output signals are defined as:

$$e_{z_{i_{k+1|k+1}}} = z_{i_{k+1}} - \hat{z}_{i_{k+1|k+1}} \qquad (9)$$

$$e_{z_{i_{k+1|k}}} = z_{i_{k+1}} - \hat{z}_{i_{k+1|k}} \qquad (10)$$

where $\hat{z}_{i_{k+1|k+1}}$ and $\hat{z}_{i_{k+1|k}}$ are elements of the estimated output vectors as defined in Eq. (7).

As implied above, an alternate way of interpreting $\hat{z}_{i_{k+1|k+1}}$ is to consider it as a "refined" estimate of $z_{i_{k+1}}$ and $\hat{z}_{i_{k+1|k}}$ as an "unrefined" estimate of $z_{i_{k+1}}$.

$$\hat{\mathbf{z}}_{k+1|k+1} = \hat{H}\hat{\mathbf{x}}_{k+1|k+1} \tag{11}$$

$$\hat{\mathbf{z}}_{k+1|k} = \hat{H}\hat{\mathbf{x}}_{k+1|k} \tag{12}$$

The corrective term K_{k+1} is a discontinuous term that is designed to guarantee the stability of the estimation process. The SVSF gain K_{k+1} is used to force the estimated states to approach the desired trajectory estimate.

The SVSF gain was derived in [5, 6] and may be chosen in the form of:

$$K_k = \hat{H}^+(\left|e_{z_{k+1|k}}\right|_{ABS} + \gamma\left|e_{z_{k|k}}\right|_{ABS})\,\mathrm{sgn}(e_{z_{k+1|k}}). \tag{13}$$

where $\gamma \in \Re^{m\times m}$ diagonal matrix, and its elements $0 \le \gamma_{ii} < 1$, the $\hat{H}^+$ is pseudo inverse of output matrix in the estimated model. The derivation for the proof of the SVSF gain is provided in [6].

If the system is completely observable and completely controllable or bijective in the case of nonlinear systems, it is possible to construct a full state observer, (one which can observe all the states rather than just some which is found in a reduced order observer). Unique to this research, for the SVSF, the state vector is divided into two parts: the state estimates with explicit measurements (measured states) and the remaining state (unavailable states) estimation. Through a series of transformation process (see Appendix A), the a priori error of the output vector between the estimations from the measured states partition and unavailable states partition may be defined as

$$e^{(u)}_{y_{k+1|k}} = \hat{\sigma}_{k+1} - \hat{\mathbf{y}}^{(u)}_{k+1|k} \tag{14}$$

where superscripts $^{(u)}$ represent the unavailable states, $\hat{\sigma}_{k+1}$ is an estimated term calculated by Eq. (35) in Appendix A.

The a posteriori error can therefore be defined as:

$$e^{(u)}_{y_{k+1|k+1}} = \hat{\sigma}_{k+1} - \hat{\mathbf{y}}^{(u)}_{k+1|k+1} \tag{15}$$

In addition, since the estimated term $\hat{\sigma}_{k+1}$ is derived from the canonical form of discrete nonlinear model, the calculation process resembles the differential of the previous states in the states vector. The system noise may also be magnified by this calculation process which is dependent on the sampling time. The SVSF corrective gain of the unavailable states may be adjusted by a gain which is nothing more than the sampling time T_s, and as such it can be defined in the same form as Eq. (13):

$$K^{(u)}{}_{k+1} = \hat{H}^+ \cdot T_s \cdot (\left|e^{(u)}_{y_{k+1|k}}\right|_{ABS} + \gamma^{(u)}\left|e^{(u)}_{y_{k+1|k+1}}\right|_{ABS})\,\mathrm{sgn}(e^{(u)}_{y_{k+1|k}}) \tag{16}$$

Note that in this example, the pseudo inverse of output matrix $\hat{H}^+$ assumes the common engineering form, a pseudo-diagonal matrix with elements equal to 1 such that $\hat{H}^+ = \left[I_{n\times m}\right]$.

For the measured state partition, since all the elements of this partition can be measured, the SVSF gain can be written as:

$$K^{(m)}{}_{k+1} = (\left|e_{z_{k+1|k}}\right|_{ABS} + \gamma^{(m)}\left|e_{z_{k+1|k+1}}\right|_{ABS})\,\mathrm{sgn}(e_{z_{k+1|k}}). \tag{17}$$

Thus, the corrective SVSF gain can be expressed as a combination of (16) and (17):

$$K_{k+1} = \begin{bmatrix} K^{(m)}{}_{k+1} \\ K^{(u)}{}_{k+1} \end{bmatrix} = \begin{bmatrix} (\left|e_{z_{k+1|k}}\right|_{ABS} + \gamma^{(m)}\left|e_{z_{k+1|k+1}}\right|_{ABS}) \\ T_s \cdot (\left|e^{(u)}_{y_{k+1|k}}\right|_{ABS} + \gamma^{(u)}\left|e^{(u)}_{y_{k+1|k+1}}\right|_{ABS}) \end{bmatrix} \circ \begin{bmatrix} \mathrm{sgn}(e_{z_{k+1|k}}) \\ \mathrm{sgn}(e^{(u)}_{y_{k+1|k}}) \end{bmatrix}. \tag{18}$$

The sign function in equation (18) leads to a high frequency switching effect that is referred to as chattering. To remove the chattering, the sgn(*vec*) in (18) may be replaced by the saturation function $sat(vec, \Psi)$ with elements defined as follows [7]:

$$sat(vec, \Psi) = \begin{cases} (vec_i / \Psi_i) \Leftrightarrow | vec_i / \Psi_i | \le 1 \\ sign(vec_i / \Psi_i) \Leftrightarrow | vec_i / \Psi_i | > 1. \end{cases} \tag{19}$$

So,

$$K_k = \begin{bmatrix} K^{(m)}{}_k \\ K^{(u)}{}_k \end{bmatrix} = \begin{bmatrix} (\left|e_{z_{k|k-1}}\right|_{ABS} + \gamma^{(m)}\left|e_{z_{k|k}}\right|_{ABS}) \\ T_s \cdot (\left|e^{(u)}_{y_{k|k-1}}\right|_{ABS} + \gamma^{(u)}\left|e^{(u)}_{y_{k|k}}\right|_{ABS}) \end{bmatrix} \circ \begin{bmatrix} sat(e_{z_{k|k-1}}, \Psi_z) \\ sat(e^{(u)}_{y_{k|k-1}}, \Psi^{(u)}_y) \end{bmatrix}. \tag{20}$$

The gain K_k so obtained by (20) is used in the SVSF process to refine the a priori state estimates as indicated by (8).

3. The Extended Kalman Filter

The Extended Kalman Filter (EKF) is an extension of the linear Kalman filtering theory to nonlinear problems. The Kalman Filter (KF) is an optimal state estimation process applied to a dynamic system with random perturbations. The goal is to minimize the estimation error for the states of a nonlinear system along a trajectory by applying a linearization technique. [8].

Consider the same nonlinear discrete model as Eq. (4) and measurement model of Eq. (5), the implementation process of EKF may be summarized as the following steps [4]:

1. The a priori state estimate $\hat{\mathbf{x}}_{k+1|k}$ may be predicted by using the same estimated model of the system in SVSF as Eq. (6). The a priori estimates of

measurements, $\hat{\mathbf{z}}_{k+1|k}$, can also be predicted by using the same estimate measurement model of (7) in SVSF.

2. A corrective EKF gain $Kf_{k+1} \in \Re^n$ may be calculated by the following steps and equations:

a) Linearize the estimation system model as:

$$\Phi_{k|k} \approx \left.\frac{\partial[\hat{\mathbf{x}}_{k|k} + T_s \hat{f}(\hat{\mathbf{x}}_{k|k}) + T_s \hat{b}(\hat{\mathbf{x}}_{k|k})u_k]}{\partial x}\right|_{x=\hat{\mathbf{x}}_{k|k}}, \tag{21}$$

where $\Phi_{k|k}$ is the linearized form of the nonlinear model.

b) Compute the a priori covariance matrix:

$$P_{k+1|k} = \Phi_k P_{k|k} \Phi_k + Q_k, \tag{22}$$

where Q_k is the covariance matrix associated with w_k and is defined as:

$$Q_k = \begin{bmatrix} E[(w_{1k})^2] & 0 & \cdots & 0 \\ 0 & E[(w_{2k})^2] & \cdots & 0 \\ \vdots & \vdots & \ddots & \vdots \\ 0 & 0 & \cdots & E[(w_{nk})^2] \end{bmatrix}.$$

The $E(\cdot)$ is the expectation which represents the central position of a random process.

c) Compute the EKF gain:

$$Kf_{k+1} = P_{k+1|k}\hat{H}[\hat{H}P_{k+1|k}\hat{H} + R_k]. \tag{23}$$

where R_k is the covariance matrix associated with v_k and is defined as:

$$R_k = \begin{bmatrix} E[(v_{1k})^2] & 0 & \cdots & 0 \\ 0 & E[(v_{2k})^2] & \cdots & 0 \\ \vdots & \vdots & \ddots & \vdots \\ 0 & 0 & \cdots & E[(v_{nk})^2] \end{bmatrix}.$$

d) Computing the a posteriori covariance matrix:

$$P_{k+1|k+1} = [I - Kf_{k+1}\hat{H}]P_{k+1|k}, \tag{24}$$

where I is identity matrix with a dimension of $m \times n$.

3. The a priori state estimate is refined into an a posteriori state estimate such that:

$$\hat{\mathbf{x}}_{k+1|k+1} = \hat{\mathbf{x}}_{k+1|k} + Kf_{k+1}(\mathbf{z}_{k+1} - \hat{\mathbf{z}}_{k+1|k}). \tag{25}$$

4. Steps 1 to 3 are iteratively repeated.

4. Numerical Example

A nonlinear hydraulic model is used in this section to illustrate the application of the SVSF method for state estimation. Consider a third order system which in its state space form is given by:

$$\begin{cases} \dot{x}_1 = x_2 \\ \dot{x}_2 = x_3 \\ \dot{x}_3 = -a_3 x_3 - a_2 x_2 - [a_{11} x_2 x_3 + a_{12} x_2^{\,2} + a_{13}]\text{sgn}(x_2) + bu \end{cases} \tag{26}$$

where x_1, x_2, x_3 are the displacement and velocity and acceleration of a load; u is the input to the system, and $a_{11}, a_{12}, a_{13}, a_3, a_4$ are constants. It should be noted that these equations are descriptive of a "real" physical plant, which is a hydrostatic system referred to as an Electrohydraulic Actuator (EHA) system [9].

The model (indeed, the physical system) is nonlinear and contains a discontinuous term involving a sign function $\text{sgn}(x_2)$ of the second state x_2. In order to satisfy the smoothness requirement, the hyperbolic tangent with a high gain of 100, i.e. $\tanh 100x_2$, is used to approximate the term $\text{sgn}(x_2)$ [6]. Using the "forward difference" approach to obtain an approximated discrete state-space model at time $T(k)$, the system model which represents the actual system and includes the system and measurement noise, is obtained as:

$$\begin{cases} x_1(k+1) = x_1(k) + T_s x_2(k) + T_s w_1(k) \\ x_2(k+1) = x_2(k) + T_s x_3(k) + T_s w_2(k) \\ x_3(k+1) = [1 - T_s a_3]x_3(k) - T_s a_2 x_2(k) - T_s[a_{11} x_2(k) x_3(k) + \\ \quad a_{12}(x_2(k))^2 + a_{13}]\tanh(100x_2(k)) + T_s bu(k) + T_s w_3(k) \end{cases} \tag{27}$$

where w_1, w_2, w_3 are system noise.

In this system model, it is assumed that displacement and velocity can be measured only and acceleration is not available, which means the output matrix H can be written as:

$$H = \begin{bmatrix} 1 & 0 & 0 \\ 0 & 1 & 0 \end{bmatrix}. \tag{28}$$

In the model of (27), the sampling time is chosen to be T_s=0.001s. This particular sampling time was chosen to satisfy Shannon's Sampling Theorem and was approximately 10 times the highest system frequency of interest. The maximum amplitude of system noise is set as:

$$W_{\max} = \begin{bmatrix} \max(T_s w_1(k)) \\ \max(T_s w_2(k)) \\ \max(T_s w_3(k)) \end{bmatrix} = \begin{bmatrix} 0.01 \\ 0.1 \\ 1 \end{bmatrix}.$$

The measurements from the system pertain to position and velocity and all the measurements are subjected to white noise of maximum amplitude: The settings of system noise and measurement noise are rough guesses based on experimental tests on the EHA and they represent real limits to the EHA system.

$V_{\max} = \begin{bmatrix} \max(v_1) \\ \max(v_2) \end{bmatrix} = \begin{bmatrix} 0.001 \\ 0.001 \end{bmatrix}$. The initial condition of states are $\mathbf{x}_0 = [0 \quad 0 \quad 0]^T$. The input to the system is a random signal with amplitude in the range of -100 to 100 Note that for the EHA example, this corresponded to a pump speed in revolutions per minute. Based on the model derived and experimentally verified in [9], the coefficients of (27) are set as:

$a_3 = -71, \quad a_2 = 78100, \quad a_{11} = 2100, \quad a_{12} = 1610,$

$a_{12} = 3.5$.

In the SVSF, the diagonal matrix γ is chosen as $\begin{bmatrix} 0.1 & 0 & 0 \\ 0 & 0.1 & 0 \\ 0 & 0 & 0.1 \end{bmatrix}$, and in the EKF, the initial condition of the predicted covariance matrix is given as:

$$P(0) = \begin{bmatrix} 1 & 0 & 0 \\ 0 & 1 & 0 \\ 0 & 0 & 1 \end{bmatrix},$$

The system noise covariance matrix is set as:

$$Q_k = \begin{bmatrix} 10^{-4} & 0 & 0 \\ 0 & 10^{-7} & 0 \\ 0 & 0 & 10^{-11} \end{bmatrix},$$

and the measurement noise covariance matrix is set as: $R_k = 10^{-9}$.

In a real application, the state variables are not available and therefore the exact value of the estimation error is unknown. However, in this study, the states and the estimation error are available and can be used to evaluate the effectiveness of the SVSF since the study is based on computer simulation, a great advantage when it comes to assessing the capabilities of any new technique. The three actual (plant) states that represent position, velocity and acceleration are shown in Fig. 2. The simulated states by the estimation model of (6) and (7), which are referred as "Non-filtered states", are shown as dotted lines in Fig. 2. It should be noted that the output position produced by the "non-filtered" system (based on equations 6 and 7) is very small and appears almost zero in the figure when compared to the actual value on the same scale. Thus, it can be concluded that the model described by Eq. (26) is a poor representation of the actual system. The estimated states using the SVSF follow and converge rapidly to the actual states as shown in Fig. 3. The estimated states using the EKF and the actual states for the same model are illustrated in Fig. 4. The estimation error by the SVSF and EKF, and the error between actual states and unrefined states from the estimation model of (6) and (7), referred to as "Non-filtered error", are shown in Fig. 5 and Fig. 6, respectively. These Figures illustrate that the use of the SVSF and EKF provides an improved performance for state estimation.

Figure 7 shows the comparison of estimation errors by the SVSF and EKF. It is clear that the SVSF produces better estimation accuracy than the EKF. In addition, the SVSF demonstrates a shorter convergence time than that of the EKF (it takes several steps to converge at the initial conditions for the acceleration estimate). This is because the SVSF is based on the same principals related to Variable Structure Control (VSC) which has shown to have a superb regulation rate [10]. In order to more clearly establish the performance differences between the SVSF and EKF, the transient dynamics (simulation time from 0s~0.02s) and steady-state conditions (simulation time from 0.3s~0.7s) of estimation errors are magnified as show in Fig. 8 and Fig. 9. It is observed that the EKF takes five steps to converge but the SVSF only takes one step. Moreover, the SVSF converges to less than half of the steady-state estimation error than EKF does, which mean the SVSF improved the estimate performance about double (100%) that of the nonlinear model in the EKF leads to larger errors. This because that the linearization approximation of the nonlinear model leads to larger errors in EKF process. In contrast, SVSF uses the nonlinear model continuously.

In practice, there exist uncertain parameter variations since the exact model is unknown, which means the coefficients in (27), such as $a_{11}, a_{12}, a_{13}, a_3, a_4$ are not exactly known. In the second simulation study, it was therefore assumed that the uncertain parameters were known within 15%. An error was deliberately injected into the estimated filter model such that $[\hat{a}_{11}, \hat{a}_{12}, \hat{a}_{13}, \hat{a}_3, \hat{a}_4] = 115\% \times [a_{11}, a_{12}, a_{13}, a_3, a_4]$. The simulation results of estimated states and estimation errors are illustrated in Fig. 10 and Fig. 11, respectively. Figure 11 is partially magnified as transient and steady-state parts as shown in Fig. 12 and Fig. 13, which indicate that SVSF obtained a more accurate estimate of the acceleration (in the order of 100%) and demonstrated faster convergence than the EKF. These results show that the SVSF is robust in the presence of uncertainties and obtains a better estimation performance than the EKF.

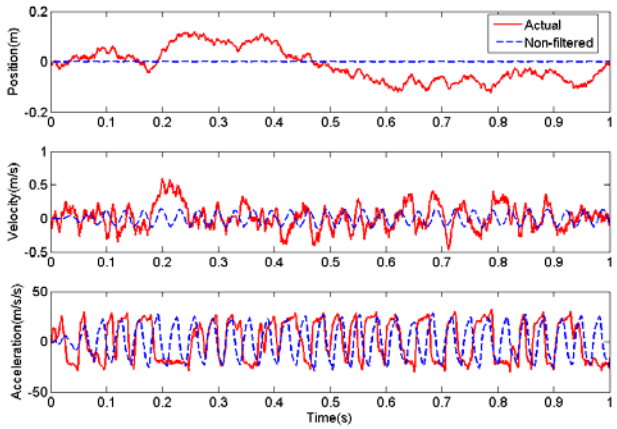

Fig. 2 Actual and Non-filter states

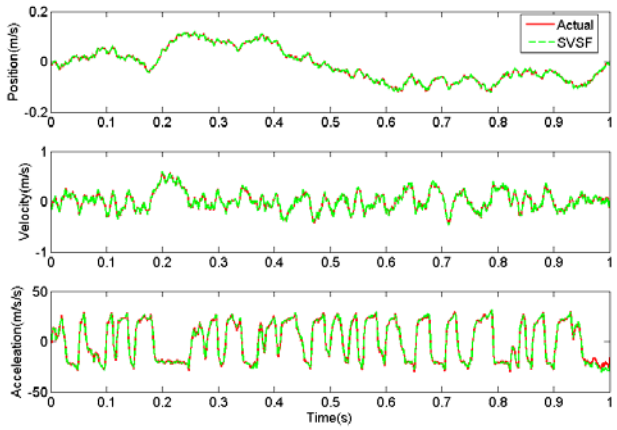

Fig. 3 Actual and estimated states by the SVSF

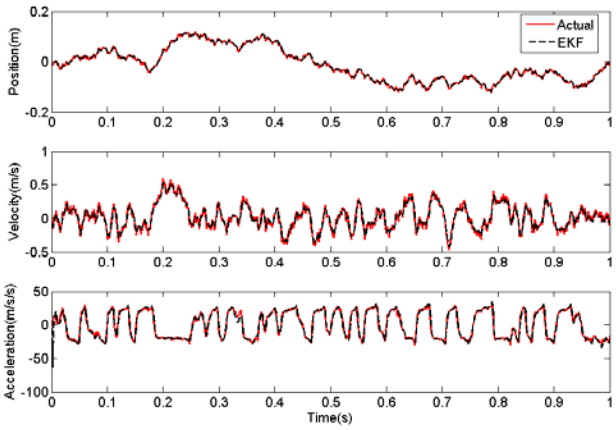

Fig. 4 Actual and estimated states by the EKF

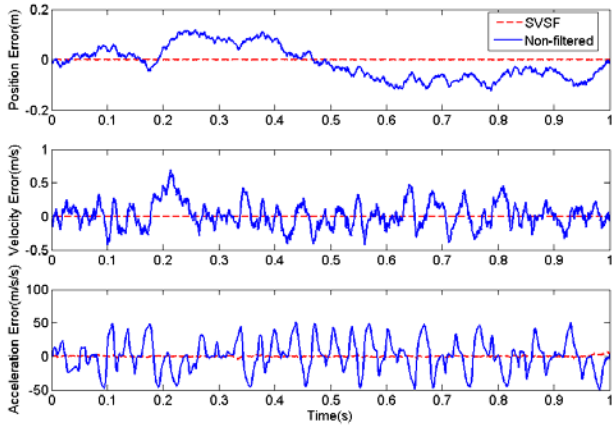

Fig. 5 State estimation errors by the SVSF and Non-filtered errors

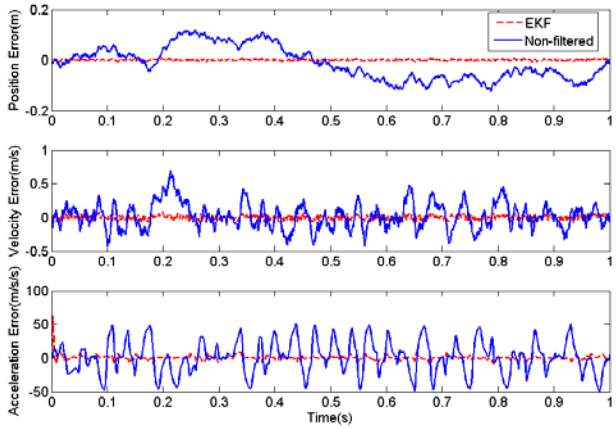

Fig. 6 State estimation errors by the EKF and Non-filtered errors

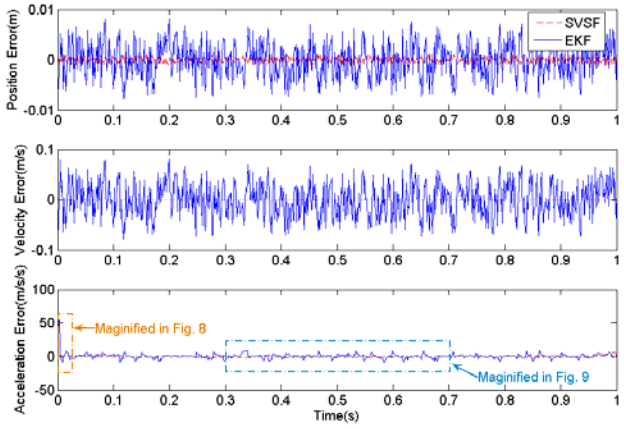

Fig. 7 State estimation errors by the SVSF and EKF

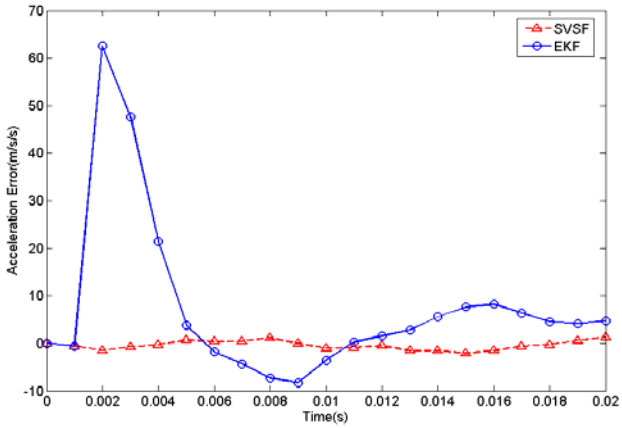

Fig. 8 State estimation acceleration errors by the SVSF and EKF (from 0.00s~0.02s)

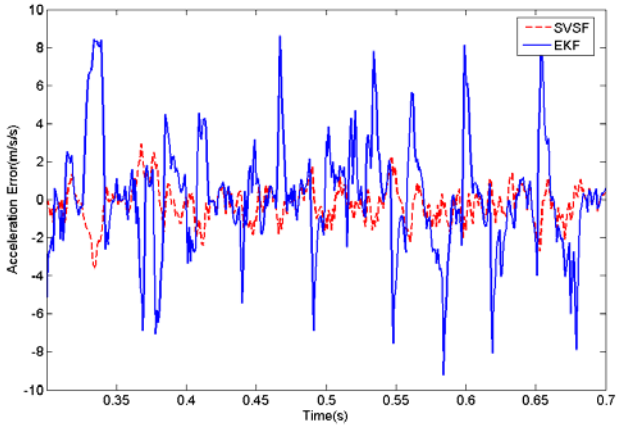

Fig. 9 State estimation acceleration errors by SVSF and EKF (from 0.3s~0.7s)

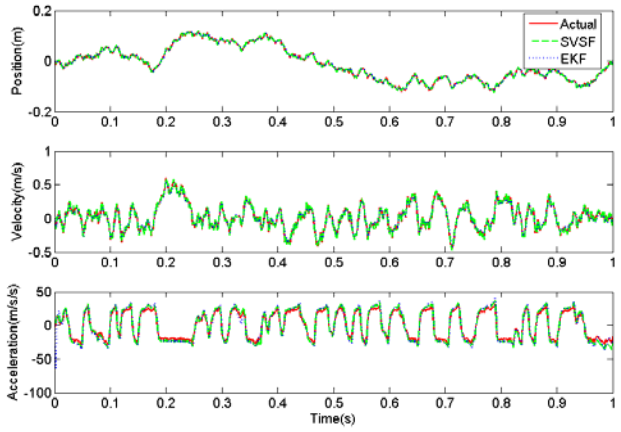

Fig. 10 Actual and estimated states by SVSF and EKF for a model with uncertainties

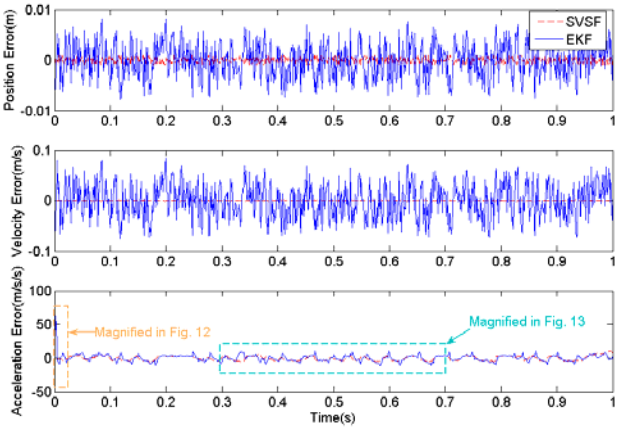

Fig. 11 State estimation errors by SVSF and EKF for a model with uncertainties

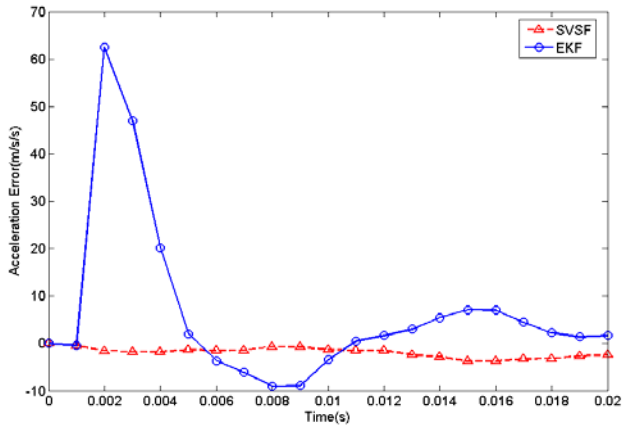

Fig. 12 State estimation acceleration errors by the SVSF and EKF with model uncertainties (from 0.00s~0.02s)

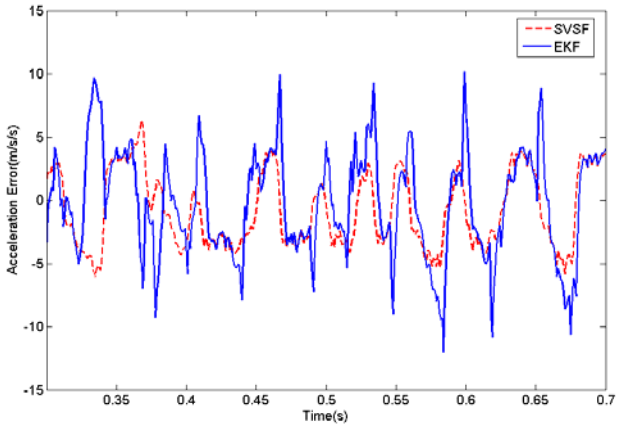

Fig. 13 State estimation acceleration errors by SVSF and EKF with model uncertainties (from 0.3s~0.7s)

5. Conclusions

The paper considers a revised form of the Smooth Variable Structure and applies this state estimation strategy, and the Extended Kalman Filter (EKF) to a nonlinear hydraulic model of a hydrostatic system. The higher convergent rate is obtained using the SVSF compared to the EKF since the SVSF is based on concepts similar to Variable Structure Control (VSC). SVSF improve the estimation accuracy more than 100% compared to the EKF because for the EKF it was necessary to linearize the nonlinear model relationships which could lead to deviations from the nonlinear model. The calculation of the SVSF gain is always based on the nonlinear model. The SVSF and EKF are both applied to an uncertain model in the presence of parameter uncertainties. The SVSF demonstrated a higher robust property than the EKF for the system studied.

The main contribution of this paper is through the comparative study, the SVSF shows significant improvement when compared to the EKF for state estimation performance. This study demonstrates the potential of the SVSF when applied to accurate models of "real" applications, the implication being that the same trends would be demonstrated for real systems. This is now being actively pursued.

Acknowledgements

The author would like to acknowledge the financial support of the University of Saskatchewan and National Science and Engineering Research Council of Canada.

Appendix A: Transformation Process of SVSF

In the SVSF, the state vector may be divided into two parts: the state estimates with explicit measurements associated with them denoted as $y_k^{(m)}$ and the remaining state estimation $y_k^{(u)}$. To facilitate the development of the SVSF, a new form of output vector is defined that would correspond to the above mentioned state vector partition as follows [5, 6]:

$$\mathbf{y}_{k+1} = T\mathbf{x}_{k+1} = \begin{bmatrix} \mathbf{y}_{k+1}^{(m)} \\ \mathbf{y}_{k+1}^{(u)} \end{bmatrix} \tag{29}$$

where T is a transformation matrix, the superscripts of $^{(m)}$ and $^{(u)}$ means measured and unavailable state variables.
Thus, the upper partition of (29) can be replaced by the actual measured output described by (5). Now the output can be written as a summation of measured output vector (with a noise term) and estimated output vector as:

$$\mathbf{y}_{k+1} = \begin{bmatrix} \mathbf{z}_{k+1} \\ \mathbf{y}_{k+1}^{(u)} \end{bmatrix}. \tag{30}$$

The problem now is to estimate $\mathbf{y}_k^{(u)}$ associated with the unavailable state partition of (30).
For the discrete system model (4), rewriting the equation using the transformation T yields:

$$\begin{aligned} \Theta(\mathbf{y}_k, u_k, w_k, v_k) &= T\mathbf{x}_{k+1} \\ &= T\{\mathbf{x}_k + T_s f(\mathbf{x}_k) + T_s b(\mathbf{x}_k) u_k + w_k\} \end{aligned} \tag{31}$$

where T=[I_n], I_n is a identity matrix with the dimension of $n \times n$. And $\Theta(\mathbf{y}_k, u_k, w_k, v_k)$ is the transformed states
The transformation model may now be written as:

$$\mathbf{y}_{k+1} = \begin{bmatrix} \mathbf{z}_{k+1} \\ \mathbf{y}_{k+1}^{(u)} \end{bmatrix} = \Theta(\mathbf{y}_k, u_k, w_k, v_k). \tag{32}$$

For a reduced order form of the system, the transformed model (31) can be partitioned as two parts as:

$$\mathbf{y}_{k+1} = \begin{bmatrix} \mathbf{z}_{k+1} \\ \mathbf{y}_{k+1}^{(u)} \end{bmatrix} = \begin{bmatrix} \Theta_1(\mathbf{z}_k, \mathbf{y}_k^{(u)}, u_k, w_k, v_k) \\ \Theta_2(\mathbf{z}_k, \mathbf{y}_k^{(u)}, u_k, w_k, v_k) \end{bmatrix}. \tag{33}$$

The model of (1) assumes all smooth functions, and therefore, Θ_1, Θ_2 are both smooth functions inherently (because the transformation T=[I_n]). The estimated output $\mathbf{y}_k^{(u)}$ can be calculated by the unique inverse functions from (33) as:

$$\begin{bmatrix} \mathbf{y}_k^{(u)} \\ \mathbf{y}_k^{(u)} \end{bmatrix} = \begin{bmatrix} \Theta_1^{-1}(\mathbf{z}_k, \mathbf{z}_{k+1}, u_k, w_k, v_k) \\ \Theta_2^{-1}(\mathbf{z}_k, \mathbf{y}_{k+1}^{(u)}, u_k, w_k, v_k) \end{bmatrix} \tag{34}$$

Similarly, as in the estimated model of (6) and (7), the a posteriori and a priori estimation, can be expressed as estimated functions following the form of (34). Define an estimated term for the upper partition of (34) without noise term as:

$$\hat{\sigma}_{k+1} = \hat{\Theta}_1^{-1}(\mathbf{z}_k, \mathbf{z}_{k+1}, u_k) \tag{35}$$

The priori estimated states can be derived from the lower partition of (34) as:

$$\hat{\mathbf{y}}_{k+1|k}^{(u)} = \hat{\Theta}_2(\mathbf{z}_k, \hat{\sigma}_k, u_k) \tag{36}$$

Thus, unavailable state estimate are refined by the SVSF gain K_k as:

$$\hat{\mathbf{y}}_{k+1|k+1}^{(u)} = \hat{\mathbf{y}}_{k+1|k}^{(u)} + K_{k+1} \tag{37}$$

The a priori error between the estimations from the measured state partition and unavailable state partition of the output matrix may be defined as

$$e_{y_{k+1|k}}^{(u)} = \hat{\sigma}_{k+1} - \hat{\mathbf{y}}_{k+1|k}^{(u)} \tag{38}$$

The a posteriori error can therefore be defined as:

$$e_{y_{k+1|k+1}}^{(u)} = \hat{\sigma}_{k+1} - \hat{\mathbf{y}}_{k+1|k+1}^{(u)} \tag{39}$$

Appendix B: Nomenclature

Table 1 Nomenclature

Table 1 lists all the constants and variable used in this paper. Vectors of state and output are denoted by using bold letters. Their elements are denoted by italic lower case letters with *i* and or *j*. *k* denotes calculation step. Subscripts *k*|*k* and *k*|*k*-1 are used to identify a posterori and a priori estimates. The symbol "^" is used to identify uncertain parameters and to denote estimated value for state variables.

Symbol	Comments	Dimension
^	Estimated variable and uncertain parameter	
(m) , (u)	Superscripts for measured and unavailable states	
$\lvert\ \rvert_{ABS}$	Absolutely value	
$a_{11}, a_{12}, a_{13}, a_3, a_4$	Coefficients of system model.	1×1
b	Input matrix	m×1
e	State estimation error	n×1
$e_{z_{k+1\|k+1}}, e_{z_{k+1\|k}}$	Output estimation error calculated by using the a posteriori and a priori output estimates	m×1
f, F	Nonlinear function	
H	Output matrix	m×n
I_m	Identity matrix	m×m
i, j	Subscripts used to identify elements of matrices and vectors	1×1
k	Calculation step index	1×1
K_k	SVSF gain	n×1
Kf_k	EKF gain	n×1
P_k, Q_k, R_k	Covariance matrix associated with system, system noise and measurement noise	
m	Number of measurements	1×1
n	Number of states	1×1
S	Switching function	
sat	Saturation function	
sgn	Signum function	
tanh	Hyperbolic tangent function	
T	Transformation matrix	n×n
T_s	Sampling time	1×1
u	Input	1×1
vec	Any vector	
v, $V_{\max}$	Measurement noise and its upper bound	m×1
w, $W_{\max}$	System noise and its upper bound	n×1
$\mathbf{x}, \mathbf{x}_0$	System states and their initial condition	n×1
$\hat{\mathbf{x}}_{k+1\|k+1}, \hat{\mathbf{x}}_{k+1\|k}$	A posteriori (refined) and a priori state (unrefined) estimates	n×1
$\mathbf{y}$	Transformed system state	n×1
$\mathbf{z}$	Measured output	m×1
$\hat{\mathbf{z}}_{k+1\|k+1}, \hat{\mathbf{z}}_{k+1\|k}$	A posteriori (refined) and a priori (unrefined) output estimates	m×1
d_k, δ_k	Uncertainty term	n×1
Θ	Transformed states	
γ	Constant diagonal gain matrix with elements $\gamma_{ij} \geq 1$	n×n

Φ_k	Linearized estimation model	
Ψ	Boundary layer	$n \times 1$

References

[1] Julier, S. J, Uhlmann, J. and Durrant-Whyte, H. F., 2000, "A new method for the nonlinear transformation of means and covariances in filters and estimators", IEEE Transactions on Automatic Control Vol. 45, no. 3, pp. 477–482.

[2] Wan, E. A. and van der Merwe, R., 2000, "The unscented Kalman filter for nonlinear estimation", In Proceedings of Symposium 2000 on Adaptive Systems for Signal Processing, Communication, and Control (AS-SPCC), Lake Louise, Alberta, Canada, pp. 153–158.

[3] Moler, C. and Van Loan, C., 1978, "Nineteen Dubious Ways To Compute The Exponential Of A Matrix", SIAM Review Vol. 20, pp. 801–836.

[4] Grewal, M. S. and Andrews, A. P., 2001, "Kalman Filtering: Theory and Practice Using MATLAB", New York: John Wiley.

[5] Habibi, S. R, and Burton, R., 2004, "Parameter Identification for A High Performance Hydrostatic Actuation System Using the Variable Structure Filter Concept", American Society of Mechanical Engineers, The Fluid Power and Systems Technology Division (Publication) FPST, Vol. 11, pp. 93-101.

[6] Wang, S., Habibi, S. R. and Burton, R., 2006, "A Smooth Variable Structure Filter for State Estimation", The 25th IASTED International Conference on Modelling, Identification, and Control, MIC 2006, (accepted).

[7] Slotine, J. E., 1984, "Sliding Controller design for nonlinear Systems", International Journal of Control, Vol. 40, pp. 421-434.

[8] Brown, R. and Hwang, P., 1997, "Introduction to Random Signals and Applied Kalman Filtering, 3rd Edition", John Wiley &Sons.

[9] Habibi, S. R., and Singh, G., 2000, "Derivation of Design Requirements for Optimization of A High Performance Hydrostatic Actuation System", International Journal of Fluid Power, Vol. 2, pp. 11-27.

[10] R. A. Decarlo, S. H. Zak, and G. P. Matthews, "Variable Structure Control of Nonlinear Multivariable Systems: A Tutorial", in Proceedings of the IEEE, vol. 76, no. 3, pp. 212-232, 1988.

Appendix E: The Smooth Sliding Mode Controller and Filter (SSMCF) (Wang, et al [2006])*

* This paper is under reviewed by the IEEE Transactions on Automatic Control. This paper is included with the express permission of the journal's publishers.

THE SMOOTH SLIDING MODE CONTROLLER AND FILTER (SSMCF)

SHU WANG **SAEID HABIBI** **RICHARD BURTON**

Department of Mechanical Engineering, University of Saskatchewan
57 Campus Drive, Saskatoon, SK, S7N 5A9 Canada
Phone: 1-306-966-5463 Fax: 1-306-966-5427
shw750@mail.usask.ca

ABSTRACT

This paper proposes a combined state feedback and control method based on the concept of Variable Structure Systems (VSS). This method is defined as the Smooth Sliding Mode Controller and Filter (SSMCF) and can be applied to a class of nonlinear systems. This paper provides a derivation of the SSMCF and defines the conditions for its stability. The experimental application of the SSMCF to a nonlinear hydraulic system is illustrated. The results indicate that the SSMCF maintains the advantages of VSS, such as fast response and robustness.

Keywords: Smooth Sliding Mode Controller and Filter, Estimation, Stability, Nonlinear systems

1 INTRODUCTION

The purpose of the control law in a closed loop system is to improve the system's error characteristics. If the controller requires full state feedback, and if some states are not available, an estimator must be designed and combined with the control law to track the reference input. As such, the control-law would be based on the estimated rather than the actual states. [1]

Sliding Mode Control (SMC) is a robust control method that can overcome system and modeling uncertainties. Sliding Mode theory can also be used for robust state estimation, (referred to as Sliding Mode Observer or SMO).

The SMO for time-invariant systems was originally developed in the Soviet Union, [2]. In 1987, Slotine et al. [3] proposed a SMO in which the output errors are fed back in both a linear and discontinuous way. Elmali et al in 1996, [4], introduced the concept of Perturbation Estimation in SMC, which resulted in a procedure called Sliding Mode Control with Perturbation Estimation (SMCPE). Korondi et al summarized the theoretical background and the three main steps in designing an Observer-based Discrete-time Sliding–Mode (ODSM) control in 1998 [5]. A new SMO was proposed for a class of uncertain nonlinear systems in [6]. A comparative study of a SMO with the standard and extended versions of the Kalman filter for full state estimation in an induction machine was done in 2002 [7]. An adaptive sliding mode observer was proposed and applied to sensorless speed control of induction motors by Li, et al in 2005 [8].

A new strategy referred to as the Variable Structure Filter was proposed in [9], which uses concepts closely related to Variable Structure Control. The VSF is a model-based strategy that can be used for estimating the states of a linear observable system. The Smooth Variable Structure Filter (SVSF) was another new estimation method, first presented in 2004 [10], which is also developed from the concept of Variable Structure Control (VSC) used for nonlinear system. The results show that the SVSF provides excellent performance both in transient and steady state when compared to the results using an Extended Kalman Filter (EKF) in a previous comparative study [11].

The implementation and experimental verification of a new Sliding Mode Controller and Filter (SMCF) was proposed and presented by Wang et al in [12] and [13]. The SMCF combined the SMC and Variable Structure Filter (VSF) to acquire a full state feedback tracking control without effects of unmatched bounded uncertainties. This paper is an extension of the work presented in [13]. In this paper, a class of nonlinear uncertain systems is considered. The approach in this paper is applied to nonlinear systems with unmatched uncertainties. A new full state feedback nonlinear control with an estimator, referred to as the Smooth Sliding Mode Controller and Filter (SSMCF) is introduced, which will “fuse” the Discrete-time Sliding Mode Controller (DSMC) and Smooth Variable Structure Filter (SVSF), as shown in Fig. 1. The DSMC proposed by Misawa [14] is employed in the SSMCF. The revised form of SVSF [15] is used as an observer or estimator in the SSMCF. Since both SMC and SVSF are model-based control strategies and are derived from the same fundamental theory, (that is, VSC), the model of nonlinear plant is used to determine

the switching surfaces and calculating procedures for both the controller and estimator as shown in Fig. 1. The measured outputs are the elements of vector Z, which has a dimension of $m\times 1$. And the desired states are X_d $(n\times 1)$. Since $n > m$, not all states from the plant are available to compare with desired states. Thus, the measured outputs Z and control input are firstly fed into the SVSF to obtain the estimate states $\hat{X}$, which has a dimension of $n\times 1$. Then full feedback control can be constructed with estimate states and the DSMC.

In practice, although the model of the plant is not exactly known (due to parametric uncertainties), it may still be used to calculate the dynamics of plant provided it has the same control input as the plant itself (ref Fig. 1). The model "reference" states X_m can be developed with the control input u shown in Fig. 1. The model reference states may be used as a "compensation" for the measurements in order to solve any observability problem which may arise.

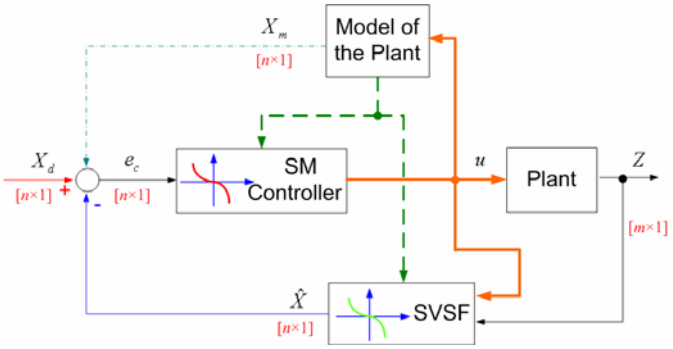

Fig. 1 SSMCF Schematic

In this paper, the method and its derivation are presented in Section 2. Section 3 provides the analysis of stability of the SSMCF. The implementation and experimental applications to a nonlinear hydraulic system are provided in Section 4. Section 5 gives the conclusions. The appendices contain the proofs of the control law, stability and sliding surface definition, and provide the nomenclature.

2 DERIVATION

Consider a particular nonlinear system which may be expressed by a smooth function, i.e. a function which is differentiable, such that,

$$\dot{X}(t) = \hat{F}(X,t,u) = \hat{f}(X,t) + \hat{b}(X,t)u(X,t) + \Delta f(X,t) \tag{1}$$

where $X(t) \in R^n$ is the state vector , $u(t)$ is the input signal and $\Delta f(x,t)$ is the time-dependent parameter uncertainties with known upper bound. $\hat{f}(X,t)$ and $\hat{b}(X,t)$ are known functions determining the system characteristics, where

$$\hat{f}(X,t) = \left[\hat{f}_1(X,t) \quad \hat{f}_2(X,t) \quad \cdots \quad \hat{f}_n(X,t)\right]^T,$$

$$\hat{b}(X,t) = \left[\hat{b}_1(X,t) \quad \hat{b}_2(X,t) \quad \cdots \quad \hat{b}_n(X,t)\right]^T$$

$$\begin{aligned}\Delta f(X,t) &= \left[\Delta f_1(X,t) \quad \Delta f_2(X,t) \quad \cdots \quad \Delta f_n(X,t)\right]^T \\ &= [\,\hat{f}_1(X,t) - f_1(X,t) \quad \hat{f}_2(X,t) - f_2(X,t) \quad \cdots \hat{f}_n(X,t) - f_n(X,t)]^T\end{aligned} \tag{2}$$

$f(.) = \left[f_1(.) \quad f_2(.) \quad \cdots \quad f_n(.)\right]$ is the exact model function describing the plant, which is unknown in practice due to system uncertainties. The unknown exact input matrix *b* can be written as the product of the uncertain input matrix $\hat{b}$ and a scalar uncertainty factor $\Delta b(\cdot)$, which is bounded such that:

$$1/\beta \le \Delta b \le \beta \quad \text{for } \beta > 1, \tag{3}$$

where $\Delta b(\cdot) = b(x(k)) / \hat{b}(X(k))$.

It is assumed that the relationship between the measurement signals and the states is linear, or at least piece-wise linear, such that

$$Z(t) = \hat{H}X(t) + v(t). \tag{4}$$

where $\hat{H}$ is the uncertain output matrix, and $v(t)$ is the measurement noise.

The approach of "forward difference" approximation is used in the discretization of the state space model at any time $T_s(k)$ and is given by:

$$\begin{aligned}&\dot{x}_i = \frac{x_i(k+1) - x_i(k)}{T_s} + \delta_i(k) \\ &i = 1,2,\cdots n\end{aligned} \tag{5}$$

where T_s is the sampling time and the terms of $\delta_i(k)$ are the numerical approximation errors.

The discrete model of Eq. (1) can be written as:

$$X_{k+1} = X_k + T_s \hat{f}(X_k) + T_s \hat{b}(X_k) u_k + w_k \tag{6}$$

where $w_k = T_s[\Delta f_k - \delta_k]$ is the lumped uncertainty term.

The discrete-time form of Eq. (4) may be expressed as:

$$Z_k = \hat{H} X_k + v_k . \tag{7}$$

The uncertainty term w_k and measurement noise v_k are assumed to have Gaussian distributions. To a high level of probability, the noise is assumed to be amplitude bounded. Furthermore, the system and measurement noise are assumed to be uncorrelated and upper bounded.

The SVSF is a predictor-corrector method that uses an internal model to predict an a priori estimate of states [10]:

$$\hat{X}_{k|k-1} = \hat{X}_{k-1|k-1} + T_s \hat{f}(\hat{X}_{k-1|k-1}) + T_s \hat{b}(\hat{X}_{k-1|k-1}) u_{k-1} \tag{8}$$

where the hat symbol "^" denotes an estimated state, function, or parameter, (it should be noted that as such, a "^" on the *f* and *b* means an estimated function or parameter that is uncertain but known). The state estimate is obtained by using the previous a posteriori state estimate $\hat{X}_{k-1|k-1}$ or at the inception of the process, by using the initial conditions, $\hat{X}_0$. The estimated states are then used for predicting the a priori estimates of measurements such that:

$$\hat{Z}_{k|k-1} = \hat{H} \hat{X}_{k|k-1} \tag{9}$$

The a posteriori state estimate can be obtained by a priori estimate refined by a corrective term, K_{k+1}:

$$\hat{X}_{k|k} = \hat{X}_{k|k-1} + K_k , \tag{10}$$

where $K_k \in \Re^n$ is calculated as a function of the error in the predicted output:

$$K_k = \hat{H}^+ (\left| e_{f_{k|k-1}} \right|_{ABS} + \gamma \left| e_{f_{k-1|k-1}} \right|_{ABS}) \operatorname{sgn}(e_{f_{k|k-1}}) , \tag{11}$$

where the superscript "+" denotes the pseudo-inverse. The derivation of the SVSF gain can be seen in [10, 15]. In Eq. (11),

$$e_{f_{k|k-1}} = Z_k - \hat{Z}_{k|k-1} \tag{12}$$

$$e_{f_{k-1|k-1}} = Z_{k-1} - \hat{Z}_{k-1|k-1} . \tag{13}$$

In state tracking or trajectory following problems, the sliding surface is defined in terms of the error of the states. Assume that the control problem is to constrain the states X to follow a prescribed trajectory X_d, let:

$$X_{d_k} = [x_{d_k}, \dot{x}_{d_k}, \cdots, x_{d_k}^{(n-1)}] \tag{14}$$

Since the actual states are not fully known, the full feedback controller can only use the estimate states.

Define the sliding surface to be

$$\hat{S}_k = \hat{S}(e_{ck}) = 0 \tag{15}$$

where $e_{c_k} = X_{d_k} - \hat{X}_{k|k}$.

The sliding surface can be approximately described using the Taylor series expansion as:

$$\hat{S}_{k+1} = \hat{S}_k + \sigma_k (e_{ck+1} - e_{ck}) + \zeta_k, \tag{16}$$

where the gradient of sliding surface is defined by

$$\sigma_k = \frac{\partial \hat{S}_k}{\partial e_{c_k}}. \tag{17}$$

The robust stability of the discrete-time sliding mode controller for the previously described systems can be guaranteed using the discrete-time Lyapunov stability theory. The Lyapunov function is chosen to be

$$V_k = \hat{S}_k^2 \tag{18}$$

The sliding surface S=0 is attractive if

$$V_{k+1} < V_k \Rightarrow \hat{S}_{k+1}^2 < \hat{S}_k^2 \quad \forall k \geq 0 \tag{19}$$

The condition may be written as:

$$\begin{aligned} \hat{S}_{k+1}^2 - \hat{S}_k^2 &= [\hat{S}_{k+1} - \hat{S}_k + 2\hat{S}_k][\hat{S}_{k+1} - \hat{S}_k] \\ &= [\Delta\hat{S}_k + 2\hat{S}_k]\Delta\hat{S}_k \\ &= \Delta\hat{S}_k^2 + 2\hat{S}_k\Delta\hat{S}_k < 0 \end{aligned} \quad . \tag{20}$$

Eq. (20) can be written as:

$$\Delta\hat{S}_k^2 < -2\hat{S}_k\Delta\hat{S}_k \tag{21}$$

where $\Delta\hat{S}_k = \hat{S}_{k+1} - \hat{S}_k$.

Thus,

$$\begin{aligned}\Delta\hat{S}_k &= \hat{S}_{k+1} - \hat{S}_k \\ &= \sigma_k[e_{c_{k+1}} - e_{c_k}] + \zeta_k \\ &= \sigma_k[\Delta X_{d_k} - \hat{X}_{k+1|k+1} + X_{k|k}] + \zeta_k\end{aligned} \tag{22}$$

From Eqs. (8) and (10), Eq. (22) can be written as

$$\begin{aligned}\Delta\hat{S}_k &= \sigma_k[\Delta X_{d_k} - \hat{X}_{k+1|k} - K_{k+1} + \hat{X}_{k|k}] + \zeta_k \\ &= \sigma_k[\Delta X_{d_k} - T_s\hat{f}(\hat{X}_{k|k}) - T_s\hat{b}(\hat{X}_{k|k})u_k - K_{k+1}] + \zeta_k\end{aligned} \tag{23}$$

where $\Delta X_{d_k} = X_{d_{k+1}} - X_{d_k}$.

The Lyapunov function Eq. (15) contains the SVSF corrective term K_{k+1} for state estimation as shown in Eq. (23). Further to Eqs. (18) to (23), it is now possible to derive a robust sliding mode controller that would include the dynamics of the state estimation. It should be noted that if the system (described by Eqs (6) and (7)) is completely controllable and completely observable, the output stability implies that all states are controlled and stable. The quality of trajectory error pertaining to each state is determined by the value of σ_k that is obtained here are using the LQ method (see appendix C). The sliding mode controller used here is based on the method proposed in [14]. Further to [14], the derivation of the control law is given in Appendix A and leads to the following control input:

$$u_k = \frac{\beta^2+1}{2\beta}\hat{p}_k + \left[\frac{\beta^2-1}{2\beta}|\hat{p}_k| + \frac{\beta K_C}{\hat{b}(\hat{X}_{k|k})\sigma_k}\right]\cdot sign(\hat{S}_k) \tag{24}$$

where

$$\hat{p}_k = \frac{\sigma_k}{T_s\hat{b}(\hat{X}_{k|k})\sigma_k}\left[-T_s\hat{f}(\hat{X}_{k|k}) + \Delta X_{d_k} - K_{k+1}\right] \tag{25}$$

and

$$K_C \geq \Sigma_k + 2\varepsilon \geq \left|\frac{\zeta_k}{T_s}\right| + 2\varepsilon \tag{26}$$

where $\varepsilon > 0$ is an arbitrary positive constant.

The proof of stability is given in Appendix B. The nonlinear system defined by Eq. (1) with the control law of Eqs. (24) and (25) is forced to reach sliding mode. However, the discontinuity and the switching nature of the control signal results in a "chattering" problem [14]. To remove chattering, a boundary layer can be used with an adjusting gain as specified in [16] and as follows:

$$\phi_k \geq \frac{T_s}{2}\left\{\frac{(\beta^2-1)\hat{b}(\hat{X}_{k|k})\sigma_k}{2\beta^2}\cdot\mu\cdot\left[(3\beta^2+1)\mid \hat{p}_k \mid +(\beta^2-1)sat\left(\frac{\hat{S}_k}{\phi_{k-1}}\right)\right]+(1+\beta^2)\Sigma_k+2\beta^2\varepsilon\right\} \tag{27}$$

where $0<\mu<1$ is the adjusting gain.

The discontinuous sign function $sign(\cdot)$ in Eq. (24) can be replaced by a saturation function to smooth the sliding motion such that:

$$sat(\frac{\hat{S}_k}{\phi_k})=\begin{cases}\hat{S}_k/\phi_k & |\hat{S}_k|\leq\phi_k\\ sign(\hat{S}_k/\phi_k) & \text{otherwise}\end{cases}. \tag{28}$$

The control signal of SSMCF contains two discontinuous switching actions, namely that of SMC ($sign(\hat{S}_k)$) and of SVSF ($\text{sgn}(e_{f_{k|k-1}})$) as seen in Eqs. (11) and (24). Although these switching actions can be smoothed by their respective boundary layers individually, it is possible that chaotic chattering may be excited by combining these two switching actions. Thus, the stability is a critical problem for this combined strategy of the SSMCF. In the next section, the combined stability pertaining to the SSMCF is further discussed.

3 STABILITY ANALYSIS

Since the SSMCF is a combined strategy that includes an estimator and a controller, the implementation process of the SSMCF can be divided into parts. The stability of the SSMCF is an "integrated" issue of three processes in that it introduces three terms into the SSMCF: 1-the Estimation Process (EP), 2- the Control Process (CP), and 3- the Integrated Process (IP). In this section, the stability will be discussed for each of these processes separately.

Figure 2 graphically shows a visual representation of the three processes of the SSMCF. The main objective of the SSMCF is for the control law of Eq. (24) to make the estimate $\hat{X}_{k|k}$ and actual X_k states to follow the desired trajectory X_{d_k}. The stability condition of the SSMCF is such that all the various error

signals shown in Fig. 2 converge to zero as quickly as possible with the prescribed control law. These error signals include EP error (the difference between actual and estimated states), CP error (the difference between desired and estimated states), and IP error (the difference between desired and actual states).

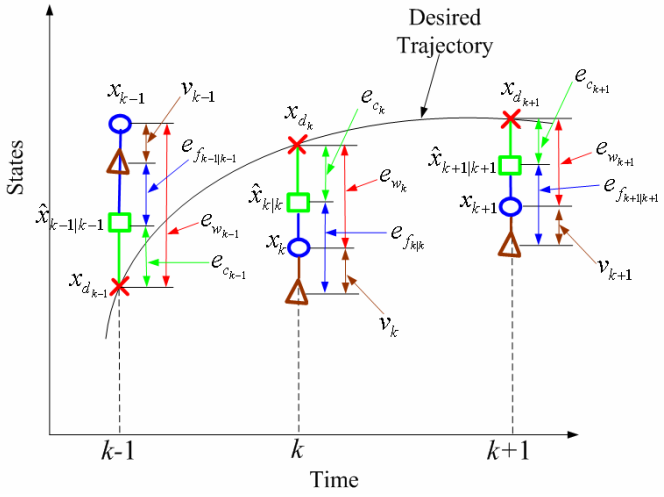

Fig. 2 The Error Processes of the SSMCF

In the SSMCF, the sliding surface is a function of the error signals of the control response as defined in Eq. (15). The CP error is chosen as:

$$e_{c_k} = X_{d_k} - \hat{X}_{k|k} \tag{29}$$

where X_{d_k} are the desired trajectories, and $\hat{X}_{k|k}$ are the a posteriori estimates for the states by the SVSF.

The control law is derived from and satisfied the Lyapunov stability criterion as shown by Eq. (19). In this case, the sliding surface can be chosen as a linear surface by the Linear Quadratic method [16], which means that $\sigma_k = \dfrac{\partial \hat{S}_k}{\partial e_{c_k}}$ is a constant *C*, such that,

$$V_{k+1} < V_k \Rightarrow \hat{S}_{k+1}^2 < \hat{S}_k^2 \tag{30}$$

Then

$$(Ce_{c_{k+1}})^2 < (Ce_{c_k})^2 \quad , \tag{31}$$

such that

$$|Ce_{c_{k+1}}| < |Ce_{c_k}| \, . \tag{32}$$

Since C is a constant vector, the pseudo inverse of C may be defined as C^+. Pre-multiplying by the absolute value of this pseudo inverse, i.e. $\left|C^+\right|$ on both sides of the inequality of (32), yields,

$$\left|C^+\left\|Ce_{c_{k+1}}\right|\right| < \left|C^+\left\|Ce_{c_k}\right|\right| . \tag{33}$$

From Eq. (33), since $\left|C^+C\right| = 1$, the error in state estimation for each step is reduced which means that the estimated states move closer to the desired trajectory. The stability of CP of SSMCF is guaranteed by the inequality as follows:

$$|e_{c_{k+1}}| < |e_{c_k}| . \tag{34}$$

In the linear system, the control gain K_c and tuning gain γ can be substituted into the system model to obtain their upper bounds to satisfy the condition of Eq. (34) and further to make the system stable. This can be verified by the error transfer function by placing all of its poles in the unit circle in the Z-domain [13]. However, due to the nonlinear characteristics in this case, it is very difficult to directly derive an upper bound of K_c. To consider the stability of the CP, the determination of K_c is a summation of its lower limit $\left|\frac{\zeta_k}{T_s}\right|$ and a small positive value 2ε shown in Eq. (26). Thus, an appropriate choice of the value of 2ε may be used to satisfy the stability condition.

The posteriori estimate can be obtained by refining the a priori estimate by the SVSF gain as Eq. (10), such that:

$$e_{c_k} = X_{d_k} - \hat{X}_{k|k-1} - K_k \tag{35}$$

From Eqs. (7), (9) and (12),

$$e_{f_{k|k-1}} = \hat{H}X_k - \hat{H}\hat{X}_{k|k-1} + v_k . \tag{36}$$

Then,

$$-\hat{X}_{k|k-1} = \hat{H}^+ e_{f_{k|k-1}} - X_k - \hat{H}^+ v_k . \tag{37}$$

where $e_{f_{k|k-1}}$ is the a priori EP error.

Substituting Eq. (37) into Eq. (35) yields:

$$e_{c_k} = e_{w_k} + \hat{H}^+ e_{f_{k|k-1}} - K_k - \hat{H}^+ v_k \,, \tag{38}$$

where $e_{w_k} = X_{d_k} - X_k$ is the error signal of IP in the SSMCF.

Computing the absolute value of Eq. (38) yields:

$$|\, e_{c_k} - e_{w_k} \,|_{ABS} = |\, \hat{H}^+ e_{f_{k|k-1}} - K_k - \hat{H}^+ v_k \,|_{ABS} \,, \tag{39}$$

Substituting the SVSF gain of Eq. (11) into Eq. (39) yields:

$$|\, e_{c_k} - e_{w_k} \,|_{ABS} = |\, \hat{H}^+ \gamma \left| e_{f_{k-1|k-1}} \right|_{ABS} \text{sgn}(e_{f_{k|k-1}}) - \hat{H}^+ v_k \,|_{ABS} \,, \tag{40}$$

It is assumed that the measurement noise v_k is upper bounded such that:

$$|\, e_{w_k} \,|_{ABS} - |\, e_{c_k} \,|_{ABS} \le \gamma \,|\, \hat{H}^+ \,|_{ABS} \left| e_{f_{k-1|k-1}} \right|_{ABS} + |\, \hat{H}^+ v_{\max} \,|_{ABS} \tag{41}$$

where $|\, v_k \,|_{ABS} \le v_{\max}$.

Eq. (41) may be written as:

$$|\, e_{w_k} \,|_{ABS} \le |\, e_{c_k} \,|_{ABS} + \gamma \,|\, \hat{H}^+ \,|_{ABS} \left| e_{f_{k-1|k-1}} \right|_{ABS} + |\, \hat{H}^+ v_{\max} \,|_{ABS} \tag{42}$$

The lag step of the IP error can be written as:

$$|\, e_{w_{k-1}} \,|_{ABS} \le |\, e_{c_{k-1}} \,|_{ABS} + \gamma \,|\, \hat{H}^+ \,|_{ABS} \left| e_{f_{k-2|k-2}} \right|_{ABS} + |\, \hat{H}^+ v_{\max} \,|_{ABS} \tag{43}$$

The stability of the SVSF estimation process (i.e. EP) is also guaranteed by the Lyapunov function (the proof is given in reference [10, 15]), i.e.:

$$\left| e_{f_{k-1|k-1}} \right|_{ABS} < \left| e_{f_{k-2|k-2}} \right|_{ABS} . \tag{44}$$

Thus, under the condition of a linear sliding surface chosen, and $\left| H^+ \right| > 0$ and $0 < \gamma < 1$, and bounded measurement noise, from Eq. (42), the IP error signals for each step are bounded by the CP and EP errors and the upper-bound of measurement noise. Eq. (42) consequently ensures that the chattering problem will not be excited in the SSMCF. Although it cannot guarantee that the IP errors reduce for each calculation step caused by the randomness of measurement noise as shown in Fig 2, the Eqs. (42) and (43) indicate that the overall tendency of IP errors will be to decrease, which is satisfied with the stability conditions.

Under an ideal condition, i.e. there exists no measurement noise, $v_k = 0$, the stability condition of the IP can be derived as shown in Appendix B as:

$$|e_{w_k}|_{ABS} < |e_{w_{k-1}}|_{ABS} . \quad (45)$$

In this case, the choice of γ will affect the convergent rate of the Integrated Process.

4 EXPERIMENTAL VERIFICATION

To illustrate the SSMCF, a high precision hydrostatic system, which is referred to as ElectoHydraulic Actuator (EHA) system was the physical system that was examined. The nonlinear model of the EHA was introduced in [16] and is given as:

$$\begin{cases} \dot{x}_1 = x_2 \\ \dot{x}_2 = x_3 \\ \dot{x}_3 = -\alpha_1 x_3 - \alpha_2 x_2 - [\alpha_{31} x_2 x_3 + \alpha_{32} {x_2}^2 + \alpha_{33}] sign(x_2) \\ \qquad + \alpha_4 u \end{cases} \quad (46)$$

where x_1, x_2, x_3 are the states representing the position, velocity and acceleration of load in the EHA system, u is the voltage input to an electric motor to control the system. The coefficients of equations for the experimental EHA are: $\alpha_1 = -71$, $\alpha_2 = 39000$ $\alpha_{31} = 2100$, $\alpha_{32} = 1610$, $\alpha_{33} = 3.5$, $\alpha_4 = 535$.

Using the discretization approach of Eq. (5) and sampling time $T_s = 0.001s$, the discrete model of the EHA system may be written as:

$$\begin{cases} x_{1k+1} = x_{1k} + 0.001 x_{2k} + w_{1k} \\ x_{2k+1} = x_{2k} + 0.001 x_{3k} + w_{2k} \\ x_{3k+1} = 1.1 x_{3k} - 39.0 x_{2k} \\ -[2.1 x_{2k} x_{3k} + 1.6 {x_{2k}}^2 + 0.0035] sign(x_{2k}) + 0.54 u_k + w_{3k} \end{cases} \quad (47)$$

where w_k is a bounded system noise.

Since the Coulomb friction was considered in the model of Eq. (47), a sign function is involved to describe the discontinuous effect. But the SVSF requires a continuous function and hence a hyperbolic tangent with high gain, $\tanh(hx)$, was used to approximate the sign function to a form, [15].

In the actual EHA, only the position could be measured directly by a digital transducer. For the model given in Eq. (47), the linearized equations of Eq (47) are unobservable if only one state variable (position, x_1) is known which means another state, i.e. velocity x_2 must be made available. In this case, the model

reference output of velocity can be used to design the SSMCF, as was shown in Fig. 1. Thus the output equation for the EHA system can be written as:

$$Z_k = \begin{bmatrix} 1 & 0 & 0 \\ 0 & 1 & 0 \end{bmatrix} X_k + v_k . \tag{48}$$

For the experimental tests, the sliding surface coefficients are chosen as a constant vector $\sigma_k = C = [35 \quad 370 \quad 1]$ using the Linear Quadratic method [16] as shown in Appendix C.

The gains were set to $\beta = 1$ (which assumes that there are no uncertainties in the model), and $\mu = 0.5$ (which is dependent on a best accuracy obtained in test results). The control gain K_C is chosen as 6 to satisfy the condition of $K_C \geq \left| \frac{\zeta_k}{T_s} \right| + 2\varepsilon$ and the adjusting gain $\gamma = 0.1$ to match the stability condition.

In the tests, the desired trajectories are given as periodic signals for the reference trajectories of position, velocity and acceleration, as shown in Fig. 3. With the control law using the SVSF estimation process as was given in Eq. (24), the actual measured position and model reference velocity are shown in Fig. 3. It is observed that the output states follow the desired trajectory effectively. The estimated states shown as dash-dot lines in Fig. 3 also track the desired states very well. Figure 4 gives the error signals for the Control Process (CP) and the Integrated Process (IP) separately. It shows that the SSMCF provides a high performance tracking control and hence, the stability of the different processes in the SSMCF is verified here experimentally.

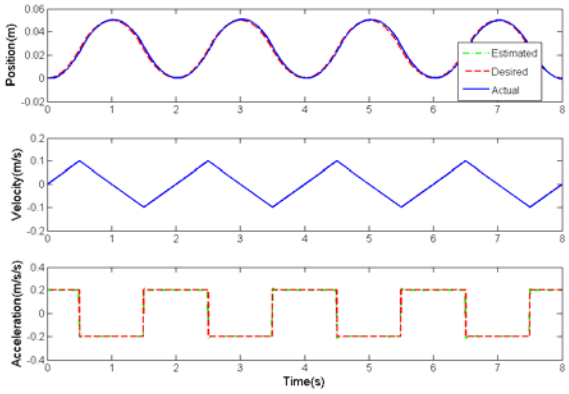

Fig. 3 The Response States of the EHA with the SSMCF

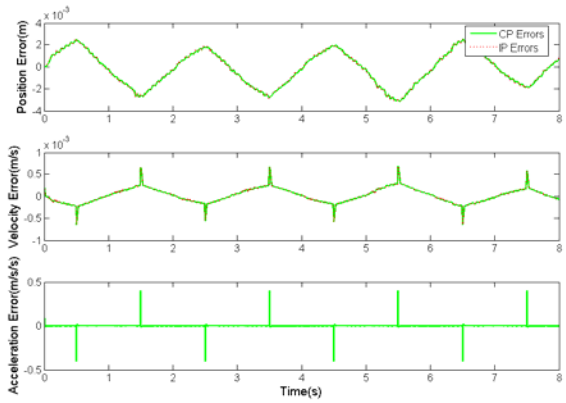

Fig. 4 The Response Errors of the EHA with the SSMCF

The SSMCF is a new combined control strategy derived using the concept of VSC. It is expected that the SSMCF will inherit the most important advantage of VSC, i.e. robustness. To verify this point, 20% percent variations of all coefficients of Eq. (47) are injected to the nonlinear model of the EHA, such that:

$\alpha_1 = -85$, $\alpha_2 = 46800$ $\alpha_{31} = 2520$, $\alpha_{32} = 1932$, $\alpha_{33} = 4.2$, $\alpha_4 = 642$.

In the experimental tests on the EHA, the tracking control of the SSMCF with the parameter variation is given the same periodic desired trajectories as the above tests. The sliding surface coefficients are determined as a vector $\sigma_k = C = [100 \quad 106 \quad 1]$. The gains set to $\beta = 1.55$ (caused by 20% parameter uncertainties in model), and the gains of μ K_C and γ are set as the same values as the above tests.

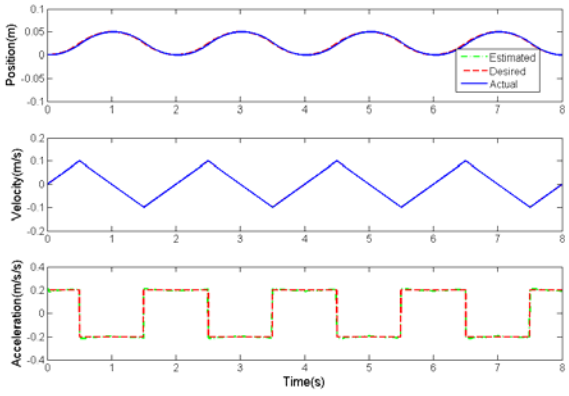

Fig. 5 The Response States of the EHA with the SSMCF (20% parameter uncertainties)

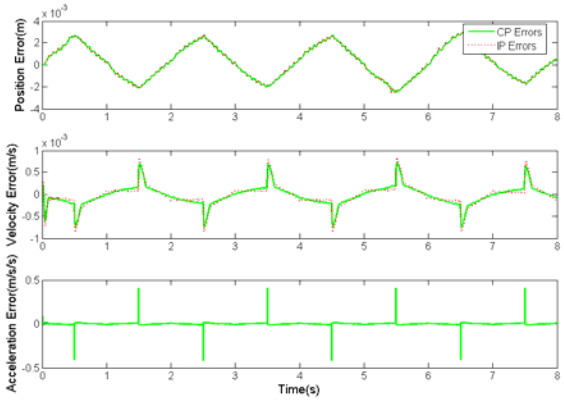

Fig. 6 The Response Errors of the EHA with the SSMCF (20% parameter uncertainties)

Figures 5 and 6 show the responses of the states and their error signals given the large parametric uncertainties. The results show that the actual states can still obtain a fast and effective tacking of the desired trajectories. The only difference is that the errors between the actual and desired states do increase as compared to those shown in Figure 4. It can be concluded that the SSMCF exhibits the robustness of the VSC as expected.

5 CONCLUSIONS

This paper introduced a new combined control and estimation strategy, which is referred to as the Smooth Sliding Mode Controller and Filter (SSMCF). This method is derived from the concepts of Variable Structure Systems. It may be used on a class of smooth nonlinear systems to provide a robust and high performance state estimation and trajectory tracking control given modeling uncertainties. The stability of this method is guaranteed given bounded uncertainties. The stability conditions are analyzed and proven by mathematically.

In this paper a nonlinear hydraulic system is used to experimentally verify the SSMCF. The robustness and performance of the SSMCF given large modeling uncertainties are experimentally demonstrated.

APPENDIX A: PROOF OF THE CONTROL LAW

The proof of the control law follows the approach used by Misawa [14]. The new defined Lyapunov function (from Eqs. (18) ~ (23)) is involved the SVSF gain and used to determine the control law of the SSMCF.

Based on the location of representative points (the values of switching function) related to sliding surface, two conditions should be considered individually:

1. When $\hat{S} > 0$, i.e. the representative points lie in the upper side of the surface, where

$$\Delta\hat{S}_k = \hat{S}_{k+1} - \hat{S}_k < 0 . \tag{49}$$

From Eq. (21),

$$0 > \Delta\hat{S}_k > -2\hat{S}_k . \tag{50}$$

Substituting Eq. (23) into Eq. (50):

$$0 > \sigma_k \Delta X_{d_k} - T_s\sigma_k[\hat{f}(\hat{X}_{k|k}) + \hat{b}(\hat{X}_{k|k})u_k] + \zeta_k - \sigma_k K_{k+1} > -2\hat{S}_k . \tag{51}$$

So

$$\begin{aligned} \frac{\sigma_k \hat{f}(\hat{X}_{k|k})}{\sigma_k} - \frac{\sigma_k \Delta X_{d_k}}{T_s\sigma_k} + \frac{\sigma_k K_{k+1}}{T_s\sigma_k} - \frac{\zeta_k}{T_s\sigma_k} &> -\hat{b}(\hat{X}_{k|k})u_k \\ &> \frac{\sigma_k \hat{f}(\hat{X}_{k|k})}{\sigma_k} - \frac{\sigma_k \Delta X_{d_k}}{T_s\sigma_k} + \frac{\sigma_k K_{k+1}}{T_s\sigma_k} - \frac{\zeta_k}{T_s\sigma_k} - \frac{2\hat{S}_k}{T_s\sigma_k} \end{aligned} . \tag{52}$$

Using Eq. (3), Eq. (52) may be written as:

$$\begin{aligned} &-\frac{\sigma_k \hat{f}(\hat{X}_{k|k})}{\hat{b}(\hat{X}_{k|k})\sigma_k} + \frac{\sigma_k \Delta X_{d_k}}{T_s\hat{b}(\hat{X}_{k|k})\sigma_k} - \frac{\sigma_k K_{k+1}}{T_s\hat{b}(\hat{X}_{k|k})\sigma_k} + \frac{\zeta_k}{T_s\hat{b}(\hat{X}_{k|k})\sigma_k} \\ &< \Delta b(\cdot)u_k < -\frac{\sigma_k \hat{f}(\hat{X}_{k|k})}{\hat{b}(\hat{X}_{k|k})\sigma_k} + \frac{\sigma_k \Delta X_{d_k}}{T_s\hat{b}(\hat{X}_{k|k})\sigma_k} - \frac{\sigma_k K_{k+1}}{T_s\hat{b}(\hat{X}_{k|k})\sigma_k} \\ &+ \frac{\zeta_k}{T_s\hat{b}(\hat{X}_{k|k})\sigma_k} + \frac{2\hat{S}_k}{T_s\hat{b}(\hat{X}_{k|k})\sigma_k} \end{aligned} . \tag{53}$$

2. When $\hat{S} < 0$, i.e. the representative point lies in the lower side of the surface, where

$$\Delta\hat{S}_k = \hat{S}_{k+1} - \hat{S}_k > 0 . \tag{54}$$

From Eq. (21),

$$0 < \Delta\hat{S}_k < -2\hat{S}_k . \tag{55}$$

Substituting Eq. (23) into Eq. (55) yields:

$$\begin{aligned} &-\frac{\sigma_k \hat{f}(\hat{X}_{k|k})}{\hat{b}(\hat{X}_{k|k})\sigma_k}+\frac{\sigma_k \Delta X_{d_k}}{T_s\hat{b}(\hat{X}_{k|k})\sigma_k}-\frac{\sigma_k K_{k+1}}{T_s\hat{b}(\hat{X}_{k|k})\sigma_k}+\frac{\zeta_k}{T_s\hat{b}(\hat{X}_{k|k})\sigma_k} \\ &> \Delta b(\cdot)u_k > -\frac{\sigma_k \hat{f}(\hat{X}_{k|k})}{\hat{b}(\hat{X}_{k|k})\sigma_k}+\frac{\sigma_k \Delta X_{d_k}}{T_s\hat{b}(\hat{X}_{k|k})\sigma_k}-\frac{\sigma_k K_{k+1}}{T_s\hat{b}(\hat{X}_{k|k})\sigma_k} \\ &+\frac{\zeta_k}{T_s\hat{b}(\hat{X}_{k|k})\sigma_k}+\frac{2\hat{S}_k}{T_s\hat{b}(\hat{X}_{k|k})\sigma_k} \end{aligned} \quad . \tag{56}$$

The control law may be given as a summation of two terms, $\hat{p}_k$, $\tilde{p}_k$, such that:

$$u_k = \hat{p}_k + \tilde{p}_k \, . \tag{57}$$

Based on inequalities of (53) and (57), $\hat{p}_k$ may be selected as:

$$\hat{p}_k = \frac{\sigma_k}{T_s\hat{b}(\hat{X}_{k|k})\sigma_k}\left[-T_s\hat{f}(\hat{X}_{k|k})+\Delta X_{d_k}-K_{k+1}\right]. \tag{58}$$

i) For the case of $\hat{S} > 0$

$$\begin{aligned} &\hat{p}_k+\frac{\zeta_k}{T_s\hat{b}(\hat{X}_{k|k})\sigma_k} < \Delta b(\cdot)[\hat{p}_k+\tilde{p}_k] \\ &< \hat{p}_k+\frac{\zeta_k}{T_s\hat{b}(\hat{X}_{k|k})\sigma_k}+\frac{2\hat{S}_k}{T_s\hat{b}(\hat{X}_{k|k})\sigma_k} \end{aligned} \quad , \tag{59}$$

and then

$$\begin{aligned} &[1-\Delta b(\cdot)]\hat{p}_k+\frac{\zeta_k}{T_s\hat{b}(\hat{X}_{k|k})\sigma_k} < \Delta b(\cdot)\tilde{p}_k \\ &< [1-\Delta b(\cdot)]\hat{p}_k+\frac{\zeta_k}{T_s\hat{b}(\hat{X}_{k|k})\sigma_k}+\frac{2\hat{S}_k}{T_s\hat{b}(\hat{X}_{k|k})\sigma_k} \end{aligned} \quad . \tag{60}$$

From the left inequality of (60),

$$\tilde{p}_k > \left[\frac{1}{\Delta b(\cdot)}-1\right]\hat{p}_k+\frac{\zeta_k}{T_s\hat{b}(\hat{X}_{k|k})\sigma_k\Delta b(\cdot)} \, . \tag{61}$$

Define $\tilde{p}_k$ as the switching form of control signal as:

$$\tilde{p}_k = q_k+\frac{\beta K_C}{\hat{b}(\hat{X}_{k|k})\sigma_k}\,sign(\hat{S}_k) \, , \tag{62}$$

where $sign(\cdot)$ is the signum function, and where β is the upper bound of $1/\Delta b(\cdot)$.

The following condition may be derived so that the inequality (62) is satisfied:

$$q_k \geq \left[\frac{1}{\Delta b(\cdot)} - 1\right]\hat{p}_k, \quad K_C \geq \Sigma_k \geq \left|\frac{\zeta_k}{T_s}\right|. \tag{63}$$

The first inequality is satisfied if

$$q_k \geq (\beta - 1)\hat{p}_k > 0, \quad \text{if} \quad \hat{p}_k > 0,$$

$$q_k \geq \frac{1-\beta}{\beta}\hat{p}_k > 0, \quad \text{if} \quad \hat{p}_k < 0. \tag{64}$$

where β and $1/\beta$ is the bound of $\Delta b(\cdot)$ defined by Eq. (3).

ii) Similarly, for the case of $\hat{S} < 0$, q_k must satisfy:

$$q_k \leq \left[\frac{1}{\Delta b(\cdot)} - 1\right]\hat{p}_k. \tag{65}$$

So

$$q_k \leq \frac{1-\beta}{\beta}\hat{p}_k < 0, \quad \text{if} \quad \hat{p}_k > 0,$$

$$q_k \leq (\beta - 1)\hat{p}_k < 0, \quad \text{if} \quad \hat{p}_k < 0. \tag{66}$$

If the inequalities of (64) and (66) can be satisfied, then q_k may be selected as:

$$q_k = \frac{\beta - 1}{2}[\hat{p}_k + |\hat{p}_k| sign(\hat{S}_k)] + \frac{1-\beta}{2\beta}[\hat{p}_k - |\hat{p}_k| sign(\hat{S}_k)]. \tag{67}$$

The control law of Eq. (57) can be written as:

$$\begin{aligned} u_k &= \hat{p}_k + q_k + \frac{\beta K_C}{\hat{b}(\hat{X}_{k|k})\sigma_k} \cdot sign(\hat{S}_k) \\ &= \frac{\beta^2 + 1}{2\beta}\hat{p}_k + \left[\frac{\beta^2 - 1}{2\beta}|\hat{p}_k| + \frac{\beta K_C}{\hat{b}(\hat{X}_{k|k})\sigma_k}\right] \cdot sign(\hat{S}_k) \end{aligned}. \tag{68}$$

To remove the chattering caused by discontinuous control signal, the boundary layer is defined as:

$$\Psi = \{e_{c_k} \,||\, \hat{S}(e_{c_k}) \leq \phi_k\}. \tag{69}$$

The control law of Eq. (68) is given as:

$$u_k = \frac{\beta^2 + 1}{2\beta}\hat{p}_k + \left[\frac{\beta^2 - 1}{2\beta}|\hat{p}_k| + \frac{\beta K_C}{\hat{b}(\hat{X}_{k|k})\sigma_k}\right] \cdot sat(\frac{\hat{S}_k}{\phi_k}). \tag{70}$$

In order to evaluate the width of boundary layer ϕ_k, the right inequality of Eq. (53) is considered:

$$\begin{aligned} &-\frac{\sigma_k \hat{f}(\hat{X}_{k|k})}{\hat{b}(\hat{X}_{k|k})\sigma_k}+\frac{\sigma_k \Delta X_{d_k}}{T_s\hat{b}(\hat{X}_{k|k})\sigma_k}-\frac{\sigma_k K_{k+1}}{T_s\hat{b}(\hat{X}_{k|k})\sigma_k}+\frac{\zeta_k}{T_s\hat{b}(\hat{X}_{k|k})\sigma_k}+\frac{2\hat{S}_k}{T_s\hat{b}(\hat{X}_{k|k})\sigma_k} \\ &> \Delta b(\cdot)u_k = \Delta b(\cdot)\left\{\frac{\beta^2+1}{2\beta}\hat{p}_k+\left[\frac{\beta^2-1}{2\beta}\mid \hat{p}_k\mid+\frac{\beta K_C}{\hat{b}(\hat{X}_{k|k})\sigma_k}\right]\cdot sign(\frac{\hat{S}_k}{\phi_k})\right\} \end{aligned} \quad . \tag{71}$$

For the worst case of $\hat{S}_k = \phi_k > 0$, Eq. (71) is given as:

$$\begin{aligned} &\frac{2\phi_k}{T_s\hat{b}(\hat{X}_{k|k})\sigma_k} > -\hat{p}_k-\frac{\zeta_k}{T_s\hat{b}(\hat{X}_{k|k})\sigma_k} \\ &+\Delta b(\cdot)\left\{\frac{\beta^2+1}{2\beta}\hat{p}_k+\left[\frac{\beta^2-1}{2\beta}\mid \hat{p}_k\mid+\frac{\beta K_C}{\hat{b}(\hat{X}_{k|k})\sigma_k}\right]\right\}, \end{aligned} \tag{72}$$

which may be given as

$$\begin{aligned} \phi_k &> \frac{T_s}{2}\left\{\hat{b}(\hat{X}_{k|k})\sigma_k\left[\left(\frac{(\beta^2+1)\Delta b(\cdot)}{2\beta}-1\right)\hat{p}_k+\frac{(\beta^2-1)\Delta b(\cdot)}{2\beta}\mid \hat{p}_k\mid\right]-\frac{\zeta_k}{T_s}+\Delta b(\cdot)\beta K_C\right\} \\ &\geq \frac{T_s}{2}\left\{\hat{b}(\hat{X}_{k|k})\sigma_k\left[\left(\frac{(\beta^2+1)\Delta b(\cdot)}{2\beta}-1\right)\hat{p}_k+\frac{(\beta^2-1)\Delta b(\cdot)}{2\beta}\mid \hat{p}_k\mid\right]-\frac{\zeta_k}{T_s}+\Delta b(\cdot)\beta(\Sigma_k+2\varepsilon)\right\}, \end{aligned} \tag{73}$$

where the sliding gain of K_C is selected as

$$K_C = \Sigma_k + 2\varepsilon\,, \tag{74}$$

and where $\varepsilon > 0$ is arbitrary positive constant, so that Eq. (63) may be satisfied.

For the case of $\hat{S}_k = \phi_k < 0$, the right inequality of (56) is given as:

$$\begin{aligned} \phi_k &\geq \frac{T_s}{2}\left\{\hat{b}(\hat{X}_{k|k})\sigma_k\left[\left(1-\frac{(\beta^2+1)\Delta b(\cdot)}{2\beta}\right)\hat{p}_k\right.\right. \\ &\left.\left.+\frac{(\beta^2-1)\Delta b(\cdot)}{2\beta}\mid \hat{p}_k\mid\right]-\frac{\zeta_k}{T_s}+\Delta b(\cdot)\beta(\Sigma_k+2\varepsilon)\right\}. \end{aligned} \tag{75}$$

The combination of these two results of Eqs. (73) and (75) gives:

$$\begin{aligned} \phi_k &\geq \frac{T_s}{2}\left\{\frac{(\beta^2-1)\hat{b}(\hat{X}_{k|k})\sigma_k}{2\beta^2}\left[(3\beta^2+1)\mid \hat{p}_k\mid+(\beta^2-1)sat\left(\frac{\hat{S}_k}{\phi_{k-1}}\right)\right]\right. \\ &\left.+(1+\beta^2)\Sigma_k+2\beta^2\varepsilon\right\}. \end{aligned} \tag{76}$$

In this result, the value of ϕ_k evaluated to be a maximum value, depends on the fact that $\Delta b(\cdot)$ is selected as β or $1/\beta$ based on the sign of $\hat{S}_k$ and $\hat{p}_k$. Thus, the width of boundary layer is a relative conservative number. To obtain a more accurate trajectory following, the boundary layer can be adjusted by a gain to get an appropriate width such that:

$$\phi_k = \frac{T_s}{2}\left\{\frac{(\beta^2-1)\hat{b}(\hat{X}_{k|k})\sigma_k}{2\beta^2}\cdot\mu\cdot\left[(3\beta^2+1)\,|\,\hat{p}_k\,|+(\beta^2-1)sat\left(\frac{\hat{S}_k}{\phi_{k-1}}\right)\right],\right. \tag{77}$$
$$\left.+(1+\beta^2)\Sigma_k+2\beta^2\varepsilon\right\}$$

where $0<\mu<1$.

APPENDIX B: PROOF OF THE STABILITY

Assuming there is no measurement noise or very small which can be neglected in systems, i.e. $v_k = 0$, from Eq. (40),

$$|\,e_{c_k}-e_{w_k}\,|_{ABS}=|\,\hat{H}^+\gamma\left|e_{f_{k-1|k-1}}\right|_{ABS}\,\mathrm{sgn}(e_{f_{k|k-1}})\,|_{ABS}\,. \tag{78}$$

Then,

$$|\,e_{c_k}-e_{w_k}\,|_{ABS}=\gamma\,|\,\hat{H}^+\,|_{ABS}\,\left|e_{f_{k-1|k-1}}\right|_{ABS}. \tag{79}$$

Thus,

$$|\,e_{w_k}\,|_{ABS}-|\,e_{c_k}\,|_{ABS}\le\gamma\,|\,\hat{H}^+\,|_{ABS}\,\left|e_{f_{k-1|k-1}}\right|_{ABS}. \tag{80}$$

The lag step of Eq. (79) may be described as:

$$|\,e_{c_{k-1}}\,|_{ABS}-|\,e_{w_{k-1}}\,|_{ABS}\le\gamma\,|\,\hat{H}^+\,|_{ABS}\,\left|e_{f_{k-2|k-2}}\right|_{ABS}. \tag{81}$$

Summing up the both sides of Eq. (80) and (81) yields:

$$\begin{aligned}&|\,e_{w_k}\,|_{ABS}-|\,e_{w_{k-1}}\,|_{ABS}\le|\,e_{c_k}\,|_{ABS}-|\,e_{c_{k-1}}\,|_{ABS}\\&+\gamma\,|\,\hat{H}^+\,|_{ABS}\,\{\left|e_{f_{k-1|k-1}}\right|_{ABS}-\left|e_{f_{k-2|k-2}}\right|_{ABS}\}\end{aligned}. \tag{82}$$

Combining Eqs (34), (44) and (82), yields:

$$|\,e_{w_k}\,|_{ABS}-|\,e_{w_{k-1}}\,|_{ABS}\le 0\,. \tag{83}$$

Thus, in the ideal condition, i.e. no measured noise, the stability condition of IP can be derived as:

$$| e_{w_k} |_{ABS} \leq | e_{w_{k-1}} |_{ABS} . \quad (84)$$

APPENDIX C: SLIDING SURFACE DEFINITION

In sliding mode control, the full-order discrete-time system given in Eq. (8) is transformed into the cascade of two reduced-order subsystems, referred to as the "regular" form,

$$Z_{1K+1} = Z_{1k} + T_s \hat{f}_1(Z_k) + T_s \Delta_{1k} , \quad (85)$$

$$Z_{2k+1} = Z_{2k} + T_s \hat{f}_2(Z_k) + \hat{b}_2 u_k + T_s \Delta_{2k} , \quad (86)$$

where $Z_{1k} \in R^{n-m}$, $Z_{2k} \in R^m$. This decomposition is done by applying a linear transformation, $Z_k = T\hat{X}_{k|k}$, where T is a diffeomorphic transformation. In order to design a linear sliding surface, only Eq. (85) is required. However, in this form, only Z_2 contains the input variable. Thus it is necessary to choose a different form of T to define a new equation that does contain the input but is still linear. One such transformation is given by: $T\hat{b} = [0 \quad \hat{b}_2]^T$, [17]. It is assumed without loss of generality that Eq. (85) is linear such that it can be written in the form:

$$Z_{1k+1} = [\hat{\Phi}_{11} \quad \hat{\Phi}_{12}] \begin{bmatrix} Z_{1k} \\ Z_{2k} \end{bmatrix} + T_s \Delta_{1k} \quad (87)$$

where $\hat{\Phi}_{11}, \hat{\Phi}_{12}$ are constants. As an example and referring to the EHA model of equations of (46) and (47), $\hat{\Phi}_{11}, \hat{\Phi}_{12}$ can be obtained using diffeomorphic transformation matrix $T = [I_3]$ such that $\hat{\Phi}_{11} = \begin{bmatrix} 1 & T_s \\ 0 & 1 \end{bmatrix}, \hat{\Phi}_{12} = \begin{bmatrix} 0 \\ T_s \end{bmatrix}$.

Defining the sliding surface is very problem dependent. For tracking control, it is not unusual to assume:

$$\hat{S}_k = \frac{\partial \hat{S}_k}{\partial e_{c_k}} e_{c_k} = C e_{c_k} = 0 , \quad (88)$$

where. $e_{c_k} = X_{d_k} - \hat{X}_{k|k}$. $C = \sigma_k = \frac{\partial \hat{S}_k}{\partial e_{c_k}}$ is a real-valued vector.

In discrete form of Eq. (16), ζ_k is the numerical approximation error for the sliding surface.

Using the transformation T, the parameter matrix of the switching function can be partitioned as:

$$S(k) = CT^T Te_{c_k} = [C_1 \quad C_2]\begin{bmatrix} Z_{1e\,k} \\ Z_{2e\,k} \end{bmatrix}. \tag{89}$$

During an ideal sliding motion, the $Z_{2e\,k}$ can be expressed in terms of $Z_{1e\,k}$:

$$Z_{2e\,k} = -FZ_{1e\,k}, \tag{90}$$

where $F = C_2^{-1}C_1$.

Assuming that the desired states satisfy the nonlinear model for a "hypothetical" control input [18], such that:

$$Z_{1d\,k+1} = [\hat{\Phi}_{11} \quad \hat{\Phi}_{12}]\begin{bmatrix} Z_{1d\,k}) \\ Z_{2d\,k} \end{bmatrix}, \tag{91}$$

then,

$$Z_{1e\,k+1} = [\hat{\Phi}_{11} \quad \hat{\Phi}_{12}]\begin{bmatrix} Z_{1e\,k} \\ Z_{2e\,k} \end{bmatrix}, \tag{92}$$

where $Z_{1e\,k} = Z_{1d\,k} - Z_{1k}$, $Z_{2e\,k} = Z_{2d\,k} - Z_{2k}$.

Consider the linear quadratic cost function:

$$J = \sum_{ksm}^{\infty} e_{ck}^T Q e_{ck}, \tag{93}$$

where $Q > 0$ are symmetric matrices, and k is the step in which the sliding motion is starting. The objective is to choose the coefficients of the linear sliding surface such as to minimize this cost function. By using the same transformation T as for the states, and by partitioning the matrix Q, then

$$TQT^T = \begin{bmatrix} Q_{11} & Q_{12} \\ Q_{21} & Q_{22} \end{bmatrix}. \tag{94}$$

Defining, [19]:

$$\Gamma = Q_{11} - Q_{12}Q_{22}^{-1}Q_{21}, \tag{95}$$

and for:

$$\Lambda_k = Z_{2e\,k} + Q_{22}^{-1}Q_{21}Z_{1e\,k}. \tag{96}$$

The quadratic cost function given in Eq. (93) can be written as:

$$J = \sum_{ksm}^{\infty} [Z_{1e\,k}^T \Gamma Z_{1e\,k} + \Lambda_k^T Q_{22} \Lambda_k], \tag{97}$$

where $Q_{22} > 0$ ensured by $Q > 0$ so that Q_{22} is nonsingular, and $\Gamma > 0$.

Combining Eqs. (92) and (96) to eliminate the Z_{2e}, the constraint equation may be written as:

$$Z_{1e\,k+1} = \hat{\Phi} Z_{1e\,k} + \Phi_{12} \Lambda_k, \tag{98}$$

where $\hat{\Phi} = \Phi_{11} - \Phi_{12} Q_{22}^{-1} Q_{21}$.

A positive-definite unique solution P is guaranteed by the discrete algebraic Riccati equation defined as:

$$P\hat{\Phi} + \hat{\Phi}^T P - P\Phi_{12} Q_{22}^{-1} \Phi_{12}^T P + \Gamma = 0. \tag{99}$$

Thus the problem becomes one of minimizing the function of Eq (97) constrained by Eq (98), which can be restated as a standard optimal control law Λ_k given as:

$$\Lambda_k = -Q_{22}^{-1} \Phi_{12}^T P Z_{1e\,k}. \tag{100}$$

Substituting (100) into (96) yields:

$$Z_{2e\,k} = -Q_{22}^{-1} (Q_{21} + \Phi_{12}^T P) Z_{1e\,k} = -F Z_{1e\,k}. \tag{101}$$

From this equation, $F = Q_{22}^{-1} (Q_{21} + \Phi_{12}^T P)$ and by hence $C_2 = Q_{22}$ and $C_1 = (Q_{21} + \Phi_{12}^T P)$.

Thus the sliding surface coefficients (embedded in F) can be determined by solving the discrete Riccati Eq. (99).

APPENDIX D: NOMENCLATURE

Table 1 gives all variables, parameters and coefficients used in this paper.

Table 1: Nomenclature

Symbol	Comments
$\hat{\cdot}$	Denotes uncertain values
+	The superscript denotes the pseudo-inverse

max	The subscripts denotes the upper bound
$\left\| \right\|_{ABS}$	Absolute value
$sign, sat$	Signum and saturation functions
a_1, a_2, a_{31}, a_{31}	Coefficients of the nonlinear model of the EHA
a_{33}, a_4	
b , $\Delta b(\cdot)$	Input vector and its scalar uncertainty factor
C	Real-valued constant vector
$e_{f_{k\|k-1}}, e_{f_{k\|k}}$	The a priori and a posteriori error signals in the Estimation Process
e_{c_k}	The error signals in the Control Process
e_{w_k}	The error signals in the Integrated Process
$f, \hat{f}, \Delta f$	Nonlinear function, uncertain nonlinear function and its uncertainties
i, j	Subscripts used to identify elements of matrices and vectors
K	Calculation step index
K_k	The SVSF gain
K_C	Sliding gain
$\hat{p}_k, \tilde{p}_k, q_k$	Nonlinear function
$\hat{S}_k$	Switching function
T_s	Sampling time
u_k	Control input
v, v_k	Measurement noise
V_k	Lyapunov function
w, w_k	System noise
x, x_k	System state elements
$X_k, X_{d\,k}$	Actual and desired system states
$\hat{X}_{k\|k-1}, \hat{X}_{k\|k}$	The a priori and a posteriori estimate of system states

Z_k	System outputs
$\hat{Z}_{k\|k-1}, \hat{Z}_{k\|k}$	The a priori and posteriori estimate of system outputs
β, γ	Adjustment gain
ε	Arbitrary positive constant
δ_k, ζ_k	Numerical approximation errors
σ_k	The gradient of sliding surface
Δ_k, Σ_k	Lumped uncertainty term
ϕ_k	Boundary layer and its element

REFERENCES

[1] G. F. Franklin, J. D. Powell, and A. Emami-Naeini, *Feedback Control of Dynamic Systems, 4th ed.*, Prentice Hall Upper saddle River, New Jersey 07458, 2002, pp. 515-529.

[2] V. I. Utkin, J. Shi, and J. Gulder, *Sliding Mode Control in Electromechanical Systems*, Springer-Verlag, Berlin, 1992, pp. 103-115.

[3] J. –J. E. Slotine, J.K. Hedrick, E. A. Misawa, "On Sliding Observers for Nonlinear Systems", *ASME Journal. of Dynamic Systems, Measurement and Control*, Sep 1987, vol. 109, pp. 245-252.

[4] H. Elmali, and N. Olgac, "Implementation of sliding mode control with perturbation estimation (SMCPE)", *IEEE Transactions on Control Systems Technology*, vol. 4, no. 1, Jan, 1996, pp. 79-85

[5] P. korondi, H. Hashimoto, and V. Utkin, "Direct Torsion Control of Flexible Shaft in an Observer-Based Discrete-Time Sliding Mode", IEEE Transactions on Industrial Electronics, vol. 45, no. 2, Apr 1998, pp. 291-296.

[6] Y. Xiong, and M. Saif, 2001, "Sliding mode observer for nonlinear uncertain systems", *IEEE Transactions on Automatic Control*, vol. 46, no. 12, , pp. 2012-2017

[7] F. Chen, and M. W. Dunnigan, 2002, "Comparative study of a sliding-mode observer and Kalman filters for full state estimation in an induction machine", *IEE Proceedings: Electric Power Applications*, vol. 149, no. 1, pp. 53-64.

[8] J. Li, L. Xu, and Z. zhang, 2005, "An adaptive sliding-mode observer for induction motor sensorless speed control", *IEEE Transactions on Industry Applications*, vol. 41, no. 4, pp. 1039-1046.

[9] S. R. Habibi and R. Burton, 2003, "The Variable Structure Filter" *ASME Journal of Dynamic Systems, Measurement and Control*, vol. 125, pp. 287-293.

[10] S. R Habibi & R. Burton, "Parameter identification for a high performance hydrostatic actuation system using the variable structure filter concept", *American Society of Mechanical Engineers, The Fluid Power and Systems Technology Division (Publication) FPST*, vol. 11, 2004, pp. 93-101.

[11] S. Wang, and S Habibi, and R. Burton, "A Comparative Study of A Smooth Variable Structure Filter and The Extended Kalman Filter", *The Proceedings of The Biennial CSME Forum 2006, Calgary, Canada*, no. 121.

[12] S. Wang, and R. Burton, and S Habibi, "Sliding Mode Controller and Filter applied to A Model of An Electrohydraulic Actuator System", *In ASME Fluid Power Systems and Technology Division Publication – 2005 International Mechanical Engineering Congress and Exposition*, Orlando, U.S., Nov, 2005, no. IMECE2005-80305.

[13] S. Wang, and R. Burton, and S Habibi, "Sliding Mode Controller and Filter applied to An Electrohydraulic Actuator System", *ASME Journal of Dynamic Systems, Measurement and Control*, 2006 (under review).

[14] E. A. Misawa, “Discrete-Time Sliding Mode Control for Nonlinear Systems with Unmatched Uncertainties and Uncertain Control Vector”, *ASME Journal of Dynamic Systems, Measurement, and Control*, vol. 119, Sep. 1997, pp. 503-512.
[15] S. Wang, and S Habibi, and R. Burton, “A Smooth Variable Structure Filter for State Estimation”, *Journal of Control and Intelligent Systems*, 2006 (under review).
[16] S. Wang, and S Habibi, and R. Burton, “Sliding Mode Control for A Model of An Electrohydraulic Actuator System with Discontinuous Nonlinear Friction”, *The Proceedings of 2006 American Control Conference, Minneapolis, Minnesota USA*, 2006, pp. 5898-5904..
[17] L. R. Hunt, R. Su, , and G. Meyer, “Global Transformations of Nonlinear Systems”, *IEEE Transactions on Automatic Control*, 1983, vol. 28, no. 1, pp. 24-31.
[18] E. A. Misawa, “Discrete-Time Sliding Mode Control: The Linear Case”, *ASME Journal of Dynamic Systems, Measurement, and Control*, 1997, vol. 119, pp. 819-821.
[19] C., Edwards, and S. K. Spurgeon, *Sliding Mode Control: Theory and Applications*, Taylor & Francis Ltd., 1998, pp. 65-74.